Table of Contents

List of Figures

List of Tables

Abbreviations

ACC	Acetyl-CoA carboxylase
AGE	Advanced glycation end products
ALP	Alkaline phosphatase
ALT	Alanine aminotransferase
Angptl4	Angiopoeitin-like protein 4
ANOVA	Analysis of variance
ANCOVA	Analysis of covariance
AP-1	Activating protein 1
AST	Aspartate aminotransferase
AT II	Angiotensin II
ATP	Adenine triphosphate
ATP7A	Cation-transporting P-type ATPase 7A
ATP7B	Cation-transporting P-type ATPase 7B
ATX1	Anti-oxidant protein 1
BSA	Bovine serum albumin
BW	Body weight
^{o}C	Temperature (degrees celsius)
CAD	Coronary artery disease
CCCP	Carbonyl cyanide m-chlorophenylhydrazone
CHAPS	3-[(3-Cholamidopropyl)dimethylammonio]-1-propanesulfonate hydrate
cmH$_2$o	Centimeters of water (pressure)
CoA	Coenzyme A
COX	Cytocrome oxidase
Cox17	Cytochrome oxidase assembly, subunit17
CPT	Carnitine palmytoyl transferase
cRNA	Complementary ribonucleic acid
CS	Citrate synthase
CTGF	Connective tissue growth factor
CTR	Copper transport protein
Cu	Copper
CV	Coefficient of variation
CVD	Cardiovascular disease
Cy-3/5	Cyanine-3/5
Cytb5	Cytochrome b5 (mitochondrial)
Da	Peptide mass (Dalton)
DAG	Diacylglycerol
DAT	N_1, N_{10}-diacetyltriethylenetetramine
DCM	Diabetic cardiomyopathy
DEPC	Diethylpyrocarbonate
DTT	Dithiothreitol
dNTP	Deoxyribonucleotide triphosphate
DNA	Deoxyribonucleic acid
DNase	Deoxyribonuclease
ECM	Extracellular matrix
EDTA	Ethylenediamine tetraacetic acid
ES	Enrichment score
ET	Endothelin
FA	Fatty acid
FAO	Fatty acid oxidation
FAT	Fatty acid transporter
FDR	False discovery rate
Fe	Iron
FFA	Free fatty acid
FMOC	9-Fluorenylthoxycarbonyl chloride

g	Mass (gram)
g	Acceleration due to gravity
γGCS	γ-glutamylcysteine synthetase
GAPDH	Glyceraldyhyde-3-phosphate dehydrogenase
GF-AAS	Graphite furnace - atom absorption spectroscopy
GFAT	Glutamine:fructose-6-phosphate amidotransferase
GEO	Gene expression omnibus
GlcNAc	UDP-N-acetylglucosamine
GLUT	Glucose transporter
GO	Gene ontology
GSEA	Gene-set enrichment analysis
GSH	Glutathione
GST	Glutathione S-transferase
HAD	Hexamethylenediamine dihydrochloride
hCTR	Human copper transport protein
HDL	High density lipoprotein
HEPES	4-(2-hydroxyethyl)-1-piperazineethanesulfonic acid
HF	Heart failure
HNO_3	Nitric acid
H_2O	Water
H_2O_2	Hydrogen peroxide
HOAD	L3-hydroxyacyl CoA:NAD^+ oxidoreductase
HPLC	High performance liquid chromatography
hr	Time (hour)
HW	Heart weight
HW/BW	Heart weight/body weight ratio
ICP-MS	Inductively coupled plasma-mass spectrometer
IDH	isocitrate dehydrogenase
IgG	Immunoglobulin G
IL-1β	Interlukin-1β
KEGG	Kyoto encyclopaedia of genes and genomes
LC-MS	Liquid chromatography-mass spectrometry
LPL	Lipoprotein lipase
LV	Left ventricle
MAT	N_1-acetyltriethylenetetramine
MCD	Malonyl-CoA decarboxylase
MES	Maximum enrichment score
μg	Mass (microgram)
mg	Mass (milligram)
MIAME	Minimum information about microarray experiments
min	Time (minute)
M	Amount of substance per litre (molar)
mm	Length (millimetre)
μM	Amount of substance per litre (micromolar)
mM	Amount of substance per litre (millimolar)
μl	Volume (microlitre)
ml	Volume (millilitre)
MMLV	Moloney Murine Leukemia virus
mol	Amount of substance
mmol	Amount of substance
MMP	Matrix metalloproteinase
Mn	Manganese
mRNA	Messenger ribonucleic acid
MRI	Magnetic resonance imaging
MT	Metallothionein
mtDNA	Mitochondrial deoxyribonucleic acid
MVEC	Microvascular endothelial cell

NAD+	Nicotinamide adenine dinucleotide
NADPH	Reduced nicontinamide adenine dinucleotide phosphate
NCBI	National Center for Biotechnology Information
NF-κB	Nuclear factor-κB
nm	Length (nannometre)
NO	Nitric oxide
NOD	Non-obese diabetic mouse
NOS	Nitric oxide synthases
NTP	Nucleotide triphosphate
OCT	Optimum cutting temperature
O/N	Overnight
ONOO$^-$	Peroxynitrite
OXPHOS	Oxidative phosphorylation
PAI-1	Plasminogen activator inhibitor-1
PARP	Poly-(ADP-ribose) polymerase
PBS	Phosphate buffered saline
PCR	Polymerase chain reaction
PDH	Pyruvate dehydrogenase
PDK	Pyruvate dehydrogenase kinase
PDP	Pyruvate dehydrogenase phosphatase
PEPK	Phosphoenolpyruvate carboxykinase
PET	Positron-emission tomography
PKC	Protein kinase C
PPAR	Peroxisome proliferator-activated receptor
RAGE	Receptor of AGE
REML	Restricted maximum-likelihood
RNA	Ribonucleic Acid
RNase	Ribonuclease
ROS	Reactive oxygen species
rpm	Revolutions per minute
RT	Room temperature
RT-qPCR	Real time quantitative polymerase chain reaction
s	Time (second)
SAPE	Streptavidin-phycoerythrin
SCO	Synthesis of cytochrome oxidase
SDS	Sodium dodecyl sulphate
SHR	Spontaneously hypertensive rat
snRNP	Small nuclear ribonucleoprotein
SOD	Superoxide dismutase
STZ	Streptozotocin
TBS	Tris buffered saline
TCA	Tricarboxylic acid cycle
TEM	Transmission electron microscope
TETA	Triethylenetetramine
Tfam	Transcription factor A, mitochondrial
TG	Triglyceride
TGF-β1	Transforming growth factor - β1
TIE	TGF-β1 inhibitory elements
TIGR	The Institute for Genomic Research
TOC	Tri-functional β-oxidation complex
TNF-α	Tumour necrosis factor-α
TXN	Thioredoxin
UCP	Uncoupling protein
UV	Ultraviolet
VLDL	Very low-density lipoprotein
yCCS	Yeast copper chaperone for superoxide dismutase
ZDF	Zucker diabetic fatty rat
Zn	Zinc

Chapter 1 General Introduction

1.0 Diabetes

Diabetes mellitus is defined as a metabolic disorder of multiple etiologies characterized by chronic hyperglycaemia and a tendency to chronic vascular complications, with disturbances in carbohydrate, fat and protein metabolism resulting from defects in insulin secretion, insulin action or both (Alberti and Zimmet 1998).

The disorder is currently estimated to affect between 6.0 and 7.6% of the population in countries with a western lifestyle. Between 1995 and 2025 it is predicted that there will be a 35% increase in the world wide prevalence of diabetes with the majority of the increase in the populations of developing countries. It is expected that more than 300 million people will have the disorder globally by 2025 (Wild et al. 2004).

In 2002 diabetes and its associated complications were the eleventh leading cause of death in the world (irrespective of economic status), and it is expected to increase to the seventh leading cause in the world and the fourth leading cause among high income countries by 2030 (Mathers and Loncar 2006).

1.1 Diabetic cardiomyopathy

Of the multiple etiologies associated with diabetes, cardiovascular disease (CVD) is responsible for approximately 50% of all deaths (http://www.who.int, fact sheet 312). The Framingham Heart Study, which aimed to identify the common factors that contribute to CVD, was the first to outline the risk of heart failure associated with diabetes. The study found that in the 45-74 year old cohort of the study heart failure was twice as common among diabetic men and five times more common in diabetic women than in those without diabetes (Kannel and McGee 1979).

1.1.1 Definition

Diabetic cardiomyopathy (DCM) was originally described in 1972 on the basis of observations made in four diabetic patients who presented with heart failure (HF) without evidence of hypertension, coronary artery disease (CAD), valvular or congenital heart

disease (Rubler et al. 1972). This finding was later confirmed in separate diabetic patients who showed evidence of myocardial dysfunction in the absence of CAD (Regan et al. 1977; D'Elia et al. 1979). DCM is characterized by early diastolic dysfunction and late systolic impairment (Mahgoub and Abd-Elfattah 1998).

Analysis of data from the Framingham Heart Study revealed echocardiographic evidence for increased heart rate, left ventricular (LV) wall thickness, LV end-diastolic dimension and mass in diabetic patients (Galderisi et al. 1991). A multivariate analysis showed that diabetes was independently associated with all of the above parameters providing substantial evidence for the existence of a distinct diabetes-associated cardiomyopathy (Galderisi et al. 1991).

Studies in experimental animal models, such as the streptozotocin (STZ)-induced diabetic model have helped to define the pathophysiology of myocardial dysfunction induced by diabetes (Fein et al. 1980; Penpargkul et al. 1980; Litwin et al. 1990; Rodrigues and McNeill 1999) via characterisation of the physiological and molecular changes that occur in the left ventricular wall.

The relationship between metabolic disturbance, fibrosis and diastolic dysfunction has been defined in a review by Fang *et al.,* (Fang et al. 2004). The authors determined that there are three stages of DCM development. Table 1.1 illustrates the changes that occur with the progression of the severity of the diabetes both at a structural and molecular level.

Table 1.1 Three stages of diabetic cardiomyopathy

Stages	Characteristics	Functional features	Structural features	Study methods
Early stage	Depletion of GLUT4 Increased FFA Carnitine deficiency Ca^{2+} homeostasis changes Insulin resistance	No overt functional abnormalities or possible overt diastolic dysfunction but normal ejection fraction	Normal LV size, wall thickness, and mass	Sensitive methods such as strain, strain rate, and myocardial tissue velocity
Middle stage	Apoptosis and necrosis Increased AT II Reduced IGFI Increased TGFβ -1	Abnormal diastolic dysfunction and normal or slightly decreased ejection fraction	Slightly increased LV mass, wall thickness, or size	Conventional echocardiography or sensitive methods such as strain, strain rate, and myocardial tissue velocity
Late stage	Microvascular changes Hypertension CAD	Abnormal diastolic dysfunction and ejection fraction	Significantly increased LV size, wall thickness, and mass	Conventional echocardiography

(AT II, Angiotensin II; CAD, coronary artery disease)

The concept of DCM is thus based upon the idea that diabetes induces changes at the cellular level, leading to structural abnormalities in the myocardium as outlined above (Hayat et al. 2004)

1.1.2 Diabetic heart function assessed in animal models

There have been numerous studies that have taken advantage of animal models in order to assess the effect of diabetes on heart function. Early work by Miller demonstrated a basic work-related defect in cardiac performance associated with diabetes at physiological concentrations of glucose only three days after induction of the disorder (Miller 1979). Using an isolated perfused heart system, cardiac performance was determined by measuring aortic pressure development, aortic output and coronary flow. With physiological concentrations of glucose (5mM) in the perfusion buffer, hearts from diabetic animals had decreased peak systolic pressure development compared to hearts from normal animals at filling pressures greater than 5cmH$_2$O. Both cardiac- and aortic-output were also decreased in the diabetic state. The conclusion from this study was that there was a premature failure in the isolated perfused working diabetic rat heart with increasing work loads (Miller 1979).

The work by Miller demonstrated that there is rapid induction of diabetes-related defects in cardiac performance. Subsequent studies, with a longer duration of diabetes (Penpargkul et al. 1980; Litwin et al. 1990), utilized isolated working hearts (Penpargkul et al. 1980) and conscious animals (Litwin et al. 1990). These studies showed that despite the model used both the active (shown by impairment of LV relaxation and systolic function) and passive (shown by increased LV chamber stiffness and increased end-diastolic volume) properties of the LV were altered as a result of diabetes (Penpargkul et al. 1980; Litwin et al. 1990).

These studies show that it is possible to produce animal models that provide a similar and reproducible pathogenesis from which DCM can be studied to broaden our understanding and allow development of potential therapies for use in humans.

1.1.3 Dysregulation of energy metabolism in the heart

In the early stages of diabetes, alterations in fuel supply and utilization as a result of the loss of insulin or of insulin insensitivity by the heart tissue are considered to be initiating factors that could lead to the development of DCM (Rodrigues and McNeill 1999). In isolated perfused studies of the diabetic heart it was observed that the heart would function normally without insulin if the perfusion buffer contained a fatty acid component (octanoate) (Miller 1979). The authors hypothesised that the diabetes-induced defect was likely to be due to the decreased ability of the heart to utilise glucose as an energy source (Miller 1979).

Presented here is a brief overview of cardiac energy metabolism and the role of mitochondria in DCM. Chapter Four of this thesis provides a further more comprehensive discussion of this area.

1.1.3.1 Energy metabolism in the normal heart

The heart consumes more energy than any other organ, in humans cycling about 6kg of ATP per day (Neubauer 2007). Mitochondrial generation of the required ATP in the heart is achieved through oxidation of various substrates that include glucose, free fatty acids (FFA), lactate and ketone bodies (Rodrigues and McNeill 1999). A recent review by Neubauer (Neubauer 2007) outlined the three main components of normal cardiac energy metabolism.

The first component discussed was substrate utilization. Substrate utilization is the process that entails the cellular uptake of substrates, predominately FFA and glucose, and the breakdown of these by β-oxidation and glycolysis before entry of intermediary metabolites into the tricarboxylic acid (TCA) cycle (Neubauer 2007).

Early studies of fatty acid and glucose metabolism in the rat heart found that perfusion with ^{14}C radio-labelled palmitate at physiological concentrations resulted in a 50% recovery of the ^{14}C label in CO_2. This indicated that about half of the available palmitic acid had undergone oxidisation within the heart (Shipp et al. 1961). Addition of unlabelled glucose had no effect on the uptake and oxidisation of the labelled lipid. When the ^{14}C-label is attached to glucose, approximately 17% appears as $^{14}CO_2$ with a further 1% being converted to glycogen. Addition of unlabelled palmitic acid to the perfusion media, however, reduces the amount of $^{14}CO_2$ produced from glucose oxidation to 2% and increases the amount of glycogen synthesised from 1% to approximately 3% (Shipp et al. 1961). These authors concluded that the heart preferentially utilises FFA as its fuel source even in the presence of glucose. A later study found that in the normal heart, the ability to switch between energy substrates, a phenomenon also known as metabolic flexibility, allows adaptation to acute and chronic changes in workload by a change to oxidisation of the most efficient fuel for respiration (Goodwin et al. 1998).

FFA for use as an energy substrate is supplied to the heart from three main sources (Rodrigues and McNeill 1999):

(1) Lipolysis of endogenous triglyceride (TG) within the cardioadipocyte or cardiomyocyte
(2) Lipolysis of adipose tissue TG with subsequent release of FFA into the blood. This is then carried to the heart and is usually bound to albumin.

(3) Lipolysis of the circulating TG found in chylomicrons and very low density lipoproteins (VLDL) by coronary endothelial-bound lipoprotein lipase (LPL). Vascular endothelial bound LPL is the rate limiting enzyme that determines the clearance of plasma TG and partially regulates FFA supply to the tissues (Eckel 1989). For a comprehensive review on myocardial utilization of carbohydrates and lipids see Neely *et al.,* (Neely et al. 1972).

The second component outlined by Neubauer (Neubauer 2007) was oxidative phosphorylation (OXPHOS) which describes the production of energy in the form of ATP by the mitochondrial respiratory chain (Cooper and Lehninger 1956; Cooper and Lehninger 1956; Devlin and Lehninger 1956; Cooper and Lehninger 1957; Cooper and Lehninger 1957). The net result of OXPHOS is the conversion of ADP to ATP which is used in all energy consuming reactions of the heart (Neubauer 2007).

The third and final component in cardiac energy metabolism discussed was the transfer of ATP to myofibrils for utilisation. This process entails an energy-transfer mechanism called the Creatine-Kinase Energy Shuttle (Neubauer 2007). This last component is beyond the scope of this thesis and so is not discussed further.

1.1.3.2 Energy metabolism in the diabetic heart

It is well established that energy uptake and metabolism are perturbed in the diabetic heart (for reviews see (Stanley et al. 1997; Lopaschuk 2002; Taegtmeyer et al. 2002; Fang et al. 2004; Taegtmeyer et al. 2004)).

Of the three components of energy metabolism outlined above (Section 1.1.3.1) one of the most well studied in DCM is the effect of diabetes on the first component, substrate utilization. Studies have shown that myocardial glucose transport is defective in both diabetic humans and STZ-induced diabetic animals (Lopaschuk 2002), which has been linked to a decrease in total glucose transporter 4 (GLUT 4) protein/mRNA (Depre et al. 2000). Additionally, the rate of glucose oxidation is severely decreased in diabetes due to a marked decrease in pyruvate dehydrogenase (PDH) activity as a result of changes in PDH regulatory enzymes (Wu et al. 1998). Inhibition of the PDH complex is believed to exacerbate the diabetic state by inappropriately sparing glucose and gluconeogenic substrates from complete oxidation in the face of abundant levels of glucose and other oxidizable fuels in the blood (Wu et al. 1998). Due to inadequate glucose transport and oxidation, energy production in the diabetic heart is almost entirely via β-oxidation of FFA (Sakamoto et al. 2000). Taegtmeyer *et al.,* provided a hypothesis regarding this phenomenon and referred to it as metabolic inflexibility. Metabolic inflexibility is defined as the loss of the ability to switch from the use of fatty acids to carbohydrates for the production of energy in the insulin deficient or resistant state (Taegtmeyer et al. 2004).
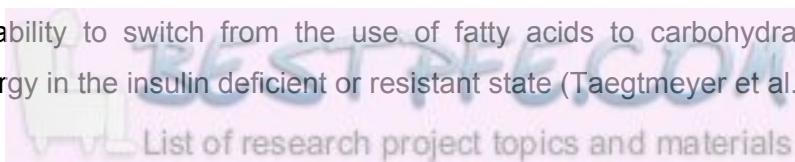
A recent proteomic study by Turko *et al.,* (Turko and Murad 2003) reported quantitative analysis of the protein profile of mitochondria from diabetic rat hearts. The primary focus of this study was on the proteins that play roles in the three major mitochondrial cycles associated with ATP production, which are: a) β-oxidation, b) TCA cycle and c) OXPHOS. These direct measurements found that various mitochondrial proteins involved in FA oxidation were up regulated, including carnitine palmitoyltransferase II (CPT II) and three different acyl-CoA dehydrogenases (Turko and Murad 2003). This work was confirmed through transcriptomic studies in this thesis that demonstrated an upregulation in genes associated with β-oxidation and a concurrent decrease in genes associated with glucose metabolism (Glyn-Jones et al. 2007). These results show that the heart from STZ diabetic rats adapts to the metabolic disorder via an up-regulation of FA β-oxidation.

There are consequences of excessive utilisation of FA which have been described in a review by Rodrigues and McNeill (Rodrigues and McNeill 1999). These include: increased susceptibility to arrhythmias, higher tissue levels of TG (due to esterification of complex lipids), increased requirement of oxygen for catabolism, modification of the structure of sarcolemmal and other subcellular membranes, inhibition of enzyme systems such as Ca^{2+}-ATPase of the sarcoplasmic reticulum and inhibition of the adenine nucleotide translocator leading to a reduction of the myocardial levels of ATP (Rodrigues and McNeill 1999). Additionally, excessive utilisation of FA may also lead to an increase in production of reactive oxygen species (ROS) by the mitochondria (Glyn-Jones et al. 2007). Section 1.2 describes the current hypothesis regarding the implications of excessive ROS production and how this may lead to complications such as DCM.

1.2 Molecular mechanisms underlying diabetic complications

Due to the prevalence and predicted increases in the number of people with diabetes, a vast amount of study has gone in to understanding its different functional and molecular aspects. The work contained within this section will focus on the molecular changes surrounding the development of DCM. Outlined in Sections 1.2.1 to 1.2.5 is the current literature related to the biology of complications arising from chronic hyperglycaemia. A unifying hypothesis was originally put forward by Brownlee *et al.,* (Brownlee 2001) which points to four main pathways in the endothelial cell. Additionally, these four pathways have been linked together under one common hyperglycaemia-induced process (Brownlee 2001).

1.2.1 Pathway 1: An increase in Polyol-pathway flux resulting in a reduction in Glutathione

Glutathione (GSH) participates in the cellular defence system against oxidative stress by reducing disulphide linkages of proteins and other cellular molecules or by scavenging free radicals and reactive oxygen intermediates (Urata et al. 1996). Synthesis of GSH requires two ATP-dependent enzymes, γ-glutamylcysteine synthetase (γ-GCS) which catalyses the rate limiting step, and glutathione synthase. The concentration of GSH and the activity of γ-GCS are decreased in mouse endothelial cells cultured at high glucose concentrations (Urata et al. 1996). It has also been reported that the activation of γ-GCS in cells exposed to normal glucose levels is due to the cytokines TNF-α and IL-1β and that this response can be eliminated by exposure of the cells to higher glucose concentrations (Urata et al. 1996). It has been proposed that a weak response of the enzymes involved in GSH synthesis to stimulation via cytokines, together with low levels of GSH reduces cellular antioxidant activity in the diabetic state (Urata et al. 1996). Arsalane *et al.,* (Arsalane et al. 1997) have shown in an *in vitro* study using lung epithelial cells that an increase in exogenous TGF-β1 enhanced susceptibility to H_2O_2 mediated cytotoxicity, and induced a marked depletion of GSH. These effects could be completely blocked by an anti-TGF-β1 specific antibody. Further, the decrease in GSH was associated with a decrease in the expression of γ-GCS (Arsalane et al. 1997).

Increases in the exogenous glucose concentration are also hypothesised to contribute to a reduction of GSH in the cell. Increased glucose levels lead to an elevation in the production of sorbitol through the enzyme aldose reductase which requires NADPH as an electron donor to allow catalysis of glucose to sorbitol (Brownlee 2001). NADPH is required in the regeneration of reduced GSH and thus reduction in the levels of NADPH will result in the subsequent reduction of GSH levels. This may induce or exacerbate oxidative stress (Brownlee 2001) as increased production of sorbitol through the polyol pathway will also ultimately result in an increase in the substrates required for the formation of AGEs ((Singh et al. 2001), see Figure 1.1). This finding demonstrates that, although each of the four pathways are described individually, they are not independent, but can act synergistically to further increase the cellular damage, leading to the development of DCM.

Transition metals such as copper can act as catalysts in the oxidative deterioration of biological macromolecules (Stohs and Bagchi 1995). GSH through its action as an antioxidant and chelating agent was able to completely prevent enhanced cytotoxicity of copper in bone marrow cells. The protective effect of GSH was attributed to its ability to stabilize copper in the Cu^I oxidation state, thus preventing redox cycling and generation of ROS (Stohs and Bagchi 1995). Depletion of GSH, by the described mechanisms, would therefore contribute to an increase in copper toxicity in diabetes. Removal of copper using

an exogenous copper chelator may aid in restoring the balance of copper homeostasis which is lost through removal of GSH activity.

1.2.2 Pathway 2: Increased intracellular formation of advanced glycation end-products

Figure 1.1 outlines the main processes involved in the formation of advanced glycation end-products (AGEs). Reducing sugars such as glucose react non-enzymatically with amino groups in proteins, lipids, and nucleic acids through a series of reactions, forming Schiff bases and Amadori products to produce AGE (Singh et al. 2001). The slow turnover of collagen makes it a prime target for modification by glucose (Qian et al. 1998).
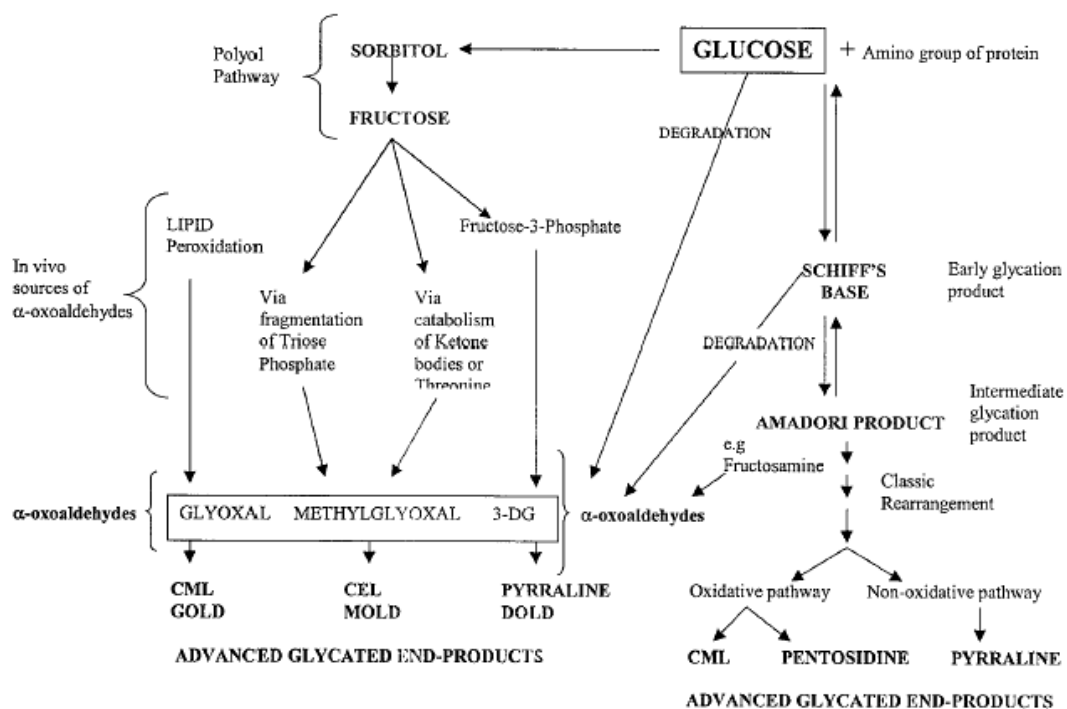
Figure 1.1 AGE formation pathways

Schematic incorporates the polyol pathway and AGE formation by the α-oxoaldehydes glyoxal, methyl glyoxal and 3-DG. 3-DG, 3-deoxyglucosone; MGO, methylglyoxal; CML, N-ε-(carboxymethyl)lysine; CEL, N-ε-(carboxyethyl)lysine; DOLD, deoxyglucasone-lysine dimmer; MOLD, methyl glyoxal-lysine dimmer; GOLD, glyoxal-lysine dimmer. (Modified picture and legend from Singh *et al.,* (Singh et al. 2001))

Cells are damaged by AGE formation through three general mechanisms:

1. Alteration in the function of AGE proteins (Brownlee 2001). For example Kang *et al*., (Kang 2003) were able to show that as the modification of Cu-Zn superoxide dismutase (Cu-Zn SOD) by methylglyoxal (AGE) increased, activity decreased. The

authors were also able to demonstrate that AGE modification of Cu-Zn SOD occurred on several important amino acid residues including glycine, histidine, lysine, and valine (Kang 2003).

2. Extra cellular matrix (ECM) components that are modified by AGEs interact abnormally with other matrix components and tend to form covalent crosslinks that result in abnormal ECM function. For example, modification of collagen by AGEs leads to decreased elasticity and solubility thus creating stiffer muscle (Brownlee 2001). AGE formation has also been shown to reduce the proteolysis of glycated protein. Interstitial collagenases (matrix metalloproteinases or MMP) mediate the initial step of collagen degradation by cleaving triple helix fibrils of the interstitial collagen types I and III at a single site, resulting in the generation of ¾ and ¼ length fragments which then become accessible to other proteases such as the gelatinases (Tamarat et al. 2003). Tamarat *et al.,* (Tamarat et al. 2003) investigated the effect of aminoguanidine (an inhibitor of AGE formation) treatment on the breakdown of collagen in the femoral artery of STZ-treated mice, and found that despite an increase in MMP content the quantity of cleaved collagen was decreased, suggesting that under these conditions the ECM is less sensitive to degradation. The authors hypothesized that the glucose derived cross-links on the collagen in diabetic animals altered the structure and function and increased the tensile strength of the collagen matrix therefore hampering protein degradation (Tamarat et al. 2003)

3. AGE receptors such as Receptor for AGE (RAGE), AGE-R1, AGE-R2, and AGE-R3 have been identified mainly through work carried out in epithelial/mesangial cells and macrophages (Singh et al. 2001). Interaction of AGE with its receptors has been found to induce receptor-mediated production of ROS (Brownlee 2001). Binding of ligands to RAGE initiates a sustained period of cellular activation mediated by receptor-dependent signalling (Schmidt et al. 2001). RAGE is expressed at low levels in normal tissues and these levels increase in areas where the ligands accumulate (Schmidt et al. 2001). Cell culture studies have shown that the AGE-RAGE interaction alters the cellular properties important to vascular homeostasis such as depleting the cells nitric oxide concentration (Singh et al. 2001). This finding suggests that AGEs have complex involvement in pathologies such as diabetes as it allows extracellular events to be internalized.

1.2.3 Pathway 3: Activation of Protein Kinase C

The Protein Kinase C (PKC) /diacylglycerol (DAG) pathway is known to be important in vascular cells via regulation of endothelial cell permeability, cardiomyocyte contractility,

ECM, smooth muscle cell growth and contraction, angiogenesis, and cytokine actions through initiating expression of signal transduction hormones and growth factors and leukocyte adhesions. Each of these factors is known to be abnormal in the diabetic state (Koya and King 1998). An increase in total DAG content has been demonstrated in a variety of tissues commonly associated with the disorder, including the heart (Inoguchi et al. 1992). Studies have shown that the glucose-induced increase in DAG content is as a result of *de novo* synthesis (Inoguchi et al. 1992; Koya and King 1998). Inoguchi *et al.,* (Inoguchi et al. 1992) reported increased membranous PKC activity and total DAG in the diabetic rat heart. They demonstrated that the β_2 isoform of PKC was preferentially increased in the rat heart and aorta, and as such, is likely to be the isoform that contributes to cardiovascular complications. PKC-β_2 activation may contribute to myocardial hypertrophy and fibrosis by altering the expression of TGF-β and connective tissue growth factor (CTGF) which has a unique TGF-β response element in its promoter region (Way et al. 2002). A more recent study by Way *et al.,* studied STZ-induced diabetes in FVB mice and Sprague-Dawley rats and found that there was an increase in TGF-β mRNA and CTGF mRNA in ventricular heart tissue (Way et al. 2002).

The increased PKC activity in diabetes may lead to alteration of several growth factors, cytokines and vasoactive molecules including Endothelin-1 (ET-1). Endothelins are a family of potent vasoactive molecules of which there are four distinct forms ET-1, ET-2, ET-3 and the vasoactive intestinal contractor. These interact with three populations of receptor: ET_A, ET_B and ET_C. It has previously been demonstrated that endothelin and its receptor mRNA are increased in the retina of diabetic rats (Chen, S. et al. 2000). This group (Chen, S. et al. 2000) investigated heart ET-1 in STZ rats six months after induction of diabetes and were able to show that ET-1 mRNA as well as ET_A and ET_B mRNA and density were increased in the diabetic heart. They proposed several mechanisms by which an increase in ET-1 may occur, including PKC β activation (Chen, S. et al. 2000).

PKC activation has also been shown to contribute to increased microvascular matrix protein accumulation through the induction of TGF-$\beta1$, fibronectin and collagen IV expression (Brownlee 2001).

1.2.4 Pathway 4: Increased flux through the Hexosamine pathway

Normally the hexosamine pathway diverts fructose-6-phosphate from glycolysis to provide substrates for reactions that require UDP-*N*-acetylglucosamine (GlcNAc), such as proteoglycan synthesis and the formation of *O*-linked glycoprotiens, for example, modification of the transcription factor Sp-1 (Brownlee 2001).

In diabetes, a greater volume of glucose is shunted through the hexosamine pathway, leading to increased amounts of UDP-GlcNAc and an increase in the donation of GlcNAc moieties to serine/threonine residues of Sp-1 (Du, X. L. et al. 2000). Studies have

indicated that the glycosylated form of Sp-1 is more active than the deglycosylated form. This finding has been used as evidence for a link between hyperglycemia, increased gene transcription and the hexosamine pathway (Brownlee 2001).

1.2.5 The common element

The link between the four pathways outlined above (activation of PKC, formation of AGEs, increased flux through the hexosamine pathway, a decrease in GSH) and the formation of ROS has been determined by Nishikawa *et al.* (Nishikawa et al. 2000). This group were able to demonstrate using cultured endothelial cells, that the TCA cycle was the source of increased ROS induced by hyperglycemia (Nishikawa et al. 2000). Further, they found that inhibition of complex II (using rotenone) and oxidative phosphorylation (using CCCP and uncoupling protein-1) completely prevented the undesired effects of hyperglycemia.

The authors then investigated the effect of CCCP, UCP-1 on PKC activation (pathway 3), formation of intracellular methylglyoxal (pathway 2, AGE formation), sorbitol accumulation (pathway 4, indicates aldose reductase activity) and activation of NFκB (ROS inducible transcription factor, pathway 1). The results showed that each of these processes were inhibited by CCCP and UCP-1 which led to the conclusion that increased ROS production from the mitochondria is the factor responsible for initiation of the four undesired pathways in the face of hyperglycemia (Nishikawa et al. 2000).

Further evidence that generation of ROS is closely associated with the onset of diabetes-induced cardiomyopathy can be found in experiments looking at other aspects of the ROS defence system. Metallothionein (MT) has a powerful ROS scavenging effect because of its high thiol content and studies have shown that MT is lowest in adult rat heart, when compared to the liver, kidney, small intestine and brain, indicating that cardiac tissue may be susceptible to oxidative stress as a result of low oxidant defence (Ye et al. 2003).

Ye *et al.,* (Ye et al. 2003) investigated whether increases in ROS are involved in the pathogenesis of DCM and the potential protective effect of MT against the effects of ROS. OVE26MT is a diabetic transgenic mouse line which has an over-expression of MT specifically in the cardiac myocytes. OVE26 (WT control) diabetic myocytes showed reduced contractility and prolonged calcium transients, suggesting that impaired contractility of the intact diabetic heart was due to defects in the individual myocytes rather than simply an increase in fibrosis (Ye et al. 2003). They also found that over expression of MT was effective in relieving the functional defects in OVE26 diabetic cardiomyocytes in the face of identical levels of hyperglycemia. The authors concluded that generation of ROS is essential to the pathogenesis of DCM (Ye et al. 2003).

Mammalian cells contain the copper-zinc form of superoxide dismutase (Cu-Zn SOD) in the cytoplasm and a manganese form in the mitochondria (Mn-SOD). These are

considered to form the most powerful defence system the cell has against ROS. Mn-SOD is known to be induced by cytokines and is one of the most important factors in combating the cytotoxicity of TNF-α (Doi et al. 2001). Doi *et al.,* investigated the effects of alterations in antioxidants and the contribution of these to the process of cardiac dysfunction. They investigated whether the activity and protein and/or gene expression of antioxidants was altered in animals with STZ-induced diabetes (Doi et al. 2001). In justification of the use of this model as one appropriate to DCM, the authors reported an increase in the expression of TGF-β1 mRNA as well as an accumulation of type IV collagen around the cardiac muscle bundles. An increase in wall thickness accompanied the cardiac dysfunction and this was attributed to the increases in collagen levels. An increase in the mRNA and protein levels of Mn-SOD was observed and GSH levels were reportedly decreased. Previous literature reports suggest that hyperglycemia causes a down-regulation of the level of GSH (Urata et al. 1996) and also the expression of one of the ATP-requiring enzymes needed to synthesize GSH (γ-GCS) (Doi et al. 2001). This result indicates that part of the defence system against ROS is not as efficient as in a normal cell and provides a potential explanation, at least in part, for the increase in oxidative stress observed in diabetes.

The damaging effect of increased ROS in diabetes is not only limited to proteins and metabolites. There is increasing evidence that increased ROS may also lead to elevated gene expression within the cell. Two of the main facilitators of this are:

1. Elevation of PKC and DAG levels, which may modulate gene expression by activating activator protein-1 (AP-1 (Nishio et al. 1998))
2. Accumulation of AGEs which then bind to their receptors, resulting in the activation of NFκB (Singh et al. 2001)

Both of these transcription factors are regulated in response to various oxidative stresses and are implicated in the alteration of expression of a variety of genes (Nishio et al. 1998). NFκB and AP-1 have both been shown to up regulate the synthesis of fibronectin, an ECM component implicated in increases in heart stiffness, through induction of ET-1 expression (Chen, S. et al. 2003). In this study mRNA levels for both ET-1 and fibronectin were increased; additionally increases in the activated forms of NFκB and AP-1 were observed in diabetic hearts (Chen, S. et al. 2003).

1.3 Treatment of diabetic cardiomyopathy

Currently there is no specific therapeutic strategy for the treatment of DCM. Due to the wide variety of perturbations which can occur in the heart, such as metabolic disturbances, myocardial fibrosis, LV hypertrophy, increased ROS production and

microvascular disease, as a result of the diabetic state, it has proven to be difficult to identify one global treatment.   Potential treatments currently include; improved diabetic control, use of calcium blockers, angiotensin-converting enzyme (ACE) inhibitors, lipid-lowering therapy or antioxidant drugs (Fang et al. 2004).

The evidence presented in Section 1.2 strongly implicates a perturbation in the molecular systems surrounding ROS generation and management in the development of complications resulting from hyperglycaemia. In light of this a sensible approach to the treatment of diabetic complications including DCM could be antioxidant therapy; however current literature provides a conflicting view of the benefits of antioxidant treatment. This literature is summarised below.

1.3.1 Antioxidant therapies

Evidence for an improvement in cardiac function as a result of antioxidant treatment was presented by Kaul *et al.,* (Kaul et al. 1996) who were able to demonstrate improved LV peak systolic pressure and aortic systolic and diastolic pressure in STZ-diabetic rats after four weeks of treatment with Probucol (Kaul et al. 1996). In support of this De Cavanagh *et al.,* (de Cavanagh et al. 2001) showed a reduction in heart fibrosis and an improvement in tissue antioxidant levels after eight months of treatment of diabetic animals with Enalapril.

Conversely, Rauscher *et al.,* published a series of studies suggesting that there was no improvement in antioxidant status in the heart as a result of treatment with antioxidants (Rauscher et al. 2000; Rauscher et al. 2001; Rauscher et al. 2001). The authors described three separate studies in which STZ-diabetic animals were treated with the antioxidants Piperine (Rauscher et al. 2000), Coenzyme Q_{10} (Rauscher et al. 2001) or Isougenol (Rauscher et al. 2001). Results from all three studies showed no reversal of STZ-diabetic compromised antioxidant status (measured as activities of catalase, SOD and glutathione peroxidase/reductase) and in the case of Piperine and Isougenol treatment actually exacerbated the diabetic state (Rauscher et al. 2000; Rauscher et al. 2001). Similarly, a randomised placebo-controlled trial conducted to assess the effects of an antioxidant vitamin supplement on high risk patients with coronary disease, other occlusive arterial disease or diabetes found no evidence of benefit in 6000 people with diabetes after five years (2002).

1.3.2 Triethylenetetramine (TETA) as a treatment for diabetic cardiomyopathy

The conclusion from the studies above is that the nature of antioxidant stress and the best treatment options are still unclear. Given the lack of current treatments, there is a great deal of interest in the development of new therapies. One such therapy has been

identified by our group (Cooper et al. 2004; Cooper et al. 2005; Gong et al. 2006; Jullig et al. 2007) and is in the process of being developed for use in humans.

TETA was first described for use in humans by Walshe (Walshe 1969) and in 1985 Triethylenetetramine dihydrochloride was approved by the USA Food and Drug administration as an orphan drug for treatment of penicillamine-intolerant patients with Wilson's disease, a genetic disorder that results in accumulation of copper within the body due to a mutation in a P-type ATPase (Bull et al. 1993).

Although the influence of trace metals such as copper had been implicated in the etiology of diabetes previously (Zargar et al. 1998; Eaton and Qian 2002), recent work by Cooper *et al.,* (Cooper et al. 2004) has indicated that removal of excess copper using the copper chelator TETA induces marked improvements in structure and function of diabetic rat hearts and also decreases in the left ventricular mass of patients with type-2 diabetes (Cooper et al. 2004). Histological analysis of LV tissue from STZ-diabetic rats showed an increase in collagen type I and III, which was proposed to increase the heart stiffness, and that treatment with TETA appeared to reverse this collagen deposition (Cooper et al. 2004). Use of TETA as a therapeutic agent in other non-Wilson's related diseases, has also been described by Keegan *et al.,* (Keegan et al. 1999) who described the effects of TETA on the aorta and corpus cavernosum of STZ-diabetic rats. Authors were able to show that treatment with TETA, from the onset of diabetes, was able to protect the aorta against defective aortic endothelium-dependent relaxation caused by hyperglycemia (Keegan et al. 1999). Gong *et al.,* (Gong et al. 2006) provided some explanation at the transcript level for the observations of Cooper *et al.,* (Cooper et al. 2004). They were able to show that treatment of STZ-diabetic animals with TETA evoked decreases in the expression of genes that are increased by the onset of diabetes, namely collagen III, TGF-β and Smad4 (Gong et al. 2006). This finding strengthens the hypothesis of Cooper *et al.,* that accumulation of loosely bound copper in the ECM may play a role in diabetic cardiac damage and that removal of such copper results in a reduction of the expression of ECM associated genes (Gong et al. 2006). The mechanism underlying these observations is, however, yet to be fully elucidated.

Evidence for the involvement of the mitochondria in the mechanism of TETA action has come from work published recently by Jüllig *et al*., (Jullig et al. 2007). These authors reported decreases with TETA treatment at the protein level of a number of key mitochondria-associated enzymes including those implicated in FA β-oxidation (CPT II, enoyl-CoA hydratase), the TCA cycle (E2 and E3 subunits of PDH) and OXPHOS (Ndufa10, ATP synthase α and β subunits). Of particular importance were changes observed in enoyl-CoA hydratase and CPT II. At the protein level, both were found to be increased with diabetes and subsequently decreased following drug treatment. CPT II activity was also increased as a result of diabetes and was restored following treatment.

This report provides evidence for an improvement in FAO in the heart as a result of treatment with TETA (Jullig et al. 2007).

1.3.2.1 Current understanding of TETA pharmacology

The current understanding of TETA metabolism has come largely from studies involving healthy volunteers or animal subjects (Gibbs and Walshe 1986; Takeda et al. 1995a; Takeda et al. 1995b; Takeda et al. 1995c; Kodama et al. 1997). Studies of TETA metabolism in humans by Kodama *et al.,* indicated that TETA was poorly absorbed with urinary levels reaching only 1-2% of the administered dose eight to ten hours after administration (Kodama et al. 1993; Kodama et al. 1997). Using an HPLC-based method to determine urinary TETA levels, Kodama *et al.,* were able to identify a secondary peak (Kodama et al. 1993). This peak was subsequently characterised as N_1-acetyltriethylenetetramine ('monoacetylated TETA' or MAT, (Kodama et al. 1997)). The authors found that MAT was excreted in the urine at levels of approximately 8% of the administered dose and was still present up to 26hr after the initial administration of TETA. They hypothesised that MAT is a biotransformation product, rather than a breakdown product, of TETA (Kodama et al. 1997).

Studies in animals using ^{14}C-labelled TETA have confirmed that this finding is not restricted to humans (Gibbs and Walshe 1986; Takeda et al. 1995a; Takeda et al. 1995b; Takeda et al. 1995c). Gibbs and Walshe described the metabolism of ^{14}C-labelled TETA in normal rats after intravenous injection and oral administration (Gibbs and Walshe 1986). The authors described poor absorption after oral administration with 6-18% of administered dose appearing in the urine (Gibbs and Walshe 1986) which concurs with that observed in humans. This work also identified a metabolite (MAT) that was able to be replicated with *in vitro* acetylation of TETA but not when TETA was chelated to metals, consistent with the work in humans of Kodama *et al.,* (Kodama et al. 1997). Autoradiographic analysis by Gibbs and Walshe of liver and kidney sections found radioactivity in the hepatocytes and renal cells providing the first evidence that TETA and/or its metabolites are able to cross the cell membrane (Gibbs and Walshe 1986).

A recent publication by Lu *et al.,* was the first to describe the metabolism of TETA in diabetic patients (Lu et al. 2007). This study analysed the levels of TETA and its metabolites in human urine from healthy and diabetic subjects treated with TETA dihydrochloride using a LC-MS based methodology (Lu et al. 2007). One of the main findings from this study was that the urine of both diabetic and normal subjects contained three species related to TETA. LC-MS comparison of pre- and post-drug samples demonstrated the presence of six extra ions in the post-drug samples of which three (of 146, 188 and 230 Da) were major. These masses were consistent with the parent compound TETA and two metabolites, the mono-acetylated TETA (MAT) described

previously (Gibbs and Walshe 1986; Kodama et al. 1993; Kodama et al. 1997)) and N_1, N_{10}-diacetyltriethylenetetramine (DAT), which was first reported in this study (Lu et al. 2007). Figure 1.2 presents the molecular structures for each of these three compounds.
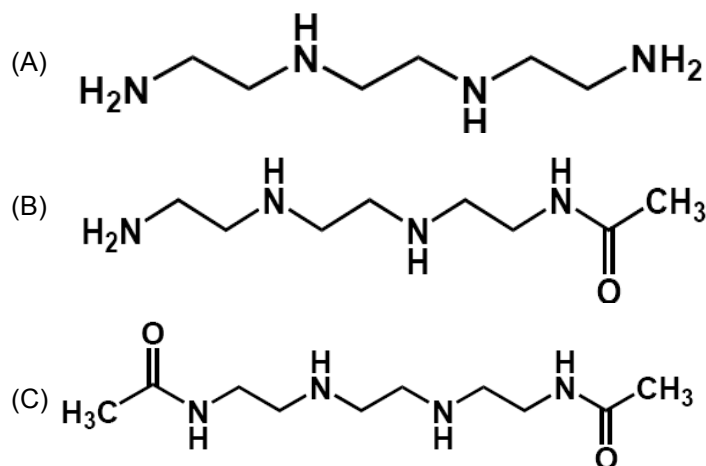
Figure 1.2 Representative molecular structures of TETA and its metabolites MAT and DAT

(A) TETA (Triethylenetetramine) free base, (B) MAT (N_1-diacetyltriethylenetetramine) and (C) DAT (N_1, N_{10}-diacetyltriethylenetetramine) (Lu et al. 2007)

Another important observation of this study was that diabetic patients' excreted greater levels of metabolised TETA (MAT and DAT) than did healthy controls (Lu et al. 2007). The authors hypothesised that this increase may result from higher hepatic metabolism of TETA (Lu et al. 2007).

1.4 Copper homeostasis

The ability of TETA to ameliorate the effects of diabetes on the heart as described by Cooper *et al.,* (Cooper et al. 2004) indicates that copper could play an important role in the development of DCM and that removal of loosely-bound copper through chelation can ameliorate the effects of hyperglycaemia. Outlined below is a description of the systems controlling copper homeostasis within the body and the issues that could arise if this system is disrupted.

1.4.1 Normal copper homeostasis

Copper ions are able to adopt distinct redox states in the body, reduced Cu^I or oxidized Cu^{II} which enables them to act as catalytic cofactors in biological redox chemistry. In

humans copper is readily absorbed and distributed to copper-requiring proteins with apparently little storage of excess copper in the body (Pena et al. 1999).

1.4.1.1 Copper uptake into the cell

Copper uptake into the cell has been widely studied in bacteria and yeast. This work has provided evidence of precise regulatory mechanisms that prevent the accumulation of toxic levels of copper ions (for a review see (Pena et al. 1999)). The first stage of cellular cooper uptake in *Saccharomyces cerevisiae* is thought to involve the reduction of Cu^{II} to Cu^{I} by one or more cell surface iron/copper reductases. Copper transcriptionally regulates these reductases through the copper metaloregulatory transcription factor Mac1 (Georgatsou et al. 1997). Cu^{I} can then be delivered to the plasma membrane-associated high affinity copper transporters encoded by the yeast CTR1 and CTR3 genes (Dancis et al. 1994; Knight et al. 1996). Comparison of the action of the CTR1 gene in yeast to early findings described in the mammalian swine model of copper deficiency yielded a number of analogous findings (Lee et al. 1968). In the yeast model, mutation of CTR1 led to abrogation not only of high affinity copper but also iron uptake (Dancis et al. 1994), while copper deficient swine were noted to have decreased total body iron levels and an anaemia indistinguishable from that observed in iron deficiency (Lee et al. 1968). These similarities indicate that the mechanism of copper and iron uptake in yeast could be related to that in mammals. Further evidence for this came from identification of a human homologue of CTR1 (hCtr1). hCTR1 was identified through complementation analysis using CTR1 deficient yeast and a human cDNA yeast expression library (Zhou, B. and Gitschier 1997). hCTR1 was characterised as a putative high affinity copper transport protein with high levels of expression in the liver, heart and pancreas (Zhou, B. and Gitschier 1997).

The predominant copper-containing protein in mammalian serum is ceruloplasmin, a glycosylated multi-copper ferroxidase first identified in plasma (Holmberg and Laurell 1948). Ceruloplasmin acts as an extracellular copper-binding and transport protein (Hsieh and Frieden 1975). Evidence for a role of ceruloplasmin as a copper transport protein comes from work demonstrating its importance for the function of copper containing proteins such as cytochrome c oxidase (Hsieh and Frieden 1975) and Cu-Zn SOD (Dameron and Harris 1987). In both cases, introduction of ceruloplasmin into a copper-deficient animal model was sufficient to restore the function of each protein (Hsieh and Frieden 1975; Dameron and Harris 1987). In the case of cytochrome c oxidase, injection of ceruloplasmin into copper deficient rats produced a faster increase in cytochrome c oxidase activity than that observed in rats receiving $CuCl_2$, copper-histidine or copper-albumin (Hsieh and Frieden 1975). Additionally, a specific receptor for ceruloplasmin has been identified in the plasma membranes of the aorta and heart tissue indicating a

potential mechanism for the transfer of copper from ceruloplasmin into the cell (Stevens et al. 1984).

1.4.1.2 Copper distribution within cells

Upon transport into the cell, copper forms complexes with small cytosolic copper trafficking proteins known as copper chaperones, which then allows delivery of the metal to specific molecules. These were originally identified in yeast; however mammalian homologues have also been identified (Pena et al. 1999).

Historically, metalloproteins such as Cu-Zn SOD were generally assumed to acquire cofactors by passive diffusion. It is now understood, however, that networks of chaperones are required for the incorporation of copper by proteins *in vivo* (Rae et al. 1999). For example yCCS is the yeast copper chaperone for superoxide dismutase, and is essential for the expression of the functional copper-bound form of yeast SOD *in vivo* (Culotta et al. 1997). yCCS is thought to insert copper into its target enzyme only if the ambient free copper concentration is extremely low (Rae et al. 1999). Absence of yCCS does not decrease the total number of yeast superoxide dismutase-1 (ySOD1) molecules but does reduce the proportion of active copper-bound ySOD1 compared to the inactive apo-form of the enzyme. yCCS was found to both sequester copper away from metal scavenging agents and to direct the cofactor into the enzyme (Rae et al. 1999).

Another copper chaperone is Cox17. This chaperone carries copper to cytochrome c oxidase in the mitochondria. Glerum *et al.,* (Glerum et al. 1996) demonstrated using a *cox17* mutant, that Cox17 is not important for synthesis, import or processing of the cytochrome c oxidase subunits but rather fits into the category of genes whose products interact during the late stages of assembly (Glerum et al. 1996). Cox17 is unusual as it has a cytoplasmic location whereas all other known cytochrome c oxidase gene products are located on the mitochondrial inner membrane. Thus, it has been proposed that the function of Cox17 is as part of the pathway responsible for delivering copper to the mitochondria (Glerum et al. 1996). These are just two examples of a rapidly expanding group of copper chaperones (another example includes antioxidant protein 1 (ATX1) (Lin and Culotta 1995; Lin et al. 1997)), each of which has its own specific role in maintaining copper homeostasis.

In order to maintain a steady state, copper ions must be exported at a rate that counters the efficient uptake system. ATP7A and 7B are integral membrane proteins designed to attach to the membrane and conduct the ATP-dependent movement of copper (Tanzi et al. 1993; Voskoboinik et al. 1998). ATP7A and 7B have been identified as being crucial to copper transport within the cell by La Fontaine *et al.,* who showed that the copper transport defect seen in fibroblasts cultured from a patient with Menke's disease could be restored with the expression of either ATP7A or B (La Fontaine et al.

1998). Current understanding suggests that vesicles containing the embedded Cu-ATPase protein pinch off from the trans-golgi network and move to the outer membrane in a continuous movement (Voskoboinik et al. 1998).

1.4.2 Copper and oxidative stress

Although copper is a dietary requirement, it is also a potent cytotoxin when allowed to accumulate in excess of cellular needs. In these circumstances copper can participate in reactions that produce ROS (Pena et al. 1999).

The toxic effects of copper are believed to be mainly due to its participation in Fenton-type reactions that include redox cycling of copper and univalent reduction of molecular oxygen to superoxide, leading to a variety of other ROS (Stohs and Bagchi 1995). Redox cycling activity is typically associated with free or loosely bound copper (Jiang et al. 2002). Copper may also manifest its toxicity by displacing other metal cofactors, for example replacement of Zn^{II} by Cu^{II} in a zinc finger binding domain. In the normal state, as described in Section 1.4.1, binding of copper by copper chaperones ensures negligibly low levels of free copper and thus prevents its redox-cycling activity. Intracellular concentrations of these copper chaperones are extremely low and may prove insufficient when cells are exposed to high levels of copper.

The thiol rich protein, MT is thought to be essential for intracellular regulation in the face of high copper concentrations, this is due to its high cysteine content which allows the protein to bind heavy metals such as zinc and copper (Ye et al. 2003). GSH is an intracellular copper chelator that is also though to play an important role in copper detoxification (Hanna and Mason 1992). Binding of copper by GSH has been shown to inhibit free radical formation of copper and H_2O_2 (Hanna and Mason 1992). It is likely that both MT and GSH are involved in protecting cells against toxic copper concentrations, particularly when challenged with a relatively high concentration of the metal (Jiang et al. 2002). Jiang *et al.,* (Jiang et al. 2002) investigated the contribution of MT and GSH to copper detoxification in mouse lung fibroblasts by utilizing cells from an MT knockout mouse line (MT -/-). They found that treatment of both MT (-/-) and its wild type counterpart, MT (+/+), cells with a GSH inhibitor resulted in an increased sensitivity of MT (-/-) cells to copper when compared to the wild type cells (Jiang et al. 2002). This result led the authors to speculate that MT and GSH may be involved in synergistic interactions and may indeed act together to maximize their protective regulatory function (Jiang et al. 2002). This provides an interesting link between accumulation of copper in diseases, such as diabetes, with increased ROS and its subsequent molecular effects. Other evidence for a link between copper and oxidative stress comes from Kang *et al.,* (Kang et al. 2001) who looked at the effect of superoxide damage on ceruloplasmin (Kang et al. 2001). During exposure to oxidative stress they found that substantial ceruloplasmin inactivation

occurred leading to the release of free copper ions. This led to speculation that ceruloplasmin may cause augmentation of free radical mediated damage to other macromolecules upon exposure to oxidative stress (Kang et al. 2001).

There are reports indicating that in addition to glucose binding, oxidation reactions catalysed by trace amounts of metal ions may also play an important role in the formation of AGEs (Sajithlal et al. 1999). Early studies by Wolff *et al.,* (Wolff and Dean 1987), found that glucose undergoes autoxidation in the presence of trace amounts of metal ions, resulting in the formation of reactive dicarbonyls and free radicals. Compared to glucose, dicarbonyls are highly reactive and formation leads to extensive modifications of various proteins (Wolff and Dean 1987). Sajithlal *et al.,* (Sajithlal et al. 1999) observed an increase in the binding of glucose to collagen in the presence of metal ions; indicating that they accelerate the glycation rate. Catalysis of collagen cross-linking by metal-ions can be explained by the increase in dicarbonyl formation. The authors concluded that metal-ions catalyse both covalent binding of glucose to collagen and glycoxidation (oxidation of glycated collagen) (Sajithlal et al. 1999).

1.4.3 Defective copper metabolism in diabetes

The biology of copper has previously been evaluated in the context of both diabetes (Wolff et al. 1991; Zargar et al. 1998; Eaton and Qian 2002; Cooper et al. 2004; Cooper et al. 2005) and in the development of cardiomyopathy (Paynter et al. 1979; Prohaska and Heller 1982; Kopp et al. 1983; Medeiros et al. 1991). Outlined below is a summary of this work.

Aguilar *et al.,* (Aguilar et al. 1998) examined copper and zinc levels as well as the ratio of the two in tissues targeted by insulin (liver, adipose tissue and skeletal muscle) of STZ-induced diabetic and normoglycemic growing Wistar rats. Results from this study demonstrated that induction of diabetes with STZ causes a decrease of total zinc levels in liver and adipose tissue and an increase in skeletal muscle zinc levels to two times the control value (Aguilar et al. 1998). The opposite was found to be true with copper. Tissue copper content was significantly affected by the duration of diabetes and was increased in the liver (Aguilar et al. 1998). Cooper *et al.,* (Cooper et al. 2004) demonstrated that Cu^{II} plays a role in the systolic deterioration of the heart that results from STZ-induced diabetes. These authors also showed that perfusion of diabetic and normal rat hearts with a copper-chelator results in a significantly greater total copper output from the diabetic animals compared to the normal animals, leading to the conclusion that an accessible copper pool accumulates in the hearts of STZ-diabetic rats (Cooper et al. 2004).

Copper absorption by diabetic rats was assessed by Uriu-Adams *et al.,* (Uriu-Adams et al. 2005), who reported the distribution of ^{67}Cu following bolus delivery in diabetic animals after five weeks on normal or low-copper diets. When on a normal copper

diet, diabetic animals showed an increase in urinary excretion of ^{67}Cu as expected; interestingly diabetic animals on a low-copper diet were also found to have increased copper excretion (Uriu-Adams et al. 2005). This result indicates that the adaptive mechanism for copper homeostasis in diabetic animals is impaired. Diabetic animals were unable to increase copper absorption and decrease copper excretion when faced with copper deficient dietary conditions. These animals also had consistently higher levels of ceruloplasmin activity even when fed a low copper diet and thus the authors hypothesised that there may be a perturbation in copper trafficking in diabetes (Uriu-Adams et al. 2005).

Patients with type-2 diabetes showed increased urinary copper output when compared to healthy controls (Cooper et al. 2004; Cooper et al. 2005). This result is in accordance with Zargar *et al.,* who reported increases in plasma copper levels in type-1 diabetic patients compared to non-diabetic subjects (Zargar et al. 1998). Together this data suggests alterations in both circulating and tissue transition metal homeostasis in the face of hyperglycemia.

1.4.4 Copper and the development of cardiomyopathy

Defective copper metabolism is implicated in the impairment of cardiac function in at least two known settings. The first arises as a result of copper deficiency. Animals receiving diets deficient in copper display cardiac hypertrophy, reduced systolic pressure development (Prohaska and Heller 1982), decreases in cellular ATP and phosphocreatine, and elevated ribose 5-phosphate and phosphocholine levels (Kopp et al. 1983). The cardiac hypertrophy in copper deficient animals is believed to be the result of increased mitochondrial volume (Medeiros et al. 1991) and transmission electron microscopic examination of cardiac tissue has revealed extensive disruption of mitochondrial fine structure (Kopp et al. 1983). Studies have also indicated depressed ceruloplasmin activity, reduced cardiac tissue levels of norepinephrine (Prohaska and Heller 1982) and Cu-Zn SOD (Paynter et al. 1979) as a result of a copper deficient diet.

The second area in which defective copper metabolism is implicated in the impairment of cardiac function is as a result of a mutation in the copper chaperone synthesis of cytochrome oxidase 2 (SCO2). Human infants with fatal cardioencephalomyopathy were found to have severe cardiac hypertrophy and reduced COX activity in both the heart and skeletal muscle (Papadopoulou et al. 1999). Using a candidate gene approach, mutations in SCO2 were identified as the source of the pathogenesis (Papadopoulou et al. 1999). Retroviral transfer of the SCO2 coding sequence into patient myoblasts led to a restoration of cytochrome oxidase (COX) function thus confirming that mutations in SCO2 were indeed the cause of the cardiac hypertrophy (Jaksch et al. 2001). The authors were also able to confirm the copper binding abilities of SCO2 through mutation analysis, suggesting that SCO2 functions as a

copper chaperone (Jaksch et al. 2001). Further evidence for a role of SCO2 as a copper chaperone was obtained by generating the identified human mutations of SCO2 in the yeast homologue Sco1p. Results of this study led authors to hypothesise that Sco1p (the yeast homologue) provides copper to the Cu_A site in COX subunit II at a step occurring late in the assembly of COX (Dickinson et al. 2000).

Taken together, these studies provide strong evidence for a role of copper in normal heart and mitochondrial function and suggest that the perturbation in copper homeostasis, such as that seen in the diabetic state, may lead to impaired mitochondrial function and thus reduced cardiac function and cardiomyopathy.

1.5 Thesis Objectives

From the work presented above it is clear that extensive study has been conducted in order to understand the underlying causative mechanism of DCM. It is also evident that there are limited therapeutic strategies to combat this potentially fatal diabetic complication. Despite comprehensive analysis, it is still not known how increases in blood glucose and changes in fuel metabolism of the heart lead to fibrosis, hypertrophy, increased ROS and mitochondrial dysfunction.

Abnormal copper metabolism in diabetes has been proposed by Cooper *et al.,* to form part of the pathway that leads to complications such as DCM (Cooper et al. 2004). Studies performed by this group have shown that treatment with the copper chelator, TETA, administered as either the dihydrochloride or the disuccinate salt forms, ameliorates the effects of diabetes on the heart at both the functional and molecular level (Cooper et al. 2004; Gong et al. 2006; Jullig et al. 2007). In the current study, a series of experiments were designed in order to generate a more complete understanding of the effects of TETA–treatment on the heart at the molecular and compositional level.

The objectives of this thesis were:

1. To characterise changes in gene expression of the LV wall of the heart after sixteen weeks of diabetes using a global microarray based approach.
2. To describe changes in gene expression of the LV wall of the heart after eight weeks of diabetes and eight subsequent weeks of treatment with the copper (Cu^{II}) chelator TETA-disuccinate, using a global microarray-based approach.
3. To use molecular techniques and biochemical assays to further elucidate the mechanism underpinning improved cardiac function occurring in the LV of the heart as a result of treatment with TETA-disuccinate.
4. To further our understanding of the metabolism of TETA-disuccinate by diabetic and sham animals, following on from the evidence presented by Lu *et al.,* which

suggested that there may be increased TETA metabolism in type-2 diabetic patients (Lu et al. 2007).

1.6 Experimental Approach

The following section explores the background of the two main experimental protocols used to address the thesis objectives outlined (Section 1.5). The first is the animal model used in order to reproduce the DCM observed in humans. For our studies, a STZ-treated diabetic rat model was chosen as this model has previously been used extensively to study DCM (Fein et al. 1980; Penpargkul et al. 1980; Litwin et al. 1990; Rodrigues and McNeill 1999; Cooper et al. 2004). The second is the technology employed to effectively measure changes in gene expression in cardiac tissue between different animals. In this instance a global microarray strategy has been employed.

1.6.1 Streptozotocin-induced diabetic animal model

It is difficult to find a single animal model that mimics all aspects of a particular disease. There are many diabetic models to choose from and some of the more common include the non-obese diabetic (NOD) mouse; the db/db mouse; the ob/ob mouse; the STZ-induced diabetic rodent; the alloxan-induced diabetic rodent; and the Zucker diabetic fatty (ZDF) rodent. Since there are numerous models, it is important to carefully consider their advantages and limitations in order to choose the optimal one which meets our specific experimental objectives.

The diabetogenic activity of [2-deoxy-2-(3-methyl-3-nitrosourea)1-D-glucopyranose] or STZ was first described by Rakieten *et al.,* who reported frank diabetes in dogs and rats after intravenous STZ administration (Rakieten et al. 1963). The diabetogenic action of STZ on the pancreatic β-cells from the islets of Langerhans was later confirmed using histological techniques and electron microscopy (Junod et al. 1967). STZ is taken up into the β-cells by the GLUT2 low-affinity glucose transporters, due to the glucose moiety in its chemical structure ((Schnedl et al. 1994; Elsner et al. 2000) Figure 1.3).
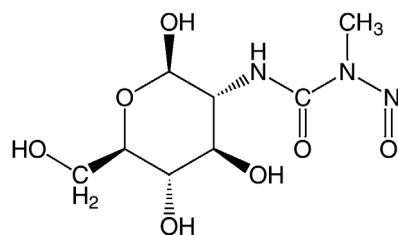
Figure 1.3 Chemical structure of streptozotocin (STZ)

STZ is a $_D$ –glucopyranose derivative of *N*-methyl-*N*-nitrosourea (Elsner et al. 2000).

The intracellular action of STZ that leads to the destruction of β-cells is now thought to be due to alkylation (Bennett and Pegg 1981) and subsequent fragmentation of DNA (Yamamoto et al. 1981), leading to activation of poly (ADP-ribose) polymerase and a reduction in cellular NAD+ and ATP content (Yamamoto et al. 1981). Separate studies have determined that it is the *N*-methyl-*N*-nitrosourea moiety that causes DNA alkylation, while the glucose moiety is required for uptake into the cell and leads to increased toxicity of the compound when compared to *N*-methyl-*N*-nitrosourea alone (Elsner et al. 2000).

In our studies a dose of between 55-60mg/kg of STZ was used to induce diabetes. Previous work has shown that at these doses, animals do not develop ketosis (Junod et al. 1969), which can be explained by incomplete though marked insulin depletion in animals receiving doses of STZ between 45mg/kg and 65mg/kg (Junod et al. 1969). Measurement of serum immunoreactive insulin after STZ injection at doses between 45mg/kg and 65mg/kg showed that levels persisted at a concentration of around 20µU/ml (Junod et al. 1969), which is similar to the levels observed in fasted animals. This residual amount of endogenous insulin allows animals to survive and means that studies can be conducted without peripheral insulin treatment which may introduce confounding variables into results.

The diabetogenic activity of STZ resembles that of alloxan, which was previously in common use for the same purpose. STZ, however, was found to differ from alloxan in several important ways which include a much greater selectivity of action on β-cells, independence from nutritional state of the animal and a broader dose range allowing for induction of mild to severe diabetic states (Junod et al. 1969).

The STZ model has also been found to reliably produce many of the symptoms of chronic human diabetes, particularly diastolic cardiac dysfunction (Wei et al. 2003) (For a review see Tomlinson *et al.,* (Tomlinson et al. 1992)). It may be suggested that given the prevalence of Type-2 diabetes in the human population when compared to that of Type-1 diabetes it may be more relevant to use a Type-2 diabteic model such as the ZDF rat or

obesity-induced insulin resistant model. Type-2 diabetic models however introduce a number of confounding factors resulting from their obsese state such as hypertension and hyperinsulinemia and it is difficult to reliably induce high blood glucose levels (for a review see (Srinivasan and Ramarao 2007)). In this experimental design an important feature of the STZ-diabetic model is that the animals remain normotensive and do not develop atherosclerosis. This allows for the characterisation of the hyper-glycemia induced changes occurring in the heart independently of the development of atheroclerosis and hypertension (Wei et al. 2003). As described in Section 1.1.1, one of the main characteristics of human DCM is that patients show evidence of myocardial dysfunction in the absence of CAD.

Therefore, the features of the STZ-diabetic model make it appropriate for studies, such as that proposed here, which aim to determine changes in the heart as a result of hyperglycaemia without the introduction of confounding factors such as hypertension. Additionally, this model is convenient for use in long term studies, such as those conducted in our lab, without the need for peripheral insulin administration.

1.6.2 Microarrays

Microarray technology has grown in application and sensitivity since it was first described in a study that utilised 45 cDNAs to look at differences in gene expression between root and leaf mRNA of *Arabidopsis thaliana* plants (Schena et al. 1995). As is evident from the experiments outlined in Sections 1.1-1.2, a plethora of molecular changes have been reported to occur in the heart as a result of hyperglycaemia. The advantage of microarray technology over other more conventional methods such as real time quantitative polymerase chain reaction (RT-qPCR) is its ability to probe the expression of thousands of genes simultaneously. Below is a description of the construction of and general experimental protocol for different microarray platforms and the subsequent handling of data for analysis and publication.

1.6.2.1 Fabrication of microarrays

Currently, microarrays are fabricated using two main techniques. The first of these utilizes purified pre-synthesised cDNA or oligonucleotide probes, which are then spotted onto a solid support, and the second is *in situ* synthesis of the probe directly onto the solid support. The most common support used in microarray synthesis is glass, as it is durable enough to withstand exposure to elevated temperatures and high-ionic-strength solutions (Xiang and Brownstein 2003). Glass surfaces can also be chemically modified to allow covalent attachment of the desired probe. Spotting of purified probe solutions or *in situ*

synthesis is carried out using robot technology (Fodor et al. 1991; Blanchard et al. 1996; Xiang and Brownstein 2003).

In situ oligonucleotide synthesis is the process by which oligonucleotide probes are assembled base-by-base on the surface of the array. This takes place by covalent reaction between the 5' hydroxyl group of the sugar of the last nucleotide to be attached and the phosphate group of the next nucleotide. Each nucleotide added to the oligonucleotide on the glass has a protective group on its 5' position to prevent the addition of more than one base during each round of synthesis. The protective group is converted to a hydroxyl group either with acid or light activation before the next round of synthesis, in a process known as de-protection (Fodor et al. 1991; Blanchard et al. 1996).

This method of array fabrication has led to the development and commercialisation of two very different microarray platforms. The first is from Agilent Technologies who have developed a chemical de-protection-based array manufacturing method that utilises inkjet printing technology (Blanchard et al. 1996). In this protocol, surface tension wells are created on the solid support through chemical modification that creates hydrophobic and hydrophilic areas. This allows the confinement of individual reagent droplets (~100pl) to an area of 100microns^2 with a space of 30microns between each well. The wells act as mini reaction vessels for the oligonucleotide synthesis (Blanchard et al. 1996). Delivery of small amounts of the synthesis reagents to the appropriate wells is achieved through micro-fabricated inkjet pumps. There are essentially four pumps, one for each nucleotide (Blanchard et al. 1996). Once the appropriate reagent is applied to each of the wells the entire slide is immersed in a chemical solution that removes the protective linker attached to each nucleotide, following this, the delivery process is repeated from the beginning. The advantage of this method is that the creation and synthesis of oligonucleotide probes is very flexible and can be easily changed, allowing new probes to be synthesised rapidly (Blanchard et al. 1996). The disadvantage of this method is that it requires space between each of the wells, which limits the number of probes that can be added to each array.

The second platform is from Affymetrix technologies, which developed a photolithographic de-protection based manufacturing method (Fodor et al. 1991). Light is directed to appropriate areas via the use of a mask that allow it to pass to some areas of the array but not others therefore creating a pattern of de-protected and protected areas. A solution containing one nucleotide is then washed over the solid support; and this nucleotide can only bind to those areas that have been de-protected. This process is repeated until an oligonucleotide of desired length is created (Fodor et al. 1991). The advantage of this method is that once a mask set has been designed and made, it is straightforward to mass produce a large number of identical arrays (Fodor et al. 1991). Additionally, the photolithographic process does not require spaces between each probe allowing the creation of much higher density arrays. However the disadvantage of this

method is that each step of the synthesis requires a different mask. The creation of new masks or new sets of masks is a complicated process. This reduces the flexibility of this platform as it becomes time-consuming to change the oligonucleotide sequence of the arrays.

1.6.2.2 Microarray general experimental outline

Once the microarray platform is constructed, RNA from the biological samples of interest is extracted, labelled and hybridised to the array. The schematic (Figure 1.4) provides a simplified overview of the processes involved in a generalised microarray experiment.
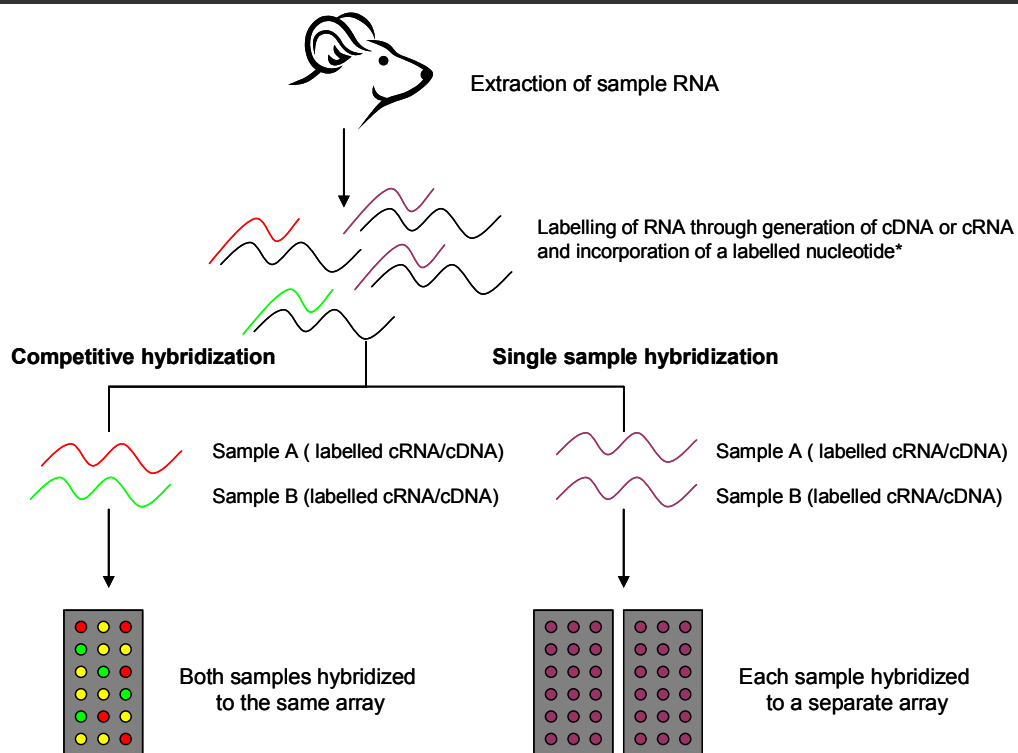
Figure 1.4 Schematic of a general microarray experiment

This schematic presents the two main kinds of microarray experiment.
*The labelled nucleotide within the cDNA or cRNA can then be coupled to a modified fluorescent dye pre-hybridisation (t Hoen et al. 2003)

Quantification of gene expression levels is achieved through fluorescent labelling of the RNA. A range of methods have been developed for labelling of RNA in microarray experiments, however the most efficient and consistent involves incorporation, into the extracted RNA, of an 5-(3-aminoallyl) dUTP (aa-UTP) that is subsequently coupled to fluorescent dies modified with *N*-hydroxysuccinamide (Richter et al. 2002; Yu, J. et al. 2002; t Hoen et al. 2003). There are two common methods for hybridisation of the

modified RNA to the microarray slide. The first is known as competitive hybridisation and involves the labelling of different samples of interest with a different fluorescent label and the subsequent hybridisation of both samples to the array. The second is a single sample hybridisation protocol that involves labelling samples with a single fluorescent label and hybridising each sample to a separate array (Figure 1.4). Post-hybridisation, the microarray slides are washed and scanned, and the data is then collected and can be analysed using a variety of statistical techniques.

A further, more comprehensive analysis of microarray experimental methodologies is conducted as part of Chapter Three of this thesis.

1.6.2.3 Minimum Information About a Microarray Experiment (MIAME)

The rapid increase in the number of both in-house and commercially-available microarray systems and the resulting non-standardised data resulting from these studies, has led to the development of MIAME standards. The goal of MIAME is to outline the *minimum* information required to unambiguously interpret and potentially reproduce and verify an array based gene expression experiment. Although particular details for each experiment may be different, MIAME aims to define the common elements of most experiments (Brazma et al. 2001). MIAME has two major sections (1) array design description and (2) gene expression experiment description. Each of these is described below and can be found at http://www.mged.org.

The first section, array design specification, consists of the description of the common features of the array as a whole (e.g., platform type: *in situ* synthesized or spotted, solid support surface coating, number of genes on the array and production protocol), and the description of each of the array design elements (e.g., the type of reporter: synthetic oligonucleotides or PCR products, reporter sequence information, sequence length, and control elements on the array).

The second section, Gene expression experiment, is defined as a set of one or more hybridizations that are in some way related (e.g., related to the same publication). The minimum information required is described in the following four parts.

1. Experimental design – this section relates to information common to all hybridizations performed in each experiment e.g., personnel, type of experiment: normal vs. diseased or treated vs. untreated, quality control steps taken, number of hybridizations performed per experiment, and experimental goal.

2. Samples used, extract preparation and labelling – The term samples refers to the biological material from which the RNA has been extracted. A detailed description of the sample is required, including: type of organism and descriptors such as sex,

age, tissue, cell type, disease state. Also included in this section is information pertaining to the manipulation of the sample such as growth conditions, *in vivo* or *in vitro* treatments and treatment type (e.g., small molecule, heat shock, food deprivation). Extract preparation refers to the extraction method, description of the type of RNA (total RNA or mRNA) used and the labelling protocol such as, amount of RNA labelled, the label used (e.g. Cy3-CTP) and the label incorporation method. Any external controls (such as the use of a spike in control samples) also need to be described.

3. Hybridization procedures and parameters – Each hybridization description should include: information about which labelled extract and type of array has been used and the hybridization protocol employed. This is particularly important for non-commercial arrays which tend to vary widely in both hybridisation reagents and protocols.

4. Measurement data and specifications of data processing – The authors of MIAME distinguish between three levels of data processing, each of which is required for completeness. The first is the raw data or original scanned image and should include scanning information; the second is a microarray quantification matrix or the image analysis output as directly generated by the image analysis software (i.e. the numbers generated from the raw image); and the third is the gene expression data for each sample. This data is likely to have been normalized, consolidated and transformed in any one of a number of ways depending on the statistical protocol utilized. An outline of these data manipulations is crucial to allow complete interpretation of the data presented.

1.7 Summary

In summary, DCM is a rapidly growing health issue globally. Despite many years of investigation into the disorder, the exact molecular mechanism is still unclear. What is known however, is that DCM arises from and results in complex molecular changes within the heart and as a result, no one treatment is yet available that fully reverses all the effects of hyperglycemia on the heart. Evidence from work in this laboratory indicates that treatment with a selective copper (Cu^{II}) chelator can restore heart function in both diabetic rats and humans (Cooper et al. 2004). In order to more completely understand the molecular changes occurring at a global level within the heart and to further characterise the mechanism of action of the Cu^{II} chelator TETA, the STZ-diabetic rat model and microarray technology have been employed in the current study.

Chapter 2 Materials and Methods

2.1. Animal model

All protocols were approved by The University of Auckland Animal Ethics Committee.
Male Wistar rats (weight range 220-250g) were obtained from University of Auckland,
School of Biological Sciences. They were maintained on Teklad TB 2018 (Harlan, UK) rat
chow and tap water *ad libitum* and randomised into two groups, 'diabetic' or 'sham', prior
to injection. Animals were anesthetised using 5% halothane, 2l/min O_2, then either
60mg.kg $^{-1}$ (Study One) or 55mg/kg (Study Two) of STZ (Fluka, 85882, Lot number:
4347341/1 13503602), which was injected into the tail vein to induce insulin-deficient
diabetes. Control rats (sham) received the corresponding volume of saline. Study one had
n = 7 (diabetic and sham groups) while Study 2 had n=5 animals per drug dose in the
sham group (total = 25) and n = 9 animals per drug dose in the diabetic group (total n =
45). Animals were recovered and housed in pairs on fibre-cycle bedding (12hr light:dark
cycle, 50-70 % humidity, 19-21 °C). Blood glucose levels (Advantage II system (Roche
Diagnostics, Basel, Switzerland) and bodyweights were measured at the time of injection
and three days thereafter to confirm the presence of diabetes; then both variables were
thereafter monitored weekly throughout. Diabetes was diagnosed as blood glucose of >
11mM on two successive occasions.

2.1.1 Administration of Triethylenetetramine (TETA)

All animals were maintained on milliQ water for this study from the time of injection.
Administration of TETA-disuccinate (TETA-disuccinate, CarboGen, Switzerland, NE-
014851-Batch-03-05, ≥ 99.8% purity) was restricted to animals in the second study. It was
administered through the drinking water over a range of doses, 3.5, 17.5, 35, and 87.5mg
per day, regardless of weight or glucose level. Drug treatment began eight weeks after
STZ injection, and continued for eight further weeks until organ collection. Outlined in
Table 2.1 below is the block design used to assign groups to a drug dose.

Table 2.1 Block design

Cage	Assigned Group
1	No Drug
2	3.5mg TETA-disuccinate
3	17.5mg TETA-disuccinate
4	35mg TETA-disuccinate
5	87.5mg TETA-disuccinate
6	No drug
7	3.5mg TETA-disuccinate
8	17.5mg TETA-disuccinate
$Cage_N$	$Group_{ND\ or\ Dose\ 1-4}$

Due to concerns about the stability of the compound in water, a TETA-disuccinate stock solution (3.5mg/ml of TETA-disuccinate in milliQ water) was made freshly each day of administration. TETA-disuccinate was fully replaced on the cage every 2 days for both STZ and sham animals. Average water intake per day was calculated each week. Stock was diluted to the appropriate level to give the required dose per day per animal using the water intake of the previous week as a guide in calculation.

2.1.2 Metabolic cage 24hr urine collection

Animals were housed in specifically designed metabolic cages for a period of 24hr. During that time, urine was collected while water intake, food intake and water bottle drips were measured in pre- and post-24hr periods to give an accurate account of fluid/food intake compared to urine excretion.

Animals were housed one per metabolic cage for the duration of the 24hr period. All collections began before 9am and stopped 24hr later. Due to the large volume of urine excreted by the diabetic animals, a container change was required at the 12hr mark. Urine was stored at 4°C until the next day and combined to give the total urine volume. All collected urine was centrifuged (4000rpm for 15min), the supernatant aliquoted and stored at -30°C until analysis.

2.2 Isolation of RNA from the left ventricle of a rat heart

2.2.1 Tissue collection

2.2.1.1 Surgical procedure (Studies One and Two)

Animals were placed in an anaesthetic induction box (either isofluorane or halothane 5%, O_2 2l/min). Once anaesthetised, rats were weighed then maintained on either isofluorane or halothane (2-3%, O_2 2l/min) via a nose cone. Complete anaesthesia was confirmed by

testing pedal withdrawal (reflex absent). A midline laparotomy was performed and 3ml of blood taken from the vena cava via a 22 gauge cannula (BD, Insyte). Heparin (200 I.U.kg^{-1}, DBL® Mayne Pharma Pty Ltd, VIC, Australia) was injected through the cannula and allowed to circulate for 2min.

2.2.1.1.1 Study One

After 2min, animals were killed by cervical dislocation. Rats were then taken from the surgery room to a laminar flow hood using a metal tray which was clean but not sterile.

2.2.1.1.2 Study Two

It was decided that for this study, the Laminar flow hood was not necessary for RNA preparation. After 2min, animals were killed via a thoracotomy. All subsequent work was carried out on the bench next to the fume hood.

2.2.1.2 Perfusion and removal of left ventricle

In order to ensure an RNase enzyme-free environment, all surgical equipment was soaked overnight in 0.5% SDS treated with DEPC and then soaked in chloroform (10min) before autoclaving prior to surgery. This included: scissors, forceps, chest spreaders, and cannula stainless steel tubing.

RNase-free microfuge tubes (Ambion, Austin TX) were used for tissue storage and subsequent RNA extraction. Sample tubes were soaked in 0.5M NaOH overnight, rinsed three times with DEPC water and then autoclaved. All surfaces and equipment were wiped clean, first with 70% ethanol and then with RNA*Zap* (Ambion, Austin TX) and rinsed with DEPC water prior to any surgery.

Table 2.2 Solutions for cleaning of equipment and surfaces, heart perfusion

Solution*	Composition
DEPC water	1ml DEPC (Applichem, Darmstadt, Germany) in 1l water
0.5% SDS in DEPC water	5g SDS in 1l DEPC water
0.5M NaOH in DEPC water	20g NaOH in 1l DEPC water
1x PBS in DEPC water	10x PBS diluted 1:10 in DEPC water

*All solutions were autoclaved.

Hearts were excised either in the laminar flow hood (Study One) or in the fume hood used for surgery (Study Two), using the procedure as defined by Dr B. Choong in his functional heart studies (personal communication). The chest was cut open and any connective tissue was cut from the heart, which was handled using sterile blunt-nosed forceps to minimise tissue damage. Incisions were made underneath the heart to free it from the chest and the aorta was then cut a short way up (below the aortic arch) to finally remove the heart. The heart was then immersed in 1x PBS (100mM NaCl, 50mM NaPO$_4$, pH7.45, treated with DEPC) at 4°C to prevent it from further spontaneous contractions.

The aortic remnant was then ligated to a metal cannula to allow perfusion using a GENIE 220 infusion pump (Kent Scientific) with 1 x DEPC-treated PBS at 4°C. Volumes used were: 40ml (diabetic) or 60ml (sham) for Study One or 60ml for all groups in Study Two. Perfusions were performed at a rate of 15ml.min^{-1}. Once perfusion was complete, the left ventricle was excised on a piece of sterile glass and tissue cut into 2 smaller pieces (new scalpel per animal) and placed in separate tubes containing 1ml RNA*later* (Qiagen). Tissue was kept at 4°C overnight before storage at -80°C.

Three layers of gloves were worn at all times and changed after each major step (removal of heart and kidney, processing of kidney and processing of heart) to minimise contamination from RNase enzymes. The remaining heart tissue was then processed and stored for subsequent study.

- Histology: A piece of tissue from the apex of each heart was embedded in Tissue-Tek optimum cutting temperature (OCT) compound (Bayer Diagnostics) and snap-frozen in isopentane cooled by liquid N$_2$. OCT blocks were stored at -80°C until sectioning.
- EM: A small cross sectional piece of tissue was immersed in 1ml of 2% glutaraldehyde in 0.1M Sorenson's phosphate buffer, and stored either at 4°C (Study One) or at -80°C (Study Two)
- Protein: Tissue was snap frozen in liquid N$_2$ (Study One only)

2.2.2 RNA Isolation

2.2.2.1 RNA isolation from tissue using Qiagen MIDI Kit protocol.

Isolation was performed as per the manufacturer's instructions. Briefly, RNA*later*-stabilized tissue was thawed and cut into smaller pieces on an RNase-free surface. Tissue was homogenised using an Ultra Turrax T8 disperser with a S8N-5G tip (IKA$^®$ Works, Inc., Staufen, Germany) in 2ml of buffer RLT (lysis buffer) until no tissue remnants were visible. Four ml of water and 65μL of Proteinase K (19131 Qiagen, >600mAU/ml) were then added and incubated at 55°C for 20min. Samples were centrifuged at 5000 x g for 5min and supernatants pipetted into new RNase-free 15ml falcon tubes. 0.5 v/v of ethanol was added to the cleared lysate and 3ml then loaded onto a MIDI column. Column + sample were centrifuged (5min at 5000 x g) repeatedly until all of the ethanol/lysate mixture had been used. Columns were washed in a series of steps using buffer RW1 (x 1) and buffer RPE (x 2, with ethanol added) both of which were provided in the kit. To elute, each column was transferred to a new RNase-free 15ml falcon tube and 50μl of RNase-free water was gently pipetted onto the top of the silica-gel membrane. Tubes were let to stand for 1min and then centrifuged for 3min at 5000 x g.

Sample quality was assessed using the Agilent Bioanalyzer (see below) and quantity using a NanoDrop® apparatus.

2.2.2.2 RNA isolation from tissue using a combined TRIZOL/Qiagen MINI method (Study Two)

In Study One, RNA yield was found to be consistently low, particularly from the diabetic samples. This was thought to be due to poor homogenisation in the buffer RLT (due to the collagenous nature of heart tissue). A new method obtained from the Affymetrix Microarray Facility (Centre for Genomics and Proteomics, School of Biological Sciences) using a combination of the Trizol (Sigma) and Qiagen Mini methods was used for Study Two to try and increase the efficiency of homogenisation and therefore increase RNA yield.

Protocol: Sample tissue weight was used to calculate the amount of Trizol required to obtain a ratio of 750µl Trizol:30mg tissue. Samples in RNA*later* were thawed and the appropriate volume of Trizol added to each sample. They were then homogenized (PRO 200 Micro-Homogenizer, RO Scientific Inc., Oxford, CT) until no tissue remnants were visible. Samples were incubated at RT for 5min, aliquoted into 750µl volumes and stored at -80°C until required. At the time of analysis, the Trizol samples were thawed and 150µl of chloroform was added. Samples were vortex-mixed for 15s and then incubated at RT for 3min before a 13200rpm spin (5min).

The aqueous phase was transferred to a fresh RNase-free tube and an equal volume of 70% ethanol (DEPC treated) added. Samples were loaded onto a Qiagen RNeasy column (maximum volume 700µl) and centrifuged (15s at 8000 x g). This step was repeated until all the mixture was used. The column was then washed in a series of steps using buffer RW1 (x 1) and buffer RPE (x 2, with ethanol added). Columns were then spun for 1min with the lids open to remove any excess ethanol which would otherwise have interfered with RNA elution.

RNA was finally eluted using 15µl RNase-free water (at 8,000 x g). A second elution was performed into a fresh RNase-free tube using 45µl RNase free water. A 1:10 dilution was performed prior to RNA quality/quantity analysis.

2.2.2.3 Assessment of RNA Quality/Quantity.

Before beginning the necessary labelling experiments, RNA quality and quantity were ascertained.

Quantity was determined using the NanoDrop® ND-1000 UV-Vis Spectrophotometer (NanoDrop Technologies, Rockland DE, USA). 1μl was placed in the NanoDrop and a print-out of concentration as well as purity was supplied.

Quality was determined for later samples using the Agilent Bioanalyzer. 1μl of sample is used in this protocol. The Bioanalyzer provides a good estimation of the quality of a sample whereas the NanoDrop provides a good estimation of the quantity. It is important that more than one method is used for complete accuracy.

2.2.2.3.1 RNA 6000 Nano assay protocol (Agilent Reagent Kit Guide, April 2003).

Analysis of RNA quality using the Agilent bioanalyser was conducted as per manufacturer's instructions.

Briefly, 9μl of the gel-dye mix pipetted into the well marked 🅖 of a RNA Nano LabChip. The plunger was set at 1ml, and the Chip Priming Station then closed. The plunger was depressed until held by the syringe clip, after which it was left for exactly 30s and then released. 9μl of the remaining gel-dye mix was pipetted into in each of the wells marked **G**

Five μl of the RNA 6000 Nano Marker was then pipetted into all other wells present on the chip and 1μl of each sample and the ladder loaded. Chips were then vortex mixed for 1min at 2400rpm. Runs were started within 5min.

2.3 Microarray Analysis

2.3.1 RNA

All RNA used in the cross-comparison study was isolated from rat LV tissue (8 sham and 8 diabetic) was kindly provided by Dr. Bernard Choong. RNA was isolated using the RNA isolation protocol outlined above in Section 2.3.2.1. RNA was pooled to increase the concentration for this section of work only.

All other RNA was isolated from rat LV tissue collected from either Study One using the RNA isolation protocol outlined in Section 2.3.2.1 or Study Two using the RNA isolation protocol outlined in Section 2.3.2.2. This RNA was not pooled.

2.3.2 Ramaciotti Rat 10K Combo Slides

This work was carried out by the Centre for Genomics and Proteomics technician Liam Willams. Slides were obtained from the Clive & Vera Ramaciotti Centre for Gene Function Analysis (School of Biotechnology & Biomolecular Sciences, University of NSW, Sydney).

Slides were epoxy-coated Eppendorf Creative Oligo glass slides. Each one contained 10,000 amino-modified 50-60mer oligonucleotides sourced from MWG-Biotech and Compugen and each spot on the slide was duplicated. Each slide had been printed with oligonucleotides containing an amino linker that had been baked for 30min at 60°C, thus permanently bonding them to the slide.

2.3.2.1 cDNA synthesis and labelling.

Prior to labelling, a precipitation and concentration step was required in order to reduce the RNA sample volume. This was performed using a sodium acetate/ethanol precipitation and sample was resuspended in 9.5µl of RNase-free water.

Oligo-dT primers were added to RNA samples in order to specifically target mRNA and allow cDNA to be formed using reverse transcription. During formation of cDNA, an amino-allyl modified dUTP was incorporated to allow labelling of cDNA post-synthesis reaction (as per manufactures protocol, GE Healthcare UK Ltd, Buckinghamshire England). All reagents were supplied in the CyScribe post-labelling kit from Amersham Biosciences (GE Healthcare UK Ltd, Buckinghamshire England).

Messenger RNA was degraded away from the newly synthesised amino allyl-labelled cDNA using sodium hydroxide and the reaction was neutralized with HEPES. Complementary DNA was then purified using a Microcon YM-30 columns (Millipore, MA, USA).

Samples were then labelled using CyDye Cy3-NHS ester or Cy5-NHS ester (GE Healthcare UK Ltd, Buckinghamshire England) which bind to the amino-allyl labelled dUTP incorporated into the cDNA. CyDye is extremely light sensitive, so once dye was removed from freezer/packaging and resuspended in sodium bicarbonate solution, care was taken to keep the sample away from light, particularly sunlight.

The samples were incubated in CyDye for 1hr with mixing at 15min intervals in order to allow maximum binding; excess dye was then removed and sample was again cleaned up using a Microcon YM-30 (Millipore, MA, USA).

2.3.2.2 Short blocking protocol for Eppendorf Creative – Epoxy

Blocking and hybridization of slides was performed as per the Clive and Vera Ramaciotti Centre protocol.

Using only glass containers and stainless steel racks, the slides were placed in a 0.1% SDS solution in milliQ H_2O at 95°C for 1min with constant stirring, then washed in a 5% ethanol solution (95% ethanol in milliQ H_2O) with constant stirring for 1min. Slides were washed finally for 1min in milliQ H_2O with constant stirring. Care was taken not to

allow slides to dry between steps. All washing steps were performed at room temperature with constant stirring. The arrays were then centrifuged dry at 1000rpm.

2.3.2.3 Hybridisation

Samples were made up into the hybridisation solution and placed in a 95°C water bath for denaturation.

The protocol for HybriSlip was used in this instance (Table 2.3). 50µl of hybridization buffer plus sample was placed on the microarray slide and the HybriSlip cover slip was then carefully positioned over the liquid and lowered so as to avoid all air bubbles.

Slides were then placed into a hybridisation chamber, sealed and incubated in a 55°C water bath overnight (12-15hr, manual chamber hybridization)

Table 2.3 Ramaciotti hybridisation solution for Hybrislip covers

20 x SSC (final conc. = 2.6x)	5.0µl
5% SDS (final conc. = 0.2%)	2.0µl
Liquid Block (Amersham)	3.0µl
Combined Samples + H$_2$O	40.0µl
Total	**50.0µl**

2.3.2.4 Post-hybridisation washing

Table 2.4 Ramaciotti solutions for washing of epoxy slides post-hybridisation

Solution	Composition	Washing Time
Washing buffer 1 (WB1)	2 x SSC, 0.2% SDS	10min
Washing buffer 2 (WB2)	2 x SSC	10min
Washing buffer 3 (WB3)	0.2 x SSC	3min

After hybridisation slide was removed from chamber and placed in WB1 shaking until cover slip fell off (~1min). Slide was washed with agitation in WB1 for 5min and then WB2 for 5min. Slide was washed finally in WB3 for 1min.

2.3.2.5 Scanning

Slide scanning was performed using the GenePix 4000B scanner (Axon Instruments, CA USA) and spot finding was performed using GenePix Pro 4.0 image analysis software.

2.3.3 Amersham Codelink

2.3.3.1 cRNA synthesis from total RNA

Two µg of total RNA from either the pooled diabetic or pooled normal samples was used. T7 oligo (dT) primer and total RNA were incubated for 10min at 70°C to anneal. First strand synthesis consisted of incubating primer:RNA mix with a master mix (a working solution of bacterial control mRNA, 5mM dNTP, RNase inhibitor and reverse transcriptase) for 2hr at 42°C. Second strand synthesis was achieved by incubating the first-strand mix with 5mM dNTP, DNA polymerase and RNase H for 2hr at 16°C.

The resulting cDNA was purified using a QIAquick spin column and the purified cDNA was dried in a SpeedVac Concentrator under medium heat for approximately 1hr. *In vitro* synthesis of cRNA was achieved by addition of dNTPs including a biotin-11-UTP to the dried cDNA solution and incubating it for 14hr at 37°C.

Complementary RNA was purified using a Qiagen RNeasy spin column and eluted in 50µl of nuclease-free water and either hybridised to the arrays immediately or stored at -70°C. Prior to hybridisation, cRNA concentration and quality was assessed using the NanoDrop.

2.3.3.2 Hybridisation

Ten µg of cRNA from Section 2.4.1.3.1 was fragmented using fragmentation buffer by heating to 94°C for 20min. Hybridisation buffers A and B (provided in kit) were added post-fragmentation to give a final volume of 260µl.

Hybridisaton mixture was loaded on to the CodeLink UniSet Rat 1 Bioarrays by injection through an array input port. 250µl was drawn into a 1ml wide-bore pipette tip. The tip was then placed over the array input port closest to the bioarray label and pressed until a seal was formed with the Flex Chamber. Sample was injected slowly without the use of the blowout feature of the pipettor. Once the chamber was full, Flex Chamber ports were sealed using special adhesive seals.

Slides were then loaded onto a shaker tray and placed in a shaker-incubator with the Flex chamber facing up. Shaker speed was set at 300rpm and slides were incubated for 18-24hr at 37°C.

2.3.3.3 Washing

Flex chambers were removed from glass microarray slides leaving the surface open for washing and staining. Bioarrays were washed in 0.75 x TNT (1 x TNT: 0.1M Tris-HCl pH

7.5, 0.15M NaCl, 0.05% Tween-20) for 1hr at 46°C prior to staining with streptavidin-Cy5 dye conjugate. Each slide was stained with the streptavidin-Cy5 dye conjugate for 30min at ambient temperature.

Slides were washed in 4 sequential washes of 1 x TNT for 5min each. The final washing of the slides was done in 0.05% Tween 20 for about 20s. Slide racks were then removed and centrifuged for 3min in a Qiagen-Sigma 4-15C centrifuge with 2 x 96well plate bucket rotor at 2000rpm to dry.

2.3.3.4 Scanning

Scanning was performed on both the GenePix 4000B scanner (Axon Instruments, CA USA) and the arrayWoRx™ "e" scanner from Applied Precision. This scanner utilizes a white-light illumination and CCD camera detection technology.

Data extraction, spot-finding and intensity analysis was done using CodeLink Expression Analysis v3.0 software 'batch analysis'. Only files from the arrayWoRx scanner were able to be processed using the analysis software.

2.3.4 Agilent

This work was carried out by the University of Auckland, Centre for Genomics and Proteomics technician Liam Williams and Dr. F. Pichler.

The Agilent system was the only two-colour system tested in the platform comparison study. The arrays used in this study were 22K rat oligo microarray.

2.3.4.1 cRNA synthesis from total RNA

500ng of total RNA from either the pooled diabetic or pooled normal samples was used. Primer and template RNA were denatured and incubated at 65°C before addition of cDNA master mix. This contained first strand buffer, DTT, dNTP and Moloney Murine Leukemia Virus (MMLV) reverse transcriptase. Solution was incubated at 40°C for 2hr to synthesise double stranded cDNA. For cRNA synthesis from cDNA, a transcription master mix was added to the cDNA samples. This contained transcription buffer, DTT, NTP mix, PEG, inorganic pyrophosphatase, T7 RNA polymerase and Cy3-CTP or Cy5-CTP modified nucleotides. After 2hr incubation, samples were purified using a Qiagen RNeasy column.

Sample quality was then assessed using a NanoDrop and Agilent Bioanalyser prior to hybridisation.

2.3.4.2 Hybridisation

As recommended by Agilent, 0.75ng of cRNA per sample was employed. The two cRNA samples were combined into a new tube with 10 x control targets, then fragmented for 30min and diluted with 2 x hybridisation buffer. 490µl was loaded onto the backing gasket in a SureHyb chamber. Microarrays were hybridised overnight (17hr) rotating (4rpm) at 60°C.

2.3.4.3 Washing

All wash solutions were provided as pre-mixed solutions by Agilent.

'Sandwiched' slides were removed from the SureHyb chamber, and quickly transferred into Wash 1 solution. After submerging, slides were pried apart and the gasket slide allowed to drop away. The microarray was then transferred into a rack in Wash 1 (low stringency). Slides were left in Wash 1 for 1min with medium mixing. Slides were then transferred to Wash 2 and left for 1min exactly (timing is critical), blotted quickly on blotting paper, then transferred to Wash 3 (Stabilisation and Drying solution). Wash 3 incorporates an atmospheric ozone scavenger in order to delay the degradation of the Cy-5 dye, which is susceptible to ozone concentrations of 10ppb and above.

Slides were left in Wash 3 for 30s and removal of the slide took at least 10s (constant speed). Dried slides were scanned immediately or stored in the dark under nitrogen until ready to scan

2.3.4.4 Scanning and analysis of slides

Slides were scanned using the Agilent DNA microarray scanner (G2565BA) which automatically loads 48-slides. Analysis software package used was Feature Extraction software (FE v7.1). Data was also imported into the Rosetta Luminator, a data analysis package from Rosetta Biosoftware. Data was calculated as a Log_{10} ratio.

2.3.5 Affymetrix

2.3.5.1 cDNA synthesis

Preparation of poly-A controls was performed as follows: each eukaryotic Genechip contains probe sets for *Bacillus subtilis* genes that are absent in eukaryotic samples. These are used as internal controls to ensure that the cRNA synthesis reaction was successful. The concentrated poly-A control stock was diluted with the poly-A control

buffer (supplied) and spiked directly into RNA samples. The controls are then amplified and labelled together with the samples.

A range of total RNA amounts (3µg-5µg) were used depending on the study. RNA + diluted poly-A controls were mixed with T7-oligo (dT) primer and incubated at 70°C for 10min, before addition of the first strand master mix. This contained 1 x first strand reaction mix, DTT and dNTP. Depending on the amount of total starting RNA different amounts of SuperScript II^{TM} enzyme was used (1ng-8µg requires 1µl Superscript II^{TM}; 8µg-15µg requires 2µl of Superscript II^{TM}). The samples were incubated for 1hr at 42°C to allow synthesis of the first strand cDNA.

At the end of the 1hr second strand master mix was added. This contained 5 x second strand reaction mix, dNTP, *Escherichia coli* DNA ligase, and *Escherichia coli* DNA polymerase. Samples were incubated for 2hr at 16°C. At the end of the 2hr, T4 DNA polymerase was added for 5min (to remove any remaining single stranded cDNA) and the reaction was stopped by addition of EDTA. All incubations were performed in a thermal-cycler. Samples were then purified using a cDNA cleanup column (Qiagen Inc, Valencia CA USA)

2.3.5.2 Synthesis of biotin-labelled cRNA

Affymetrix GeneChip IVT labelling kit is used for this step.

Depending on the starting RNA concentration, either the whole amount of purified cDNA (~12µl) or half (6µl) of the purified cDNA was used in this step. To the cDNA, IVT labelling NTP, enzyme mix and 10 x IVT buffer was added. Samples were incubated at 37°C for 16hr in an oven incubator for even temperature distribution. Samples were then purified using a cRNA cleanup column (Qiagen Inc, Valencia CA USA)

Biotin labelled-cRNA quality and quantity was assessed using the NanoDrop and the Agilent Bioanalyzer.

2.3.5.3 Target hybridisation

Samples were incubated in fragmentation buffer (MgOAc, KOAc) at 94°C for 35min.
Array used was the 49 format (standard) which meant that 15µg of fragmented cRNA was added.

Table 2.5 Affymetrix GeneChip® hybridisation cocktail

Component	49 Format (standard)/64 format array
Fragmented cRNA	Volume variable depending on concentration
Control oligonucleotide B2 (3nM)	5µl
20X Eukaryotic hybridisation controls (bioB 1.5pM, bioC 5pM, bioD 25pM, cre100pM)	15µl
Herring Sperm DNA (10mg.ml)	3µl
BSA (50mg/ml)	3µl
2X Hybridisation buffer	150µl
DMSO	30µl
Water to final volume of 300µl	variable
Final volume	**300µl**

Arrays were equilibrated to room temperature before use (~30min). Each array was wetted prior to injection of hybridisation mix, by filling it with 250µl of 1 x hybridisation buffer (100mM MES, 1M [Na$^+$], 20mM EDTA, and 0.01% Tween-20).

200µl of hybridisation cocktail was then injected into each array. It was important to check that there was a visible bubble, which ensured that the solution could move around easily while in the hybridisation oven. The array was then rotated at 60rpm for 16hr in a 45°C hybridisation oven.

2.3.5.4 Washing, staining and scanning

All buffers for this section of the array process were prepared by Microarray technician Liam Williams.

To wash, stain and scan the probe array, the experiment had to be registered in the GCOS (GeneChip Operating Software, Affymetrix). After 16hr hybridisation, the hybridisation cocktail was removed from the array, which was then filled completely with non-stringent wash buffer A (6 x SSPE, 0.01% Tween-20, 250µl)

The Microarray facility contains two Affymetrix GeneChip Fluidics Station 450 machines, which between them allow the washing and staining of eight Affymetrix GeneChips® simultaneously. The Fluidics Script (protocols used by GeneChip® Fluidics Stations) for the washing and staining of Rat 230 2.0 GeneChip arrays used for all experiments was EukGE-WS2v5_450.

Each chip was stained with a Streptavidin-phycoerythrin dye (SAPE). This is used to bind to the biotinylated nucleotide incorporated into the transcript of interest during the *in vitro* transcription (IVT) reaction.

Table 2.6 Affymetrix stain components

Stain 1 & 3		Stain 2	
2 × Stain Buffer	600µl	2 × Stain Buffer	300µl
50mg/ml BSA	48µl	50mg/ml BSA	24µl
1mg/ml SAPE	12µl	10mg/ml Goat IgG	6µl
H_2O	540µl	0.5mg/ml Biotinylated antibody	3.6µl
		H_2O	266.4µl
Total Volume	1200µl	Total Volume	600µl

Stain 2 was incorporated to increase the probe signals.

All .CEL files (raw data files) created for each scanned slide by Affymetrix GCOS were then collected for statistical analysis.

2.4 Real-time quantitative PCR validation

Validation of all Affymetrix microarray experiments was performed through quantitative real time PCR analysis of the same RNA samples that had been analysed using the Affymetrix GeneChips.

Total RNA from each of the 14 samples from Study One (7 sham animals and 7 diabetic animals) or 20 samples (Study Two) hybridised to the microarrays was used for cDNA synthesis. An additional 8 samples not used in the microarray experiment were run from tissue collected in Study Two (final group numbers: 8 diabetic, 7 diabetic + 87.5mg, 7 sham and 6 sham + 87.5mg). The new RNA was extracted in the same manner as all RNA used in Study Two.

Briefly, RNA underwent a DNase 1 digestion to remove any contaminating DNA. cDNA was then synthesised using SuperScript III® (Invitrogen) and random hexamer primers as per the manufacturer's instructions.

In total, 14 Taq-Man Primers and reagents were purchased from Applied Biosystems. Primers used were: Cpt1, CytB5 (mitochondrial), MCD, Tfam, TXN1, PDK4, Ctr1 Col3a1, TGF-β1, Sco1, Angptl4, Receptor for AGE (RAGE), CD36, and COX17. 18s rRNA was used as the endogenous control for all experiments.

Two ng of cDNA was used per reaction with the Taq-Man primer MasterMix, as per the manufacturer's instructions. Each sample was analysed in triplicate.

Samples were run on the Applied Biosystems 7900HT Real Time PCR System and analysed using the Comparative C_t Method as described in the instructions of ABI PRISM 7700 User Bulletin #2 (P/N 4303859) from Applied Biosystems.

2.5 Histology

Part of the LV was used for cardiac histology, which was obtained after heart perfusion. The LV tissue was immediately fixed in OCT (10.24% (w/w) polyvinyl alcohol, 4.26% (w/w) polyethylene glycol, 85.5% (w/w) non-reactive ingredients) and frozen in liquid nitrogen-chilled isopentane. Samples were stored at -80 $^{\circ}$C until sectioning. Tissues were cryosectioned to 5µm using a Leica Cryocut 1850 Cryomicrotome and adhered to SuperFrost slides. Samples were stored at -80 ºC until staining.

2.5.1 Indirect *in situ* immunofluorescence labelling of collagen

Prior to staining slides are dried for 2hr (RT) before fixing in cold acetone for 10min. Slides were re-hydrated in PBS (100 mM NaCl, 50 mM NaPO$_4$, pH 7.45) for 5min. A square was drawn around each section using DakoCytomation pen (Dako, Carpinteria, CA). To each section, 50µl of 10% goat serum in PBS (block) was applied and left for ~60min at RT on shaker. Slides were immunostained using 50µl/section rabbit anti-rat collagen type III (AB757P, Chemicon), 1:100 diluted in PBS/1% BSA. The collagen antibody was omitted as a negative control. Optimal titer for the collagen primary antibody had been determined previously in the laboratory (Dr. D. Crossman, personal communication). Slides were kept in a light proof box with a wet paper towel in it (to prevent slides drying out) o/n at 4°C on a shaker.

Slides were washed a final 3 x 5min in PBS and stained for 2hr with the secondary antibody Alexa Fluor 488 goat anti-rabbit (diluted 1:100 with PBS containing 1%BSA at 50µl per section; RT on a shaker). Alexa Fluor 488 goat anti rabbit (2° antibody) was from Molecular Probes (Eugene, OR). After incubation, slides were washed 3 x for 5min with PBS and mounted in aqueous antifade mount (Dako, Carpinteria, CA) and stored in the dark at 4°C until imaging.

2.5.2 Nile red staining of lipid in frozen left ventricle heart sections

Nile red specifically targets neutral lipids (Greenspan et al. 1985) and can be used as an alternative for Oil Red O staining. It was decided to use this particular stain because it is fluorescent and can be visualised using confocal microscopy.

A stock solution of Nile Red was prepared at a concentration of 1mg/ml by dissolving 1mg of powder in 1ml of acetone and stored in the dark at 4°C. A 1:200 working solution was prepared by diluting 5µl Nile red stock + 5µl 100% acetone in 990µl TBS (137mM NaCl, 2.68mM KCl, 25mM TRIS, pH 8).

Slides were not fixed prior to staining as lipids are soluble in alcohol and immersing slides in acetone would wash away all of the lipid. Sections were incubated in 100µl Nile Red working solution for 10min, in the dark, at RT.

Following the 10min incubation period, excess dye was removed by one quick rinse of the slides in TBS followed by a 5min TBS wash. Slides were mounted in aqueous antifade mount (Dako, Carpinteria, CA) and stored in the dark at 4°C until imaging.

2.5.3 Transmission electron microscopy (TEM) ultrastructural analysis

Approximately 20-50mg of endomyocardial tissue was dissected from the LV side (medial) of the septum and placed into a high energy relaxing biopsy buffer (10 mM EGTA-Ca$_2$EGTA buffer, free Ca^{II} concentration 0.1µM, 9.5mM MgCl$_2$, 3mM KH$_2$PO$_4$, 20mM taurine, 5mM ATP, 15mM creatine phosphate, 49mM K$^+$ MES, 29mM imidazole-HCl, pH7.1) and dissected into fibre bundles of 0.5 x 1 mm using fine sharp forceps into fibre bundles. Several fibres were then placed into sucrose 250mM, 10mM HEPES (pH7.1) containing 2.5% glutaraldehyde and stored at 4°C for ultrastructural analysis by TEM.

Fibre samples were washed three times for 10min in 100mM Sörenson's phosphate buffer, then post-fixed in 1% osmium tetroxide/100 mM Sörenson's phosphate buffer for 1hr. Samples were then dehydrated by serial ethanol washes (30% to 100% 10min each) with a final 100% acetone wash (10min). Samples were then infiltrated with 1:1 812 epoxy resin for 24hr, and embedded within moulds with fresh resin and cured at 60°C for 48hr. Samples were sectioned to 1µm and stained with toluidine blue. Ultrathin sections were then cut to 70nm, mounted on copper mesh grids and stained with uranyl acetate. Samples were scanned using a Philips CM12 transmission electron microscope at 120kV.

2.5.4 Imaging

2.5.4.1 Confocal imaging of collagen III

Confocal Microscopy was used for histological analysis of tissues in Study Two. It was decided to use this technique because of the superior ability of the confocal to resolve images to a much finer detail. The confocal microscope (LEICA TCS SP2, Leica Microsystems, Germany) was set up as follows: 40 x objective lens (oil) at a 1.0 x zoom, line average set at four. An argon laser with an excitation wavelength of 488 nm was used. For each field, a z-series was taken in 512 x 512-format with six images per series. The beginning and end of each series were determined by the operator but in general these were as close to the top and bottom of section as possible. Three fields were taken
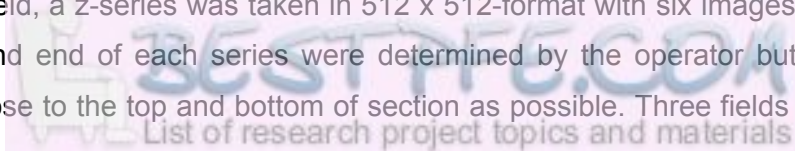
for each section with two sections per animal to give a total of six images per animal. The field to take the z-series was chosen at random and image capture and analysis was undertaken with the operator blinded both as to the status of the animal and the drug group. A maximum projection of all six images was created using LCS Software (Leica Microsystems, Germany) for analysis.

Semi-quantitative analysis was performed for Collagen III. Captured images (as .tif files) for analysis of collagen staining were processed in ImageJ (version 1.37r, http://rsb.info.nih.gov/ij/). A background intensity measurement for each picture with standard deviation was taken and the threshold minimum level was set to median background intensity + six standard deviations and maximum to 255. In order to calculate percentage areas occupied by collagen, the black pixels (or 0 on the gray scale) were divided by the total number of pixels (sum of black and white pixels) and multiplied by 100.

2.5.4.2 Confocal Imaging of cardiac tissue lipid (Nile red)

The confocal microscope (LEICA TCS SP2, Leica Microsystems, Germany) was employed with the following set up: 63 x objective lens (oil) at a 1.0 x zoom, line average set at four. Images were taken in 1024 x 1024-format to improve ability to visualize lipid. For each field, a single image was taken with four fields per section (eight images in total per animal). Care was taken to ensure that the field was chosen at random and both image capture and analysis were undertaken by an operator blinded to both the status of the animals and the drug group.

A background intensity measurement for each picture with standard deviation was taken and the threshold minimum level was set to median background intensity + three standard deviations and the maximum to 255. In order to calculate the percentage area occupied by collagen, the black pixels (or 0 on the gray scale) were divided by the total number of pixels (sum of black and white pixels) and multiplied by 100.

2.6 Serum biochemistry

All tests were performed on the Synchron CX5CE (Beckman Coulter, Inc., 4300 N. Harbor Blvd., Fullerton, CA) by an accredited technician. The Synchron CX5CE is a discrete, random access clinical analyzer capable of performing a wide variety of chemistry tests in a single run. All system functions are automated and under control of the onboard microprocessors. Each of the assays used is described briefly below. All information for the assays was obtained from the Beckman Coulter Synchron CX® Systems Chemistry Information Manual (2001) and the Beckman Coulter Synchron CX5CE/CX5 DELTA Clinical Systems Operating Instructions (2001)

2.6.1 Albumin

Albumin was measured by a timed-endpoint method, in which albumin is reacted with bromocresol purple (BCP) to form a coloured product. A precise volume of sample was mixed with the reagent in a 1 to 100 ratio. The change in absorbance at 600 nm was directly proportional to the concentration of albumin in the sample.

Albumin + BCP ⟶ Albumin-BCP complex

E015174L.EPS

2.6.2 Alkaline phosphatase (ALP)

ALP was measured by a kinetic rate method using a 2-amino-2-methyl-1-propanol (AMP) buffer. Alkaline phosphatase catalyzed the hydrolysis of the colourless organic phosphate ester substrate, p-nitrophenylphosphate, to form a yellow coloured product, p-nitrophenol, and phosphate, the latter being measured spectrophotometrically. The reaction was performed at a pH of 10.3. A precise volume of sample was mixed with the reagent in a 1 to 50 ratio. The change in absorbance at 410 nm was directly proportional to the activity of ALP in the sample.

$$\text{p-Nitrophenylphosphate} + H_2O \xrightarrow[\text{pH 10.3, Mg}^{++}]{\text{ALP}} \text{p-Nitrophenol} + \text{Phosphate}$$
(colorless) (yellow)

E015176L.EPS

2.6.3 Alanine aminotransferase (ALT)

ALT was measured by a kinetic rate method. Alanine aminotransferase catalyzed the reversible transamination of L-alanine and α-ketoglutarate to pyruvate and L-glutamate. The pyruvate was then reduced to lactate in the presence of lactate dehydrogenase (LDH) with the concurrent oxidation of reduced nicotinamide adenine dinucleotide (NADH) to nicotinamide adenine dinucleotide (NAD). A precise volume of sample was mixed with the reagent in a 1 to 11 ratio. The change in absorbance at 340 nm was directly proportional to the activity of ALT in the sample.

2.6.4 Aspartate aminotransferase (AST)

AST was measured by an enzymatic rate method. AST catalyzed the reversible transamination of L-aspartate and α-ketoglutarate to oxaloacetate and L-glutamate. Oxaloacetate was then reduced to malate in the presence of malate dehydrogenase (MDH) with the concurrent oxidation of reduced β -nicotinamide adenine dinucleotide

(NADH) to β-nicotinamide adenine dinucleotide (NAD). A precise volume of sample was mixed with the reagent in a 1 to 11 ratio. The change in absorbance at 340 nm was directly proportional to the activity of AST in the sample.

$$\text{L-Aspartate} + \alpha\text{-ketoglutarate} \xrightleftharpoons{\text{AST}} \text{Oxaloacetate} + \text{L-glutamate}$$
$$\text{Oxaloacetate} + \text{NADH} + \text{H}^+ \xrightleftharpoons{\text{MDH}} \text{Malate} + \text{NAD}^+$$

E015186L.EPS

2.6.5 Calcium

Calcium was measured by a timed endpoint method. Calcium combined with Arsenazo III to form a bluish-purple coloured product. A precise volume of sample is mixed with the reagent in a 1 to 100 ratio. The change in absorbance at 650 nm is directly proportional to the concentration of calcium in the sample.

$$\text{Calcium} + 2 \text{ Arsenazo III} \longrightarrow \text{Ca-Arsenazo complex (bluish-purple color)}$$

E015277L.EPS

2.6.6 Chloride

Chloride was determined by measurement of electrolyte activity in solution. A precise volume of sample (69µL) was mixed with a buffered solution in a 1 to 20 ratio. High molar-strength buffer was used to establish a constant ionic strength that served to set a constant activity coefficient for the electrode, which was then calibrated to concentration values. The chloride ion-selective electrode was a two-phase Ag/AgCl type. Equilibrium was developed at the surface of the electrode. This equilibrium depends on the solubility product (K_{sp}) of the silver and chloride ions in the solution, according to the following reaction:

$$\text{AgCl} \longrightarrow \text{Ag}^+(\text{ag}) + \text{Cl-(ag)} \qquad (1)$$
$$K_{sp} = \frac{[\text{Ag}^+][\text{Cl}^-]}{[\text{AgCl}]} = [\text{Ag}^+][\text{Cl}^-] \qquad (2)$$
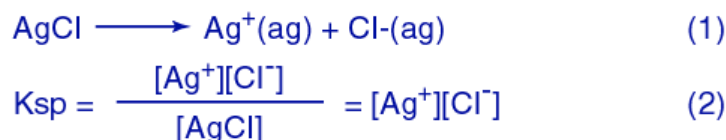
E015279L.EPS

When chloride ions are introduced into this system, the developed equilibrium is disrupted as Ag$^+$ ion concentration at the electrode surface changes. This change results in a shift of the electrode potential according to the Nernst equation, which is indirectly related to the chloride activity in the sample. The potential developed at the chloride electrode is referenced to a sodium electrode in which small temperature variations and electrical noise are compensated.

2.6.7 Cholesterol

Cholesterol was measured by a timed-endpoint method in which cholesterol esterase (CE) hydrolyzed cholesterol esters to free cholesterol and fatty acids. Free cholesterol was then oxidized to cholestene-3-one and hydrogen peroxide by cholesterol oxidase (CO). Peroxidase catalyzed the final reaction of hydrogen peroxide with 4-aminoantipyrine (4-AAP) and phenol which produced a coloured quinoneimine product.

A precise volume of sample was mixed with the reagent in a 1 to 100 ratio, the change in absorbance at 520 nm being directly proportional to the concentration of cholesterol in the sample.

$$Cholesterol\ ester \xrightarrow{CE} Cholesterol + Fatty\ Acid$$

$$Cholesterol + O_2 \xrightarrow{CO} Cholestene\text{-}3\text{-}one + H_2O_2$$

$$2H_2O_2 + 4\text{-}AAP + Phenol \xrightarrow{Peroxidase} Quinoneimine + H_2O$$
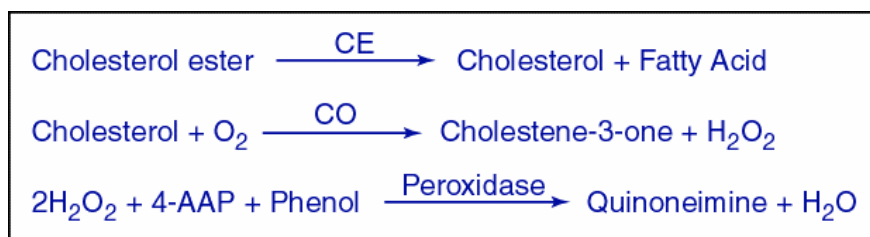
E015196L.EPS

2.6.8 Creatinine

Creatinine was measured by a modified rate Jaffé method, in which creatinine combined with picrate in an alkaline solution to form a creatinine-picrate complex. A precise volume of sample was mixed with the reagent in a 1 to 11 ratio for serum. The change in absorbance at 520 nm was directly proportional to the concentration of creatinine in the sample.

$$Creatinine + picric\ acid \xrightarrow{Alkaline\ solution} creatinine\text{-}picrate\ (Red\ colored\ complex)$$
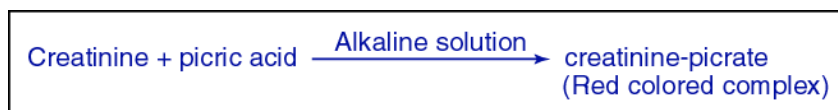
E015281L.EPS

2.6.9 Ferroxidase

Ferroxidase I activity was determined by measuring the ceruloplasmin-catalyzed conversion of Fe^{II} to Fe^{III}. After 4min incubation at 37°C, the Fe^{II} specific chromagen 3-(2-pyridyl)-5,6-bis(2-[5-furylsulphonic acid])-1,2,4-triazine (PFTDA) was added as a stopping reagent. The Fe^{II}-PFTDA chromagen concentration was determined by measuring an absorbance change at 600 nm. Ferroxidase activity in the sample is inversely proportional to colour formation

$$\mathbf{Fe^{II}} + ferroxidase \longrightarrow \mathbf{Fe^{III}}$$

chromogen = +++ colour Fe^{3+} + chromogen = +/- colour
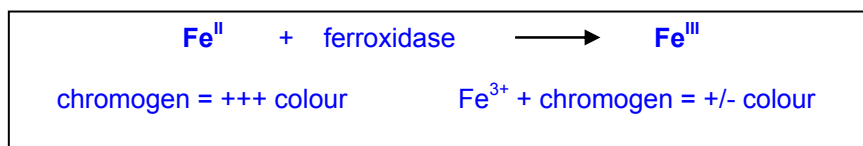
2.6.10 HDL cholesterol

HDL cholesterol was measured by a direct timed-endpoint method. The method used depends on a unique detergent which solubilises only the HDL lipoprotein particles and releases HDL cholesterol to react with CE and CO in the presence of chromogens, to produce a colour product. The same detergent also inhibits the reaction of the cholesterol enzymes with LDL, VLDL, and chylomicrons lipoproteins by adsorbing to their surfaces. A polyanion contained in the reagent enhances the selectivity for HDL cholesterol assay by complexing LDL, VLDL, and chylomicrons lipoproteins.

A precise volume of sample was mixed with the reagent in a 1 to 93 ratio. The change in absorbance at 560 nm measured was directly proportional to the concentration of cholesterol in the sample.

$$\text{LDL, VLDL, Chylomicrons} \xrightarrow[\text{Polyanion}]{\text{Detergent}} \text{Stable Complexes}$$

$$\text{HDL Cholesterol} \xrightarrow[\text{Cholesterol Oxidase}]{\text{Cholesterol Esterase}} \Delta^4 \text{ Cholestenone} + H_2O_2$$

$$H_2O_2 + \text{DSBmT} + \text{4-AA} \xrightarrow{\text{Peroxidase}} \text{Color Product}$$

DSBmT: N,N-bis (4-sulphobutyl) - m - toluidine - disodium

4-AA: 4-aminoantipyrine
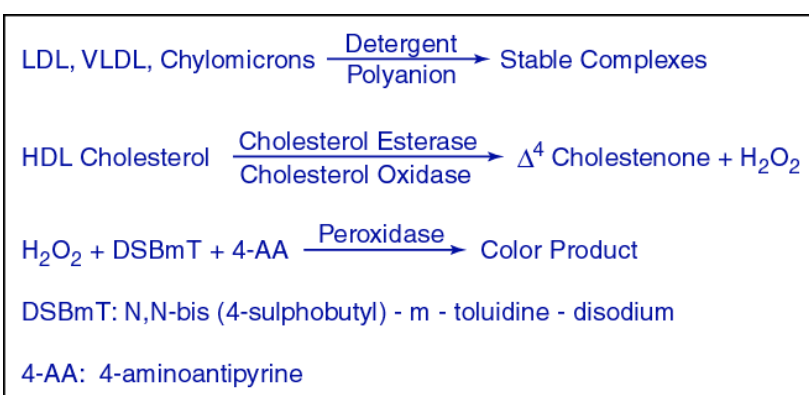
E015231L.EPS

2.6.11 Iron

Iron was measured by a timed endpoint method. Iron was released from transferrin by acetic acid and reduced to the ferrous state by hydroxylamine and thioglycolate. The ferrous ion was immediately complexed with the FerroZine Iron Reagent. A precise volume of sample was mixed with the reagent in a 1 to 8 ratio. The change in absorbance at 560 nm was measured and is directly proportional to the concentration of iron in the sample.

$$\text{Transferrin–}(Fe^{3+})_2 \xrightarrow{\text{Acetic Acid pH 4.3}} \text{Transferrin} + 2Fe^{3+}$$

$$Fe^{3+} + \text{Hydroxylamine} + \text{Thioglycolate} \longrightarrow Fe^{2+}$$

$$Fe^{2+} + 3\text{FerroZine} \longrightarrow Fe^{2+} + (\text{FerroZine})_3$$
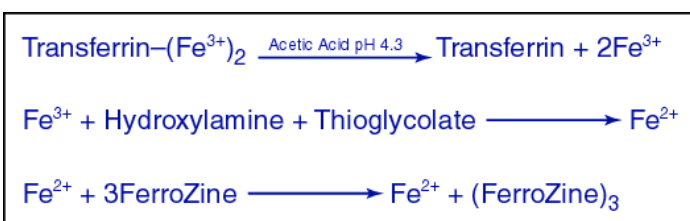
E015160L.EPS

2.6.12 Non-esterified (free) fatty acids (NEFA)

NEFA in serum was treated with acyl-CoA synthetase (ACS) in the presence of adenosine triphosphate (ATP), magnesium cations and CoA, to form the thiol esters of CoA known as acyl-CoA as well as the by-products adenosine monophosphate (AMP) and pyrophosphate (PPi). The acyl-CoA was then oxidised with the addition of acyl-CoA oxidase (ACOD) to produce hydrogen peroxide which in the presence of added peroxidase (POD) allowed the oxidative condensation of 3-methyl-N-ethyl-N-(β-hydroxyethyl)-aniline (MEHA) with 4-aminoantipyrine to form a purple coloured adduct with an absorption maximum at 550 nm.

A calibration graph was produced, from which the amount of NEFA in the sample was determined.

2.6.13 Phosphate

Phosphate was measured by a timed endpoint method. Inorganic phosphorus reacts with ammonium molybdate in an acidic solution to form a coloured phosphomolybdate complex. A precise volume of sample was mixed with the reagent in a 1 to 67 ratio. The change in absorbance at 340 nm was measured, which is directly proportional to the concentration of PO4 in the sample.

$$Phosphorus + Molybdate \xrightarrow{\quad H_2SO_4 \quad} Phosphomolybdate\ Complex$$

E015251L.EPS

2.6.14 Potassium

Potassium was measured by measuring electrolyte activity in solution. A precise volume of sample (69µl) was mixed with a buffered solution in a 1 to 20 ratio. High molar-strength buffer was used to establish a constant ionic strength, which served to set a constant activity coefficient for the electrode, which can then be calibrated to concentration values. The potassium electrode consists of a valinomycin membrane. The physical structure of this membrane is such that the complexing sites in the membrane nearly equal the diameter of the potassium ion. When complexing occurs, a voltage (potential) change takes place within the membrane. This potential is referenced to a sodium reference electrode in which small temperature variations and electrical noise are compensated. The potential follows the Nernst equation and allows the calculation of potassium concentration in the solution:

$$E = Constant + (slope)(log[K^+])$$

E015237L.EPS

Under ideal conditions, the electrode imparts a selectivity of 1000:1 over sodium and is insensitive to hydrogen ions in solutions buffered from pH 3 to 9.

2.6.15 Sodium

The sodium electrode together with a reference electrode was used to determine the activity of ions in the unknown solution. A precise volume of sample (69μl) was mixed with a buffered solution in a 1 to 20 ratio. High molar-strength buffer was used to establish a constant ionic strength, which served to set a constant activity coefficient for the electrode, which can then be calibrated to concentration values.

The Beckman sodium electrode uses a solid membrane produced from aluminium silicate (LAS). When the sample/buffer mixture contacts the electrode, sodium ions undergo an ion exchange with the hydrated outer layer of the glass sodium electrode, resulting in a change in potential (voltage) at the face of the electrode. This potential is referenced to a sodium reference electrode in which small temperature variations and electrical noise are compensated. The potential follows the Nernst equation and allows the calculation of sodium concentration in the solution:

$$E = Constant + (slope) (log[Na^+])$$

E015247L.EPS

Under ideal conditions, the electrode imparts a selectivity of 300:1 over potassium and is insensitive to hydrogen ions in solutions buffered from pH 6 to 10.

2.6.16 Total bilirubin

Total bilirubin was measured by a timed endpoint Diazo method. Bilirubin reacted with the diazo reagent in the presence of caffeine, benzoate, and acetate as accelerators to form azobilirubin.

A precise volume of sample was mixed with the reagent in a 1 to 35 ratio. The change in absorbance at 520 nm was measured and is directly proportional to the concentration of total bilirubin in the sample.

$$Total\ Bilirubin + Diazo + H^+ \xrightarrow{Caffeine,\ Benzoate,\ Acetate} Azobilirubin\ (blue\ color)$$

E015257L.EPS

2.6.17 Total protein

Total protein was measured by a timed-endpoint biuret method. The peptide bonds in the protein sample bind to cupric ions in an alkaline medium to form colored peptide/copper complexes.

A precise volume of sample was mixed with the reagent in a 1 to 50 ratio. The change in absorbance at 560 nm was measured and is directly proportional to the concentration of total protein in the sample.

$$Protein + Cu++ \xrightarrow{Alkali} Protein\text{-}Copper\ Complex$$

E015292L.EPS

2.6.18 Triglyceride

Triglycerides were measured by a timed-endpoint method. The triglycerides in the sample were hydrolyzed to glycerol and free fatty acids by the action of lipase. A sequence of three coupled enzymatic steps using glycerol kinase (GK), glycerophosphate oxidase (GPO), and horseradish peroxidase (HPO) caused the oxidative coupling of 3,5-dichloro-2-hydroxybenzenesulfonic acid (DHBS) with 4-aminoantipyrine to form a red quinoneimine dye.

A precise volume of sample was mixed with the reagent in a 1 to 100 ratio. The change in absorbance at 520 nm was measured and is directly proportional to the concentration of triglycerides in the sample.

(a) Triglycerides $\xrightarrow{Lipase}$ Glycerol + Fatty Acids

(b) Glycerol + ATP $\xrightarrow[Mg^{++}]{GK}$ Glycerol-3-phosphate + ADP

(c) Glycerol-3-phosphate + O_2 $\xrightarrow{GPO}$ Dihydroxyacetone + H_2O_2

(d) $2H_2O_2$ + 4-Aminoantipyrine + DHBS $\xrightarrow{HPO}$ Quinoneimine Dye + HCl + $2H_2O$
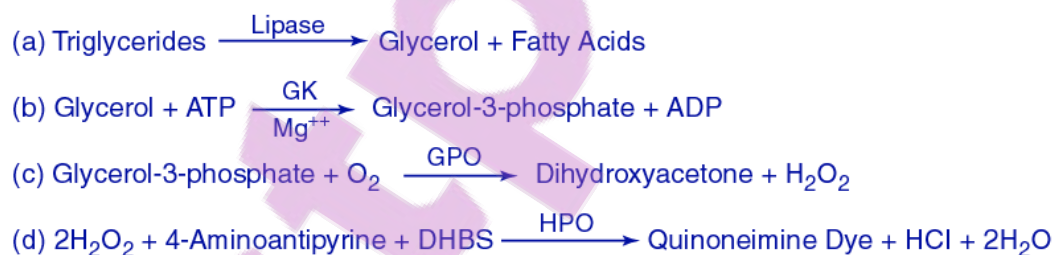
E015258L.EPS

2.6.19 Urea

Urea was measured by an enzymatic rate method. Urea was hydrolyzed by urease to ammonia and carbon dioxide. Glutamate dehydrogenase (GLDH) catalyzed the condensation of ammonia and 〈-ketoglutarate to glutamate with the concomitant oxidation of reduced nicotinamide adenine dinucleotide (NADH) to nicotinamide adenine dinucleotide (NAD).

$$\text{Urea} + H_2O \xrightarrow{\text{Urease}} 2NH_3 + CO_2$$

$$NH_3 + \alpha\text{-Ketoglutarate} + NADH + H^+ \xrightarrow{\text{GLDH}} \text{Glutamate} + NAD^+ + H_2O$$
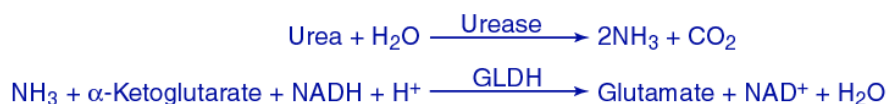
E015266L.EPS

A precise volume of sample was mixed with the reagent in a 1 to 100 ratio. The change in absorbance at 340 nm was measured and is directly proportional to the concentration of urea in the sample.

2.7 Determination of TETA, monoacetylated-TETA (MAT) and diacetylated-TETA (DAT) levels using an HPLC based methodology

All work was carried out by the School of Biological Sciences Reference Laboratory. Serum used was collected from the second study only and urine used was collected from the metabolic cages.

HPLC analysis was performed on a Shimadzu HPLC System with online solvent degassing unit, autosampler, sample cooling unit, column oven and fluorescent detector. Software used for analysis was Shimadzu LC Solution.

The column used was a Luna 3µC18 (1) 150 x 3.0mm (Part number 00F-4251-YO Phenomenex). When not in use the column was stored at room temperature. On the instrument columns were maintained at 25 °C.

The associated guard column was a security guard cartridge system. Cartridge holder using C18 (ODS Octadecyl) cartridges 4mm (length) x 3mm (internal diameter), 10 pack (Phenomenex.)

2.7.1 Reagents

Standard composition:

- Triethylenetetramine Dihydrochloride (MW 219.16, Carbogen Lot C-013740 – Astd-2)
- Monoacetyl triethylenetetramine trihydrochloride (MW 297.65, Carbogen Lot C-017436 – STD 01)
- Diacetyl triethylenetetramine dihydrochloride (MW 303.23, Carbogen Lot C-017452 – STD 01)

Human serum used for preparation of the serum standard was obtained from NZ Blood Service and Human urine used in preparation of the urine standard was obtained from Asma Othman, School of Biological Sciences Reference Laboratory.

Calibration curve: Standards were prepared in pooled human serum or urine.

Points on curve were equal to: 5mg/l, 3mg/l, 1.5mg/l, 0.75mg/l, 0.5mg/l, 0.25mg/l, 0.125mg/l, and 0.0625mg/l mixed standard. Samples were also run without internal standard.

The internal standard used for all experiments was Hexamethylenediamine dihydrochloride (HAD, MW 189.13 Aldrich Lot JO 07808LI). A 60µM working solution was prepared fresh each day from the 1mM Stock Solution for all runs. The derivitisation compound used was 9-Fluorenylthoxycarbonyl chloride (FMOC chloride, MW 258.70 Sigma-Aldrich Lot 04303TC) diluted in acetonitrile. For all serum analysis a 7.5mM solution was used and for the partially validated urine analysis a 10mM solution was used.

2.7.2 Protocol

To 25µl of sample, 10µl of 60µM HAD, 20µl of 1mM EDTA, 25µl of water, 25µl of Borax buffer (Sodium tetraborate, Sigma) and 75µl of Acetonitrile were added. Mixture was vortexed for approximately 10s and then let stand for 10min at room temperature to allow deproteinisation. Samples were then spun for 3min at 10,000rpm and 100µl of supernatant transferred to a new glass HPLC vial. 100µl of 7.5mM (Serum) or 10mM (Urine) FMOC chloride was added, samples were shaken and then allowed to stand for a further 10min. Samples were centrifuged for 4000rpm for 5min to remove any remaining particulate matter and run on the HPLC using the appropriate method.

2.7.3 Sample dilution

Occasionally it was necessary to dilute a sample. Dilution was estimated by assessing the original chromatogram. Two dilutions within the measuring range were required for example, if the sample appeared to be 20 mg/l, 5 x 1:2 dilutions will be required. Two of the 1:2 dilutions should yield a result within the measuring range of 0.0625 – 5.0mg/l. Calculated results (multiplied by dilution factor) were within 15 % of each other. The average of the two calculated duplicates is reported.

2.7.4 HPLC protocol

Pump Parameters

Pressure Lower Limit	5 bar
Pressure Upper Limit	400 bar
Pump Mode	Gradient program
Mobile phase:	C is 10mM Ammonium acetate; A is acetonitrile

Gradient program:

0.01	Pumps Pump C Conc.	50
7.00	Pumps Pump C Conc.	30
7.50	Pumps Pump C Conc.	20
17.00	Pumps Pump C Conc.	20
19.00	Pumps Pump C Conc.	5
23.00	Pumps Pump C Conc.	5
25.00	Pumps Pump C Conc.	50
35.00	Controller	Stop
Flow		0.500 ml/min
B. Flow		0.000 ml/min
C. Flow		0.000 ml/min
LC Stop Time 35.0min		

Detector Parameters

Response	1.5sec
Excitation Wavelength	263nm
Emission Wavelength	317nm
Emission Gain	4
Sensitivity	Low

2.8 Graphite Furnace - Atom Absorption Spectroscopy (GF-AAS) analysis of copper, zinc, manganese or iron levels in 24hr rat urine

2.8.1 Sample preparation

50µl 1% CHAPS (1g/100ml w/v) + 50µl 5% HNO_3 (3.55ml 69% solution in 44.8ml H_2O, v/v) was added to 400µl of straight urine in a clean sterile 15ml falcon tube and stored in the fridge until collection.

Samples were given to the GF-AAS technician and stored in the freezer prior to dilution and analysis. Prior to analysis they were removed from the freezer and allowed to thaw to room temperature. All samples were diluted to approximately 3ml in clean sterile 15ml polypropylene tubes using an accurately weighed volume of Ultrapure water.

For Zn, some samples required additional dilution prior to analysis. In this case, diluted samples were further diluted between 3 to 6 times with Ultrapure water.

2.8.2 Instrument details and specific settings for the detection of Cu, Zn, Mn or Fe

Graphite furnace instrumentation and software was obtained from GBC Scientific Equipment Pty Ltd (Victoria, Australia)

Atom Absorption: GBC 933 AA

Graphite Furnace: GBC GF 3000

Auto Sampler: GBC Pal 3000

Program: GBC Avanta Version 2.0

Table 2.7 GF-AAS settings

Metal	Lamp Current	Wavelength	Slit Width
Copper	3.0 mA	324.7nm	0.5nm
Zinc	5.0mA	213.9nm	0.5nm
Manganese	5.0mA	279.5nm	0.2nm
Iron	7.0mA	248.3nm	0.3nm

2.8.3 Analysis by GF-AAS

Trace metal standards of known concentration (50µg/l for Cu, 40µg/l for Fe and 30µg/l for Zn and Mn) were prepared from SpectrosoL® standard solutions (1000mg/l, VWR International Ltd, Leicestershire, UK) and ultrapure water. The average of three absorbance readings for each known standard was used to construct the calibration curve.

Using the calibration curve, sample concentrations were calculated from the average of triplicate absorbance measurements. A reference standard of known concentration (prepared from the trace metal standard) was prepared and analysed after each consecutive fourth sample analysed. A rescale calibration was undertaken periodically to correct for any drift in the calibration curve.

For some samples, sample was lost during the injection stage when the sample leaked out of the furnace tube hole. To reduce this problem, the probe tip was gently rubbed with clean ethanol. This procedure introduced little contamination to the measured concentrations. Samples were stored in the refrigerator between analyses.

The limits of detection for the GF-AAS are as follows: Mn, Fe and Zn, 1ppb and Cu, 0.5ppb.

2.9 Flame ionisation detection thin-layer chromatography (Iatroscan) determination of lipid in heart tissue

2.9.1 Lipid extraction

Heart tissue samples from the Study Two only were used in this analysis. Due to the limited amount of tissue available, some samples were taken from storage in OCT (previously used in histology). These samples were thawed and removed from OCT before a brief rinse in chloroform to remove any residual compound.

After this point all samples then underwent the same treatment. Sample tissue was weighed and snap frozen in liquid N_2. Tissue was ground in liquid nitrogen with mortar and pestle and the tissue powder transferred to a pre-weighed eppendorf tube and weighed again. To the tissue powder 1ml of MilliQ water was added.

This solution was sonicated with a Vibra Cell sonicator (3mm fitted head) at amplitude of 150 on ice for 2 x 30s. Samples were then aliquoted into 4 x 250µl lots.

Lipid extraction was performed as described by Sewell (Sewell 2005) with minor modifications. Briefly, 1 x 250µl aliquot was transferred to a 1ml clean glass V-Vial with a pulled Pasteur pipette. To the sample 25µl internal Standard (3-hexadecanone, Sigma H-7504 Lot: 125H0815), 100µl chloroform and 250µl methanol was added. 3-hexadecanone (ketone) was used as an internal control because it did not interfere with any of the peaks of interest (triglyceride, free fatty acid or cholesterol) and was deemed to be negligible in the samples. Samples were shaken for 2-3min and then centrifuged (1500rpm for 6min) at room temperature. Both the aqueous and chloroform fractions were transferred to a new clean glass V-Vial leaving the solid non-lipid material behind and to the new V-Vial 250µl of both chloroform and water were added. Samples were again shaken for 2-3min and then centrifuged (1500rpm for 7min) at room temperature. From this the bottom chloroform layer was transferred to a third clean glass V-Vial. Samples were dried down in a stream of nitrogen gas and prepared for immediate use or otherwise, the vial was filled with nitrogen and stored at -20°C. Samples were never stored longer than overnight.

2.9.2 Rod spotting and Iatroscan run

For this analysis the Iatroscan Mark V[new] TLC/FID system and new silica gel S-III Chromarods were used. As per the protocol outlined by Sewell (Sewell 2005), 25µl of chloroform was added to the dried down sample. 1µl of this 25µl was applied to clean chromarods using a fixed volume Drummond Microdispenser fitted with Drummond Precision Glass Bores (volumetric tolerance of ±1%).

Chromarods were developed in the Parrish triple development system (Parrish 1999) with minor modifications. Briefly, here two rather than three developments were used as it was deemed unnecessary to determine the levels of the phospholipid classes.

In the first development chromarods were placed in a solution containing: 69.3ml hexane, 0.7ml diethyl-ether and 0.035ml formic acid. Rods were then partially scanned (80% down the rod) to allow visualization the ketone peak while leaving the remaining lipids at the base of the rod for subsequent developments (second development). This process allows separation of all the lipid classes of a single sample (Sewell 2005)

In the second development chromarods were placed in a solution containing 55.3ml hexane, 14ml diethyl-ether, and 0.7ml formic acid. Rods were scanned 100% in this second development.

Prior to each scan the Chromarods were dried for 3min in a Rod Dryer TK-8 (Iatron Laboratories) at 60°C.

2.9.3 Quantification of lipid

Quantification of the lipid per sample was based on calibration curves generated for each lipid class on the same rack of 10 Chromorods used for analysis as described by Sewell (Sewell 2005). Rods were calibrated with an eight component composite standard made from highly purified lipid standards (99%) in HPLC-grade chloroform. The lipid classes used in this instance were phospholipid (L-α-phosphoditylcholine), free sterol (cholesterol), fatty alcohol (1-hexadecanol), free fatty acid (palmitic acid), triglyceride (tripalmitin), ketone (3-hexadecanone), wax ester (lauryl acid myristyl ester), and aliphatic hydrocarbon (nonadecane).

Standards were purchased from ICN Biomedicals (FFA), Acros Organics (HC) or SIGMA (all others). Peak areas for the calibration curves were based on the mean of two separate Chromarods; r^2 values were > 0.97 for all lipid classes. Due to the large amount of phospholipids present in these tissues some modification to the calibration curve was required.

For each group (sham, sham + 87.5mg TETA-disuccinate, diabetic, diabetic + 87.5mg TETA succinate) three replicate lipid extractions were performed per animal (3 x 250μL aliquots). Each lipid class per sample was determined based on the percent recovery of the internal standard and the calibration curve appropriate for the lipid class. The amount of each lipid class was calculated from the standard curve using peak area. Each lipid class value is the average of the three replicates.

2.10 Cardiac mitochondria functional assays

Analysis of enzyme function was performed on homogenate and isolated mitochondria of the septum from animals in Study Two only.

2.10.1 Isolation of cardiac mitochondria

The mitochondria isolation procedure was performed in a cold room (4ºC). Following heart perfusion, the septum was cut into small pieces in 5ml of ice-cold mitochondrial isolation buffer (MIB; 225mM D-mannitol; 75mM sucrose; 20mM HEPES; 1.0mM EGTA, 0.5mg/ml BSA (fraction V, IgG free, free fatty acid-poor); pH7.4 at 4ºC). The protease nagarase (2.5mg per septum; Sigma Proteinase type XXIV) was added to MIB and incubated for 10min. Following exposure to protease digestion, the septum was homogenised (Ultra-Turrax T25) for 3 x 5 sec and then diluted with 15ml of MIB to limit the exposure to concentrated protease. A portion of the homogenate was collected for each sample and stored at -80 ºC for future experiments. The remaining homogenate was centrifuged at low speed (1,000 x g) for 5min at 4ºC. The resulting pellet was discarded and the supernatant was filtered through a clean mesh into a SS-34 centrifuge tube. The filtrate was centrifuged at 7,700 x g using (RC-Sorvall; SS-34 Rotor, 4ºC) for 10min. The resultant pellet following the high-speed spin contained the mitochondria, and was gently re-suspended with a soft brush in MIB (without BSA), and centrifuged at 7,700 x g for a further 10min. The pellet was then re-suspended in 100µl of MIB (without BSA), transferred to Eppendorf tubes and centrifuged for 2min in a cooled Eppendorf centrifuge at top speed. The resulting supernatant was discarded, and the mitochondria pellets were stored at -80ºC.

2.10.2 Enzyme functional assays

Septum homogenates and mitochondria were used in the enzyme activity assays. The activities of five enzymes were measured: citrate synthase (CS), carnitine palmitoyl transferase (CPT), L3-hydroxyacyl CoA:NAD$^+$ oxidoreductase (HOAD), isocitrate dehydrogenase (IDH), and cytochrome c oxidase (COX). The activity of CS, CPT, HOAD and IDH were measured spectrophotometrically, while COX activity was measured polarographically using an oxygen electrode. Mitochondrial pellets were thawed and reconstituted in a re-suspension buffer (40mM KCl; 25mM Tris-HCl (pH7.5); 2.0mM EDTA; 0.2% (v/v) Triton X-100). Protein concentrations for both homogenates and mitochondria were determined using the Bradford method. A standard curve was constructed using BSA standards of 2.0mg/ml, 1.0mg/ml and 0.5mg/ml, and a blank

containing the reconstitution buffer. Protein concentrations were determined using a spectrophotometer (SpectraMax^{TM} 340, Molecular Devices, Sunnyvale, CA) at 595nm, and the final protein concentrations were determined from the standard curve constructed using SOFTMax Prov.3.1 (Molecular Devices). All assays were conducted in duplicates and adjusted with the appropriate extinction coefficients. The micromolar extinction coefficients used were 13.6 (CS and CPT) and 6.22 (HOAD and IDH). The averaged enzyme activities were expressed in µM/min/µg of tissue.

2.10.2.1 Citrate synthase (CS, E.C.4.1.3.7)

This enzyme catalyses the entry of acetyl-Coenzyme A into the TCA, and was determined as described (Newsholme and Crabtree 1986). The reaction mixture contained 50mM Tris-HCl (pH 8.0), 0.1mM acetyl Coenzyme A, and 0.2mM 5,5'-dithiobis-(2-nitrobenzoic acid) (DTNB). Reactants and sample were incubated for 5min prior to measurement by addition of 5mM oxaloacetate, which was omitted in controls.

2.10.2.2 L3-hydroxyacyl CoA:NAD$^+$ oxidoreductase (HOAD, E.C.1.1.1.35)

HOAD, a principal lipolytic enzyme, was determined as described (Newsholme and Crabtree 1986). Assays contained 100mM Tris-HCl (pH7.5), 0.15mM NADH, 1mM KCN and were started by the addition of 0.15mM acetoacetyl Coenzyme A, which was omitted in controls.

2.10.2.3 Carnitine palmitoyl transferase (CPT, E.C. 2.3.1.21)

CPT is required for the uptake and metabolism of lipid by the mitochondria. It was assayed as described (Schafer et al. 1993). The assay buffer contained 50mM Tris-HCl pH7.4 and 0.1mM palmitoyl-CoA, 150mM KCl, 0.2mM 5,5'-dithiobis-(2-nitrobenzoic acid) (DTNB) and 5mg/ml lipid free BSA. The assay was started by addition of 5mM carnitine, which was omitted for controls.

2.10.2.4 Isocitrate dehydrogenase (IDH-NADP+, E.C. 1.1.1.42)

IDH is an intrinsic enzyme of the TCA cycle, and was measured using an assay mixture that contained 50mM Tris-HCl (pH8.5), 0.15mM NADP, 1mM DTT, 5mM MgCl$_2$ 100mM NaCl and 4 mg/l BSA. The reaction was started by the addition of 0.23mM isocitrate.

Activities of IDH and HOAD enzymes were determined at $25^{o}C$ following the absorbance of NADH/NAD^{+} at 340 nm. CS and CPT followed the absorbance of DNTB at 412 nm.

2.11 Inductively coupled plasma – mass spectrometer (ICP-MS) Analysis

Cu and Zn levels in serum were determined at Hill Laboratories (Hamilton, New Zealand) using either a PE Sciex Elan-DRCII or PE Sciex Elan-6100 DRC Plus ICP-MS. The operating parameters are summarised in Table 2.8 below. The method used in this instance was APHA 3125B (Metals by Inductively Coupled Plasma/Mass Spectrometry).

A calibration was performed for every batch of 40 samples, and a calibration verification QC standard was analysed immediately following the calibration standards. This calibration verification standard was obtained from a source independent of the elements used in the calibrating standards. Interference-check solutions were analysed with every batch in order to monitor potential interferences and ensure the Dynamic Reaction Cell was removing these interferences efficiently.

Check standards were analysed at least every 20 samples in order to monitor and correct for any drift in the instrument response. Check blanks were analysed at least every 3-4 samples in order to monitor the instrument baseline.

Internal standards were automatically added to each sample as they were introduced into the instrument. The internal standards were used to correct for any sample transport or ionisation effects within the plasma. A range of internal standards was used to span the mass range being analysed.

Samples were diluted 40-fold (from an original volume of 150µl) prior to analysis to reduce matrix interferences and provide enough volume for ICP-MS analysis

Table 2.8 Instrumental operating parameters for ICP-MS

Parameter	Value
Inductively coupled plasma	
Radiofrequency power	1400W
Argon plasma gas flow rate	15l/min
Argon auxiliary gas flow rate	1.2l/min
Argon nebuliser gas flow rate	0.9l/min
Ammonia (reaction gas) flow rate	0.3 – 0.4ml/min
Interface	
Sampler cone and orifice diameter	Ni / 1.1mm
Skimmer cone and orifice diameter	Ni / 0.9mm
Data acquisition parameters	
Scanning mode	Peak hopping
Dwell time	50-500ms
Sweeps / replicate	7
Replicates	3
Sample uptake rate	1ml/min

2.11.1 Method detection limits and analytical range

The following table lists the method detection limit and the upper ranges of the analytes in the biological fluids analysed.

The ICP-MS is linear over six orders of magnitude and the upper ranges reported in Table 2.9 below represent highly conservative linear ranges.

Table 2.9 ICP-MS detection limits

Method	Analyte	MDL µg/l	Upper values µg/l
ICP-MS	Cu	0.05	100.00
ICP-MS	Zn	0.2	1000.0

2.12 Statistical Analysis

2.12.1 General

All general statistics such as one- or two-way ANOVA and Student's *t*-test were carried out using GraphPad Prism 4 for Windows (v.4.03, January 2005, San Diego CA, USA) unless otherwise stated.

2.12.2 Microarray statistics

2.12.2.1 Agilent

All data analysis was carried out in the R computing environment (Ihaka and Gentleman 1996) using the Limma package (Smyth 2005). For each array, no background correction was performed, and global loess smoothing was used to remove intensity dependent dye bias from each channel of each array (via application of the loess approach to the MA plot for each array). The three arrays contained one normal and one diabetic sample in each channel were then used in a linear models analysis to identify differentially expressed genes. Specifically, a modified *t*-statistic of Smyth (Smyth 2004) was calculated for each gene, along with a corresponding P-value. The Benjamini and Hochberg method of false discovery rate control (Benjamini and Hochberg 1995) was then used to adjust these P-values, resulting in a putative list of significantly differentially expressed genes.

2.12.2.2 Amersham

All data analysis was carried out in the R computing environment (Ihaka and Gentleman 1996). Each diabetic sample was arbitrarily matched to a normal sample for the purposes

of normalization, with no background correction performed. Loess smoothing was then used to remove non-linear trend from the scatter plot of each pair of samples, under the assumption that a large proportion of genes would not undergo differential expression between the two samples (thus implying that there should be good agreement between the two arrays for the majority of genes). Smoothed local variances were calculated across the intensity range of each normal-diabetic pair, with these variability estimates used to form standardized z-scores for each gene in each array pair. A standard multiple comparison procedure (Benjamini and Hochberg method of false discovery rate control (Benjamini and Hochberg 1995)) in conjunction with a normality assumption was then used to determine if genes were differentially expressed in each normal-diabetic array pair. Consistency of differential expression detection was then assessed by comparing the per-gene results across the array pairs.

2.12.2.3 Affymetrix

Data files used were .CEL files as produced by GCOS. All data analysis was carried out in the R computing environment (Ihaka and Gentleman 1996), using the Bioconductor suite of analysis packages (Gentleman et al. 2004). Normalization was performed using the Robust Multichip Averaging (RMA) algorithm of Irizzary *et al.,* (Irizarry et al. 2003), as implemented in the Affymetrix Bioconductor package (Gautier et al. 2004). Background correction was not performed as part of the normalization process. Detection of probe sets undergoing changes in expression level was performed using the Limma package (Smyth 2005), with the modified *t*-statistic of Smyth (Smyth 2004) used to assess the strength of differential expression (relative to variability) for each probe set. The false discovery rate controlling method of Benjamini and Hochberg (Benjamini and Hochberg 1995) was used to produce adjusted P-values in order to limit the expected proportion of false positive results to below 5%. Probe sets with an adjusted P-value less than 0.05 were considered to have undergone statistically significant changes in expression level across treatment conditions.

2.12.3 GSEA

A second method for analysing microarray datasets known as Gene Set Enrichment Analysis (GSEA) described by Subramanian *et al.,* (Subramanian et al. 2005) and Mootha *et al.,* (Mootha et al. 2003) was applied to the data from this study.

Briefly, genes $R_1 \ldots R_N$ were ordered into a list using an appropriate gene expression difference measure, such as signal to noise ratio. To determine whether the members of a gene-set *S* were enriched at the top of a list a Kolmogorov-Smirnov (K-S)

running sum statistic was computed, beginning with the top-ranking gene. The running sum increased when a member of gene-set *S* was encountered and decreased otherwise. The enrichment score (ES) for a single gene-set was defined as the greatest positive deviation of the running sum across all genes. When many members of *S* appear at the top of the list ES was high. The ES was computed for every gene-set using actual data and the maximum ES (MES) was recorded. To determine whether one or more of the gene-sets were enriched in one group relative to the other, the entire procedure was repeated 1000 times using permuted group assignments and building a histogram of the maximum ES achieved by any pathway in a given permutation. As only two data sets were able to be compared per analysis, planned comparisons sham vs. diabetic and diabetic vs. diabetic-treated were carried out.

The MES achieved for the actual data was then compared to this histogram, providing a global P-value for assessing whether any gene-set is associated with the diagnostic characterisation. A false discovery rate correction (25%) was then applied to the final P-value to account for the multiple comparisons.

Analysis of the data was carried out using GSEA software v2.0 available from http://www.broad.mit.edu/gsea. Gene sets were defined using Gene Ontology (GO) annotations (as described in Chapter 4) and KEGG pathway identifiers. Five categories of gene-sets in total were created for this analysis: 1. GO Biological Process (239 pathways with greater than 15 genes per pathway, less than 500 genes per pathway); 2. GO Molecular Function (413 pathways with greater than 15 genes per pathway, less than 500 genes per pathway); 3. GO Cellular Component (128 pathways with greater than 15 genes per pathway, less than 500 genes per pathway); 4. KEGG pathways (115 pathways with greater than 15 genes per pathway, less than 500 genes per pathway); and 5. a smaller *Apriori* gene-set (51 pathways with greater than 5 genes per pathway, less than 500 genes per pathway) based on work from Chapter Four and previously published work from this laboratory (Cooper et al. 2004; Cooper et al. 2005; Gong et al. 2006).

The GSEA program parameters were set as described below:

1. Gene set data base: varied depending on comparison

2. Number of permutations: 1000

3. Permutation type: phenotype

Phenotype: Random phenotypes were created by shuffling the phenotype labels on the samples. For each random phenotype, GSEA ranked the genes and calculated the enrichment score for all gene-sets. These enrichment scores were used to create a null distribution from which the significance of the actual enrichment score (for the actual expression data and gene-set) was calculated. This is the recommended method when there are at least seven (7) samples in each phenotype.
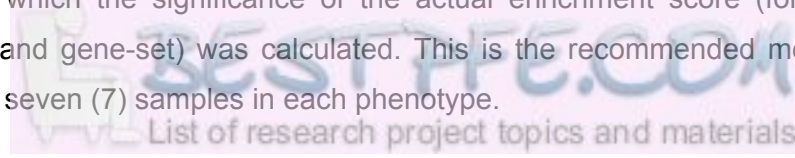
2.12.4 Mixed model statistics

Mixed model statistics for the Iatroscan lipid and RT-qPCR data was conducted using the SAS PROC MIXED mixed model function ((Littell et al. 2006), SAS v 9.1 SAS Institute Incorp., Cary, NC, USA).

2.12.4.1 Iatroscan data

As described in section 6.2.6.2 the data used in this analysis was amount of TG, FFA, cholesterol or phospholipid (µg) per mg of tissue. Each data set was transformed as required.

2.12.4.1.1 The mixed procedure model information
Estimation Method: REML
Degrees of Freedom Method: Satterthwaite

2.12.4.1.2 Description of REML covariate parameters
Mixed model methodology proceeds only if variances and covariances among the observations are known or after they have been estimated. One of the recommended methods for estimating variances and co-variances is to use the Restricted Maximum Likelihood (REML) method. Using REML, the covariates estimated in this mixed model were as follows; Set: Encompasses variation occurred as a result of all runs involving the same set of four rats (within a day, in triplicate). Rat (set): Between-animal variance within a set, pseudoRun (set): Variation between Iatroscan runs within a set.

2.12.4.2 RT PCR data

The data used in this analysis was the ΔC_t value and was obtained using the following formula:
C_t (gene of interest) – C_t (endogenous control, 18S rRNA), as per the instructions of ABI PRISM 7700 User Bulletin #2 (P/N 4303859) from Applied Biosystems.

2.12.4.2.1 The mixed procedure model information
Estimation Method: REML
Degrees of Freedom Method: Satterthwaite

2.12.4.2.2 Description of REML covariate parameters

Plate: As there were 28 samples, two plates were required to analyse all samples. This parameter accounted for any variation that may have occurred between the two plates.

Block (Plate): The experiment was designed so that each plate consisted of three blocks of samples that had been randomly assigned. This parameter accounts for any block-to-block variation that occurred once plate variation had been removed.

2.12.5 Dose-response data

Mixed model statistics for the dose response data was conducted using the SAS PROC MIXED mixed linear model or SAS PROC GLM general linear model functions ((Littell et al. 2006), SAS v 9.1 SAS Institute Incorp., Cary, NC, USA) as indicated.

2.12.5.1 Split-plot in time ANOVA or ANCOVA

A split-plot analysis was conducted as data represented measurements from the same animal at two time points (Week 10 & Week 15).

A mixed linear model was used in place of a general linear model in these analyses as the general linear model was unable to estimate the means or standard error for each group due to uneven group numbers. For all analyses, the random error estimation method used was REML and the degrees of freedom method was Satterthwaite.

For urine TETA, percentages of un-metabolised TETA, MAT and sham DAT, a mixed linear model split-plot in time ANOVA was conducted and for urine metal levels (Cu, Zn, Mn and Fe) a split-plot in time ANCOVA using Week 0 as covariate was conducted. ANOVA/ANCOVA tables are presented within the relevant figures for each variable measured.

2.12.5.2 General linear model ANOVA or ANCOVA

A general linear model ANOVA was conducted for urine DAT at Week 10 (sham and diabetic groups), serum biomarkers, final HW, HW/BW, serum metals and serum TETA and MAT levels. A general linear model ANCOVA was conducted for urine Cu, Fe, Zn, Mn at six weeks using respective metal levels at Week 0 as a covariate. ANOVA/ANCOVA tables are presented within the respective figures for each variable measured.

2.12.5.3 Repeated measures ANVOA (Mixed Linear Model)

Repeated measures analysis of blood glucose (BG) levels was conducted on data collected post-administration of TETA to determine if TETA had caused any change. Data used in the repeated measures analysis of body weight (BW) was split into two groups as described in the text (Section 5.2.2.2). The covariance structure used for all analyses was Autoregressive (1). This structure has homogeneous variances and correlations that decline exponentially with distance. This means that two measurements next to each other in time are highly correlated but that as measurements get further and further away they become less correlated.

2.12.5.4 Regression analysis

A Pearson's correlation was used to determine association between factors (TETA and Cu, Zn, Fe, Mn or MAT) in both serum and urine. Significance of the association was determined using repeated measures mixed linear model ANCOVA for urine values (to adjust for the two time points, Week 10 & Week 15, used in the analysis) and general linear model ANCOVA for serum (no time adjustment required). Analysis was split across status as the amount of TETA or MAT excreted is dependent on whether animals were in the diabetic or sham group. This violates the ANCOVA assumption that the x values (TETA or MAT) are independent of treatment (Status).

Chapter 3 Pilot study to assess suitability of three commercially available microarray platforms for assessment of changes in gene expression

3.1 Introduction

Microarrays are important tools for analysing global changes in gene expression. Microarray technology has continued to develop since it was first described in 1995 by Schena *et al.,* (Schena et al. 1995). Improvements in the methodology have led to more consistent and robust results while requiring fewer replicates (Holloway et al. 2002, Hughes, 2001 #158, Gershon, 2002 #282). There are now a number of microarray providers from both commercial companies and academic institutions; however cost is often a major factor in the decision of which microarray system to use. It was decided initially to use the rat 10K combo microarray slides available from the Clive & Vera Ramaciotti Centre for Gene Function Analysis (School of Biotechnology & Biomolecular Sciences, University of NSW, Sydney) in a pilot study, as they were not as expensive as the commercially available slides. These slides were used with the intention of switching to a commercially available slide should results prove interesting. The pilot study involved hybridising pooled RNA from 8 diabetic and 8 sham animals to the arrays. However results from initial work indicated that these particular slides would be unable to provide results of the quality required, and also revealed inherent faults that we were unable to correct. These are discussed more fully in Section 3.2.1.

Our experiments require stringent quality control and robust results as they may be subject to scrutiny by regulatory bodies such as the Food and Drug Administration (FDA) of the United States and therefore it was decided to assess three major commercial microarray systems.

The three systems were:

- Amersham 'Codelink'
- Agilent
- Affymetrix 'GeneChip'

Outlined below is a description of some of the most important aspects for consideration when choosing an appropriate microarray system

3.1.1 Hybridising the probe to the array

Hybridisation protocols of older microarray systems, including that of the Ramaciotti Centre, introduce a major source of bias. Many of the older microarray hybridisation techniques were subject to a phenomenon called 'spatial bias', which results from the hybridisation solution containing the cRNA (or cDNA) being unequally distributed around the array. In these earlier array systems, the hybridisation method was static. The hybridisation solution was sandwiched between the microarray slide and a plastic 'lifter slip' and distributed around the slide as the result of capillary action. This led to uneven distribution and thus resulted in some areas of the slide being exposed to higher concentrations of sample than others. There are a number of solutions used by the newer commercial systems to overcome this problem, such as the introduction of rotating hybridisation chambers, as used by both Affymetrix and Agilent. In these newer protocols, slides are rotated in a warm oven at low rpm. This allows the solution to be constantly moved around the microarray slide over the hybridisation period (typically 16hr).

3.1.2 Washing and staining of slides

This is the area of greatest user variability. Most systems require manual washing. This creates error from both user handling and focus on the day the slides are processed. Other factors such as ambient temperature and centrifuge model can cause slides to be less than perfect. Additionally, washing and staining methods provide another source of spatial bias. If the stain solution is not washed from the slide evenly, it can leave a streaking effect across the slide. Streaking can occur at either the actual wash station or when the slide is dried in the centrifuge. If drying of the slide is not performed promptly, partially evaporated droplets of wash buffer can leave streaks across the slide when the slide is spun.

A good commercial system should have a stringent wash protocol that reduces the chance of introduced variation.

3.1.3 Spot finding

Computer algorithms known as feature extraction software, convert the image into the numerical information that enables quantification of gene expression. The image processing involved in feature extraction has a major impact on the quality of the data. One of the main steps in the feature extraction procedure is known as 'segmentation'. This is the process by which the software determines which pixels are a part of each individual feature, and so determines the overall intensity that will count towards a

quantitative measurement (Stekel 2003). The GenePix software provided by the Centre for Genomics and Proteomics at the School of Biological Sciences uses a process known as 'variable circle segmentation'. This fits a circle of a variable size onto the region containing the feature. The software then requires the user to manually 'spot find' the array to ensure that spots haven't been missed, or eliminate contamination such as specks of dust. Spot finding also allows the user to identify poor quality spots missed by the program, such as those surrounded by an area with a large mark or 'blob' of intense signal created by poor washing, as well as allowing the user to increase the size of spots underestimated by the program.

A disadvantage of this method is that any irregularly shaped feature may be imperfectly quantified (Stekel 2003) due to the circle segmentation process. Additionally the spot finding required can create user bias, as operators will tend to identify varying numbers of 'bad' spots in a given microarray. This leads to different numbers of spots being included in the analysis and thus a different outcome for the same experiment. This problem has been overcome by many of the commercially available systems which have their own spot finding software. This software contains quality control measures that include a grid system placed over the array reducing the likelihood of missing or incorrectly identifying a spot.

3.1.4 Single versus competitive hybridisation

Another important consideration is whether to use the well established two-dye competitive hybridisation method with both target samples (in our case diabetic and sham) being hybridised to a single array, or the single dye method with each sample hybridised to its own individual array.

The advantage of the competitive hybridisation system is that both samples undergo identical hybridisation conditions compared to separate conditions with the one colour system.

A disadvantage of this system is that competitive hybridisation requires a 'dye swap' experiment in order to overcome the inherent differences between the two dyes as the Cy3 (green) fluorescent dye will give a greater fluorescence signal than that of the Cy5 (red) dye, even at a one-to-one ratio. This is known as non-linear dye effects. In a dye-swap experiment, slide one is has sample A labelled with Cy3 and sample B labelled with Cy5, while slide two has sample A labelled with Cy5 and sample B labelled with Cy3. If the same change is observed between the samples in both slide one and slide two, it is more likely to be a biologically-relevant change and not related to the properties of the dye. Both one- and two-colour commercially available systems are analysed in this study.

3.1.5 Cost and ease of use

Many groups are unable to use commercially available microarray systems because of expense, thus an assessment of cost/benefit is another important aspect when deciding which system to employ.

Ease of use relates to the ability of different users to become proficient in the experimental procedure and to achieve reproducible results.

This chapter aims to provide a qualitative analysis of three commercially available microarray systems taking into account the five considerations outlined above and employing a semi-quantitative analysis using statistical criteria. Each system was found to have its own inherent strengths and weaknesses and so we aimed to determine the system that best suited our requirements for use in subsequent studies.

3.2 Results

To ensure homogeneity within the sample population, as only a limited number of microarrays were available from each of the platforms, all studies used pooled RNA from cardiac tissue of six week diabetic (n = 8) and sham rats (n = 8, provided by Dr. B. Choong). Pooling was considered to enable statistically significant results to be obtained despite small replicate numbers.

3.2.1 Spotted arrays from Clive & Vera Ramaciotti Centre for Gene Function Analysis

Slides from the Clive & Vera Ramaciotti Centre for Gene Function Analysis (School of Biotechnology & Biomolecular Sciences, University of NSW, Sydney) were oligonucleotide-spotted epoxy-coated Eppendorf Creative Oligo glass slides that contained 10,000 amino-modified 50-60mer oligonucleotides sourced from MWG-Biotech and Compugen. The Ramaciotti Centre uses an ESI microarrayer configured with a 120-slide capacity, a six microtitre tray auto loader and 48 PointTech split pins (Section 2.3.2).

In order to ensure that the RNA extraction gave the best quality product, a protocol was developed that included a defined procedure for the removal and perfusion of the rat heart to remove any contaminating blood (Sections 2.2.1 and 2.2.2). The protocol was designed to minimize the risk of contamination with RNase enzymes which would degrade the sample.

An initial dye-swap experiment was done using two slides assess the quality of both our RNA preparation and the microarray slides. Figure 3.1 is a representative picture of the scanned slides.
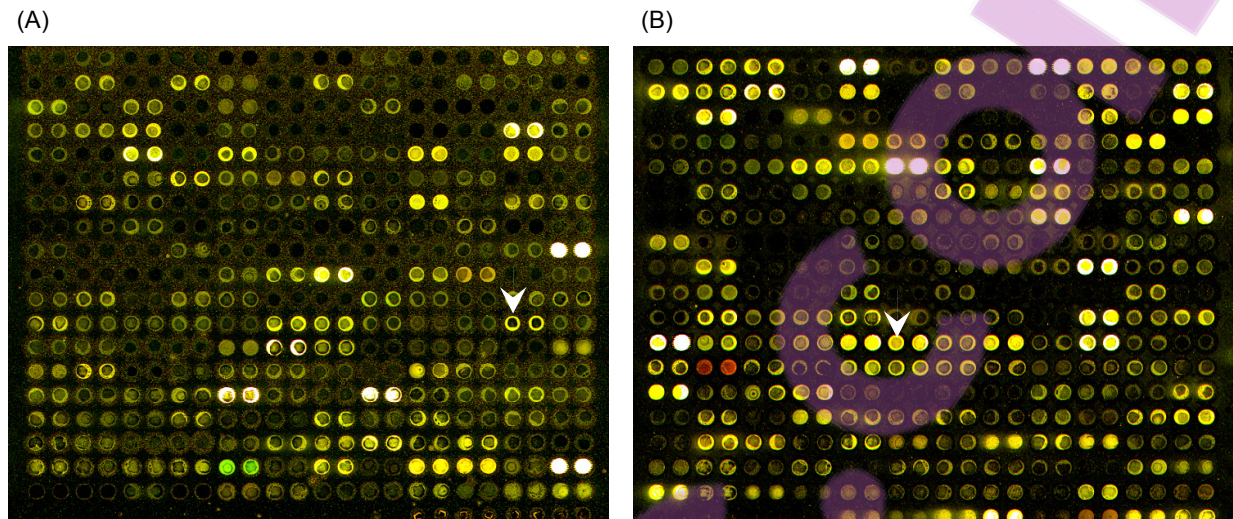
Figure 3.1 Ramaciotti 10K Combo microarray slides

RNA was extracted from LV heart tissue of diabetic or sham male Wistar rats after six weeks as described in Section 2.2.2.1. 80μg of pooled RNA (eight diabetic and eight sham animals) was used in a first strand cDNA synthesis reaction during which amino-allyl modified nucleotides (AA-dUTP) were incorporated. cDNA samples labelled were post-synthesis using a CyDye Cy3-NHS ester or Cy5-NHS ester. Labelled cDNA was hybridised to epoxy-coated Eppendorf Creative Oligo glass slides under a Sigma HybriSlip at 55°C for 15h. Slides were washed and scanned as described in Sections 2.3.2.4 and 2.3.2.5.

(A) Slide 220792. Sham cDNA labelled with Cy5-NHS ester (red) fluorescent dye and diabetic cDNA labelled with Cy3-NHS ester (green) fluorescent dye. White arrow indicates doughnut spot.

(B) Slide 220813. Sham RNA labelled with Cy3-NHS ester (green) fluorescent dye and diabetic RNA labelled with Cy5-NHS ester (red) fluorescent dye. White arrow indicates good spot.

Eppendorf Creative Oligo glass slides contain 10,000 amino-modified 50-60-mer oligonucleotides sourced from MWG-Biotech and Compugen. Slides are courtesy of Clive and Vera Ramaciotti Centre for Gene Function Analysis in Sydney

These initial slides led to the discovery of a phenomenon known as 'doughnut' spots. Doughnut spots reportedly result from an irregular distribution of the cDNA or oligonucleotide probe over the spot area. This occurs most often if the spots are allowed to dry rapidly, as may occur when the humidity in the printing machine is too low. As the spots dry, the oligonucleotide mixture migrates to the edge of the spot leaving a distinctive ring shape. Many researchers have assumed that this effect occurred when the slides were printed and so after printing, slides were rehumidified, so that the spots would re-moisten and swell with the liquid (Dr. F. Pichler, School of Biological Sciences, personal communication). The slides were then snap dried on a heating block, and the whole

process repeated a few times. The resulting spot was no longer a doughnut shape and the probe could then be fixed to the slide surface with UV cross-linking.

Overly-rapid drying provides a plausible explanation for the poor spot quality of the Ramaciotti Slides used here. As mentioned in Section 2.3.2, these slides were cross-linked prior to dispatch, which meant that rehydration of the slides, as outlined above, was not possible. Doughnuts may also be caused by faulty pins, but then only a few areas of the slide would likely be affected (Dr. F. Pichler, School of Biological Sciences, personal communication). As can be seen in Figure 3.1, this was not the case with the Ramaciotti slides.

Most microarray analysis/spot finding programs will regard doughnut spots as 'bad', and so the information is excluded from the analysis. With the Ramaciotti slides, over 50% of the potential data would have been disregarded. This drastically reduces the resolving power of the microarray platform and means that numerous repetitions would be required to provide results with statistical robustness, increasing both time and cost of the experiment.

3.2.2 Amersham, Agilent and Affymetrix commercially available microarray systems

Each of the three commercial companies (Amersham Biosciences/GE Healthcare, Agilent and Affymetrix) provided the necessary equipment, reagents and microarray slides in order to carry out the experiments.

The RNA used for each of the platforms was prepared in exactly the same way (Section 2.2.2.1) in order to ensure that each assessment was based on the platform itself and not the RNA preparation method.

Two of the three systems (Affymetrix and Agilent) are *in situ* synthesis oligonucleotide arrays and are fabricated using the methodologies described in Section 1.6.2. Amersham Codelink arrays are made using the covalent attachment of prefabricated and purified oligodeoxyribonucleotides. The Motorola platform used by Amersham is based on a cross-linked polyacrylamide substrate which is photo-crosslinked to the glass slides and has specific functional groups to which the 5' end of an oligonucleotide is attached via a hexylamine linker. Then 5' amine-terminated oligonucleotides are deposited onto the polymer using piezoelectric dispensing robots (Ramakrishnan et al. 2002).

Statistical analysis of the microarray data was performed by Dr. Michael A. Black of the Statistics Department at the University of Auckland (Section 2.12.2), employing three main criteria to define whether a gene was considered to be significantly expressed.

1. P-value: < 0.05
2. LogOdds: Positive value

3. False discovery rate (FDR (Benjamini and Hochberg 1995)): < 0.1. This is the most stringent of the three criteria. Setting the FDR at 10% means that on average it is expected that there will be one false positive out of every ten genes identified as differentially expressed

These statistical criteria were used as a basis to determine whether a system could provide consistent and robust results or not.

3.2.2.1 Amersham Codelink

The Amersham system was initially trialled during a three day workshop and the experimental protocol was carried out in its entirety under the supervision of an expert Amersham representative. Subsequent arrays were done independently.

The Amersham processes uses a one colour experimental approach, therefore each sample was hybridised to its own array.

Slide specifications:

- 30mer oligonucleotide attached to the slide
- A unique polyacrylamide gel surface which the manufacturers believe creates less steric hindrance and so allows better binding of the probe to the target
- At the time only 10,000 genes were available; however, Amersham (GE Healthcare) have since released a whole rat genome array (29,000 genes spotted onto the array)
- The port injection system is this company's answer to the problem of 'spatial bias'. The slide is covered in a plastic 'flex-chamber' which allows the hybridisation solution to be injected onto the slide and to move over the slide while it is in the shaker
- A manual washing system utilising a series of wash containers, the slides are placed in a holder and moved from container to container.

Nine slides were used in total, two at the workshop and seven subsequently. There were a number of problems encountered with the Amersham protocol, including breakage of slides when injecting the hybridisation solution into the port, cRNA synthesis giving low yields due to incorrect estimation of speed-vac times and poor washing technique. Of the nine arrays prepared, five were judged good (no background, good spot definition), three poor (high background, poor spot definition) and one failed (cRNA degradation).
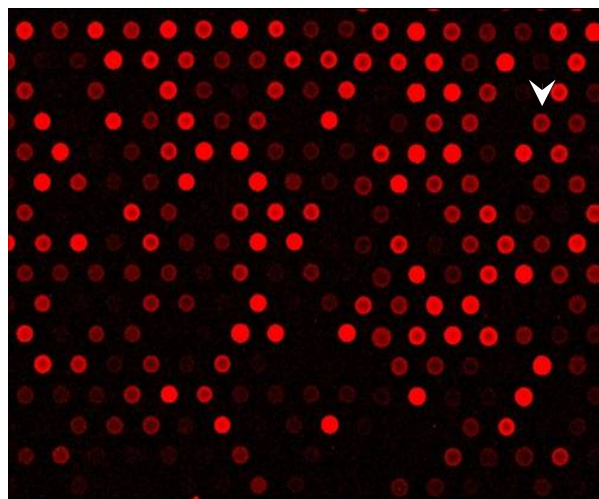
Figure 3.2 Amersham CodeLink UniSet Rat 1 Bioarrays

RNA was extracted from LV cardiac tissue of diabetic or sham male Wistar rats after six weeks as described in Section 2.2.2.1. 2µg of pooled RNA (eight diabetic and eight sham animals) was required to synthesise double stranded cDNA which was then used to make cRNA in an *in vitro* reaction during which a fluorescently labelled nucleotide (Cy5-dUTP) was incorporated. 10µg of fragmented labelled cRNA from either the diabetic or sham group were hybridised to a CodeLink UniSet Rat 1 Bioarray at 37°C for 18-24hr in a shaker incubator set at 300rpm. In this experiment, cRNA from sham or diabetic tissue was hybridised to separate arrays. Slides were washed and scanned according to Sections 2.3.3.3 and 2.3.3.4. This image represents a small section of Slide T00230236 which was hybridised with the pooled sham labelled cRNA. White arrow indicates doughnut spot.

Once the arrays were completed, the best six (three diabetic and three sham) of the nine raw data files were analysed statistically (results described below).

In order to ascertain the level of variation within this system and therefore its reproducibility, a series of comparisons were performed. These comparisons examined the Pearson's correlation coefficient values as calculated using the normalised intensity from the scanner output. For this analysis, the normalised intensity of a 'diabetic' array was plotted against the normalised intensity of another 'diabetic' array and the correlation coefficient calculated. This process was repeated for all diabetic and normal arrays. Only like arrays were compared. The expected value of the correlation coefficient was ≥ 0.98.

Table 3.1 Amersham slide comparison

A. Sham Pearson's correlation coefficient

	2	3	4	5
1	0.9225	0.6804	0.8284	0.8237
2		0.6321	0.8943	0.7913
3			n/a	n/a
4				0.9922

B. Diabetic Pearson's correlation coefficient

	2	3	4
1	0.9712	0.6801	0.873
2		0.7247	0.923
3			n/a

The highest Pearson's correlation coefficient obtained was 0.9922 (Table 3.1(A and B)); however the values ranged from as low as 0.621 to 0.9922, indicating a high degree of variation between slides from the same experimental group.

Table 3.2 Diabetes vs. sham top 10 genes

LocusID	Name	Fold Change	M	t	P-value	LogOdds
29669	NM_017279_Probe1	49.8	5.6	7.7	0.9	-4.6
0	AI169353_Probe1	-13.9	-3.8	-4.4	1.0	-4.6
0	BLANK	15.0	3.9	4.3	1.0	-4.6
0	BF284818_Probe1	-10.1	-3.3	-4.3	1.0	-4.6
0	BLANK	-13.2	-3.7	-4.1	1.0	-4.6
306764	BF392695_Probe1	12.9	3.7	4.1	1.0	-4.6
79220	Z17239_Probe1	-9.4	-3.2	-4.0	1.0	-4.6
361538	AI233266_Probe1	14.4	3.9	4.0	1.0	-4.6
25372	M87855_Probe1	14.6	3.9	4.0	1.0	-4.6
24504	NM_012590_Probe1	-13.3	-3.7	-4.0	1.0	-4.6

(Data from six arrays only)

Table 3.2 above presents data from a small subset of genes, based on fold-change. Statistical analysis found that although there were large fold-changes, none were statistically significant. This is due to the high variation in signal intensity between the slides, as indicated by the correlation analysis.

When studying the values from the Amersham analysis, it was of note that none of the three statistical criteria (P-value, LogOdds and FDR) were met. These findings indicated lack of sensitivity of this system in detecting significant changes in gene expression due to wide variability between the slides.

3.2.2.2 Agilent

Agilent provided a workshop at Melbourne University attended by Dr. F. Pichler and Liam Williams of the Centre for Genomics and Proteomics, School of Biological Sciences. The pooled diabetic and sham RNA samples were shipped to Australia for use in the experiment. These were run on the Agilent Bioanalyzer (see section 2.2.2.3 for method description), in Melbourne to ensure they were still of the highest quality (see Appendix 1 for images from Bioanalyzer).

Slide specifications:

- 60mer oligonucleotide - the longer oligonucleotides on the Agilent array have been found to provide the best compromise between specificity and sensitivity (Hughes et al. 2001).
- Inkjet array synthesis method - using chemical deprotection with synthesis via

inject technology. The bases are fired onto the array using modified inkjet nozzles. This technology is very flexible and of the highest quality achieving regular even spots. (Blanchard et al. 1996)

- This system incorporates a hybridisation chamber, where metal casings hold the arrays while still providing room for the hybridisation solution to move over the slide and thus reduce the effects of spatial bias (SureHyb® Chamber)

- Two-colour system (competitive hybridization) thus two samples are labelled, one with a green fluorescent dye (Cy3) and one with a red fluorescent dye (Cy5).
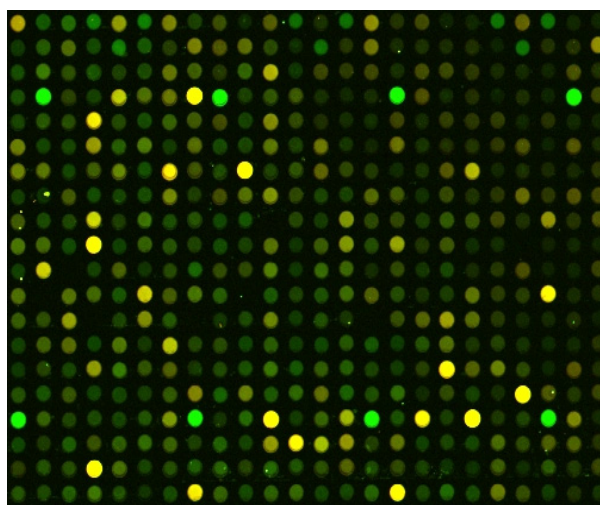
Figure 3.3 Agilent 22K Rat Oligo Microarray

RNA was extracted from LV heart tissue of diabetic or sham male Wistar rats after six weeks as described in Section 2.2.2.1. 500ng of pooled RNA (eight diabetic and eight sham animals) was required to synthesise double stranded cDNA which was then used to make cRNA in an *in vitro* reaction during which a fluorescently-labelled nucleotide, either Cy3-UTP or Cy5-UTP was incorporated. 0.75ng of labelled cRNA from each group (diabetic or sham) was combined and then hybridised to an Agilent 22K Rat Oligo microarray slide at 60°C for 16hr in a hybridisation oven rotating at 4rpm. Slides were washed and scanned according to Sections 2.3.4.3 and 2.3.4.4. The figure represents a small section of Slide PBC_251186824772. In this slide, sham cRNA labeled with Cy3-UTP (green fluorescent dye) and diabetic cRNA labeled with Cy5-UTP (red fluorescent dye) were hybridized to an Agilent 22K Rat Oligo Microarray. Streaking is visible across the right corner with lower spot intensity than when compared to left corner.

Agilent provided us with five microarray slides. Of the five processed slides only one was considered satisfactory (no background or streaking on the slides) and four were poor (streaking and high background). Figure 3.3 represents a sham vs. diabetic Agilent slide and highlights the streaking which occurred on four of the five slides. This streaking meant that some areas of affected slides gave stronger signals than others and may have contributed to an increase in variation within the results. This was verified in the statistical analysis provided by Dr. Michael A. Black for these slides.

Agilent is a two-dye system; therefore a slightly different method was used to analyse within-platform variability. Two of the five slides used were 'self-slides' where either normal or diabetic were labelled with both the green (Cy3) and red (Cy5) and applied to a slide. By plotting the red and green intensities against each other, an understanding of within-slide variation can be obtained.

Two of the five slides were sham vs. diabetic so a second way of identifying inter-slide variation was to take the Cy3 sham data from both slides and plot them against each other and the Cy5 diabetic data from both slides and plot them against each other.

Table 3.3 Agilent slide comparison

	Pearson's r
Sham Cy3vCy5 Self Slide	0.9851
Diabetic Cy3vCy5 Self Slide	0.9705
Sham Cy3 labelled samples from slides 71 and 72	0.9924
Diabetic Cy5 labelled samples from slides 71 and 72	0.9951

The Pearson's r values for Agilent (Table 3.3) were much higher than that seen with the Amersham data; however there was still some variation, particularly in the 'self' slides which was of concern as these slides are the same sample and as such should have had the highest correlation.

Table 3.4 Diabetes vs. sham top 10 genes

LocusID	Name	Fold Change	M	A	t	P-value	LogOdds	FDR
0	203514_Rn	5.7	2.5	13.4	22.9	0.01	4.3	0.01
0	222177_Rn	5.3	2.4	14.0	21.6	0.01	4.2	0.01
0	218109_Rn	7.9	3.0	12.4	21.4	0.01	4.2	0.02
29237	NM_017139	5.7	2.5	13.9	20.8	0.01	4.1	0.02
117543	NM_057197	5.7	2.5	13.2	20.5	0.01	4.1	0.02
363499	AI579422	12.1	3.6	10.6	20.4	0.01	4.1	0.02
0	201227_Rn	4.0	2.0	10.8	19.0	0.01	4.0	0.02
0	200418_Rn	3.9	2.0	10.0	17.8	0.01	3.8	0.02
0	327164_Rn	13.3	3.7	10.3	17.2	0.01	3.7	0.02
0	297985_Rn	4.0	2.0	11.4	16.8	0.01	3.7	0.02

Table 3.4 above presents data from a subset of the total number of genes identified by Agilent microarrays. From this it can be concluded that the Agilent data met all the statistical criteria and so could be considered robust enough for use in our subsequent microarray studies.

However there were some concerns about reproducibility of the data when the reports of the experimental process (Liam Williams and Dr. F. Pichler, School of Biological Sciences, personal communication) and subsequent correlation analysis were taken into account.

3.2.2.3 Affymetrix

Affymetrix also provided a workshop to trial their system. The cRNA was produced using the pooled RNA diabetic and sham samples, prior to the arrival of the Affymetrix representative. The cRNA was made according to the protocol described in Section 2.3.5.1 and the quality was assessed using the Agilent Bioanalyzer at each of the stages required.

Affymetrix supplied eight arrays, four for the diabetic and four for the sham samples. Four of the arrays were from one batch and four from another to test for batch-to-batch variability. Affymetrix uses a one-colour experimental method, similar to that of Amersham.

The specifications of the slides (GeneChips®) are:

- 25mer oligonucleotide target – each gene is represented by 11 perfect match/mismatch pairs scattered randomly around the array. The signal intensity from each of the 11 pairs is combined to give the overall signal intensity. The perfect match-mismatch system is designed to reduce the error introduced through non-competitive hybridisation. The mismatch oligonucleotide is identical to the perfect match oligonucleotide with one base pair difference. When analysing the signal intensity of any given gene the Affymetrix software looks at the intensity of the signal from the mismatch oligonucleotide compared with that of its perfect match pair. If the signal is equal or higher than the perfect match pair then the oligonucleotide target is discarded from the analysis as having too much interference (Affymetrix 2001). 28,000 genes were represented

- Photolithographic printing method – Another *in situ* oligonucleotide synthesis method that uses light to convert the protective group on the terminal nucleotide into a hydroxyl group to which further bases can be added. Affymetrix technology is well suited to making large quantities of 'standard arrays' that can be widely used (Stekel 2003)

- Port injection/Rotating hybridisation

- Biotin-UTP label / Phycoerythrin-streptavidin detection

- Automated washing using the Affymetrix Fluidics Station 450, which is able to wash and stain up to four arrays at a time per station. Stations can be linked together to increase throughput.

The Affymetrix system is quite different from the other three systems trialled. Instead of using conventional glass slides as in the Agilent or Amersham systems, the Affymetrix slides start out as a 5″ x 5″ quartz wafer, and depending on the demands of the experiment and the number of probes required per array, each quartz wafer can be diced into tens or hundreds of individual arrays (http://www.affymetrix.com). Each individual

array is protected by a special plastic casing (illustrated in Figure 3.6(B)), which ensures that the array itself does not need to be handled by the investigator, something which was of great concern when processing the Agilent and Amersham arrays. The septa at the back of the plastic cartridge provide a port into which hybridisation or wash solutions can be injected (Figure 3.4(B)). This design allows the Affymetrix system to have an automated wash protocol. The fluidics station design includes two needles that insert into the septa and inject in or withdraw the wash/staining buffers at different stages of a wash protocol that is computer controlled.
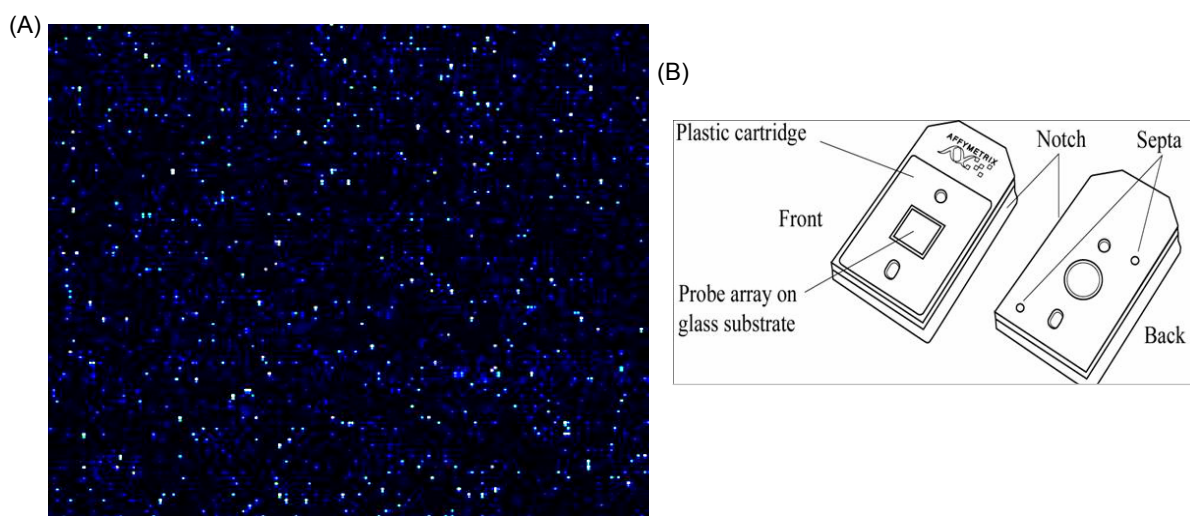
Figure 3.4 Affymetrix Rat 230 2.0 GeneChip

RNA was extracted from LV heart tissue of diabetic or sham male Wistar rats after six weeks as described in Section 2.2.2.1. 5µg of pooled RNA (eight diabetic and eight sham animals) was required to synthesise double stranded cDNA which was then used to make cRNA in an *in vitro* reaction during which a biotin label was incorporated. 15µg of fragmented biotin-labelled cRNA from either the diabetic or sham group were hybridised to an Affymetrix Rat 230 2.0 GeneChip® at 45°C for 16hr in a rotating hybridisation oven set at 60rpm. In this experiment sham or diabetic cRNA were hybridised to separate arrays. Slides were washed and scanned according to Section 2.3.5.2. Fluorescent signal is obtained using streptavidin-phycoerythrin which binds to the biotin-labelled cRNA.
(A) Image represents a section of Slide 4002970, RNA from the LV of eight sham animals (pooled).
(B) Schematic of Affymetrix GeneChip cartridge with all major features labelled to illustrate the different microarray slide format utilised by Affymetrix.

Of the eight arrays processed, all were considered to be of good quality due mostly to the automated washing system which ensured very little user bias or variability was introduced during this vulnerable part of the process. The data from this study was again analysed by Dr. Michael A. Black.

As with the Amersham platform variability comparison, the normalised intensity of a 'diabetic' or 'sham' array was plotted against the normalised intensity of the other

'diabetic' or 'sham' arrays and the correlation coefficient was calculated. The expected value of the correlation coefficient was ≥ 0.99.

Unlike the Amersham arrays, the Affymetrix arrays (Table 3.5) consistently had Pearson's correlation coefficient values >0.99, consistent with a high correlation between replicates.

Table 3.5 Affymetrix slide comparison

(A) Sham Pearson's correlation coefficient

	2	3	4
1	0.9979	0.994	0.9975
2		0.9938	0.9962
3			0.9968

(B) Diabetic Pearson's correlation coefficient

	2	3	4
1	0.9979	0.9978	0.9975
2		0.9975	0.9975
3			0.9975

Table 3.6 presents data from a subset of the total number of genes identified by Affymetrix GeneChips®. From this we can conclude that the Affymetrix data met the inclusion criteria for all three statistical tests and so, like the Agilent platform, met the requirements for our subsequent microarray studies. Unlike with the Agilent arrays, however, there were no concerns with reproducibility or questions over the experimental process.

Table 3.6 Diabetes vs. sham top 10 genes

LocusID	Affymetrix ID	Fold Change	M	A	t	P-value	Log Odds
116720.00	1369050_at	28.2	4.8	6.9	71.1	0.000	22.1
89813.00	1369150_at	7.5	2.9	9.8	68.5	0.000	21.1
0.00	1388924_at	40.2	5.3	7.0	68.4	0.000	21.1
0.00	1374765_at	-9.5	-3.3	5.7	-65.5	0.000	21.7
50559.00	1398250_at	24.4	4.6	4.9	62.0	0.000	21.3
0.00	1388802_at	15.3	3.9	7.3	57.3	0.000	20.9
25139.00	1367989_at	-5.9	-2.6	8.7	-55.0	0.000	20.6
24450.00	1370310_at	28.6	4.8	7.0	53.2	0.000	20.4
29557.00	1367928_at	4.4	2.1	11.1	53.1	0.000	20.4
0.00	1396165_at	-5.1	-2.4	10.2	-51.7	0.000	20.2

3.2.3 Definition of significant change in gene expression

At the time these experiments were conducted, a commonly used method to define a 'significant' gene change was the level of fold-change between two groups (F. Pichler, Michael A. Black, University of Auckland, personal communication). If we use this rationale for looking at the current array data, then the Amersham arrays provided the greatest number of significant changes as shown in Figure 3.5 below.
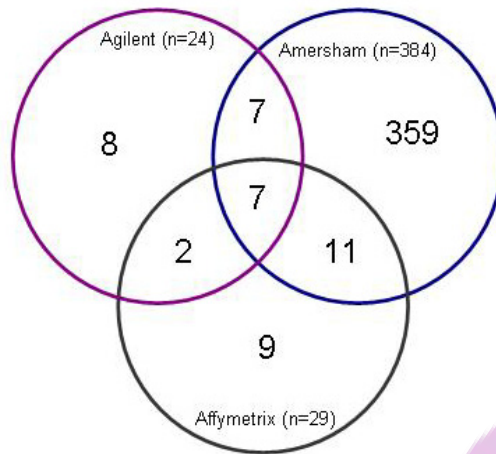
Figure 3.5 Venn diagram of the distribution of significant genes, using a 1.5-fold cut off, of the subset of genes that are common between all three systems

Fluorescent image data obtained from the Amersham, Agilent and Affymetrix microarray systems using pooled RNA collected from LV heart tissue of eight sham and eight diabetic animals after six weeks were collected and analysed as in Section 2.12.2.

This Venn diagram represents fold-change values generated for each common gene represented on the Agilent, Amersham or Affymetrix microarray systems which were ranked from the greatest positive fold-change to the greatest negative fold-change. Genes were identified as common to all three systems using GenBank accession numbers as this identifier was general to all three systems.

The number of genes with a fold-change of >1.5 and > (-1.5) for each system that was unique (outside circles), common to one other system (two circles interconnected) or common to all systems (all three circles interconnected) are displayed. n= total number of common genes in that system with a fold-change >1.5 and > (-1.5)

Figure 3.5 shows that there is very little correlation between the three systems and that the Amersham system provided the greatest number of gene changes. However, when using this fold-change method the slide variability described previously, was not taken into account and could have led to the misidentification of important or relevant gene expression changes.

Another way of looking at significance is to consider the P-value of the change in gene expression. Use of this method allows even very small fold-changes in gene expression to be considered. If this criterion is applied to the three data sets then we can see that the data from the Amersham platform no longer contains any genes that would be considered significant compared to the data from the Affymetrix or Agilent platforms (see Figure 3.6). The degree of variation observed, although not as great as that seen with the Amersham data, in the data from the Agilent system also becomes apparent with a very low number of significant differentially expressed genes reported.
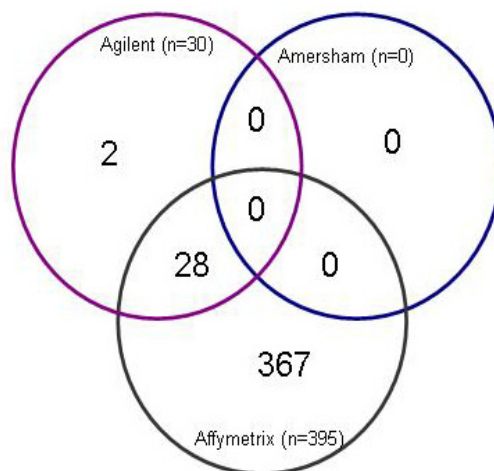
Figure 3.6 Venn diagram of the distribution of significant genes, at a P<0.05 cut-off, of the subset of genes that are common between all three systems

Fluorescent image data obtained from the Amersham, Agilent and Affymetrix microarray systems using pooled RNA collected from LV heart tissue of eight sham and eight diabetic animals after six weeks was collected and analysed as in Section 2.12.2.

This Venn diagram represents fold-change values generated for each common gene represented on the Agilent, Amersham or Affymetrix microarray systems which were ranked according to their P-value. Genes were identified as common to all three systems using GenBank accession numbers as this identifier was general to all three systems.

The number of genes with a P<0.05 for each system that was unique (outside circles), common to one other system (two circles interconnected) or common to all systems (all three circles interconnected) are displayed: n= total number of common genes in that system with a P<0.05.

The results from the Amersham system were therefore not included in any subsequent analysis, as the results described here and in Section 3.2.2.1 give a clear indication that this system would not have provided the calibre of data required.

3.2.4 Inter-platform variability

One of the main points considered in this study is that, as well as providing the highest possible quality of data, the results obtained should be comparable to those that would be obtained by other research groups, if they repeated these experiments.

Each platform had its own set of unique identifiers for each gene. In order to be able to compare between platforms, a common identifier was required; in this study genes represented on the array platform with the same GenBank accession number were matched. This resulted in 2888 genes that were detected in common by both the Affymetrix and Agilent systems. It is interesting to note how few genes the platforms have in common compared to the total number of genes printed on each array system.

The first step of this analysis was to create a pairwise scatter plot of the two array systems being compared (Affymetrix and Agilent), using only the genes with the same accession number (Figure 3.7). This comparison included all fold-change values from each of the platforms looked at, regardless of significance.
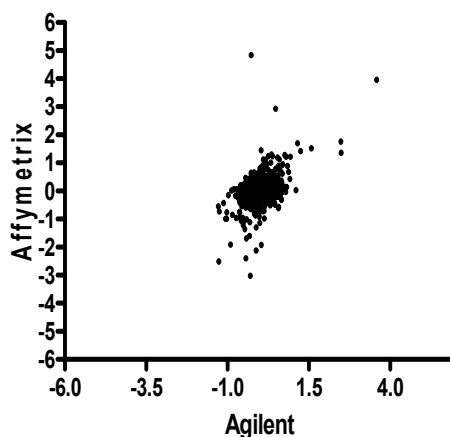
Figure 3.7 Plot of all fold-change values from Agilent slides plotted against all fold-change values from Affymetrix slides

Fluorescent image data obtained from the Agilent and Affymetrix microarray systems using pooled RNA collected from LV heart tissue of eight sham and eight diabetic animals after six weeks, were collected and analysed as in Section 2.12.2. A total of 2888 genes were identified as common to both systems using the GenBank number as a common identifier. Fold-change values were plotted against each other regardless of whether they were identified as significant. The Pearson's correlation coefficient for this correlation was 0.3787

Correlation between the two platforms was found to be only 37%. It has been hypothesised that the reason for the low correlation between different microarray systems was due to very little consistency between the sequences used to identify a gene (Park et al. 2004, Mecham, 2004 #184). In order to determine whether this was true for our cross-platform analysis, 1000 of the 2888 probes common to both Affymetrix and Agilent (based on GenBank ID) were randomly selected (regardless of P-value to give a larger pool from which to choose) and submitted to eArray (http://earray.chem.agilent.com). This website enables the user to extract Agilent's 60mer sequence for any queries. The 1000 GenBank ID's returned 825 probes from Agilent that corresponded to actual sequences that were able to be used for further study. Figure 3.8 is the scatter plot of these 825 probes.
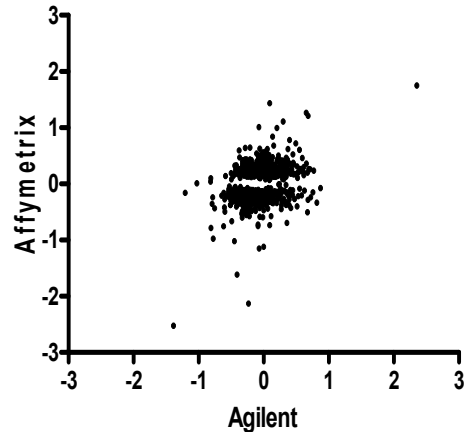
Figure 3.8 Initial correlation analysis of 825 probes common to the Agilent and Affymetrix microarray systems to be used in probe match analysis

Fluorescent image data obtained from the Agilent and Affymetrix microarray systems using pooled RNA collected from LV heart tissue of eight sham and eight diabetic animals after six weeks were collected and analysed as in Section 2.12.2. Of the total 2888 genes identified as common to both systems using GenBank accession numbers as the common identifier, the Agilent probe sequence for 825 genes was obtained from the eArray website (http://earray.chem.agilent.com). Fold-change values are plotted against each other regardless of whether they are identified as significant. The Pearson's correlation coefficient for this correlation is 0.3783

Next the 'Probe Match' function which is available through the Affymetrix website (https://www.affymetrix.com) was used to identify which Affymetrix 25mer-oligonuclotide probes these Agilent sequences matched. Each was then manually checked to ensure that the Affymetrix Probe ID supplied from the 'Probe Match' analysis corresponded to the Affymetrix Probe ID given in the original data. Due to the high level of redundancy within the Affymetrix system some of the probes ID's identified by the 'Probe match' analysis were not the same as the GenBank ID from the original data but did correspond to the same gene. These were included in the analysis.

Of the 825 genes studied, 410 had the same probe sequence. Figure 3.9 illustrates the correlation between these matched genes. Once this analysis is performed the correlation between the two platforms increased slightly from 0.3783 to 0.4133.
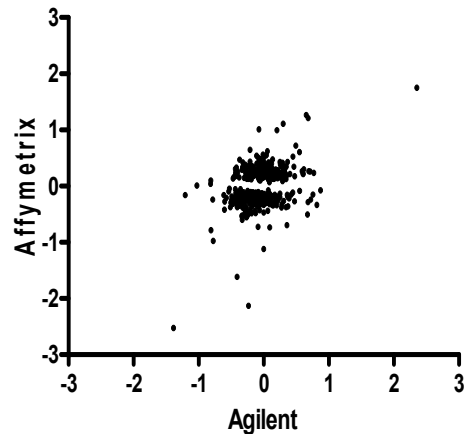
Figure 3.9 Correlation between sequence matched probes of the Agilent and Affymetrix microarray systems

Fluorescent image data obtained from the Agilent and Affymetrix microarray systems using pooled RNA collected from LV heart tissue of eight sham and eight diabetic animals after six weeks were collected and analysed as in Section 2.12.2. Sequence matching was performed using 825 probes with known sequence from the Agilent system and the Affymetrix website probe match function (https://www.affymetrix.com). Of the 825 original Agilent probes 410 had a corresponding Affymetrix sequence as identified by the probe match function. The Pearson's correlation coefficient for this correlation is 0.4133

Given the low level of correlation between the systems observed in the study above and the high level of variation seen within the Agilent system we decided to look at the correlation between genes with a P-value of P≤0.05 regardless of probe sequence matching. It was decided that the system and user introduced variation had strongly influenced the the resulting changes in gene expression identified by the Agilent system. In order to truly identify a correlation between the two systems, only results with low variation (such as those with a significant P-value) should be used for comparison. The resulting scatter plot can be seen in Figure 3.10. Here we see that the correlation coefficient from this analysis was much stronger than any previously observed between platforms indicating that variation has a strong influence on the ability to compare between two systems and should be considered carefully when assessing data from microarray systems.
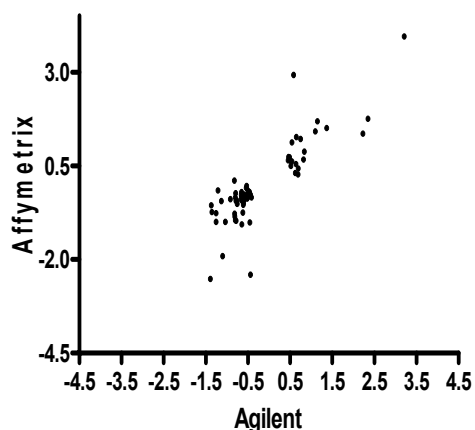
Figure 3.10 Correlation between Agilent and Affymetrix, fold-change values with P<0.05

Fluorescent image data obtained from the Agilent and Affymetrix microarray systems using pooled RNA collected from LV heart tissue of eight sham and eight diabetic animals after six weeks were collected and analysed as in Section 2.12.2. Fold change values generated for each common gene (as defined by their GenBank accession number) represented on the Agilent or Affymetrix microarray systems were ranked according to their P-value. Of the 2888 genes identified as common to both systems 67 were deemed significant at the P<0.05 cut off. Fold-change values are plotted against each other and the Pearson's correlation coefficient for this correlation is 0.8533.

Figure 3.10 also indicates that even genes with a very small fold-change (even those close to zero) correlated with each other. The low number of XY pairs in this correlation is due to the low number of significant genes in the Agilent data set which correspond to significant genes in the Affymetrix data set. The low level of significant genes identified by Agilent is likely due to the problems which occurred when the slides were washed (as described in Section 3.2.2.2).

3.3 Discussion

3.3.1 Overview of the three commercially available systems

The objective of this work was to identify a microarray system that would provide us with data of the highest quality and reproducibility, given the poor quality of results seen with the original microarray platform chosen.

Table 3.7 below presents an overview of the three commercially available systems reviewed in this study.

Table 3.7 Overview of all three systems

	Amersham	**Agilent**	**Affymetrix**
Oligonucleotide Length	30 bases	60 bases	25 bases
Gene number	10,000 rat genes (Whole genome now available 29,000 rat genes)	20,000 rat genes	28,000 rat genes (230 2.0 Array)
Array Type	One colour	Two Colour	One Colour
Printing method	Spotted Inkjet	Inkjet	Photolithography (masks)
Arrays used	9 used, 5 good, 3 poor & 1 fail	5 used, 1 good & 4 poor	8 used, 8 good
Cost per array* (NZD)	$1757	$1453	$1453
Unique Features/Benefits	3D gel matrix on slide "Flex-Chamber" technology Potential for 4 chambers per slide.	Hybridisation chamber Printing technology	Well established Package system Internal controls Automated washing
Potential problems	Doughnut spots Background Manual washing	Two colour system Manual washing	Cost Light leaking through masks potentially giving poor spot quality

*Costing includes cost of array and all reagents required to carry out one slides hybridisation and washing steps. Values were accurate as of 2004.

As mentioned in the introduction to this chapter, the most important factors to consider when choosing a microarray platform are: hybridising the probe to the array, the washing and staining of slides, spot finding, single versus competitive hybridisation, cost and ease of use. It has become apparent throughout the course of this study that of these, perhaps the most critical is the washing and staining of the slides. This part of the experimental procedure impacted greatly on the quality of the results and is also the cause of greatest user variation.

The wash/stain protocol can also affect other aspects of the experimental design. For example, one issue with both the Amersham and Agilent systems was that their inherent experimental variability (seen through our own work) meant that single animal arrays were not feasible. In a true experimental situation, these two systems would require pooling of the RNA samples. This has implications for assessing variation within the population, as outliers may skew results (Affymetrix 2004). This problem was overcome by the Affymetrix system. As indicated in Section 3.2.2.3, the correlation between arrays hybridised with RNA from the same experimental group was consistently greater than 0.99 compared to the other two systems, which showed lower correlations, indicative of greater variation. This was particularly evident with the Amersham system. The ability of the Affymetrix system to perform single animal arrays was judged to be able to provide us with a very powerful data set for further analysis.

The results of this particular study have provided a valuable insight into the ability of each of the systems to perform in untrained hands. Affymetrix was the only system which provided consistently good results for an inexperienced operator. Although the other two systems might eventually provide data of a similar standard to that of Affymetrix, the time and associated costs of the work required would have negated the lesser initial outlay of the systems.

In light of both the qualitative results and semi-quantitative statistical analysis performed we decided that the Affymetrix GeneChip system would provide the required high standard of data for subsequent studies. Affymetrix gave superior results in all of the five original qualitative criteria compared with the other systems and also had the lowest user-associated variation.

3.3.2 Correlation between Affymetrix and Agilent Systems

Analysis of the correlation between different systems is an important factor in the understanding of data from microarray analyses between different research groups. Our initial analyses found that there was a very poor correlation between the Agilent and Affymetrix systems and that the number of common genes represented on each set of arrays was minimal when compared to their overall gene potential. The low number of common genes and variations in nomenclature makes comparison of the two systems very difficult.

Other available comparison studies such as that by Mecham *et al*., (Mecham et al. 2004) discussed the idea that sequence matching between two systems was necessary to obtain good correlation. They reported an increase of mean Pearson's correlation coefficient from 0.35 to 0.61 when looking at unmatched versus matched probe sequences (Mecham et al. 2004). In this study, the correlation did increase with sequence matched probes, but it was not to a substantially greater level.

In another study, by Yauk *et al.* (Yauk et al. 2004), wherein six different microarray systems were compared, comparable results between Affymetrix, Agilent Oligonucleotide and Amersham Codelink without sequence matching, were reported. This result indicates that, perhaps between shorter oligonucleotide arrays, sequence matching is not necessary (Yauk et al. 2004).

In the current study variation within systems played a major role in determining correlation between systems. Due perhaps to the lack of operator experience in using microarrays, a number of mistakes occurred that increased the variation within the data. This was particularly evident with both the Amersham arrays providing no significant data due to variation and the much improved correlation between Affymetrix and Agilent when

the data set was reduced to genes with a significant (P<0.05) change in gene expression (Figure 3.10).

In a study by Park *et al.,* (Park et al. 2004), three different microarray systems were studied: Affymetrix, a custom cDNA array (Agilent) and a custom oligo array (MEG biotech). The authors found that by filtering the genes according to intensity (low intensity genes tend to have a higher and more variable differential expression ratio), the correlation coefficient increased as the signal intensity increased. They concluded that even though the overall correlation may be low, the log ratios of the highly expressed genes (defined by a greater intensity) could be strongly correlated and were likely to be more reliable estimates than is suggested by the overall correlation coefficient (Park et al. 2004). The phenomenon is evident in the current study, when only the genes with a significant P-value of ≤0.05 are included in the correlation analysis. These genes have less variation and are therefore more reliable and thus give a stronger correlation.

A more recent report (Larkin et al. 2005) also emphasised this point. The hypothesis in this study was 'given a biological question evaluated on two different microarray platforms are there platform-specific differences that mask the underlying biological response' (Larkin et al. 2005). This group compared a cDNA platform (TIGR) and the Affymetrix array platform and concluded that there is a variety of factors that may contribute to the independence of results from a platform. These included:

1. Advancement of technology – technology has progressed rapidly over the last 5 years; however, if only one of the two platforms gives reliable consistent data, then comparisons between the two platforms are meaningless.

2. Gene expression values can be compared effectively only if the genes are accurately identified on both platforms using techniques such as sequence matching.

In our current study it appears to be the former that is having the greatest influence on platform comparability.

3.4 Conclusions

Overall it can be concluded that the Affymetrix GeneChip system provided the most consistent and reliable data and met each of the five qualitative measures outlined in the introduction. This study highlights the impact of user variation on microarray results The results presented here suggest that by reducing this variation it is possible to not only increase the robustness of the data but also to reduce the overall cost of the experiment by lowering the number of arrays required to obtain statistically significant results.

Chapter 4 Assessment of differences in the transcriptome between STZ-diabetic and sham LV heart tissue at sixteen weeks

4.1 Introduction

As stated in Section 1.1, the existence of diabetic cardiomyopathy as a distinct clinical entity is still uncertain (Fang et al. 2004). However, there is a large body of literature related to the pathogenesis of DCM and increasing evidence suggests that altered substrate supply and utilization by cardiac myocytes could be a primary injury in the pathogenesis of the disease (Fang et al. 2004).

In the normal heart, use of carbohydrate or FA as the predominant energy source varies, depending on carbon substrate supply, myocardial workload and relative oxygen supply (Lopaschuk 2002). The normal heart is able to adapt to acute and chronic changes in its workload by alternating between fuels to achieve the most efficient respiration (Taegtmeyer et al. 2004). In diabetes, however, there is an altered metabolic environment due to increased blood glucose, resulting in impaired glycolysis and glucose oxidation, decreased lactate oxidation and a greater dependence of the heart on FFA as a source of acetyl-CoA (Section 1.1.3) (Taegtmeyer et al. 2004). In uncontrolled diabetes FA oxidation provides most, if not all (90-100%) of the ATP requirements of the heart. This switch to almost exclusive use of FA, over carbohydrate, as a fuel appears to be induced by high circulating levels of FA and alterations in the control of its oxidation (Sakamoto et al. 2000).

Until now, the complex nature of DCM has made it difficult to examine all the concomitant changes in gene expression that interact to generate the observed pathophysiology. The advent of microarray technology, which provides a global view of changes in gene expression (Schena et al. 1995), has meant that it is now possible to simultaneously determine alterations in the expression of thousands of genes and thus get an understanding of modifications to the complex metabolic pathways involved in the disease. Previous technology such as quantitative real-time PCR was limited by the number of reactions that could be carried out at any one time and cost.

The overall aim of this study was to assess all the changes in gene expression of the left ventricle occurring after 16 weeks of STZ-induced diabetes using microarray technology. A global study of this nature had not been conducted previously and by using this experimental design the analysis of multiple changes occurring over a range of

pathways is possible. Through understanding all the changes that are occurring at the gene level, this study will enable the combination of the vast majority of work that has been conducted at a single pathway level in this area previously.

This chapter describes an initial pilot study that was set up in order to ascertain whether a stable model of STZ-induced diabetes could be established and maintained for a period of sixteen weeks to allow analysis of the rat heart LV at the transcriptomic level. The analysis of data from the comparison of diabetic vs. sham animals provides not only an indication of gene changes occurring in the development of diabetes but also the baseline data required for any subsequent studies. This study also aimed to enable further optimisation of the Affymetrix GeneChip system, which we had previously determined would achieve the most reliable results (see Chapter Three).

In addition, two main areas were chosen as a research focus for the study. The first related specifically to the changes in diabetic cardiomyopathy and metabolic inflexibility in energy utilisation and the second attempted to apply a more general hypothesis, consistent with that presented by Brownlee *et al.,* ((Brownlee 2001),Section 1.2) to this data set, to see if a correlation was able to be found between these two bodies of work. A paper encompassing a major portion of data from this work has been published previously (Glyn-Jones et al. 2007).

4.2 Results

4.2.1 Characterisation of the STZ-diabetic model at sixteen weeks

Diabetes was induced as described in Section 2.1, and subsequently confirmed in the experimental animals three days later. Diabetic (STZ) rats were maintained for the duration of the sixteen week study without insulin supplementation. As a result of this, diabetic animals had an average blood glucose level of 27.7 ± 1.4mM, compared to sham animals which had average blood glucose of 4.8 ± 0.1mM (Table 4.1, Figure 4.1 (A)). Figure 4.1(A) shows the persistent elevation of blood glucose levels of the diabetic rats over the course of the sixteen week study. Here it is evident that the diabetic animals maintained high blood glucose levels for the entire length of the study while sham animals continued to display blood glucose levels within the normal range. Diabetic animals also displayed attenuated weight gain (final weight: STZ, 314 ± 54g; sham, 506 ± 45g) and hyperphagia (STZ animals consumed an average of 649 ± 60g of food/week compared to the sham average of 391 ± 27g). Figure 4.1(B) is a representation of animal weights over the course of the sixteen week study.
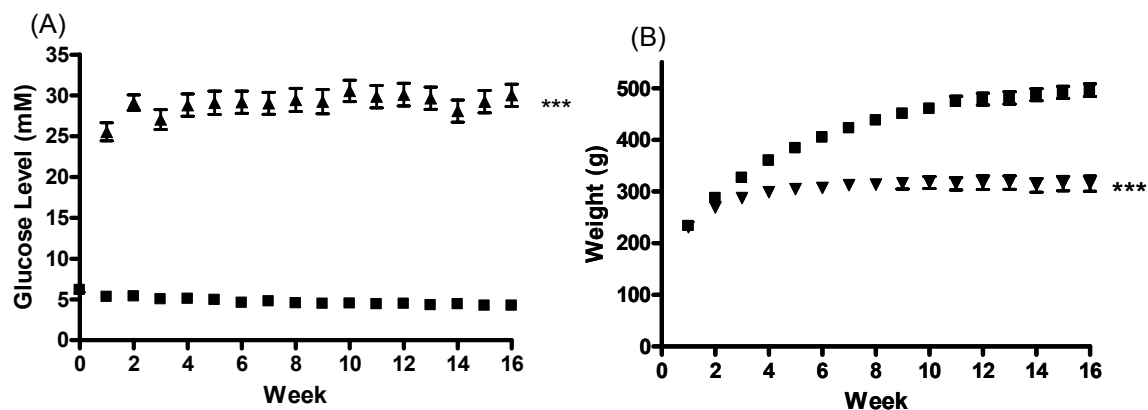
Figure 4.1 Gross characterisation of STZ diabetic model

Male Wistar rats (220-250g) anesthetised using 5% halothane, 2l/min O_2, and 60mg/kg streptozotocin (STZ) dissolved in saline was immediately injected into the tail vein to induce diabetes. Sham rats received the corresponding volume of saline only. Animals were housed in pairs on fibrecycle bedding (12-hr light:dark cycle, 50-70% humidity, 19-21°C) and maintained on Teklad TB 2018 (Harlan, UK) rat chow and tap water *ad libitum*. Values are means ± SEM (n=19 for each group).

(A) Animal blood glucose measurements were made weekly between 8-11am using the Advantage II system (Roche Diagnostics, Basel, Switzerland). Sham (■), diabetic (▲),*** $P < 0.0001$

(B) Animals were weighed on a weekly basis for sixteen weeks. The diabetic animals (▲) only gained weight for the first 3 weeks and then levelled off, while the sham animals (■) continued to gain weight over the course of the study. *** $P < 0.0001$

Table 4.1 illustrates a selection of biochemical serum markers from tests carried out on terminal serum samples. Diabetic animals were hyperlipidaemic, with significant increases in both triglycerides and FFA compared to the sham animals. These same animals had impaired liver function with increases in both alanine aminotransaminase (ALT) and alkaline phosphatase (ALP). ALT leaks into the circulation following hepatocyte damage, while acute liver damage sees a dramatic rise in its levels. ALP is an enzyme present in the cells lining the biliary ducts of the liver. Its levels in plasma rise due to a large bile-duct obstruction, intrahepatic cholestasis or infiltrative diseases of the liver (2006). These alterations may be indicative of diabetes-induced steatosis or steatohepatitis. Indications consistent with impaired kidney function presented here were decreased albumin and total protein levels (Table 4.1).

Diabetic animals also showed signs of electrolyte imbalance, with decreased plasma sodium concentrations and increased chloride values. This may be due to polydipsia, at least in part, since the STZ animals drank on average 222 ± 37ml of water per day compared to the sham average of 37 ± 8ml.

Table 4.1 Biochemical markers in serum from STZ-diabetic and sham rats

	Sham	Diabetic
Glucose	4.8 ± 0.1 n=15	27.7 ± 1.4 n=15***
Triglyceride	1.6 ± 0.2 n=15	4.4 ± 0.9 n=15**
FFA	1.2 ± 0.1 n=15	2.4 ± 0.2 n=15***
Cholesterol	1.9 ± 0.16 n=5	1.4 ± 0.1 n=5*
ALP	99.9 ± 2.9 n=17	420 ± 44.3 n=15***
ALT	41.5 ± 1.5 n=17	76.6 ± 7.0 n=13***
Bilirubin	5.2 ± 0.4 n=17	6.8 ± 0.6 n=14*
Albumin	15.8 ± 0.3 n=16	13.5 ± 0.2 n=13***
Total Protein	61 ± 0.7 n=12	52 ± 1.3 n=12 ***
Sodium	142 ± 0.6 n=15	133 ± 0.7 n=11***
Potassium	4.3 ± 0.1 n=15	4.0 ± 0.2 n=9
Chloride	90 ± 1.3 n=7	103 ± 0.5 n=7***
Ferroxidase	314 ± 12 n=17	314 ± 13 n=13

*$P< 0.05$, **$P< 0.01$, ***$P< .0001$ vs. respective controls.
Values represent mean ± SEM.

Data presented in Figure 4.2 (A) show that the absolute heart weight of the diabetic animals was significantly reduced compared to that of the sham animals. Figure 4.2(B), however, demonstrates that there was an increase in the heart weight/body weight ratio (HW/BW) in diabetic animals compared to that of the sham. This finding is consistent with cardiac hypertrophy in the diabetic animals in the current study, and coincides with the previous findings (Chen, S. et al. 2000; Depre et al. 2000; Candido et al. 2003; Cooper et al. 2004).

Collectively this data demonstrates the model has mild to severe diabetes and changes consistent with developing diabetic cardiomyopathy.
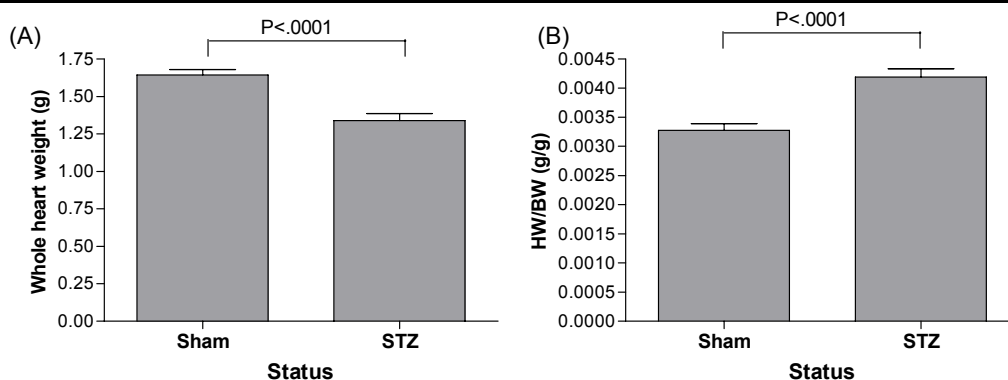
Figure 4.2 Heart weight and heart weight/body weight comparison

Sixteen weeks after injection with either STZ (diabetic) or saline (sham), male Wistar rats were placed in an induction box with halothane 5%, O_2 2l/min. Once under anaesthetic, animals were weighed (Final BW). They were thereafter maintained on halothane 2-3%, O_2 2l/min and complete anaesthesia was confirmed by testing pedal withdrawal (reflex absent). Animals were euthanized by cervical dislocation, a mid-line laparotomy was performed and hearts were excised in a laminar flow hood as described in Section 2.2.1.2.

(A) Heart weight. Hearts were weighed at the time of excision, prior to perfusion. Values are means ± SEM (n=16 for each group).

(B) HW/BW. HW/BW was calculated based on the heart weight at the time of excision and the final weight of the animal taken just prior to euthanasia. Values are means ± SEM (n=16 for each group)

4.2.2 Microarray changes in gene expression

Changes in gene expression of the LV of the heart sixteen weeks after induction of diabetes, were determined using Affymetrix Rat 230 2.0 GeneChip arrays.

As discussed in Chapter Three, the Affymetrix system produced only low level variation and thus allowed an experimental design utilising individual animal arrays rather than relying on pooling of RNA samples. This reduced the risk of both significant loss of sensitivity of the microarray and of skewing data towards animals with extreme outlying data sets (Affymetrix 2004). Data was analyzed using the RMA algorithm from the Bioconductor Website (www.bioconductor.org) as described in Section 2.12.2.3.

Probability, rather than fold-change, was used here to determine whether a gene showed significant differential expression; this method incorporates a much larger proportion of potential gene candidates. As discussed in Chapter Three, a large fold-change in expression is not always necessary to generate a significant biological effect within the cell. The use of probability means that the smaller, potentially interesting, gene changes are included in the analysis. Additionally, the use of probability ensures that large fold-changes that may be the result of one or two outlying data points and thus not a true change in gene transcript levels, are excluded from the analysis. For example, when significance was determined as a 2-fold difference in transcript levels in either direction, a total of 138 genes out of 31100 (total number of spots on the Affymetrix array) were included in the analysis whereas a 1.5-fold cut off returned 521 significant changes in gene expression. However, when a probability cut-off of $P<0.05$ is used, 1614 significant changes in mRNA transcript levels were detected, providing us with a larger initial pool of genes from which to draw our conclusions.

Since the sensitivity of the Affymetrix chips may have been reduced by high background in some of the arrays, data from low copy number genes may have been masked. In order to exclude this possibility, further analysis by quantitative real-time PCR were performed (Section 4.2.3) to test whether the array data presented here were accurate.

Microarray systems generate a large amount of data and this presented the interesting dilemma of having too much information to process within the scope of this study. As a result, we have chosen to present the gene expression data from two main areas of interest, the biological implications of which have been discussed in Section 4.3. The data set discussed in this chapter was deposited in Gene Expression Omnibus of the NCBI (GEO, http://www.ncbi.nlm.nih.gov/geo/) and is accessible through GEO Series accession number GSE5606.

4.2.2.1 Mitochondrial energy utilisation

Genes implicated in energy utilisation in the mitochondria were identified through analysis of the location/spread of changes occurring within the cell using the Gene Ontology (GO) annotation 'Cellular Component'. Of the 1614 significant genes identified, 750 had two or more GO annotations, and of those 394 had GO Cellular component descriptions. A pie chart distribution of the percentage of GO cellular component classifications was created using this subset of genes. Figure 4.3 indicates that the largest proportion of annotated changes involved "membrane-associated" compartments of the cell (29%). Interestingly though, the second largest proportion of annotated changes involved genes from the mitochondria (13%). It has long been established that mitochondria are important organelles in the pathogenesis of diabetes due at least in part to the role that they play in fuel metabolism (Stanley et al. 1997; Taegtmeyer 2000; Thompson and Cooney 2000; Taegtmeyer et al. 2004). Therefore, these changes provided us with our first area of interest and thus warranted a more in depth analysis, which is provided below.
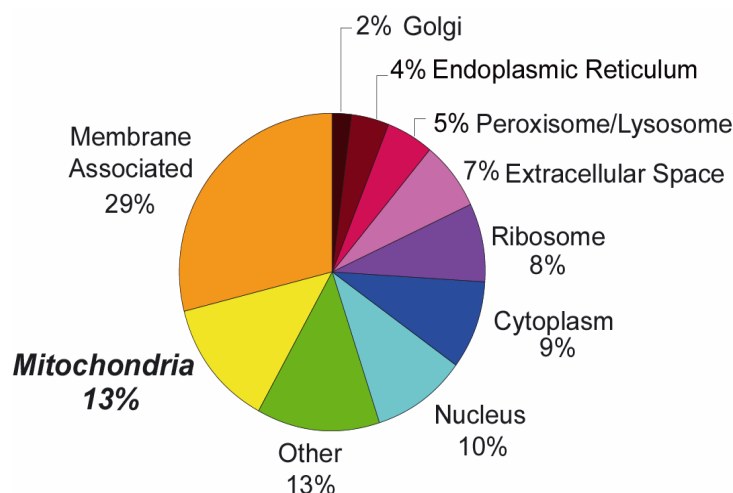
Figure 4.3 Pie chart illustrating the global distribution of genes in rat LV myocardium with expression significantly altered by diabetes

This graph is based on GO Cellular Component classification (Ashburner et al. 2000). The total number of genes with a GO Cellular Component Classification term and at least one other associated GO term were used in this analysis, yielding a total of n = 394 out of an overall total of n = 1614 significantly modified genes. Genes were sorted according to their GO classification and the total in each category then divided by the total number of genes analyzed (n = 394) to generate respective percentages, as shown.

4.2.2.1.1 Metabolic Inflexibility

The normal heart possess the ability to use both lipid (in the form of FA) and carbohydrate as fuels, but these processes become modified in diabetes, producing a state known as metabolic inflexibility (Taegtmeyer et al. 2004). As stated earlier, this leads to the almost exclusive use of FA as a fuel source. The major derangement in the carbohydrate metabolic pathways in the diabetic myocardium occurs not in the glycolytic pathway, as would be expected, but in pathways that control pyruvate oxidation (Fang et al. 2004). Additionally, glucose utilization in the diabetic heart is restricted due to a decrease in the rate of glucose transport. Table 4.2 outlines the genes associated with carbohydrate metabolism whose expression was found to be significantly altered after sixteen weeks of hyperglycaemia.

Table 4.2 Genes involved in carbohydrate metabolism (as defined by their GO annotation) whose expression in LV myocardium was significantly altered by diabetes

Gene Symbol	*Fold Change	P-value	Gene Title	GO Biological Process and Molecular Function Description	
Transport					
Gckr	1.61	0.000*	glucokinase regulatory protein	protein-nucleus import	cell glucose homeostasis
Slc3a2	1.45	0.000*	solute carrier family 3 (activators of dibasic and neutral amino acid transport), member 2	alpha-amylase activity	calcium:sodium antiporter activity
Slc2a3	1.26	0.027	Solute carrier family 2 (facilitated glucose transporter), member 3	carbohydrate transport	sugar porter activity
Abcc8	0.76	0.043	ATP-binding cassette, sub-family C (CFTR/MRP), member 8	potassium ion transport	nucleotide binding
Slc2a1	0.54	0.000*	solute carrier family 2 (facilitated glucose transporter), member 1	response to osmotic stress	sugar porter activity
Slc2a4	0.25	0.000*	solute carrier family 2 (facilitated glucose transporter), member 4	carbohydrate transport	sugar porter activity
Pdp2	0.41	0.000*	pyruvate dehydrogenase phosphatase isoenzyme 2	protein amino acid dephosphorylation	carbohydrate utilization
Glycolysis					
Pfkp	1.38	0.011	phosphofructokinase, platelet	magnesium ion binding	catalytic activity
Ldha	0.78	0.000*	lactate dehydrogenase A	TCA cycle intermediate metabolism	lactate dehydrogenase activity
Pgam2	0.73	0.019	phosphoglycerate mutase 2	striated muscle contraction	bisphosphoglycerate phosphatase activity
Eno3	0.49	0.000*	enolase 3, beta	magnesium ion binding	phosphopyruvate hydratase activity
Hk2	0.24	0.000*	hexokinase 2	hexokinase activity	
Glucose Metabolism					
Pdk4	7.59	0.000*	pyruvate dehydrogenase kinase, isoenzyme 4	acetyl-CoA biosynthesis from pyruvate	two-component sensor molecule activity
Fabp5	1.40	0.032	fatty acid binding protein 5, epidermal	lipid metabolism	transport
G6pd	1.23	0.018	glucose-6-phosphate dehydrogenase	glucose 6-phosphate utilization	glucose-6-phosphate 1-dehydrogenase activity
Pgm1	0.84	0.019	phosphoglucomutase 1	magnesium ion binding	phosphoglucomutase activity
Pdk1	0.74	0.028	pyruvate dehydrogenase kinase 1	protein amino acid phosphorylation	[pyruvate dehydrogenase (lipoamide)] kinase activity

Gene	Fold-change	P	Description	Biological Process	Molecular Function
Gpd2	0.70	0.008	glycerol-3-phosphate dehydrogenase 2	glycerol-3-phosphate metabolism	gluconeogenesis
Gluconeogenesis					
	0.76	0.001	dimethyl-Q 7	ubiquinone biosynthesis	
Gpt1	0.65	0.000*	glutamic pyruvic transaminase 1, soluble	nitrogen compound metabolism	alanine transaminase activity
Pc	0.54	0.000*	Pyruvate carboxylase	lipid biosynthesis	pyruvate carboxylase activity
Other Carbohydrate Metabolism					
RGD1309821_predicted	1.58	0.000*	Similar to KIAA1161 protein (predicted)	hydrolase activity, hydrolyzing O-glycosyl compounds	
Fbp2	1.39	0.003	fructose-1,6-bisphosphatase 2	gluconeogenesis	fructose-2,6-bisphosphate 2-phosphatase activity
Fuca	1.38	0.000*	fucosidase, alpha-L- 1, tissue	glycosaminoglycan catabolism	alpha-L-fucosidase activity
Manba	1.36	0.010	mannosidase, beta A, lysosomal (predicted)	glycoprotein catabolism	beta-mannosidase activity
Idh1	1.34	0.005	isocitrate dehydrogenase 1 (NADP+), soluble	main pathways of carbohydrate metabolism	glyoxylate cycle
Gpd1	1.32	0.016	glycerol-3-phosphate dehydrogenase 1 (soluble)	glycerol-3-phosphate metabolism	glycerol-3-phosphate dehydrogenase (NAD+) activity
Man1a_predicted	1.27	0.004	mannosidase 1, alpha (predicted)	N-linked glycosylation	mannosyl-oligosaccharide 1,2-alpha-mannosidase activity
Pygb	1.26	0.033	brain glycogen phosphorylase	glycogen catabolism	phosphorylase activity
---	1.21	0.030	similar to mannosyl-oligosaccharide alpha-1,2-mannosidase	N-linked glycosylation	mannosyl-oligosaccharide 1,2-alpha-mannosidase activity
Galt	1.19	0.036	galactose-1-phosphate uridyl transferase (predicted)	galactose metabolism	UTP-hexose-1-phosphate uridylyltransferase activity
	0.81	0.005	junctophilin 2 (predicted)	positive regulation of cytosolic calcium ion concentration	xylose isomerase activity
Naga	0.78	0.039	N-acetyl galactosaminidase, alpha (predicted)	hydrolyzing O-glycosyl compounds	alpha-galactosidase activity
Neu2	0.74	0.043	neuraminidase 2	exo-alpha-sialidase activity	hydrolase activity
Prkab1	0.74	0.003	protein kinase, AMP-activated, beta 1 non-catalytic subunit	fatty acid biosynthesis	AMP-activated protein kinase activity
Dcxr	0.28	0.000*	dicarbonyl L-xylulose reductase	monosaccharide metabolism	xylulose metabolism

*Fold-change: The fold-change in the diabetic compared to control animals. >1 is increased expression in the diabetic and <1 is decreased expression in the diabetic compared to control: * at least $P < 5.0E-05$

In the diabetic state, the heart is exposed to an environment that is both hyperglycaemic and hyperlipidaemic ((Taegtmeyer et al. 2004), Table 4.1). It has been proposed that the enzymes involved in the mitochondrial fatty acid oxidation (FAO) pathway are up-regulated in the diabetic heart because the organ becomes reliant on this pathway for energy production due to diminished glucose uptake and utilisation (Su et al. 2005). Table 4.3 below gives a summary of a number of the lipid metabolism-associated genes with altered mRNA expression levels in the diabetic state.

Table 4.3 Genes associated with lipid metabolism (as defined by their GO annotation) whose expression was significantly altered in diabetic LV

Gene Symbol	*Fold Change	P value	Gene Title	GO Biological Process and Molecular Function	
Transport of lipid into the mitochondria					
Cpt1a	2.16	0.000*	carnitine palmitoyltransferase 1, liver	carnitine O-palmitoyltransferase	
Cpt2	1.41	0.0026	carnitine palmitoyltransferase 2	carnitine O-palmitoyltransferase	
Cpt1b	1.22	0.036	carnitine palmitoyltransferase 1b	carnitine O-palmitoyltransferase	
Mlycd	1.53	0.000*	malonyl-CoA decarboxylase	fatty acid biosynthesis	methylmalonyl-CoA decarboxylase activity
Slc25a20	1.30	0.002	solute carrier family 25 (carnitine/acylcarnitine translocase), member 20	lipid transporter	
β-oxidation					
Acadvl	1.40	0.000*	acyl-Coenzyme A dehydrogenase, very long chain	electron transport	acyl-CoA dehydrogenase
	1.33	0.000*	hydroxyacyl-Coenzyme A dehydrogenase (trifunctional protein), beta subunit	3-hydroxyacyl-CoA dehydrogenase activity	
Hadha	1.58	0.000*	hydroxyacyl-Coenzyme A dehydrogenase/3-ketoacyl-Coenzyme A thiolase/enoyl-Coenzyme A hydratase (trifunctional protein), alpha subunit	metabolism	3-hydroxyacyl-CoA dehydrogenase
Ehhadh	1.79	0.001	enoyl-Coenzyme A, hydratase/3-hydroxyacyl Coenzyme A dehydrogenase	acyl-CoA metabolism	3-hydroxyacyl-CoA dehydrogenase
Acox1	1.16	0.049	acyl-Coenzyme A oxidase 1, palmitoyl	electron transport	acyl-CoA oxidase
Lipid Transport (General)					
Slc27a1	2.01	0.000*	solute carrier family 27 (fatty acid transporter), member 1	lipid transport	catalytic activity
Apoe	2.01	0.002	apolipoprotein E	response to reactive oxygen species	beta-amyloid binding
Vldlr	0.63	0.000*	very low density lipoprotein receptor	neuron migration	low-density lipoprotein receptor activity
Lipid Metabolism					
Mte1	2.89	0.000*	mitochondrial acyl-CoA thioesterase 1	acyl-CoA metabolism	serine esterase activity
	1.77	0.000*	brain acyl-CoA hydrolase	acyl-CoA binding	catalytic activity
CD36/FAT	1.41	0.000*	CD36 antigen/similar to fatty acid translocase	receptor activity	
Mal	1.39	0.005	myelin and lymphocyte protein	lipid raft polarization	intracellular protein transport
Lpl	0.83	0.002	lipoprotein lipase	circulation	lipoprotein lipase
Chka	0.73	0.038	choline kinase alpha	lipid transport	choline kinase
Fatty Acid Metabolism					
Dci	1.87	0.000*	dodecenoyl-coenzyme A delta isomerase	fatty acid β-oxidation	dodecenoyl-CoA δ-isomerase activity
Gpam	1.73	0.000*	Glycerol-3-phosphate acyltransferase, mitochondrial	phospholipid biosynthesis	glycerol-3-phosphate O-acyltransferase activity
Acaa2	1.46	0.000*	acetyl-Coenzyme A acyltransferase 2 (mitochondrial 3-oxoacyl-Coenzyme A thiolase)	acetyl-CoA C-acyltransferase activity	
Dhrs3_predicted	1.26	0.003	dehydrogenase/reductase (SDR family) member 3 (predicted)	visual perception	electron transporter activity
Hadhsc	1.20	0.002	L-3-hydroxyacyl-Coenzyme A dehydrogenase, short chain	3-hydroxyacyl-CoA dehydrogenase activity	
Gnpat	0.82	0.024	glyceronephosphate O-acyltransferase	fatty acid metabolism	acyltransferase activity
Fatty Acid Biosynthesis					

Cte1	17.24	0.000*	cytosolic acyl-CoA thioesterase 1	long-chain fatty acid metabolism	serine esterase activity
Elovl6	1.38	0.013	ELOVL family member 6, elongation of long chain fatty acids (yeast)	fatty acid elongation	fatty acid elongase
Degs1	1.32	0.031	Degenerative spermatocyte homolog (Drosophila)	fatty acid desaturation	lipid biosynthesis
---	0.70	0.007	Similar to hypothetical protein (predicted)	lipid biosynthesis	oxidoreductase
Acsl6	0.40	0.000*	acyl-CoA synthetase long-chain family member 6	long-chain fatty acid metabolism	magnesium ion binding
Scd2	0.33	0.000*	stearoyl-Coenzyme A desaturase 2	lipid biosynthesis	stearoyl-CoA 9-desaturase activity
Electron Transport					
Nudt7_predicted	2.22	0.000*	nudix (nucleoside diphosphate linked moiety X)-type motif 7 (predicted)	coenzyme A catabolism	acetyl-CoA catabolism
Acadl	1.17	0.003	acetyl-Coenzyme A dehydrogenase, long-chain	long-chain-acyl-CoA dehydrogenase activity	
Cyb5	0.63	0.000*	cytochrome b-5	stearoyl-CoA 9-desaturase activity	
Other					
Angptl4	25.10	0.000*	angiopoietin-like protein 4	negative regulation of lipoprotein lipase activity	protein oligomerization
Mgll	2.41	0.000*	monoglyceride lipase	proteolysis and peptidolysis	lipid metabolism
Pla2g2a	1.83	0.002	phospholipase A2, group IIA (platelets, synovial fluid)	regulation of cell growth	lipid catabolism
Prkar2b	1.53	0.005	protein kinase, cAMP dependent regulatory, type II beta	protein amino acid phosphorylation	fatty acid metabolism
	1.40	0.000*	hydroxysteroid (17-β) dehydrogenase 4	steroid biosynthesis	fatty acid metabolism
Pla2g5	0.80	0.033	phospholipase A2, group V	phospholipid metabolism	lipid catabolism
Ucp3	2.53	0.000*	uncoupling protein 3 (mitochondrial, proton carrier)	response to superoxide, lipid metabolism	transporter activity, oxidative phosphorylation uncoupler activity

*Fold-change: The fold-change in the diabetic compared to control animals. >1 is increased expression and <1 is decreased expression in the diabetic compared to control. * at least P< 5.0E-05

Of particular interest with regards to the glucose- and lipid-associated changes in gene expression presented in Tables 4.2 and 4.3 is that in the results in Table 4.2 (glucose-associated) 53% of the genes are down-regulated, compared to Table 4.3 (lipid-associated) where 76% of the genes are up-regulated. This provides evidence in support of the theory of Taegtmeyer *et al.,* which holds that the heart in diabetes becomes reliant on lipid as its major fuel source (Taegtmeyer et al. 2002).

4.2.2.2 Diabetic complications as a consequence of excess ROS.

The second area of interest to be covered in this chapter follows on from work published by Brownlee *et al.,* (Brownlee 2001; Brownlee 2005). This group hypothesised that complications of diabetes arise as a result of an increase in the production of ROS from the mitochondria (Brownlee 2001). The hypothesis states that there are four main

metabolic pathways perturbed by hyperglycaemia leading eventually to diabetic complications.

In order to asses whether this theory fits into an *in vivo* model of cardiomyopathy that results from diabetes, we present an analysis of the changes in expression of genes which may be associated with these four pathways. The results from this section are discussed in Section 4.3

4.2.2.2.1 Pathway one: reduction in GSH

Several genes involved in GSH metabolism were found to have changes in gene expression, such as members of the glutathione S-transferase (GST) family (Table 4.4). This family of enzymes utilize glutathione in reactions contributing to the transformation and detoxification of a wide range of compounds, including carcinogens, therapeutic drugs, and products of oxidative stress (Strange et al. 2001). Classically the GST enzymes are described as being involved in cellular defence against numerous harmful chemicals produced both endogenously and exogenously (Strange et al. 2001).

Table 4.4 Genes involved in GSH metabolism

Gene Symbol	*Fold Change	P value	Gene Title	GO Biological Process and Molecular Function	
Gsta5	2.93	0.000*	glutathione S-transferase A5	glutathione metabolism	glutathione transferase activity
Glrx1	1.83	0.000*	glutaredoxin 1 (thioltransferase)	electron transport	glutathione disulfide oxidoreductase activity
Gstm5	1.74	0.000*	glutathione S-transferase, mu 5	metabolism	glutathione transferase activity
Mgst1	1.68	0.000*	microsomal glutathione S-transferase 1	glutathione metabolism	glutathione transferase activity
Gstt2	1.6	0.003	glutathione S-transferase, theta 2	glutathione metabolism	glutathione transferase activity
Gstm1	1.55	0.000*	glutathione S-transferase, mu 1	perception of smell	glutathione transferase activity
Gsta4_predicted	1.47	0.011	glutathione S-transferase, alpha 4 (predicted)	response to stress	glutathione transferase activity
Glrx2_predicted	1.29	0.028	Glutaredoxin 2 (thioltransferase) (predicted)	electron transport	glutathione metabolism
Gstp1/Gstp2	1.24	0.047	glutathione-S-transferase, pi 1 / glutathione S-transferase, pi 2	xenobiotic metabolism	glutathione transferase activity
Gsto1	0.76	0.003	glutathione S-transferase omega 1	metabolism	glutathione transferase activity
Gstm3	0.65	0.000*	glutathione S-transferase, mu type 3	metabolism	glutathione transferase activity
Gstk1	0.6	0.000*	glutathione S-transferase kappa 1	protein targeting	glutathione transferase activity

*Fold-change: The fold-change in the diabetic compared to control animals. >1 is increased expression and <1 is decreased expression in the diabetic compared to control. * at least P< 5.0E-05

4.2.2.2.2 Pathway two: increased intracellular formation of AGEs

No changes specifically related to AGEs were found in this microarray study. The relevance and implications of this are discussed in Section 4.3.2.2

4.2.2.2.3 Pathway three: activation of PKC

The PKC /DAG pathway is known to play important roles in vascular cells in the regulation of endothelial cell permeability, cardiomyocyte contractility, extracellular matrix (ECM), smooth muscle cell growth and contraction, angiogenesis, and cytokine actions through the initiation of expression of signal transduction hormones, growth factors and leukocyte adhesions. All of these processes are known to be abnormal in the diabetic state (Koya and King 1998).

Of the PKC isoforms present on the array (α, β, δ, ε, η, ι, γ, ζ, θ, μ), only PKC δ showed a significant change in gene expression. Data presented in Table 4.5 show a selection of representative PKC isoforms for which no significant change in gene expression was observed and the data obtained for the δ isoform. Increased PKC activity in diabetic state may lead to alteration of several growth factors, cytokines and vasoactive molecules including endothelin-1 (ET-1) (Griendling et al. 1989; Chen, S. et al. 2000). Included in Table 4.5 is the data obtained for endothelin receptor type A and B, which were both found to be increased in LV tissue sixteen weeks after induction of diabetes.

Table 4.5 Expression changes in genes associated with activation of PKC

Gene Symbol	*Fold Change	P-value	Gene Title	GO Biological Process and Molecular Function	
PKCα	1.15	0.317	Protein kinase C, α type	calcium ion homeostasis, regulation of muscle contraction	protein serine/threonine kinase activity
PKCβ	1.08	0.714	Protein kinase C, β type	protein amino acid phosphorylation, calcium ion	protein kinase C activity
PKCδ	1.34	0.003	protein kinase C, δ type	protein amino acid phosphorylation, induction of apoptosis	nucleotide binding, protein kinase C activity
Ednrb	1.92	0.000	endothelin receptor type B	neural crest cell migration	endothelin-B receptor activity
Ednra	1.59	0.003	endothelin receptor type A	smooth muscle contraction	endothelin-A receptor activity

*Fold-change: The fold-change in the diabetic compared to control animals. >1 is increased expression and <1 is decreased expression in the diabetic compared to control: * at least P< 5.0E-05

4.2.2.2.4 Pathway four: increased flux through the Hexosamine pathway

In a normal system, the hexosamine pathway diverts fructose-6-phosphate away from the glycolytic pathway to provide substrates for reactions that require UDP-*N*-acetylglucosamine (GlcNAc), such as proteoglycan synthesis and the formation of *O*-linked glycoproteins (Brownlee 2001). Kolm-Litty *et al.,* (Kolm-Litty et al. 1998),

presented work that indicated inhibition of glutamine:fructose-6-phosphate amidotransferase (GFAT), the rate limiting enzyme in the conversion of glucose to glucosamine in the hexosamine pathway, can lead to a blocking of the hyperglycaemia-induced increase in the transcription of TGF-α, TGF-β1 and PAI-1. They hypothesised from this work that GFAT was a major contributor to the perturbation of the hexosamine pathway as a result of increased blood glucose.

  Table 4.6 shows data obtained for genes associated with the hexosamine pathway and their changes in the diabetic heart. Of the six genes analysed only PAI-1 and UDP-N-acetyl-alpha-D-galactosamine:polypeptide N-acetylgalactosaminyltransferase 1 showed significant alteration in gene expression.

Table 4.6 Expression changes of genes associated with the Hexosamine pathway

Gene Symbol	*Fold Change	P-value	Gene Title	GO Biological Process and Molecular Function	
PAI-1	1.47	0.007	Plasminogen activator inhibitor-1 (PAI-1)	blood coagulation/regulation of angiogenesis	serine-type endopeptidase inhibitor activity
Tgfb1	1.13	0.780	transforming growth factor, beta 1	skeletal development , regulation of cell growth, inflammatory response	transforming growth factor beta receptor binding
Gfpt2	1.16	0.396	glutamine-fructose-6-phosphate transaminase 2	glutamine metabolism, carbohydrate metabolism	glutamine-fructose-6-phosphate transaminase (isomerizing) activity
Tgfa	1.16	0.617	transforming growth factor alpha	Angiogenesis, anti-apoptosis	protein-tyrosine kinase activity epidermal growth factor receptor binding
Sp1	1.14	0.069	Sp1 transcription factor	transcription regulation of transcription, DNA-dependent	DNA binding
Galnt1	0.810	0.003	UDP-N-acetyl-alpha-D-galactosamine:polypeptide N-acetylgalactosaminyltransferase 1	protein amino acid O-linked glycosylation	polypeptide N-acetylgalactosaminyl-transferase activity

*Fold-change: The fold-change in the diabetic compared to control animals. >1 is increased expression and <1 is decreased expression in the diabetic compared to control.

4.2.2.2.5 The common element: linkage of the four pathways

The link between activation of PKC, formation of AGEs, increased flux through the polyol pathway, a decrease in GSH, and formation of reactive oxygen species has been described by Nishikawa *et al.* (Nishikawa et al. 2000). This group used cultured endothelial cells to demonstrate that the hyperglycemia-induced increase in ROS production is caused through the TCA cycle (Nishikawa et al. 2000). Further, they reported that inhibition of mitochondrial respiration complex II (using the inhibitor rotenone) and oxidative phosphorylation (using the inhibitor CCCP and uncoupling protein-1 (UCP-1)), completely prevented the negative effects of hyperglycemia. Finally, they investigated the effects of CCCP and UCP-1 on PKC activation, formation of

intracellular methylglyoxal (an AGE precursor), sorbitol accumulation (indicates aldose reductase activity) and activation of NFκB (ROS inducible transcription factor). The results showed that all these processes can be inhibited by CCCP and UCP-1 and led to the conclusion that increased ROS production from the mitochondria is the initial cause of the perturbation in the four pathways described above (Nishikawa et al. 2000).

Table 4.7 is a representation of all genes associated with oxidative stress as defined by the Kyoto Encyclopaedia of Genes and Genomes (KEGG) pathway annotation. Also included in the table are the data for glyceraldyhyde-3-phosphate dehydrogenase (GAPDH) and TCDD-inducible poly (ADP-ribose) polymerase. Their inclusion here is discussed in section 4.3.2.5.

Table 4.7 Genes that play roles in oxidative stress (as defined by their KEGG pathway description) whose expression was significantly altered in diabetic LV

Gene Symbol	*Fold Change	P-value	Gene Title	GO Biological Process and Molecular Function	
Cat	1.36	0.001	catalase	response to reactive oxygen species, hydrogen peroxide catabolism	catalase activity, oxidoreductase activity, metal ion binding
Cyba	1.08	0.621	cytochrome b-245, alpha polypeptide	oxygen and reactive oxygen species metabolism, superoxide metabolism	iron ion binding, oxidoreductase activity
Cyp1a1	2.10	0.004	cytochrome P450, family 1, subfamily a, polypeptide 1	dibenzo-p-dioxin metabolism, electron transport	monooxygenase activity, oxygen binding
Gclc	1.16	0.331	glutamate-cysteine ligase, catalytic subunit	glutamate metabolism, glutathione biosynthesis	glutamate-cysteine ligase activity, nucleic acid binding
Gpx1	1.00	0.952	glutathione peroxidase 1	response to reactive oxygen species, induction of apoptosis by oxidative stress	glutathione peroxidase activity, selenium binding
Gpx3	1.04	0.923	glutathione peroxidase 3	response to lipid hydroperoxide, hydrogen peroxide catabolism	selenium binding, oxidoreductase activity, glutathione peroxidase activity
Gsr	1.00	0.989	glutathione reductase	response to pest, pathogen or parasite, glutathione metabolism	glutathione-disulfide reductase activity, FAD binding
Gstt2	1.60	0.003	glutathione S-transferase, theta 2	glutathione metabolism	glutathione transferase activity
Mt1a	1.04	0.855	metallothionein 1a	zinc ion homeostasis, nitric oxide mediated signal transduction	copper ion binding, zinc ion binding
Mgst1	1.70	0.000*	microsomal glutathione S-transferase 1	glutathione metabolism	glutathione transferase activity
Nqo1	0.92	0.666	NAD(P)H dehydrogenase, quinone 1	xenobiotic metabolism, nitric oxide biosynthesis	NAD(P)H dehydrogenase (quinone) activity, cytochrome-b5 reductase activity
Nfix	1.10	0.824	nuclear factor I/X	transcription from RNA polymerase II promoter, DNA replication	double-stranded DNA binding, RNA polymerase II transcription factor activity, enhancer binding
Sp1	1.38	0.069	Sp1 transcription factor	regulation of transcription, DNA-dependent, positive regulation of transcription, DNA-dependent	DNA binding, transcription factor activity
Srd5a2	-1.152	0.135	steroid 5-alpha-reductase 2	steroid biosynthesis, androgen metabolism	3-oxo-5-alpha-steroid 4-dehydrogenase activity

	Fold-change*	P-value			
Sod1	0.86	0.957	superoxide dismutase 1	activation of MAPK activity, superoxide metabolism, removal of superoxide radicals	copper, zinc superoxide dismutase activity, copper ion binding
Sod2	0.86	0.088	superoxide dismutase 2, mitochondrial	age-dependent response to reactive oxygen species, removal of superoxide radicals	manganese superoxide dismutase activity, manganese ion binding
Sod3	1.00	0.998	superoxide dismutase 3, extracellular	response to superoxide, response to hypoxia	copper, zinc superoxide dismutase activity, copper ion binding, zinc ion binding
Txn2	0.87	0.620	thioredoxin 2	electron transport	thiol-disulfide exchange intermediate activity
Txnrd1	1.20	0.025	thioredoxin reductase 1	thioredoxin pathway, response to oxidative stress	thioredoxin-disulfide reductase activity, selenium binding
Txnrd2	0.88	0.520	thioredoxin reductase 2	response to oxygen radical, electron transport	thioredoxin-disulfide reductase activity, electron carrier activity
Xdh	0.87	0.491	xanthine dehydrogenase	response to aluminum ion, steroid biosynthesis	xanthine dehydrogenase activity, 3-oxo-5-alpha-steroid 4-dehydrogenase activity, iron-sulfur cluster binding
Gapdh	0.91	0.352	glyceraldehyde-3-phosphate dehydrogenase	glycolysis, apoptosis	glyceraldehyde-3-phosphate dehydrogenase (phosphorylating) activity, oxidoreductase activity
Gapdhs	0.92	0.626	glyceraldehyde-3-phosphate dehydrogenase, spermatogenic	glycolysis, sperm motility	glyceraldehyde-3-phosphate dehydrogenase (phosphorylating) activity
Tiparp_predicted	1.28	0.027	TCDD-inducible poly(ADP-ribose) polymerase (predicted)	protein amino acid ADP-ribosylation	protein binding

*Fold-change: The fold-change in the diabetic compared to control animals. >1 is increased expression and <1 is decreased expression in the diabetic compared to control. * at least $P < 5.0E\text{-}05$

4.2.3 Real time quantitative PCR (RT-qPCR) validation of microarray results.

There are inherent limitations of microarray technology including non-specific hybridisation, poor hybridisation, false positive signals, background levels and issues raised by statistical analysis methods used for this technology. Consequently, independent confirmation of microarray results is frequently required for the publication of microarray results (Chuaqui et al. 2002; Firestein and Pisetsky 2002). As described by Chauaqui *et al.,* (Chuaqui et al. 2002) there are a number of techniques that could potentially be used for validation, each with their own technical issues; however, the one most commonly used is RT-qPCR (Firestein and Pisetsky 2002). In this study and in all subsequent microarray studies RT-qPCR has been used as the microarray validation method.

In this study, five genes were selected for RT-qPCR-based confirmation of expression changes observed with the Affymetrix GeneChips®. Carnitine palmitoyl transferase I (CPT I), malonyl-CoA decarboxylase (MCD), and pyruvate dehydrogenase kinase 4 (PDK4) were selected because of their roles in mitochondrial energy metabolism.

Cytochrome b5 (CytB5) has been used previously to quantitate mtDNA copy number (Shen et al. 2004) and is presented here as a marker for mitochondrial content. Transcription factor A, mitochondrial (Tfam) is another marker of mitochondrial replication (Ekstrand et al. 2004) and was chosen here as a negative control because it was not significantly changed on our microarrays. Fold-change was calculated using the $\Delta\Delta C_t$ method (see Section 2.4). Table 4.8 shows a high correlation between the RT-qPCR results and the changes seen using microarray technology, indicating that the results observed using microarray technology are consistent with those occurring *in vivo*.

Table 4.8 Comparison between gene expression differences determined by RT-qPCR and microarray methods

Gene	$\Delta\Delta C_t$	$\Delta\Delta C_t$ (SD)	RTqPCR *Fold-change	Microarray Fold-change
CPT1	-1.26	0.21	2.39	2.16
MCD	-0.61	0.27	1.52	1.53
PDK4	-3.24	0.38	9.44	7.59
CytB5	0.3	0.59	0.81	0.63
Tfam	-0.11	0.23	1.07	1.14 (ns)

*Fold-changes in diabetic tissues are expressed in relation to respective control values.

4.3 Discussion

The results presented in the first section of this chapter indicate that the STZ model used here provides a stable pattern of diabetes that can be maintained for at least sixteen weeks without insulin administration. Analysis of the physiological characteristics of this model (Figure 4.1, Table 4.1) indicate that the STZ-treated animals exhibit all the hallmark indicators of a mild to severe diabetes (Alberti and Zimmet 1998), such as attenuated weight gain, polydipsia, hyperphagia, hyperglycemia and hyperlipidemia. Previous studies carried out by this group and others (Fein et al. 1980; Penpargkul et al. 1980; Litwin et al. 1990; Rodrigues and McNeill 1999; Cooper et al. 2004) have described reduced heart function in the STZ model of diabetes. The aim of this chapter was to characterise changes within the transcriptome of the diabetic heart (LV) after sixteen weeks of diabetes. From the large number of changes in gene expression observed in this study, two main areas were chosen as a focus. The first related specifically to diabetic cardiomyopathy and metabolic inflexibility and the second attempted to determine if support could be found for the more general hypothesis of Brownlee *et al.* (Brownlee 2005).

The following discussion outlines in detail the significance of the results found in this microarray study.

4.3.1. Metabolic Inflexibility

4.3.1.1 Carbohydrate metabolism

The inability to undergo metabolic substrate switching is a well documented phenomenon in the diabetic heart (Stanley et al. 1997, Lopaschuk, 2002 #48, Taegtmeyer, 2004 #160). In this study, a number of genes important in carbohydrate metabolism showed altered expression and the results match those in previously published studies. Using RT-qPCR, Depre *et al.,* found a decrease in GLUT4 transporters of the LV after one week (acute) and six months (chronic) of STZ-induced diabetes (Depre et al. 2000). This result is consistent with the microarray results obtained here, which showed a decrease in GLUT4 expression in the diabetic group to 25% of normal and a decrease of 50% of GLUT1 in the diabetic group compared with the sham group. This indicates a consistency between results obtained in this study and that of others, and importantly highlights a perturbation in glucose uptake.

The failure of the diabetic heart to utilise glucose is also highlighted in this study with changes in key metabolic regulatory enzymes such as pyruvate dehydrogenase phosphatase 2/pyruvate dehydrogenase kinase 4 (PDP2/PDK4) which are involved in transport of pyruvate into the mitochondria. In mitochondria, the kinase (PDK4) and phosphatase (PDP2) are simultaneously active and their relative activities determine the occupancies of phosphorylation sites in the pyruvate dehydrogenase (PDH) complex and hence the proportion of the inactive (phosphorylated) complex (Karpova et al. 2003). Inactivation of the PDH complex limits the use of glucose by peripheral tissues and conserves three carbon (3C) compounds for glucose synthesis by the liver and kidney (Wu et al. 1998). Under normal feeding conditions, approximately 70% of PDH complex in heart muscle is phosphorylated and inactive. Under starvation and diabetes, the proportion of phosphorylated and inactive complex increases to 99% (Karpova et al. 2003). As can be seen in Table 4.2, gene expression of PDK4 increased 7.5-fold in the diabetic group compared to the normal group (this result was confirmed with RT-qPCR, Table 4.8), while the gene expression of PDP2 was decreased 59% in the diabetic compared to the normal. In support of this hypothesis, a previous study reported a more than 10-fold increase, in the amount of PDK4 protein in heart mitochondria of diabetic rats. A similarly large increase in PDK4 mRNA was also observed (Wu et al. 1998). In addition, it has been shown that STZ-induced diabetes (of 48hr duration) decreased both protein and mRNA levels of PDP2 in the heart and kidney (Huang et al. 2003). This result is consistent with the 59% decrease in PDP2 observed in the data presented in this chapter. The effects observed by Huang *et al.,* were completely reversed by insulin treatment (Huang et al. 2003). Taken together, these findings are consistent with an

hypothesis that concurrent up regulation of PDK expression and down-regulation of PDP expression, contribute to hyper-phosphorylation of PDH complex in diabetes. This conserves 3C compounds for hepatic gluconeogenesis and contributes to the hyperglycemia seen in diabetes (Huang et al. 2003).

Another gene that is related to the glucose pathway that was found to have altered expression in the present study was hexokinase. As can be seen in Table 4.2, hexokinase mRNA was decreased in the diabetic state to approximately 25% of normal. Hexokinase performs the first step in glycolysis, transferring a phosphate from ATP to glucose to form glucose-6-phosphate. The consequence of this is a reduction in the amount of activated substrate available for conversion into pyruvate and subsequent entry into mitochondria and the TCA cycle (Taegtmeyer et al. 2002).

4.3.1.2 Lipid metabolism

A consequence of metabolic inflexibility and decreased glucose availability observed in diabetes is an increase in the use of lipid as the main fuel source (Sakamoto et al. 2000).

CD36/fatty acid translocase (CD36/FAT), a FA transporter, is known to be increased in the diabetic state (Greenwalt et al. 1995), consistent with the concept that the disease causes increased FA uptake in the heart. Although not directly connected with the mitochondria, CD36/FAT has been identified as one of three fatty acid transport proteins responsible for increased FA uptake when over-expressed in cell lines (Luiken et al. 2002) and is thought to be the primary FA transporter in heart/skeletal muscle (Luiken et al. 2002). Results from this study show that expression of CD36/FAT increased 1.41-fold in the diabetic group compared to the sham group. This finding, together with the observed disproportionate increase in genes involved in lipid metabolism has recently been confirmed in LV tissue after only two weeks of diabetes (Knoll et al. 2005) indicating that this is an early and sustained change.

Fatty acid oxidation is limited by the transport of FA moieties into the mitochondria through the specific shuttle CPT I (Depre et al. 2000). The two isoforms of CPT I, CPTα and CPTβ are both expressed in the rat heart. Results from the current study show that expression of the genes encoding CPTα and CPTβ increased 2-fold and 1.22-fold respectively. In addition, levels of other genes known to be involved in the channelling of FA into the mitochondrial oxidative pathway were also altered. Specifically, expression of carnitinie:acylcarnitine translocase (solute carrier family, member 20) increased 1.3-fold and expression of CPT II increased 1.4-fold in the diabetic group.

A study by Cook *et al.,* (Cook et al. 2001) found that a consequence of STZ-induced diabetes was an increase in CPT Iα levels, while CPT Iβ levels remained the same. CPT Iα is predominantly expressed in the fetal heart and its expression levels

gradually reduce as the animal develops. CPT Iβ expression was found to remain the same throughout the development of the animal (Cook et al. 2001). The observed increase in both CPT I isoforms in the diabetic state indicates increased reliance on fatty acids as a fuel source in the heart and perhaps provides an explanation for the accumulation of acyl-carnitine and its intermediates known to occur in the diabetic heart (Su et al. 2005).

Regulation of CPT Iα is mainly via inhibition of its activity by malonyl-CoA, which is produced by acetyl-CoA carboxylase (ACC) and degraded by malonyl-CoA decarboxylase (MCD) to acetyl-CoA (Sakamoto et al. 2000). A study by Sakamoto *et al.,* (Sakamoto et al. 2000) found no change in the activity of ACC; however they did find a significant increase in both the activity and expression of MCD. An increase in the expression of MCD would be expected to result in a decrease in the amount of malonyl-CoA and thus a reduction in the inhibition of CPT I. This result is consistent with the data from this current microarray study. Here, no change in the gene expression of ACC was observed; however, there was a significant increase in MCD of 1.5-fold in the diabetic group compared to the normal group (result confirmed with RT-qPCR, Table 4.8).

Taken together, these results indicate that there likely to be at least three contributing factors to the increased transport of fatty acylcarnitine into the mitochondria, the first being increased FA uptake into the heart through the CD36 transporter, the second being reduced inhibition of CPT by malonyl-CoA and the third, being increased expression of CPT itself.

Fatty acids transported into the mitochondria are broken down into acetyl-CoA through β-oxidation and the trifunctional β-oxidation complex (TOC). This complex consists of long-chain enoyl-CoA hydratase, L-3-hydroxyacyl-CoA dehydrogenase, and long-chain 3-ketoacyl-CoA thiolase, which exist in the inner mitochondrial membrane. Very long-chain acyl-CoA dehydrogenase is also an enzyme of the inner mitochondrial membrane and thus may also act in concert with the enzymes above (Yao and Schulz 1996). In this study we found that three of the four genes in the TOC, enoyl-CoA hydratase, L-3-hydroxyacyl Coenzyme A dehydrogenase and acyl-Coenzyme A dehydrogenase (very long chain) were increased in the diabetic state when compared with normal (Table 4.2).

A proteomic analysis of changes in mitochondrial proteins associated with the diabetic state found a similar array of changes in proteins involved in β-oxidation, including carnitine palmitoyltransferase 2, acyl-Coenzyme A dehydrogenase (very long chain), L-3-hydroxyacyl-Coenzyme A dehydrogenase (short chain), acyl-Coenzyme A dehydrogenase (long-chain) and acyl-Coenzyme A dehydrogenase, (short/branched chain) (Turko et al. 2003). All of these genes were also altered in this study (Table 4.2),

giving weight to the hypothesis that any changes at the genetic level are potentially being translated into changes at the protein level and perhaps even the functional level.

Of interest was the observation that, in the proteomic study, a number of the proteins involved in the TCA cycle, including pyruvate dehydrogenase (lipoamide), aconitase, malate dehydrogenase, dihydrolipoamide dehydrogenase, fumarase, isocitrate dehydrogenase 3 and succinyl-CoA ligase (ADP-forming), showed no change from normal in the diabetic state (Turko et al. 2003). This result is consistent with our data in which no differences in the expression of these genes were observed. Given that the TCA cycle is potentially functioning at the same rate (no change in gene expression) despite an increase in both CPT isoforms, and a decrease in MCD observed in this study, there is possibly an increase in lipid (likely as acyl-carnitine) occurring in the mitochondria in this model of diabetes. This hypothesis is supported by a recent review (Taegtmeyer et al. 2004) which proposed that as the diabetic state progresses, the excessive availability of lipids and fatty acids exceeds the rate of FA oxidation in the heart and lipids accumulate within the cardiomyocyte. Further, Su *et al.,* (Su et al. 2005) found a four-fold increase in acyl-carnitine in the diabetic myocardium (six weeks of STZ diabetes) using electrospray ionization mass spectrometry indicating that the heart is unable to process the acyl-carnitine as quickly as it is being synthesised.

A novel finding of the current study was the observed up regulation of angiopoietin-like protein 4 (Angptl4) in the diabetic heart (25-fold increase relative to normal tissue). This finding was repeated and independently verified using RT-qPCR in a later study (Chapter 6, Table 6.16). Angptl4 is also known as PPARγ angiopoietin-related fasting-induced adipose factor or hepatic fibrinogen/angiopoietin-related protein (Ge, H. et al. 2004) and has been shown to be a potent inhibitor of lipoprotein lipase (LPL) activity, leading to increased serum triglyceride levels (Yoshida et al. 2002). Under normal conditions, the highest expression levels of Angptl4 are found in white adipose tissue, with significant expression also found in the normal liver, heart and skeletal muscle (Kersten 2005). As a transcriptional target of PPARγ, it has been hypothesized that Angptl4 plays a role in the modulation of adipogenesis, insulin sensitivity or energy metabolism and elevated levels of the protein are found in genetically obese mice (Ge, H. et al. 2004). A recent study published by Yu *et al.,* looking at specific over-expression of Angptl4 in the heart tissue of mice, found that increased levels caused an 80% reduction in cardiac LPL activity and a greater than two-fold increase in fasted plasma triglyceride levels (Yu, X. et al. 2005). Our current work supports this finding with observed 25-fold up regulation of Angptl4 and 2.8-fold increase in serum triglycerides (see Table 4.1). Further studies by Yu *et al.,* found that over expression of Angptl4 also leads to altered substrate oxidation and impaired cardiac function that is similar to that seen in cardiomyopathy. They were also

able to show a 60% reduction in triglyceride (intralipid) utilization in the Angptl4 transgenic mouse during isolated perfused heart studies (Yu, X. et al. 2005).

As described in Section 1.1.3, there are three sources from which the heart obtains FA for use as a fuel source. One such source is VLDL, which contains FA in the form of TG that must be hydrolysed by LPL in the cardiomyocyte before the fuel can be utilized (Yu, X. et al. 2005). The major increase in Angptl4 mRNA expression found in our current study supports the view that the heart is unable to use the LPL pathway to obtain FA for energy from VLDL and therefore it is likely that the FA used by the heart comes from one of the other two pathways. Further study using the Angptl4 transgenic mouse or even a knock-out model inconjunction with a diabetic model (such as STZ) together may provide further understanding of the impact perturbation of this enzyme has on the diabtetic heart.

In summary, there is a large body of evidence in support of the role played by increased fatty acid oxidation and FA accumulation in the damage to the heart seen in the diabetic state. Figure 4.4 schematically represents a number of the changes in gene expression described above.
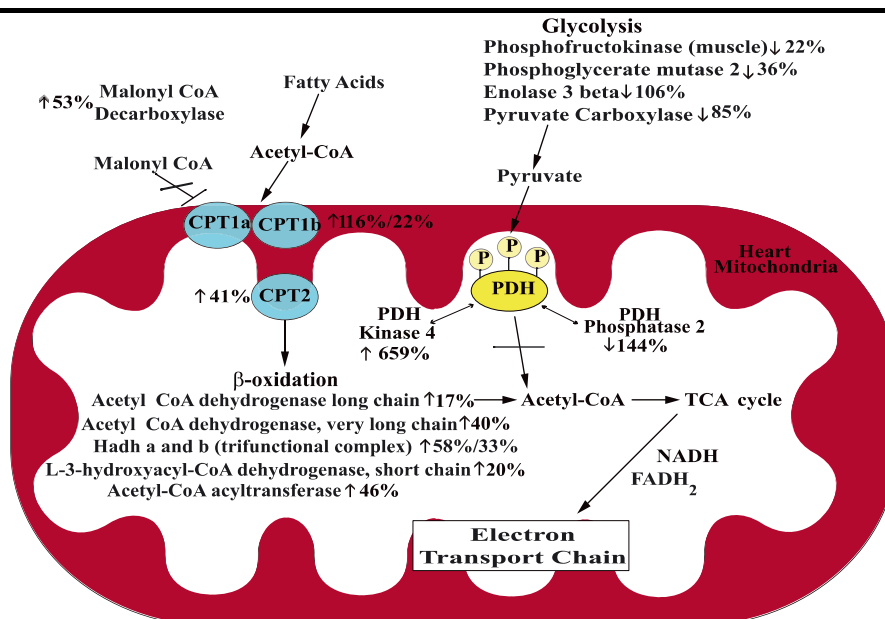
Figure 4.4 Schematic representation of fuel-metabolic pathways affected by diabetes in the heart.

Changes occurred in the expression of genes encoding enzymes that regulate PDH, consistent with a decrease in its activity and therefore ability to catalyze use of pyruvate for energy generation. Concurrent increases in expression of genes encoding mitochondrial fatty acid uptake and β-oxidation are consistent with reliance of the heart on fatty acids as its main energy source in severe diabetes.

4.3.2 Hypothesis for damage caused in heart by ROS.

Discussed below are the findings from an attempt to correlate the microarray data in this study with the hypothesis for diabetic complications as presented by Brownlee *et al.,* (Brownlee 2001). This group proposed that complications of diabetes arise as a result of an increase in the production of ROS from the mitochondria (Brownlee 2001). The hypothesis states that there are four main metabolic pathways perturbed by hyperglycaemia leading eventually to the complications observed in the diabetic state.

4.3.2.1 Reduction in GSH

GSH participates in the cellular defence system against oxidative stress by reducing disulphide linkages of proteins and other cellular molecules or by scavenging free radicals and reactive oxygen intermediates (Urata et al. 1996). The GST enzymes have classically been viewed as playing a role in cellular defence against numerous harmful chemicals produced endogenously and in the environment (Strange et al. 2001). The general reaction of GST enzymes is the addition of GSH to electrophiles which have a wide variety of chemical structures (Strange et al. 2001).

Several genes involved in GSH metabolism, such as members of the glutathione S-transferase (GST) family showed alterations in gene expression (Table 4.4). As stated in Section 4.2.2.2.1, this family of enzymes utilize glutathione in reactions contributing to the transformation and detoxification of a wide range of compounds (Strange et al. 2001). The expression of nine GSH S-transferase family members, including one member that is specific to mitochondria, was significantly altered. Of these, six were increased in diabetes, providing a possible explanation for decreased GSH availability for cellular defence and implicating this pathway as one which may contribute to increases in ROS.

4.3.2.2 Increased intracellular formation of AGEs

Of note, none of the genes linked to AGE formation were found to have associated expression changes. This may be changes occurring at levels other than transcription. Evidence for this comes from the three general mechanisms of AGE formation known to cause cell damage. The first of these, alteration in the function of proteins after modification by AGEs (Brownlee 2001; Kang 2003) would likely lead to changes in function rather than expression of a gene. The second, modification of ECM components by AGEs is thought to result in abnormal interaction with other matrix components and cause formation of covalent crosslink's leading to decreased elasticity and solubility of collagen, creating a stiffer muscle (Brownlee 2001), but not necessarily changing gene expression. This was confirmed by a lack of observed changes in gene expression of

collagen I, III and IV in this study. The third mechanism, interaction of AGE products with their receptors inducing receptor-mediated production of ROS (Brownlee 2001) may induce changes in gene expression; however, it would be difficult to relate any changes specifically back to AGE accumulation. No changes in gene expression were observed for any of the receptors for AGE.

4.3.2.3 Activation of PKC

An increase in total DAG content associated with diabetes has been demonstrated in a variety of tissues, including the heart (Inoguchi et al. 1992). Inoguchi *et al.,* (Inoguchi et al. 1992) reported increased membranous PKC activity and total DAG in the hearts of diabetic animals. This group found that the PKC-β_2 isoform was preferentially increased in the rat heart and aorta, suggesting that it might contribute to cardiovascular complications. The gene expression levels of PKC-β_2 were not altered in the diabetic state compared to normal in our study (see Table 4.5). However the δ isoform of PKC (PKC-δ) was found to show a 1.3-fold increase in gene expression in the diabetic state. Recent literature using immunoblotting in the aorta and heart of diabetic animals suggests that of the various isoforms of PKC, both PKC-β and PKC-δ appear to be preferentially activated in diabetes (Koya and King 1998).

4.3.2.3.1 Downstream effectors activated by PKC

Both endothelin receptors A and B were increased in the diabetic animals as shown in the Table 4.5. Endothelins are a family of potent vasoactive molecules of which there are four distinct forms ET-1, ET-2, ET-3 and the vasoactive intestinal contractor; these four forms interact with three populations of receptor: ET_A, ET_B and ET_C. It has previously been demonstrated that endothelin and its receptor mRNA are increased in the retina of diabetic rats (Chen, S. et al. 2000). Chen *et al.,* (Chen, S. et al. 2000) also investigated heart ET-1 in STZ rats six months after induction of diabetes and showed that ET-1 mRNA as well as ET_A, ET_B mRNA were increased in the diabetic heart.

4.3.2.4 Increased flux through the Hexosamine pathway

As stated in Section 4.2.2.2.4, inhibition of the rate limiting enzyme in the conversion of glucose to glucosamine in the hexosamine pathway was able to block hyperglycemia-induced increases in the transcription of TGF-α, TGF-β1 and PAI-1. Our study found no change in the GFAT mRNA expression and only one change in any of the downstream molecules, this being PAI-1.

4.3.2.5 The common element

A link between overproduction of ROS and the activation of the four pathways has been proposed recently by Du *et al.,* (Du, X. et al. 2003). This group found that the increase in ROS leads to the inhibition of GAPDH, an enzyme involved in the glycolysis/gluconeogenesis pathway that acts by converting d-glyceraldehyde-3-phosphate into 3-phospho-D-glycerol phosphate. These researchers postulated that inhibition of GAPDH would activate all of the four pathways of hyperglycaemic damage described, by diverting upstream glycolytic metabolites into each of these pathways (Du, X. et al. 2003). Du *et al.,* ultilized an *in vivo* model to investigate the mechanism by which hyperglycemia-induced overproduction of superoxide inhibits GAPDH. They reasoned that because hyperglycemia-induced loss of endothelium-dependent vasodilation can be normalised by inhibition of poly-(ADP-ribose) polymerase (PARP), the best starting place would be to study the relationship between PARP, hyperglycemia-induced overproduction of superoxide and GAPDH activity. PARP is a nuclear DNA repair enzyme which catalyses the attachment of ADP-ribose units from NAD$^+$ to nuclear proteins. Replacement of the NAD$^+$ that is lost by PARP results in consumption of ATP; thus excessive activation of PARP leads to excessive ATP consumption and this can cause cell death due to the resulting energy deficit (Du, X. et al. 2003). This theory has been confirmed by a separate group, who found that inhibition of PARP significantly improved systolic and diastolic pressure in an STZ-model of diabetes (Pacher et al. 2002).

Normally, PARP is present in the nucleus in an inactive form that is activated by DNA damage. In conditions where there are increased levels of intracellular glucose, it has been demonstrated that the generation of ROS is increased in the mitochondria and that these free radicals subsequently induce DNA strand breaks, thereby activating PARP. Once activated, PARP splits the NAD molecule into its two component parts: nicotinic acid and ADP-ribose. PARP then proceeds to make polymers of ADP-ribose, which accumulate on GAPDH and other nuclear proteins. Although GAPDH is commonly thought to reside exclusively in the cytosol, it does in fact, in normal tissues, shuttle in and out of the nucleus, where it plays a critical role in DNA repair (Brownlee 2001).

PARP-induced modification of GAPDH reduces its activity leading to activation of the polyol pathway, which causes increases in intracellular AGE formation and thus activation of PKC and subsequently NFκB, and finally activates hexosamine pathway flux (Brownlee 2005). There were no changes in expression of the gene encoding GAPDH in this study (Table 4.7). This result is not unexpected, as there is evidence that it is inhibition of GAPDH activity through accumulation of ADP-ribose polymers that causes the derangement as outlined above. This highlights the need to consider the regulation of protein expression in addition to gene expression when analysing microarray data.

There was observed however, a modest increase in expression of a 2,3,7,8-tetrachlorodibenzo-p-dioxin (TCDD)-inducible PARP (Table 4.7) by 1.3-fold in the diabetic group compared to the sham. This finding strengthens the correlation between the results from this microarray study and the hypothesis as proposed by Brownlee *et al.,* (Brownlee 2001).

4.3.2.6 Relationship between fatty acid oxidation, ROS generation and mitochondrial function

Brownlee's hypothesis has been derived from studies performed mainly in endothelial cells which lack the GLUT4 transporter, therefore allowing the large influx of glucose required to initiate events outlined throughout this chapter (Brownlee 2001). The paradox in cardiomyocytes is that glucose transport is actually reduced and fatty acid transport is increased. However, as stated in the Banting Lecture 2004 (Brownlee 2005), since β-oxidation of FA and oxidation of the resulting acetyl-CoA by the TCA cycle generates the same electron donors as glucose oxidation, increased fatty acid oxidation may result in mitochondrial overproduction of ROS by exactly the same mechanism (Brownlee 2005). Further evidence to support this theory is from work done by St-Pierre *et al.,* (St-Pierre et al. 2002) which showed that rat skeletal muscle and heart mitochondria produced measurable levels of H_2O_2 (a precursor of ROS) when respiring on palmitoyl carnitine compared to no measurable H_2O_2 produced when respiring on pyruvate or succinate (St-Pierre et al. 2002).

 Further evidence for a role of FA in the generation of ROS has come from work done on the uncoupling protein (UCP) gene family. It has been shown that UCP3 mRNA expression is increased when heart FA levels are high (St-Pierre et al. 2002) and a further study also demonstrated this in the skeletal muscle of db/db mice (Clapham et al. 2001). In this microarray study, UCP-3 was found to be increased by 2.5-fold in the diabetic animal (Table 4.3).

The functional role of UCP3 is currently under active debate. One review (Brand and Esteves 2005) identified four models with which it is possible to describe the function of UCP2 and UCP3. Each model was required to incorporate the following observations:

- That fatty acids increase the expression of UCP2/3 mRNA thus implying that they are somehow involved in FA metabolism.
- That UCP2/3 catalyse net proton conductance but only when activated by fatty acids and free radical derived alkenals
- That UCP2/3 can probably export fatty acids and other anions

The model for which there was the best evidence suggests that the functional role of UCPs is to attenuate mitochondrial production of free radicals and protect against

oxidative damage. Because mitochondrial ROS production is very sensitive to the proton-motive force set up across the inner membrane by electron transport, the mild uncoupling caused by activation of UCP2 or UCP3 may lower this force slightly, and thus attenuate mitochondrial ROS production, and protect against ROS-related cellular damage (Brand and Esteves 2005). The increase in UCP3 seen in this study would indicate that in the STZ model of diabetes the observed increase in fatty acids leads to an increase in ROS production which requires UCP3 as a protective agent. Whether the protective effect of UCP3 is via attenuation of free radical production or export of fatty acids and fatty acid peroxides from the mitochondria (another functional role proposed by Brand and Esteves, (Brand and Esteves 2005)) is not known and requires further study. This study could be achieved using transgenic models of UCP-3 such as that employed by Changani et al., (Changani *et al.* 2003) coupled with STZ as a diabetiogenic agent. Studies of mitochondrial respiration and uncoupling are currently being undertaken in this laboratory (Dr A Hickey, personal communication) and use of this technique on such a model may further our understanding of how UCP-3 protects the mitochondria.

As mentioned in Section 4.3.1.2.2, the diabetic state leads to an increase in the fatty acid transporter CD36/FAT (with an increase of 1.4-fold observed in this study). This transporter has also been implicated in an increase in oxidative stress damage to the heart. Farhangkhoee *et al.,* (Farhangkhoee et al. 2005) reported that incubation of cultured MVECs in a high background of glucose results in up regulation of CD36/FAT, this was followed by an increase in levels of oxidized-LDL (thought to be a ligand for the CD36/FAT transporter) and haeme oxygenase 1, a marker of ROS. This effect was able to be prohibited by CD36/FAT gene silencing. Further to this, the group was able to show in a STZ rat model of diabetes, an increase in CD36/FAT using RT-PCR as well as an increase in oxidative stress markers nitrotyrosine (protein) and 8-OHdG (DNA) (Farhangkhoee et al. 2005).

Taken together these results support the hypothesis of oxidative stress damage in the heart being a result of increased fatty acid metabolism rather than glucose metabolism as is classically believed.

4.4 Conclusions

Results presented in this chapter show that the genes corresponding to proteins that are expressed in mitochondria account for a disproportionate number of those whose expression was significantly modified in DCM. These findings are consistent with the hypothesis that mitochondria act as key targets of the pathogenic processes that cause diabetic heart disease. Furthermore, this microarray analysis is also consistent with the hypothesis that the diabetic state induces global perturbations in the expression of genes

regulating fatty acid metabolism, whose dysfunction is likely to play a key role in the promotion of oxidative stress, thereby contributing to the development of myocardial disease. In particular, our study points to impaired regulation of mitochondrial β-oxidation as central in the mechanisms contributing to DCM pathogenesis. These conclusions are based on the gene changes described within this chapter and are consistent with other available lines of evidence (Sakamoto et al. 2000; Lopaschuk 2002; Taegtmeyer et al. 2002; Taegtmeyer et al. 2004)

Chapter 5 Characterization the physiological effects on and metabolism of TETA-disuccinate in diabetic and sham rats after eight weeks of treatment

5.1 Introduction

TETA is a selective Cu^{II}-chelator originally used in the treatment of Wilson's disease (Walshe 1982), as described in Section 1.3.2. Use of TETA as a potential therapeutic treatment in rodents was first described by Cameron and Cotter (Cameron and Cotter 1995) and in humans by Cooper *et al.* (Cooper et al. 2004).

A recent publication by Lu *et al.,* (Lu et al. 2007) characterised the excretion of TETA and its metabolites (MAT and DAT) in human subjects with or without diabetes. In this study it was discovered that healthy subjects metabolised TETA differently to diabetic subjects, resulting in different ratios of TETA to metabolite present in the urine (Lu et al. 2007). Results from a metal balance study conducted concurrently with this work also found abnormalities in metal ion excretion as a result of the diabetic state and that levels of both copper and zinc were affected in a dose responsive manner with TETA treatment (Cooper et al. 2005)

Much of the work looking at the metabolism of TETA in rats has come from studies that focussed on the analysis of either intravenous or single oral dose administration, providing important information regarding the uptake and distribution of TETA in normal animals acutely (Takeda et al. 1995a; Takeda et al. 1995b; Takeda et al. 1995c) but not for chronic treatment or treatment of animals with STZ-induced diabetes.

Work from this laboratory (Cooper et al. 2004; Gong et al. 2006) has suggested a change in the physiology of treated diabetic animals, with changes in total body weight and heart weight/body weight observed, however a comprehensive analysis of the physiological effects of TETA treatment on sham or diabetic rats over time has not been conducted.

This aim of this chapter was therefore to evaluate the effects of continuous TETA-disuccinate administration on the physiological characteristics of male Wistar rats with or without STZ-induced diabetes over an eight week period. Collected data included blood glucose levels, total body weight, heart weight, serum biochemistry, urine and serum TETA, MAT, DAT and metal levels (Cu, Zn, Fe and Mn). Quantification of TETA, MAT and

DAT was achieved using an HPLC-based method developed by the School of Biological Sciences Reference Laboratory.

This work aimed to establish whether the difference in metabolism observed in humans is also present in this animal model of diabetes. The current study was designed to include a variety of TETA-disuccinate doses with a view to understanding whether treatment elicits a dose-response and what the effects of an extreme high and low dose are, as these have not previously been studied in diabetic animals.

5.2 Results

5.2.1 Experimental design

As in Chapter Four (Section 4.2.1), this study utilized animals with diabetes caused by STZ, or matched saline-injected controls (Section 2.1). As a direct result of the work published previously (Cooper et al. 2004; Cooper et al. 2005), this study included a series of TETA-disuccinate arms in an attempt to elucidate the effect that the drug was having on the phenotypic, biochemical and molecular characteristics of this model. Analyses of the molecular changes associated with TETA-disuccinate were restricted to those in the LV of the heart and are discussed fully in Chapter Six. The design of this study is outlined below in Figure 5.1.
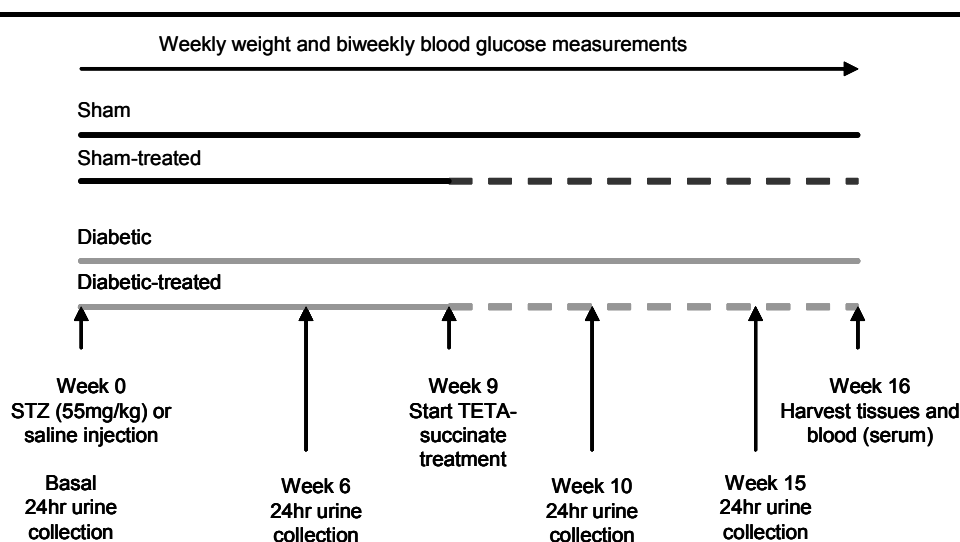
Figure 5.1 General experimental design

Experiment included four main arms, sham untreated (——, n= 6), sham treated with TETA succinate (- - -, n= 6 per dose), diabetic untreated (——, n= 8), diabetic treated with TETA succinate (- - -, n= 8 per dose). STZ or saline were injected at Week 0 (Section 2.1). At four time points (basal, 6 week, 10 week and 15 weeks), 24hr urine collections were performed as described in Section 2.1.2. Administration of TETA-disuccinate (Section 2.1.1) was begun eight weeks after injection of STZ or saline. 16 weeks after administration of STZ or saline terminal serum, heart, kidney and liver tissue was collected as described in Section 2.2.1.2

Included in this study was administration of four doses of the compound TETA-disuccinate (3.5mg, 17.5mg 35mg and 87.5mg) as described in Section 2.1.1. All doses were per rat per day independent of body weight or blood glucose. This range of doses was chosen in order to identify whether the effects of TETA occurred in a dose responsive manner. The lowest dose (3.5mg) has not previously been studied. The lower limit of drug efficacy in STZ-induced diabetes was unknown prior to this study, so a 3.5mg dose was included in order to ascertain whether changes could be observed even at this very low dose.

As indicated in Figure 5.1, this study included four 24hr urine collections from animals in specially designed metabolic cages (Section 2.1.2). Collections were performed at a basal time point (pre-injection of either STZ or saline), Week 6 (six weeks post-STZ or saline injection), Week 10 (two weeks post start of TETA-disuccinate administration) and Week 15 (seven weeks post start of TETA-disuccinate administration). During the 24hr period water-intake, food-intake and urine volume were measured. Table 5.1 outlines the amounts of water, food or urine that animals either consumed or excreted over the course of a 24hr collection, irrespective of TETA-disuccinate administration. This table indicates a marked increase in all three parameters analysed in the diabetic animals within six weeks of STZ injection compared to sham. Urine collection enabled the analysis of levels of TETA-disuccinate and its metabolites (MAT and DAT, in Week 10 and 15 24hr collections only), and trace metal levels (all time points) previously identified as altered in the diabetic state (Cooper et al. 2005).

Table 5.1 Amounts of water and food consumed and urine excreted during 24hr

	Sham				Diabetic			
	Basal	6 week	10 week	15 week	Basal	6 week	10 week	15 week
Water intake (ml)	31.2±1.5	38.8±2.7	36.4±2.9	36.8±4.0	32.7±0.9	138.9±7.9	153.0±7.5	143.5±6.8
Food intake (g)	18.5±0.6	10.1±0.9	8.0±0.7	5.5±0.7	18.4±0.5	27.7±1.1	29.1±1.2	27.8±1.3
Urine Excretion (ml)	13.5±1.1	25.9±2.3	23.4±2.3	22.7±2.8	13.1±0.8	125.9±5.8	141.5±5.7	126.5±5.9

5.2.1.1 Stability study of TETA-disuccinate in water

As described in Section 2.1.1, TETA-disuccinate was administered via the drinking water at concentrations calculated to deliver 3.5, 17.5, 35 or 87.5mg per rat per day. In order to ensure that drug concentration in the water remained stable over time, a drug stability study was performed prior to initial administration, using the HPLC serum method developed by the School of Biological Sciences Reference laboratory (Section 2.7)
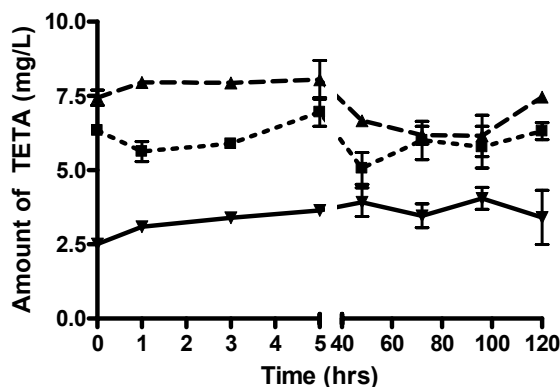
Figure 5.2 Stability of TETA-disuccinate in milliQ water

Prior to administration of TETA-disuccinate stability in milliQ water (18 MΩ) was assessed. TETA levels were determined (Section 2.7) at eight time points over three representative doses, Stock (▲, 6.69 mg/l), sham (■, 5.35mg/l) and diabetic (▼, 3.75mg/l).Time points at which a sample of TETA dissolved in water were taken: Baseline (at the time TETA was dissolved), and then 1, 3, 5, 48, 72, 96, and 120hrs after TETA was dissolved into milliQ water.

Samples were taken at baseline (when the drug was made), then at 1, 3 and 5hr intervals to assess whether there was any acute degradation and then daily (day 2-5) in order to ascertain whether the drug was stable for up to a week. As can be seen in Figure 5.2, loss of TETA occurred at only minimal levels even at the very low concentration intended for the diabetic animals. The percentage CV for this data is within the 15% required by the FDA.

In order to ensure a constant level of TETA-disuccinate taken in by the animals, water intake was measured weekly from week eight and used to calculate the concentration of TETA-disuccinate.

5.2.2 Physiological characterization

5.2.2.1 Blood glucose

Consistent with the results described in Chapter Four (Table 4.1, Figure 4.1A); diabetic animals had raised levels of glucose three days after STZ injection. On average, diabetic animals had blood glucose levels of 26.6 ± 2.4mM compared to sham animals with average blood glucose values of 5.0 ± 0.2mM. This increase in blood glucose was sustained for the duration of the sixteen week study (see Figure 4.1B for a representative graph).

Previous work has shown that TETA administration has no effect on the blood glucose (Cooper et al. 2004; Jullig et al. 2007). Repeated measures ANOVA (Section

2.12.5.3) analysis of blood glucose levels using data from Week 10 onwards (post-drug) confirmed this in the present study with the blood glucose levels of the different treatment groups showing no significant difference over Dose or Time (Dose P=0.8754, Time P=0.3970).

5.2.2.2 Total body weight

Animals were weighed weekly. The combined weight of the diabetic group (all doses) compared to the combined weight of the sham group (all doses) was similar to that presented in Chapter Four (Figure 4.1C). Diabetic animals had an average body weight of 308.7 ± 5.6g compared to the sham average body weight of 440.4 ± 20.1g.

For the statistical analysis the data was split into two in order to ensure analysis was carried out on comparable data.

The first part of the analysis aimed to determine if there was a difference in the weight of diabetic and sham animal's pre-drug administration (Week Two to Week Eight). Assessment of animals weight prior to injection of STZ or saline (Week One) found that groups were not significantly different (Status P=0.6322). A repeated measures ANOVA (Section 2.12.5.3) was conducted on the absolute weights of sham and diabetic animals from Week Two to Week Eight, and results are presented in Figure 5.3 There was a significant Status*Time interaction (P<.0001) indicating that the weight of the animal at a particular time point is dependent on its disease status. In this figure, we can see that the diabetic group track lower than the sham group from about Week Three onwards. As in Chapter Four, the sham animals continue to gain weight while the diabetic group plateaus.

(A)

Source	Num DF	Den DF	F value	Pr>F
Status	1	73.6	250.42	<.0001
Time	6	163	212.74	<.0001
Status*Time	6	163	49.76	**<.0001**

(B)
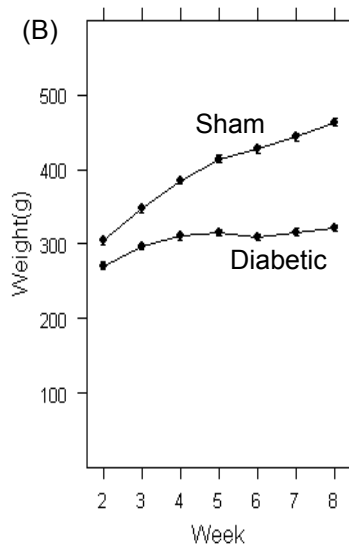
Figure 5.3 Analysis of changes in weight as a result of STZ or saline injection

Male Wistar rats (220-250g) were anesthetised using 5% isoflurane, 2l/min O_2, and 55mg/kg STZ dissolved in saline was immediately injected into the tail vein to induce diabetes. Control rats (sham) received the corresponding volume of saline. Animals were housed in pairs on fibrecycle bedding (12 hr light:dark cycle, 50-70 % humidity, 19-21 °C) and maintained on Teklad TB 2018 (Harlan, UK) rat chow and tap water *ad libitum*. Animals were weighed on a weekly basis from weeks 1-16. Data presented represents adjusted mean ± SEM for weeks 2-8 (pre-TETA administration).

(A) Results of the repeated measures ANOVA conducted to assess the effect of status over time on the body weights of animals with or without diabetes. Variance structure used was Autoregressive (1).

(B) Body weight over time. Animals were weighed on a weekly basis from Week 1-16. Data presented represents adjusted mean ± SEM for Weeks 2-8 (pre-TETA administration).

The purpose of the second part of the analysis was to elucidate any changes that may have occurred as a result of treatment with TETA. To ensure that there was no difference in weight between animals assigned to a particular drug dose, an assessment of either sham animals at Week Eight or diabetic animals at Week Eight was conducted using dose as the main effect. It was found in the analysis of sham weights that there was weak evidence for a difference in weight between drug dose groups prior to administration of TETA (Dose P=0.0579) and moderate evidence for difference in weight between drug dose groups in the diabetic group (Dose P=0.0353). This result may be due to the non-random allocation of animals to dose (Section 2.1.1, Table 2.1). In light of this difference in pre-TETA administration, an assessment of the change in body weight was conducted (change = (Week 9-16)-Week 8, repeated measures ANOVA Section 2.12.5.3). By subtracting the weight of an animal at Week Eight, any change associated with different

starting weights is removed and more meaningful results can be obtained. Results of this analysis are presented in Figure 5.4.

There were three significant interactions in this analysis. Figure 5.4 (B) represents the Status*Time interaction (P<.0001). As seen in Figure 5.3 (pre-TETA treatment), the diabetic animals' weights remained level for the duration of the study, while the sham animals continued to gain weight. Figure 5.4 (C) represents the Status*Dose interaction (P=0.0182). Here, the effect of TETA on the weight of the animal was dependent on the status. In this analysis it can be seen that for both groups the change in weight was generally increased over dose administered. The diabetic group showed a dose-responsive increase in weight change, with the change in weight shifting from negative to positive as the dose of TETA increased. This finding was further confirmed by Tukey's *post-hoc* tests, which showed that the change in weight for the 87.5mg group was significantly greater than that of the 0, 3.5, and 17.5mg groups (P=0.0448, P=0.0161, P=0.067 respectively). Overall, the sham animals also showed an increase in weight with treatment. The same dose response was not observed in the sham group, with the 3.5mg group showing an abnormally large weight gain. This may be due to the non-randomisation of dose groups. The third significant interaction, Figure 5.4 (D) was a Dose*Time interaction (P=0.0012). This interaction indicates that there is a change in weight with time that is dependent on the dose of TETA administered. The 87.5mg group had the greatest change in weight as time progressed while the animals receiving no drug showed the lowest change in weight as time progressed.

(A)

Source	Num DF	Den DF	F value	Pr>F
Status	1	60.1	210.81	<.0001
Dose	4	60.1	2.31	0.0685
Status*Dose	4	60.1	3.23	**0.0182**
Time	7	207	21.52	<.0001
Status*Time	7	207	28.79	**<.0001**
Dose*Time	28	207	2.15	**0.0012**
Status*Dose*Time	28	207	1.34	0.1258

(B)   (C)   (D)
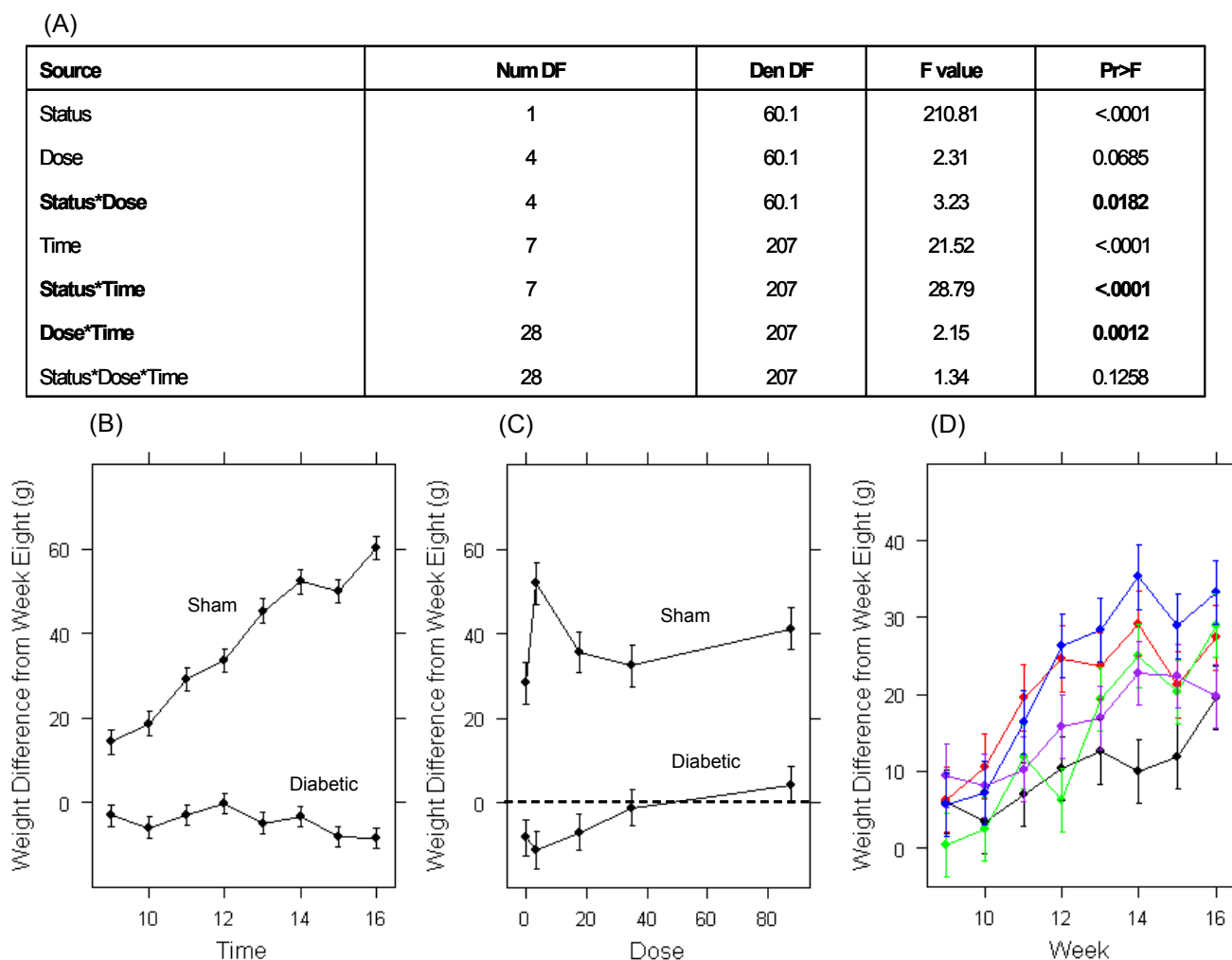
Figure 5.4 Analysis of changes in weight as a result of TETA administration

Male Wistar rats (220-250g) were anesthetised using 5% isoflurane, 2l/min O2, and 55mg.kg^{-1} STZ dissolved in saline was immediately injected into the tail vein to induce diabetes. Control rats (sham) received the corresponding volume of saline. Animals were housed in pairs on fibrecycle bedding (12 hr light:dark cycle, 50-70 % humidity, 19-21 °C) and maintained on Teklad TB 2018 (Harlan, UK) rat chow and tap water *ad libitum*.
Animals were weighed weekly basis from Week 1-16.
(A) Results of the repeated measures ANOVA conducted to assess the effect of either status or dose over time on the adjusted body weights of treated or untreated animals. Variance structure used was Autoregressive (1).
(B) Change in body weight over time (fixed effect: Status). Animals were weighed on a weekly basis from Week 1-16. Data presented represents adjusted mean ± SEM for the difference in body weight of Week 9-16 (minus Week 8)
(C) Change in body weight over dose (fixed effect: Status). Animals were weighed on a weekly basis from Week 1-16. Data presented represents adjusted mean ± SEM for the difference in body weight of Week 9-16 (minus Week 8)
Change in bodyweight over time (fixed effect: Dose). Animals were weighed weekly from Week 1-16. Data presented represents adjusted mean ± SEM for the difference in body weight of week 9-16 (minus Week 8) (⎯⎯ 0mg, ⎯⎯ 3.5mg, ⎯⎯ 17.5mg, ⎯⎯ 35mg, ⎯⎯ 87.5mg)

5.2.2.3 Heart weight

Analysis of change in heart weight as a result of treatment with TETA-disuccinate was conducted after tissue collection. Data was assessed for changes in Status (diabetic vs. sham), Dose (treatment with TETA) and Status*Dose (changes occurring with TETA treatment that are dependent on the status of the animal). Results of the heart weight and heart weight/body weight ANOVA (Section 2.12.5.2) found that, as in Chapter Four, the diabetic hearts were significantly smaller than those of the sham animals but that the ratio to bodyweight was increased (Table 5.2).

Table 5.2 Heart weight and heart weight body weight measurements

	Status	Mean	*LSE	*USE	P value	Change
HW (g)	Sham	1.7	1.6	1.7	P<.0001	↓ Diabetes
	Diabetic	1.4	1.4	1.5		
HW/BW (g/g)	Sham	3.2E-03	3.1E-03	3.3E-03	P<.0001	↑ Diabetes
	Diabetic	4.6E-03	4.5E-03	4.7E-03		

*LSE = Lower standard error, USE=Upper standard error

In the initial assessment of HW, it was noted that there was very weak evidence for a response to administration of TETA in both groups (Dose P=0.0626). Further investigation of the data revealed an outlying value from the diabetic untreated group (Animal ID # 42, Figure 5.5 (B) and (C)). Removal of this animal from the analysis reduces the P-value from P=0.0626 to P=0.0033. Visual assessment of the data indicates that the change observed is an increase in heart weight with treatment across all groups; however this does not occur in a dose responsive manner. The significant increase was lost when HW was corrected for body weight (data without animal ID #42 P=0.1167), so the significance of this result is uncertain.

(A)

Source	DF		Type III SS		Mean Square		F value		Pr>F	
	HW	HW No #42	HW	HW No #42	HW	HW No #42	HW	HW No #42	HW	HW No #42
Status	1	1	0.16028	1.15452	0.16028	1.154526	22.72	37.36	**<.0001**	**<.0001**
Dose	4	4	0.06683	0.54959	0.016708	0.137396	2.37	4.45	0.0626	**0.0033**
Status*Dose	4	4	0.02097	0.132783	0.005243	0.033196	0.74	1.07	0.5664	0.3774
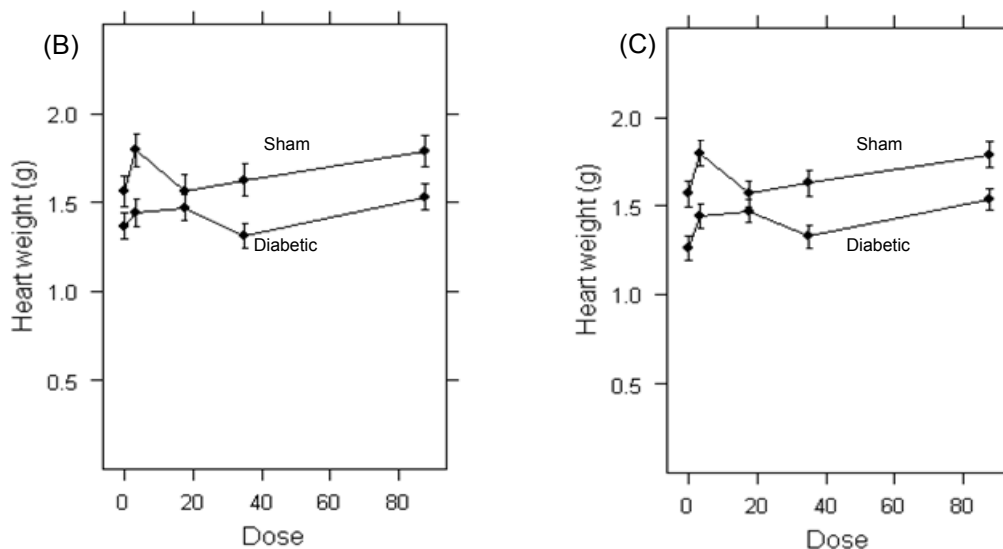
Figure 5.5 Effects of TETA-disuccinate treatment on absolute heart weight with and without animal ID # 42

Sixteen weeks after injection with either STZ (diabetic) or saline (sham), male Wistar rats were placed in an induction box with isoflurane 5%, O_2 2l/min. Once anaesthetized, animals were weighed (Final BW). Animals were thereafter maintained on isoflurane 2-3%/, O_2 2l/min and once complete anaesthesia was confirmed a midline laparotomy was performed. After 2min, animals were killed via thoracotomy. Heart weight values for each dose are displayed separately for the sham and diabetic groups

(A) Results of the ANOVA conducted to assess the effect of either status or dose on the heart weights of treated animals compared to untreated controls

(B) Heart weights with animal 42. Hearts were weighed at the time of excision, prior to perfusion. Values are adjusted means ± SEM (n=6 for all doses in the sham group and 8 for all doses in the diabetic groups)

(C) Heart weights without animal 42. Hearts were weighed at the time of excision, prior to perfusion. Values are adjusted means ± SEM (n=6 for all doses in the sham group and 8 for all doses in the diabetic groups)

5.2.3 Serum biochemistry

A terminal serum sample was taken from each animal and used for a number of different biochemical tests as indicated below.

Data were analysed using ANOVA (Section 2.12.5.2) with Tukey's *post-hoc* tests and were again assessed for changes in Status, Dose and Status*Dose. The results of the ANOVA indicated that in the majority of serum biomarkers tested, a significant change

occurred only in the diabetic vs. sham (Status) comparison. The results of the Status comparison are presented below.

5.2.3.1 Liver function tests

Table 5.3 Indicators of liver function

	Status	Mean	LSE	USE	P value	Change
ALP (U/L)	Sham	124	118	131	P<.0001	↑ Diabetes
	Diabetic	628	598	660		
ALT (U/L	Sham	50	48	53	P<.0001	↑ Diabetes
	Diabetic	111	106	117		
AST (U/L)	Sham	67	65	71	P=0.0135	↑ Diabetes
	Diabetic	81	77	85		
Billirubin (μmol/L)	Sham	6.6	6.3	6.9	P<.0001	↑ Diabetes
	Diabetic	8.7	8.3	9.0		

Significant increases in ALP, ALT, aspartate transaminase (AST, which is similar to ALT in interpretation, but was not measured in Chapter 4) and bilirubin indicate that modest liver disease was present in the diabetic animals in this study (Table 5.3). The liver disease present is of an unspecific nature as the changes within each of the four enzymes measured were small, but could have been caused by steatohepatitis, which is known to accompany diabetes.

5.2.3.2 Lipid markers

Table 5.4 Lipid levels in serum

	Status	Mean	LSE	USE	P value	Change
TG (mmol/L)	Sham	1.4	1.2	1.6	P<.0001	↑ Diabetes
	Diabetic	3.0	2.7	3.3		
HDL (mmol/L)	Sham	1.2	1.2	1.3	P<.0001	↑ Diabetes
	Diabetic	1.7	1.6	1.7		
FFA (mmol/L)	Sham	0.7	0.6	0.8	P=0.0247	↑ Diabetes
	Diabetic	1.1	1.0	1.3		
Cholesterol (mmol/L)	Sham	1.3	1.3	1.3	P<.0001	↑ Diabetes
	Diabetic	2.1	2.0	2.2		

Increases in the levels of all four lipid markers (Table 5.4) are consistent with those observed in Chapter Four. These changes indicate a perturbation in the ability of the diabetic animals to process lipid as well as glucose, as has been previously documented (Taegtmeyer et al. 2002; Taegtmeyer et al. 2004; Glyn-Jones et al. 2007). No changes were observed in any of the different lipid markers as a result of treatment.

5.2.3.3 Renal function

Table 5.5 Indicators of renal function in serum biochemical markers

	Status	Mean	LSE	USE	P value	Change
Urea (mmol/L)	Sham	7.0	6.8	7.3	P=0.0043	↑ Diabetes
	Diabetic	8.2	7.9	8.5		
Albumin (g/L)	Sham	16.3	16.1	16.6	P<.0001	↓ Diabetes
	Diabetic	14.1	13.9	14.3		
Total Protein (g/L)	Sham	62.7	61.8	63.6	P<.0001	↓ Diabetes
	Diabetic	54.9	53.9	55.9		
Creatinine (μmol/L)	Sham	42.3	42.2	43.5	P=0.5553	–
	Diabetic	43.3	42.2	44.4		

A decrease in albumin and total protein in the diabetic animals indicates an overall perturbation in the synthetic function of the kidney in the diabetic state; however, there was no change with treatment. There was no significant change in creatinine even between diabetic and normal. The absence of change associated with drug treatment indicates that the drug did not adversely affect renal function in these animals

5.2.3.4 Metal ion homeostasis

As TETA is a copper chelator and has been found to affect both copper and zinc levels within the body (Cooper et al. 2005), it was important to assess the serum levels of a number of different metals to understand the effect of TETA treatment on circulating metal levels and associated protein activities. In this study, serum levels of Cu, Zn and Fe were assessed. Ferroxidase levels indicate the activity of the copper-carrier protein ceruloplasmin (Section 1.4.1) and levels have been found to be severely decreased in studies of copper deficient rats (Uriu-Adams et al. 2005).

Figure 5.6 presents the results for analysis of copper and ferroxidase levels in the serum of treated and untreated animals. Of all the serum biomarkers assessed, only copper levels and ferroxidase activity were found to be affected by treatment with TETA.

(A)

Source	DF		Type III SS		Mean Square		F value		Pr>F	
	Cu	Ferroxidase	Cu	Ferroxidase	Cu	Ferroxidase	Cu	Ferroxidase	Cu	Ferroxidase
Status	1	1	0.00055	124968.6	0.00055	124968.6	88.5	37.54	<.0001	<.0001
Dose	4	4	0.00026	152561.1	6.4E-05	38140.27	10.3	11.46	<.0001	<.0001
Status*Dose	4	4	9.0E-05	45088.55	2.2E-05	11272.14	3.6	3.39	**0.0107**	**0.0152**
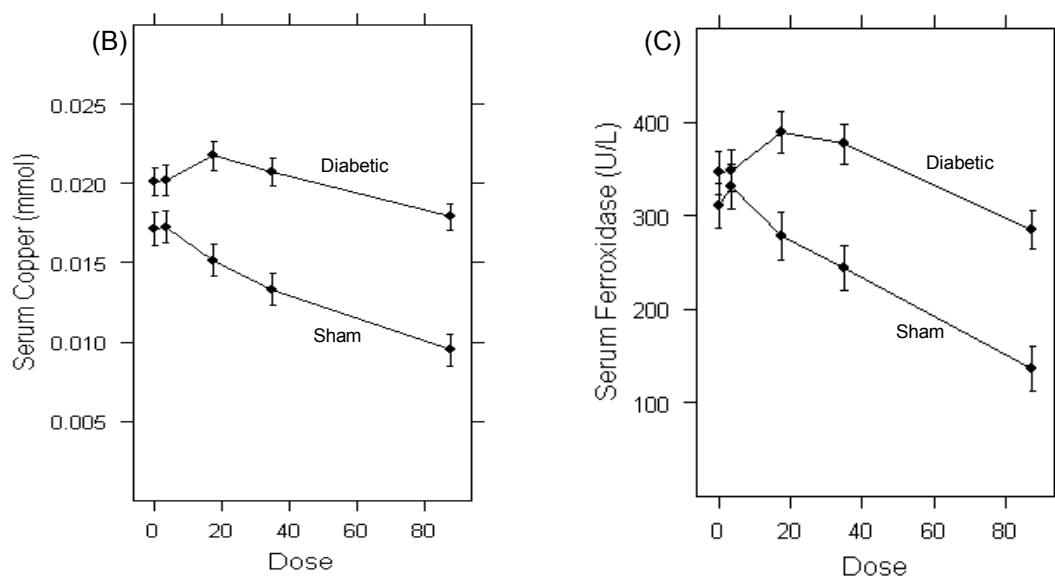
Figure 5.6 Serum copper and ferroxidase Levels

Sixteen weeks after injection with either STZ (diabetic) or saline (sham), male Wistar rats were placed in an induction box with isoflurane 5%, O_2 2l/min. Animals were thereafter maintained on isoflurane 2-3%, O_2 2l/min and once complete anaesthesia was confirmed, a midline laparotomy was performed. A 22 gauge cannula (BD, Insyte) was inserted into the vena cava and approximately 3ml of blood was extracted and aliquoted into serum tubes (BD, Insyte). Copper levels were determined as described in Section 2.11 and ferroxidase activity as described in Section 2.6.9.
Values are presented as adjusted means ± SEM
(A) Results of the ANOVA conducted to determine if there was a significant effect of either status or dose on the on the levels of copper and ferroxidase in diabetic and sham treated groups
(B) Copper levels as a function of dose administered in the diabetic and sham animals
(C) Ferroxidase levels as a function of dose administered in the diabetic and sham animals

In this study (Figure 5.6), it was observed that there is a Status*Dose interaction for the effect of TETA on both copper levels and ferroxidase activity. The similar outcome for both copper and ferroxidase activity indicates the dependence of ceruloplasmin activity on copper levels. Overall, TETA significantly reduced the levels of copper and active ceruloplasmin in a dose dependent manner in both the sham and diabetic groups. The significant interaction indicates that TETA-induced changes were dependent on whether the animal is in the diabetic or sham group. It was observed that both copper levels and ferroxidase activity had much steeper downward slopes across dose in the sham group than in the diabetic group.

(A)

Source	DF	Type III SS	Mean Square	F value	Pr>F
Status	1	61.1696254	61.1696254	1.29	0.2632
Dose	4	319.8732363	79.9683091	1.68	0.1731
Status*Dose	4	271.0084549	67.7521137	1.43	0.2431

(B)

(C)
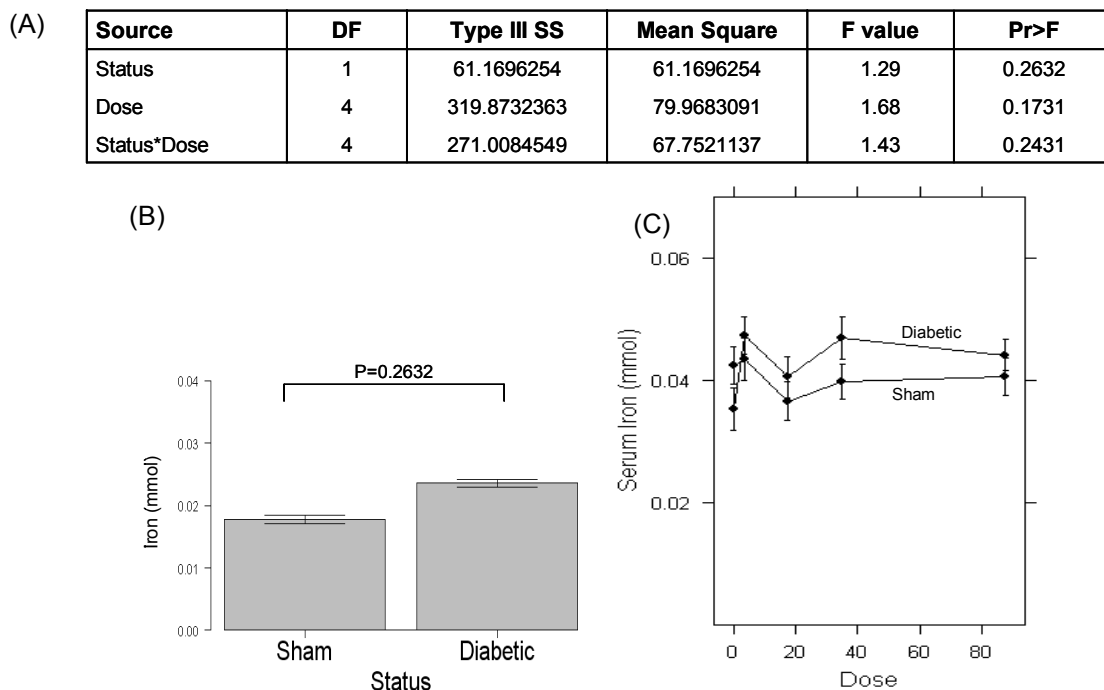
Figure 5.7 Iron levels in serum

Sixteen weeks after injection with either STZ (diabetic) or saline (sham), male Wistar rats were placed in an induction box with isoflurane 5%, O_2 2l/min. Animals were thereafter maintained on isoflurane 2-3%, O_2 2l/min and once complete anaesthesia was confirmed, a midline laparotomy was performed. A 22 gauge cannula (BD, Insyte) was inserted into the vena cava and approximately 3ml of blood was extracted and aliquoted into serum tubes (BD, Insyte). Iron levels were determined as described in Section 2.6.11.
Values are presented as adjusted mean ± SEM
(A) Results of the ANOVA conducted to assess if there was a significant effect of either status or dose on the on the levels of iron in diabetic and sham treated groups
(B) Levels of iron in the sham groups compared to that in the diabetic groups
(C) Iron levels as a function of dose administered in the diabetic and sham animals

Iron levels were found to be the same between the diabetic and sham groups (Status P=0.2632) and TETA treatment resulted in no change in iron levels (Treatment P=0.1731, Figure 5.7).

(A)

Source	DF	Type III SS	Mean Square	F value	Pr>F
Status	1	0.00057423	0.00057423	41.86	**<.0001**
Dose	4	0.00006784	0.00001696	1.24	0.3052
Status*Dose	4	0.00000618	0.00000154	0.11	0.9777

(B)

(C)
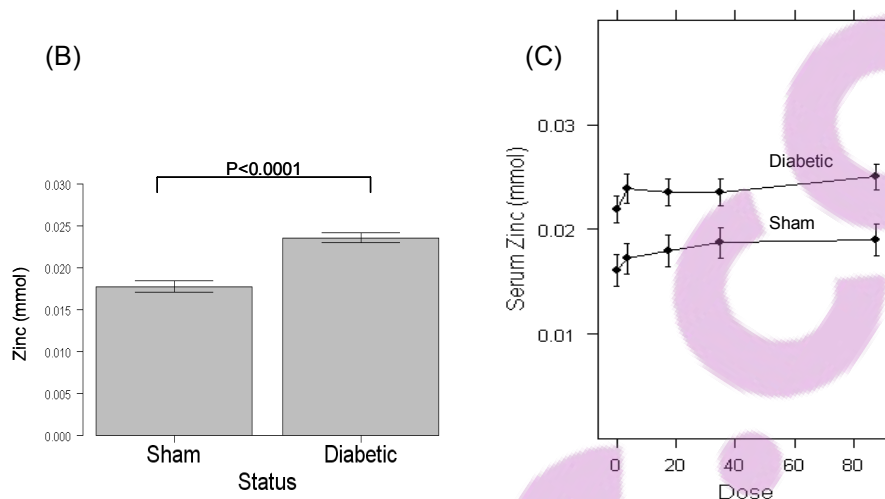
Figure 5.8 Zinc levels in serum

Sixteen weeks after injection with either STZ (diabetic) or saline (sham), male Wistar rats were placed in an induction box with isoflurane 5%, O_2 2l/min. Animals were thereafter maintained on isoflurane 2-3%, O_2 2l/min and once complete anaesthesia was confirmed, a midline laparotomy was performed. A 22 gauge canula (BD, Insyte) was inserted into the vena cava and approximately 3ml of blood was extracted and aliquoted into serum tubes (BD, Insyte). Zinc levels were determined as described in Section 2.11.
Values are presented as adjusted mean ± SEM
(A) Results of the ANOVA conducted to assess if there was a significant effect of either status or dose on the on the levels of zinc in diabetic and sham treated groups
(B) Levels of Zinc in the sham groups compared to that in the diabetic groups
(C) Zinc levels as a function of dose administered in the diabetic and sham animals

Zinc levels were found to be increased in the diabetic group compared to sham groups, but did not change with TETA treatment (Figure 5.8).

5.2.4 TETA and metabolite analysis

As well as measuring the effects of TETA on physiological parameters and serum biomarkers, it was also important to measure TETA and metabolite levels within the serum and urine of both diabetic and sham animals. This would enable assessment of whether diabetes affected the ability of animals to process TETA.

133

5.2.4.1 Serum

Analysis was performed on terminal serum collected during the tissue harvest. Similar to that of the serum biomarkers, an ANOVA was carried out to assess if there were any significant effects of Status, Dose and Status*Dose on the levels of TETA and MAT in sixteen week terminal serum. No DAT was detected in any serum sample and so DAT was not included in the analysis.

(A)

Source	DF	Type III SS	Mean Square	F value	Pr>F
Status	1	19.741	19.741	54.89	**<.0001**
Dose	3	24.278	8.093	22.5	**<.0001**
Status*Dose	3	1.20315634	0.40105211	1.12	0.3547
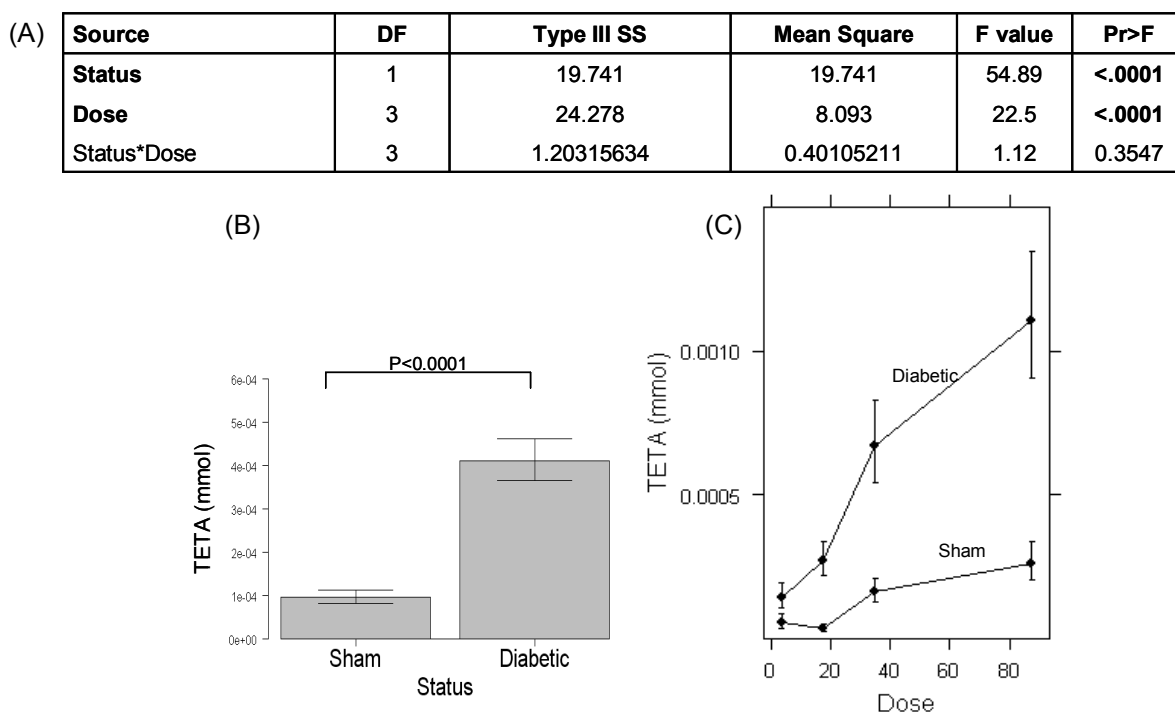
Figure 5.9 TETA levels in 16 week terminal serum

Sixteen weeks after injection with either STZ (diabetic) or saline (sham), male Wistar rats were placed in an induction box with isoflurane 5%, O_2 2l/min. Animals were thereafter maintained on isoflurane 2-3%, O_2 2l/min and once complete anaesthesia was confirmed, a midline laparotomy was performed. A 22 gauge cannula (BD, Insyte) was inserted into the vena cava and approximately 3ml of blood was extracted and aliquoted into serum tubes (BD, Insyte). TETA levels were determined as described in Section 2.7. Values are presented as adjusted mean ± SEM
(A) Results of the ANOVA conducted to assess if there was a significant effect of either status or dose on the on the levels of TETA in diabetic and sham treated groups
(B) Levels of TETA in the sham groups compared to that in the diabetic groups
(C) TETA levels as a function of dose administered in the diabetic and sham animals

The results of the analysis (Figure 5.9) indicate that there were greater levels of TETA in the serum of diabetic animals compared to sham animals receiving the same dose (Status P<.0001) and that, in both sham and diabetic animals, as the dose of TETA administered rose so did the level of TETA in the serum (Dose P<.0001). There was no Status*Dose interaction, however, indicating that although there is more TETA in the

diabetic serum the change associated with increasing dose was proportional to that observed in the sham animals.

A similar analysis was conducted for MAT levels in serum and the results of this analysis have been presented in Figure 5.10. MAT levels were below the limit of detection for the 3.5mg dose in both the sham and diabetic groups and so were not included in the analysis.

(A)

Source	DF	Type III SS	Mean Square	F value	Pr>F
Status	1	28.62803595	28.62803595	74.72	**<.0001**
Dose	2	13.51923819	6.7596191	17.64	**<.0001**
Status*Dose	2	0.7623463	0.38117315	0.99	0.3806
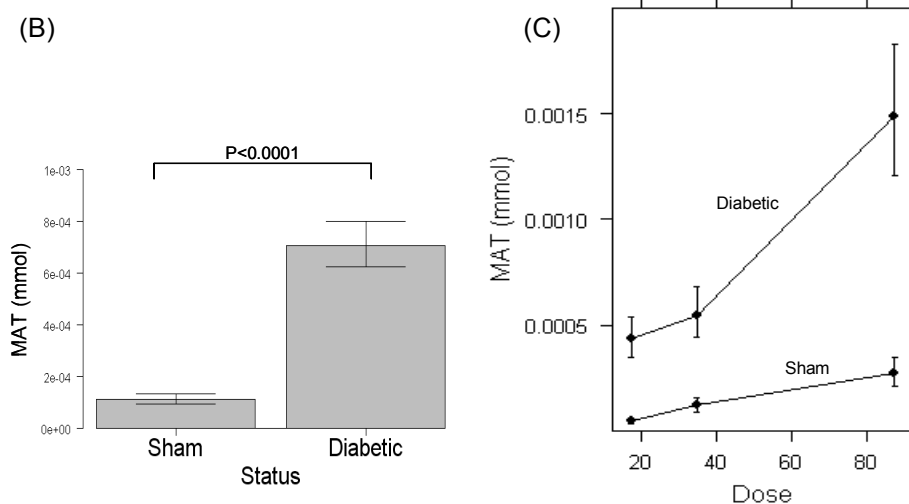
Figure 5.10 MAT levels in 16 week terminal serum

Sixteen weeks after injection with either STZ (diabetic) or saline (sham), male Wistar rats were placed in an induction box with isoflurane 5%, O_2 2l/min. Animals were thereafter maintained on isoflurane 2-3%, O_2 2l/min and once complete anaesthesia was confirmed, a midline laparotomy was performed. A 22 gauge cannula (BD, Insyte) was inserted into the vena cava and approximately 3ml of blood was extracted and aliquoted into serum tubes (BD, Insyte). MAT levels were determined as described in Section 2.7. Values are presented as adjusted mean ± SEM
   (A) Results of the ANOVA conducted to assess if there was a significant effect of either status or dose on the levels of MAT in diabetic and sham treated groups
   (B) Levels of MAT in the sham groups compared to that in the diabetic groups
   (C) MAT levels as a function of dose administered in the diabetic and sham animals

As with TETA, MAT levels were higher in the diabetic animals than in the sham animals (Status P<.0001) and greater doses of TETA administered resulted in greater levels of MAT present in the serum (Dose P<.0001). It is observed in MAT as with TETA that the change in MAT levels across the dose of TETA given was not different between the diabetic and sham groups (Status*Dose P=0.3806).

Overall, there were greater levels of TETA and MAT present in the serum of the diabetic animals, and in both groups TETA and MAT levels increased with increasing drug dose. There was no significant effect on the level of TETA or MAT across dose as a result of the status of the animal as the slopes for each are the same (no Status*Dose interaction, Figure 5.9 and 5.10 (C)).

5.2.4.2 Urine

Collection of 24hr urine enabled the measurement of TETA, metabolite and metal levels in urine in order to try and partly elucidate the metabolism of the drug in rodents.

The method used to detect TETA and its metabolites (Section 2.7) has been validated by the School of Biological Sciences Reference lab for serum only and had not been tested in rodent urine before. There were initially some problems resolving the metabolites in the urine as MAT is at very high concentrations compared to DAT which is at very low concentrations. Further validation was performed by Reference lab technician Asma Othman that led to minor modifications being incorporated in order to ensure that all three compounds were detectable (Othman et al. 2007).

These modifications included decreasing the volume of urine added for derivatisation and increasing the concentration of FMOC (derivatising agent). This allowed both MAT and DAT to be measured in the same HPLC chromatogram.

All values were corrected for total 24hr urine volume. Only urine from Week 10 and Week 15 collections were used for measurement as these were both post-drug administration. As expected the No Drug groups (both sham and diabetic) did not contain any detectable TETA, MAT or DAT. These values were not included in the subsequent statistical analyses as they did not provide any useful information.

A number of the values obtained were considered to be below the lower limit for clinical sample detection for the method but were still used in this analysis as the limit was a threshold designed for clinical trial analysis and not animal based research. The assay can resolve below the clinical threshold but it has more variation associated with its values (noted particularly in the 3.5mg drug group).

Table 5.6 indicates that, based on the amount of water drunk over the 24hr period and the calculated concentration of TETA in the water on that day, the sham and diabetic animals took in approximately the same amount of TETA at each of the time points.

Table 5.6 Average TETA-disuccinate intake (24hr urine collection)

Dose(mg)	Sham				Diabetic			
	3.5mg	17.5mg	35mg	87.5mg	3.5mg	17.5mg	35mg	87.5mg
Week 10	3.1±0.5	20.6±3.1	35.0±4.7	64.5±10.3	2.4±.0.5	11.7±1.0	23.1±2.4	67.1±9.5
Week 15	3.2±0.5	11.9±2.1	24.6±4.5	71.6±27.2	2.4±0.2	12.6±1.0	31.6±2.8	65.5±7.7

Previous studies have indicated that TETA has low absorption in humans (Walshe 1982; Takeda et al. 1995a; Takeda et al. 1995b; Takeda et al. 1995c; Lu et al. 2007), when administered as the dihydrocholoride salt. Initial analysis of total drug (TETA + MAT + DAT) excreted in urine as a percentage of the theoretical TETA-disuccinate intake (Table 5.6) indicated that this is again the case with TETA-disuccinate. Urinary recovery of drug expressed as a percentage of administered dose was 9.8 ± 1.25% (range 0.2-36.3%) in sham animals and 15.6 ± 2.16% (range 4.9-96.8%) in diabetic animals, indicating low absorption of TETA in both groups. The diabetic animals excreted a significantly greater percentages of administered dose than sham animals ($P<.0001$, Mann-Whitney non-parametric test). Note that the Mann-Whitney test was applied in this instance as all tests indicated that the data was not normally distributed.

5.2.4.2.1 TETA and metabolite levels in urine as a function of time

The next step in the analysis was to identify what levels of TETA, MAT and DAT were being excreted in the urine and whether there were any differences comparable to those observed in the serum. Due to the collection of urine at the 10 Week (two weeks post-drug administration) and 15 Week (seven weeks post drug administration) time points, changes in excretion over time were incorporated into the analysis. In this analysis the three main effects, Status, Dose and Time were assessed. Data for TETA and MAT were analysed using a split-plot in time ANOVA as described in Section 2.12.5.1. One variable not accounted for in this analysis is the level of drug in the faeces of the animals as the metabolic cage study was not designed as a balance study.

Results of the analysis over time gave a Status*Time interaction (Figure 5.11 (A)) indicating that the level of TETA in the urine over time is dependent on the status of the animal. Tukey's *post-hoc* tests reveal that the diabetic animals excrete greater levels of TETA at the Week 10 time point (diabetic: 3.1×10^{-4} mmol/24hr TETA compared to sham: 1.5×10^{-4} mmol/24hr TETA, $P=0.0033$) and that, over time, the diabetic animals increased TETA excretion (3.1×10^{-4} mmol/24hr TETA at Week 10 to 4.7×10^{-4} mmol/24hr TETA at Week 15, $P=0.0112$) while the sham animals decreased TETA excretion (1.5×10^{-4} mmol/24hr TETA at Week 10 to 8.6×10^{-5} mmol/24hr TETA at Week 15 $P=0.0058$). This change over time resulted in an even greater difference between diabetic and sham TETA excretion at the Week 15 time point (diabetic: 4.7×10^{-4} mmol/24hr TETA compared to sham: 8.6×10^{-5} mmol/24hr TETA, $P<.0001$). This change over time suggests that both groups (diabetic and sham) are changing their ability to metabolise TETA as exposure to the drug increases.

(A)	Source	Num DF	Den DF	F value	Pr>F
	Status	1	47	48.1	**<.0001**
	Dose	3	46.9	27	**<.0001**
	Status*Dose	3	46.9	0.98	0.4091
	Time	1	45.3	0.25	0.6209
	Status*Time	1	45.3	22.72	**<.0001**
	Time*Dose	3	45.2	2.72	0.0552
	Status*Time*Dose	3	45.2	2.09	0.1151
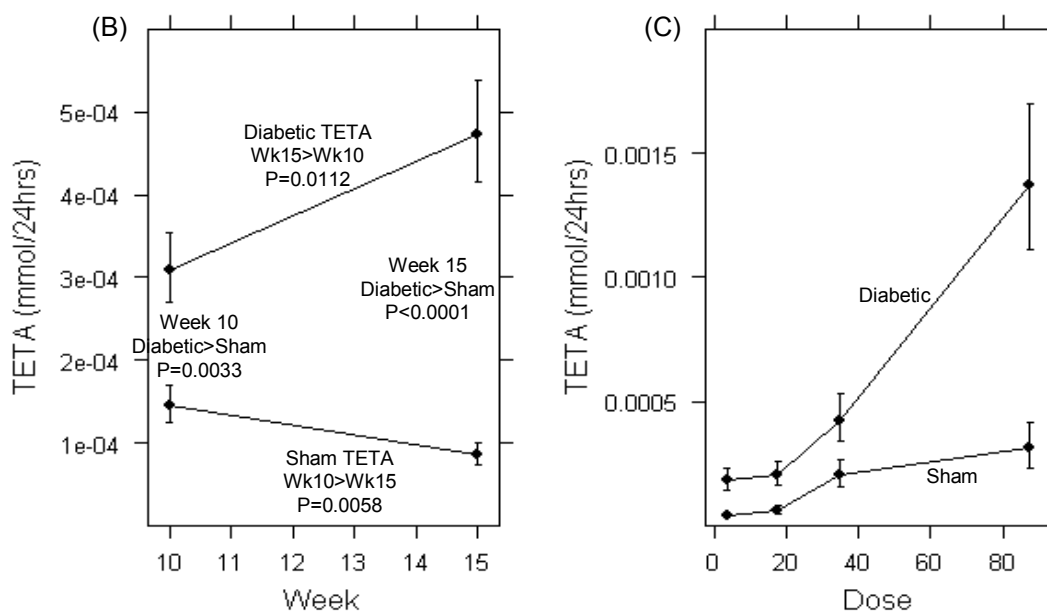
Figure 5.11 TETA in urine over Week 10 and 15 time points

Male Wistar rats (220-250g) were anesthetised using 5% isoflurane, 2l/min O_2, and 55mg/kg STZ dissolved in saline was immediately injected into the tail vein to induce diabetes. Control rats (sham) received the corresponding volume of saline. At 10 and 15 weeks post-injection, animals were placed in metabolic cages for 24hr and urine excreted over that time was collected (Section 2.1.2). TETA levels were determined as described in Section 2.7 and corrected for 24hr volume. Values are presented as adjusted means ± SEM
(A) Results of the ANOVA conducted to assess if there was a significant effect of either status, dose or time on the levels of TETA in treated animals
(B) Levels of TETA in the sham groups compared to that in the diabetic groups over time
(C) TETA levels as a function of dose administered in the diabetic and sham animals

As with the serum analysis, there was a significant increase in the amount of TETA excreted as a greater dose of TETA was administered and this occurred at the same rate in both groups (Figure 5.11 (C)).

Analysis of MAT levels in the urine was conducted in the same manner as for TETA. The results of this analysis are presented in Figure 5.12 below.

Similar to TETA excretion, MAT levels were higher in the diabetic animals compared to the sham animals (Status P=0.011) and increased the same amount in both

groups as the dose of TETA administered increased (Dose P<.0001). Unlike the TETA case however, MAT levels remained constant in both groups over time (Status*Time P=0.6921).

(A)

Source	Num DF	Den DF	F value	Pr>F
Status	1	47	7.01	**0.011**
Dose	3	47	38.62	**<.0001**
Status*Dose	3	47	1.3	0.2864
Time	1	47	1.22	0.2757
Status*Time	1	47	0.16	0.6921
Time*Dose	3	47	1.29	0.2895
Status*Time*Dose	3	47	1.57	0.2088

(B)

(C)

Figure 5.12 Levels of MAT in 24hr urine at 10 and 15 weeks

Male Wistar rats (220-250g) anesthetised using 5% isoflurane, 2l/min O_2, and 55mg/kg STZ dissolved in saline was immediately injected into the tail vein to induce diabetes. Control rats (sham) received the corresponding volume of saline. At 10 and 15 weeks post-injection, animals were placed in metabolic cages for 24hr and urine excreted over that time was collected (Section 2.1.2). MAT levels were determined as described in Section 2.7 and corrected for 24hr volume.
Values are presented as adjusted means ± SEM
(A) Results of the ANOVA conducted to assess if there was a significant effect of either status, dose or time on the levels of MAT in treated animals
(B) Levels of MAT in the sham groups compared to that in the diabetic groups over time
(C) MAT levels as a function of dose administered in the diabetic and sham animals

DAT levels were analysed differently to that of TETA and MAT as it was found that no DAT was detectable in the diabetic urine at Week 15. The analysis of DAT was therefore broken down into two parts.

The first part of the analysis concerned the level of DAT in sham urine only at the Week 10 and 15 time points (Figure 5.13).

(A)

Source	Num DF	Den DF	F Value	Pr > F
Dose	3	37.2	14.62	**<.0001**
Time	1	32.7	44.84	**<.0001**
Dose*Time	3	33	1.14	0.349

(B)
(C)
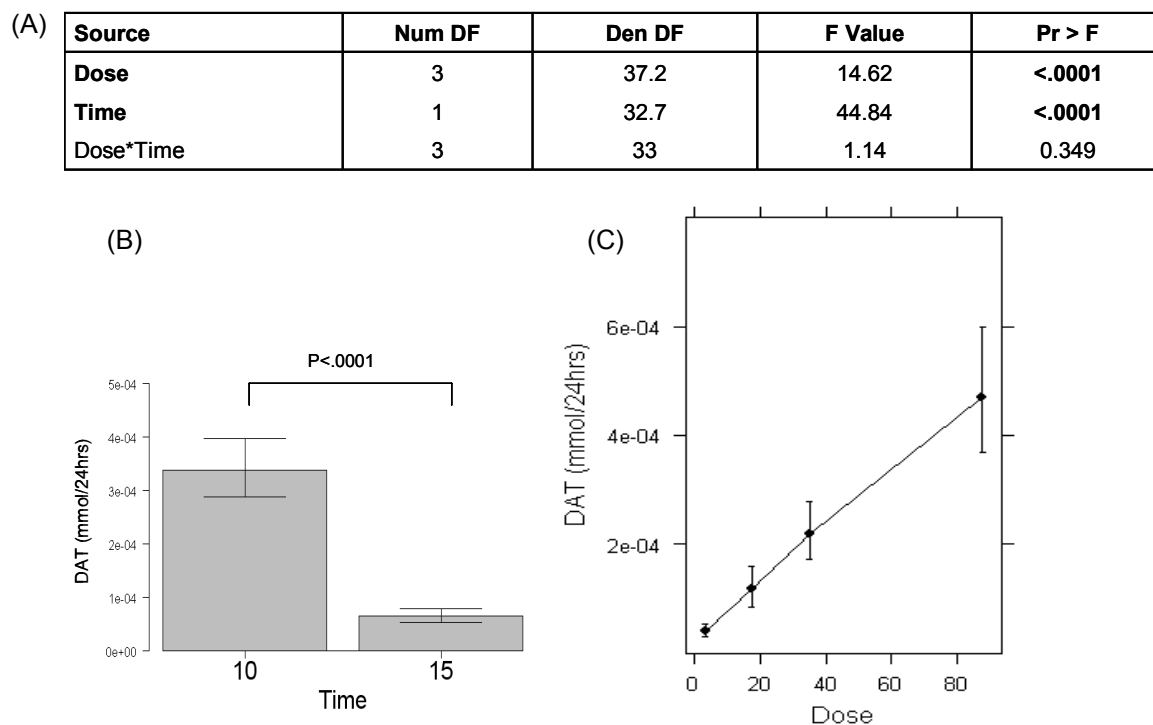
Figure 5.13 Levels of DAT in 24hr sham urine at Week 10 and 15

Male Wistar rats (220-250g) were anesthetised using 5% isoflurane, 2l/min O_2, and 55mg/kg STZ dissolved in saline was immediately injected into the tail vein to induce diabetes. Control rats (sham) received the corresponding volume of saline. At 10 and 15 weeks post-injection animals were placed in metabolic cages for 24hrs and urine excreted over that time was collected (Section 2.1.2). DAT levels were determined as described in Section 2.7 and corrected for 24hr volume
Values are presented as adjusted means ± SEM
(A) Results of the ANOVA conducted to assess if there was a significant effect of either dose or time on the levels of DAT in treated sham animals
(B) Levels of DAT at the Week 10 time point compared to the Week 15 time point in sham animals
(C) DAT levels as a function of dose administered in the sham animals (Week 10 and 15 time point combined)

Here it was found that DAT levels decrease in the sham group over time (P<.0001). This is consistent with that observed in the diabetic animals, where levels of DAT decreased to below the detectable limit of the method. As seen with TETA and MAT, the increase in TETA administered (Dose P<.0001) resulted in an increase in DAT excreted.

The second analysis conducted looked at the differences in DAT excretion between diabetic and sham groups at the Week 10 time point only (Figure 5.14). In this analysis only the 35mg and 87.5mg groups from both diabetic and sham animals contained enough data for comparison.

(A)

Source	DF	Type III SS	Mean Square	F Value	Pr > F
Status	1	5.979	5.979	34.26	**<.0001**
Dose	1	1.284	1.284	7.36	**0.0122**
Status*Dose	1	0.051	0.051	0.29	0.5952

(B)

(C)
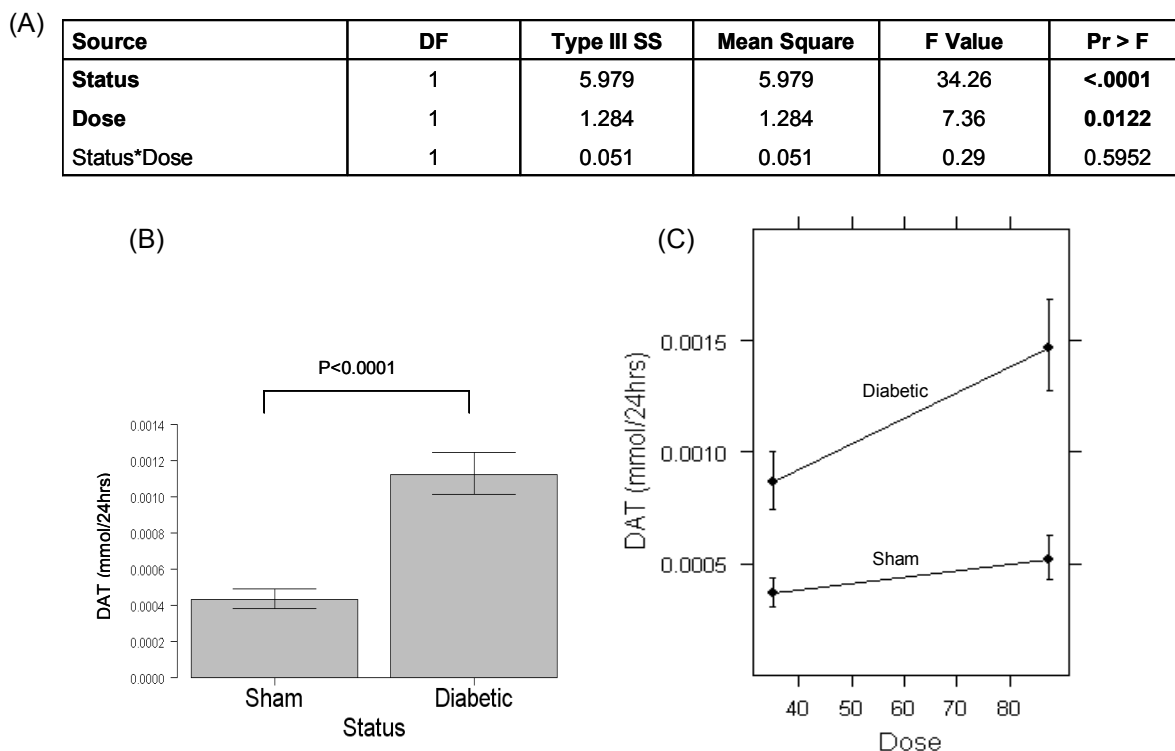
Figure 5.14 Levels of DAT in 24hr sham and diabetic urine at Week 10

Male Wistar rats (220-250g) were anesthetised using 5% isoflurane, 2l/min O_2, and 55mg/kg STZ dissolved in saline was immediately injected into the tail vein to induce diabetes. Control rats (sham) received the corresponding volume of saline. At 10 and 15 weeks post-injection, animals were placed in metabolic cages for 24hr and urine excreted over that time was collected (Section 2.1.2). DAT levels were determined as described in Section 2.7 and corrected for 24hr volume
Values are presented as adjusted means ± SEM
(A) Results of the ANOVA conducted to assess if there was a significant effect of either status or dose on the levels of DAT in treated animals (at the Week 10 time point)
(B) Levels of DAT in the sham groups compared to that in the diabetic groups at the Week 10 time point
(C) DAT levels as a function of dose administered in the diabetic and sham animals (35mg and 87.5mg dose at the Week 10 time point only)

DAT levels were found to be greater in the diabetic animals than the sham animals across both doses (Status P<.0001). The diabetic and sham animals increased their DAT level as the administered dose of TETA increased; however, this occurred at similar rates in both groups, so no Status*Dose interaction was observed (P=0.5952).

Overall, TETA and metabolite levels were greater in the diabetic animals than in the sham animals. This is consistent with both the observed TETA and MAT levels in the serum and the percentage urinary recovery. These results taken together indicate that the diabetic animals are likely to be absorbing a greater amount of administered TETA. No significant Status*Dose interaction was observed for any of the three compounds, indicating that although the diabetic animals excrete more TETA, MAT and DAT at the Week 10 time point, and more TETA and MAT at the Week 15 time point, the slope of

TETA excreted over the range of administered doses is the same for both diabetic and sham animals.

Both TETA and DAT appear to undergo a change in excretion over time, with an increase in TETA excretion and a decrease in DAT excretion in the diabetic animals and a decrease in both TETA and DAT in the sham animals. These findings point towards a change in the enzyme systems that control the processing of these two compounds. There was no change in MAT levels over time in either diabetic or sham groups indicating stability in the processing of this compound.

5.2.4.3 Percentage of unmetabolised TETA in Serum and Urine

The results presented so far indicate that overall the diabetic animals have a greater amount of all three compounds (TETA, MAT and DAT) present in their urine at the Week 10 time point and more TETA and MAT present in their serum and at the Week 15 time point. The next step in the analysis was to identify in what proportion of the total excreted drug (TETA + MAT + DAT) unchanged or metabolised TETA was present and if there was an observable difference between diabetic and sham animals. This analysis helps to determine how much of the TETA absorbed was metabolised and how much remained as unmetabolised TETA.

The results presented here focus on unmetabolised TETA only. Results are presented as a percentage of total drug in the urine (unmetabolised + metabolised TETA) so changes in unmetabolised TETA will reflect changes in metabolised TETA.

5.2.4.3.1 Urine

In accordance with previous findings, the percentage of unmetabolised TETA present in the urine was lower than metabolised TETA at both time points (Kodama et al. 1993; Takeda et al. 1995b; Kodama et al. 1997; Lu et al. 2007).

A split-plot in time ANOVA (Section 2.12.5.1) analysis of the percentage of unmetabolised TETA in the urine of diabetic and sham animals revealed evidence for a Time*Dose interaction and a Status*Time interaction (Figure 5.15).

Source	Num DF	Den DF	F value	Pr>F
Status	1	46	34.97	<.0001
Dose	3	45.9	9.76	<.0001
Status*Dose	3	45.9	0.75	0.5268
Time	1	44	36.15	<.0001
Status*Time	1	44	37.64	**<.0001**
Time*Dose	3	44	2.82	**0.0499**
Status*Time*Dose	3	44	0.63	0.5983

(A)
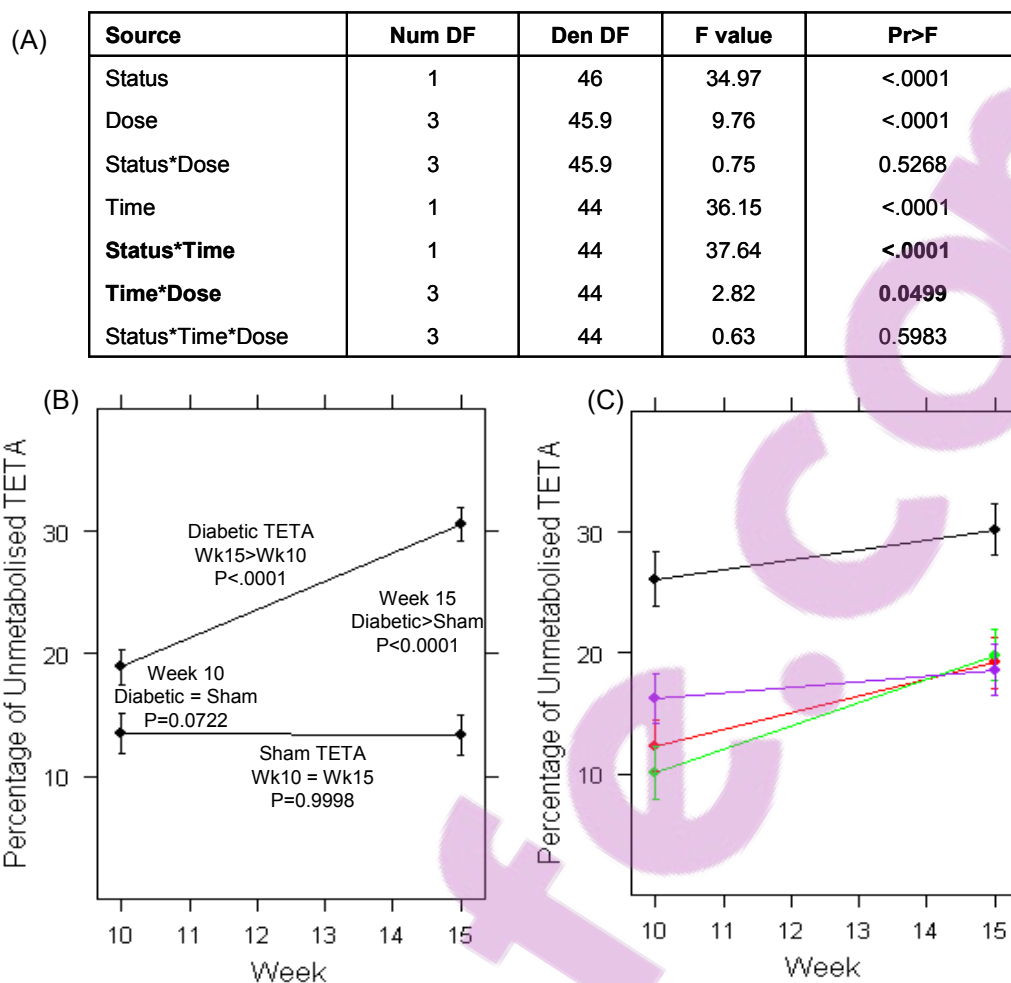
Figure 5.15 Percentage of unmetabolised TETA in urine

Male Wistar rats (220-250g) were anesthetised using 5% isoflurane, 2l/min O_2, and 55mg/kg STZ dissolved in saline was immediately injected into the tail vein to induce diabetes. Control rats (sham) received the corresponding volume of saline. At 10 and 15 weeks post-injection animals were placed in metabolic cages for 24hr and urine excreted over that time was collected (Section 2.1.2). TETA levels were determined as described in Section 2.7 and corrected for 24hr volume. Percentage values = (measured TETA/ (TETA+MAT+DAT))*100.
Values are presented as adjusted means ± SEM
(A) Results of the ANOVA conducted to assess if there was a significant effect of either status, dose or time on the percentage of unmetabolised TETA in treated animals
(B) Percentage of unmetabolised TETA in the sham groups compared to that in the diabetic groups over time
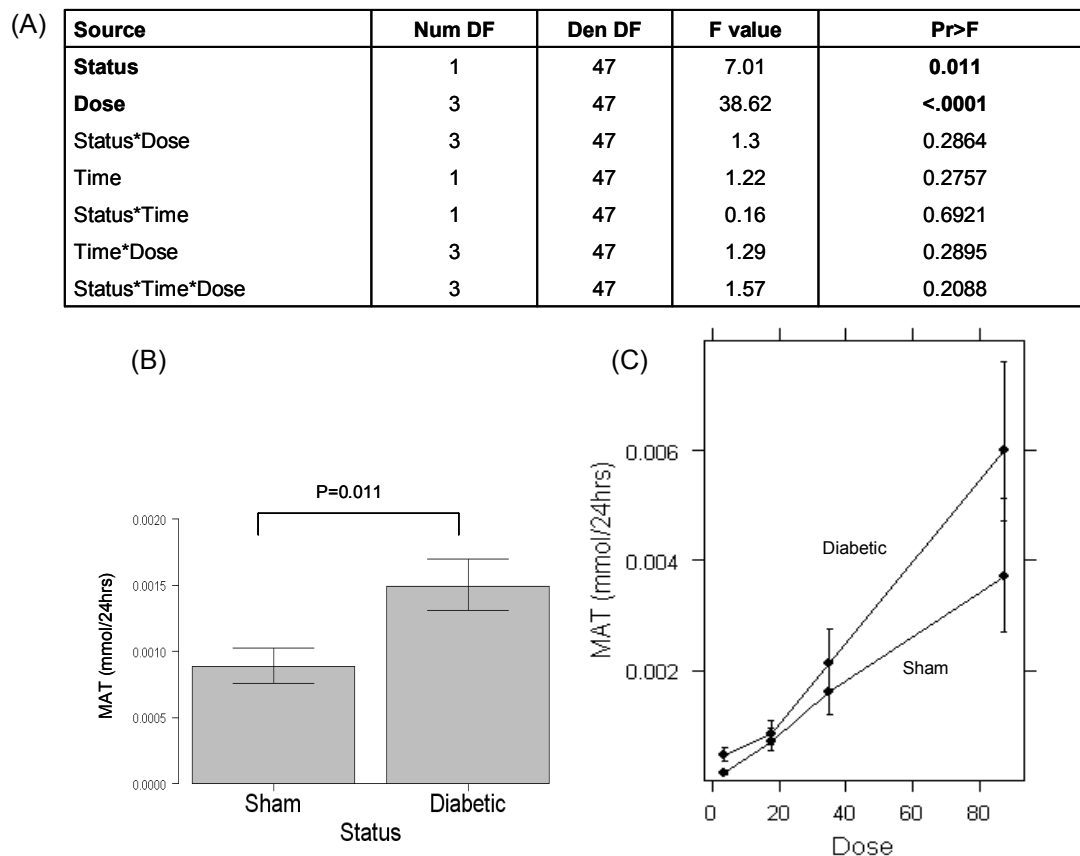(C) TETA levels as a function of dose administered in the diabetic and sham animals over time
(⎯ 3.5mg, ⎯ 17.5mg, ⎯ 35mg, ⎯ 87.5mg)

Weak evidence for a Time*Dose interaction (P=0.0499) indicates that the percentage of unmetabolised TETA at a particular time point (Week 10 or Week 15) is dependent on the dose administered. Figure 5.15 (C) reveals that it is the 3.5mg dose that is driving this observation.

There is strong evidence for a Status*Time interaction (P<.0001) indicating that the percentage of unmetabolised TETA at a particular time point (Week 10 or Week 15) is

143

dependent on the status of the animal. Closer inspection of the data (Tukey's *post-hoc* tests) found that at Week 10, there was no significant difference between the percentage of unmetabolised TETA in the diabetic animals (18.9 ± 1.4%) when compared to the sham animals (13.5 ± 1.6%, P=0.0722). However at Week 15, unmetabolised TETA in the diabetic animals increased to 30.6±1.4% and while the sham unmetabolised TETA remained constant at 13.4 ± 1.6% (P<.0001, Figure 5.15 (B)).

Altogether these data indicate that although the diabetic animals have greater absolute amounts of TETA, MAT and DAT in their urine at Week 10, the proportion of unmetabolised TETA was the same as in the sham animals. As time progresses however this changed in the diabetic animals, and the proportion of unmetabolised TETA increased. This is consistent with the results presented in Figure 5.11 which show an increase in the amount of TETA excreted by the diabetic animals at Week 15 compared to Week 10.

5.2.4.3.2 Serum

In order to calculate the percentage of unmetabolised TETA in serum, the amount of TETA for each group (diabetic or sham) was divided by the sum of TETA + MAT (deemed to be the total amount of drug in the serum). It was found that the percentage of unmetabolised TETA in the diabetic animals was significantly lower than the percentage of unmetabolised TETA in the sham animals (diabetic: 48.1 ± 2.7% compared to sham: 63.9 ± 6.0%, Status P=0.0088). This result was expected, given that the proportion of unmetabolised TETA in the diabetic animals at the Week 15 time point was greater than that of the sham animals, indicating a higher level of unmetabolised TETA excretion in the urine. Higher levels of excretion could be responsible for the observed lower serum levels.

5.2.5 Levels of trace metals, copper, zinc, iron and manganese in 24hr urine

Urine metal analysis was performed using GF-AAS as outlined in Section 2.8. Urine was analysed from all four 24hr urine collection time points to give an idea of the change in metal excretion levels over time as well as with STZ-induced diabetes.

5.2.5.1 Changes in metal ion excretion with the onset of diabetes

The analysis of metal levels in urine was split into two parts to ensure that it was conducted across comparable data sets. The first part looked solely at the change in metal levels with the induction of diabetes (six week urine metal levels). As the treatment arm of this study did not begin until week nine, animals were grouped as either diabetic or

sham only. A 24hr urine sample was taken for all animals at Week 0 (pre-STZ or saline injection) and so the metal levels at this time point were used as a covariate in the analysis to increase accuracy. Results from the ANCOVA are presented in Figure 5.16. As this is a one-way ANCOVA with only Status as the main effect, the ANCOVA table for each metal is not included. Data presented in Figures 5.16-5.19 represent total levels of metal ion excretion over 24hrs corrected for body weight of the animal. This correction was made as the diabetic animal's weight was much lower than the sham animals and this may skew metal ion excretion results.
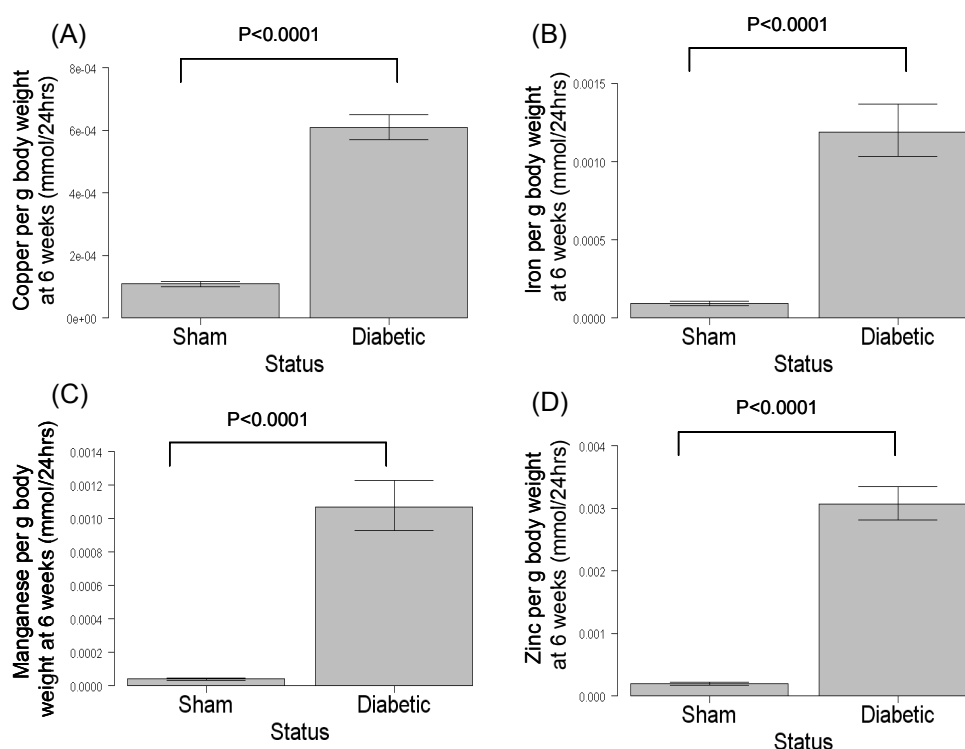
Figure 5.16 Metal ion levels six weeks after injection with STZ or saline

Male Wistar rats (220-250g) were anesthetised using 5% isoflurane, 2l/min O_2, and 55mg/kg STZ dissolved in saline was immediately injected into the tail vein to induce diabetes. Control rats (sham) received the corresponding volume of saline. At 0, 6, 10 and 15 weeks post-injection, animals were placed in metabolic cages for 24hr and urine excreted over that time was collected (Section 2.1.2). Urine metal analysis was performed using GF-AAS as outlined in Section 2.8. All metal values were corrected for 24hr volume and body weight of the animal. (A) Copper, (B) Iron (C) Manganese, (D) Zinc

Overall it was found that all four transition metals were increased with diabetes as described previously (Lau and Failla 1984). As illustrated in Table 5.1, the level of food intake by diabetic animals is increased due to hyperphagia. If the increase in metal levels is solely the result of increased food intake, it could be assumed that the fold increase as a result of diabetes in either would be similar. The differences between food intake and

urine metal levels of the diabetic group pre-STZ injection (basal 24hr urine collection) and post-STZ injection (Week 6 urine collection) were calculated. It was found that the average fold difference for food intake was 1.6 ± 0.1-fold, which was significantly lower than the average fold difference in copper (3.6 ± 0.3-fold P<.0001), zinc (11.0 ± 1.0-fold P<.0001), iron (11.7 ± 2.0-fold P<.0001) and manganese (18.1 ± 4.0-fold P<.0001) excretion, indicating that the rise in metal ion excretion shown by the diabetic animals cannot solely be accounted for by a rise in food intake.

This result is consistent with that of Uriu-Adams *et al.,* who reported that urinary excretion of copper was higher in diabetic rats and remained high despite a low copper intake (Uriu-Adams et al. 2005).

5.2.5.2 Change in metal ion excretion with TETA treatment over time.

The second part of the analysis looked at the effect of status, dose and time on the level of the four metal ions measured. Data from the Week 10 and 15 24hr urine collections was used for this analysis with correction for baseline (Week 0 collection) in a split-plot in time ANCOVA. The main effects assessed for each metal was dose, status and time.

Results from the ANCOVA of each of the four metals are presented in Figures 5.17-5.19 below. The levels of iron and manganese (Figure 5.17) were found only to significantly increase with status, with no change as a result of dose or time or any of the interactions associated with the three main effects.

(A)

Source	Num DF		Den DF		F value		Pr>F	
	Iron	Manganese	Iron	Manganese	Iron	Manganese	Iron	Manganese
Status	1	1	59.7	56.7	373.33	376.17	**<.0001**	**<.0001**
Dose	4	4	59.5	56.6	1.08	0.32	0.3749	0.8629
Status*Dose	4	4	59.6	56.7	0.48	1	0.749	0.416
Time	1	1	60.2	51.6	0.4	0.38	0.5308	0.5421
Status*Time	1	1	60.2	51.6	0.17	0.32	0.6823	0.5727
Time*Dose	4	4	60.2	50.9	1.98	3.01	0.1083	0.0266
Status*Time*Dose	4	4	60.2	50.9	1.5	0.79	0.2127	0.5397
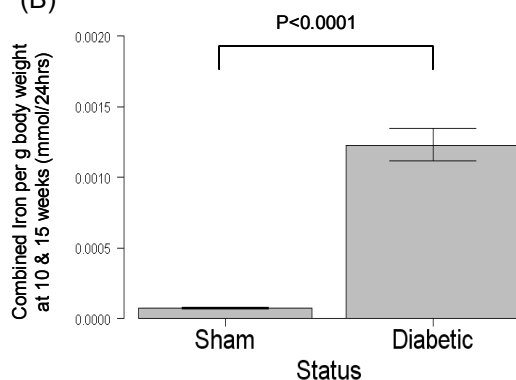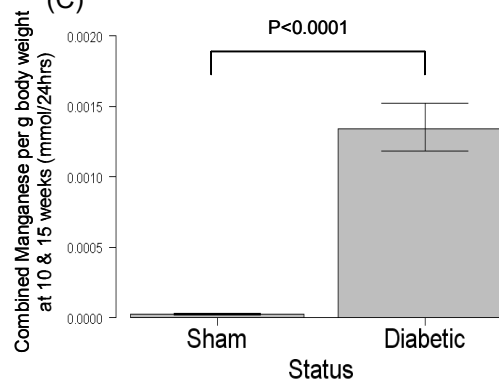
Figure 5.17 Change in iron and manganese excretion combined over the Week 10 and 15 24hr collection corrected for body weight

Male Wistar rats (220-250g) were anesthetised using 5% isoflurane, 2l/min O_2, and 55mg/kg STZ dissolved in saline was immediately injected into the tail vein to induce diabetes. Control rats (sham) received the corresponding volume of saline. At 0, 6, 10 and 15 weeks post-injection, animals were placed in metabolic cages for 24hr and urine excreted over that time was collected (Section 2.1.2). Urine metal analysis was performed using GF-AAS as outlined in Section 2.8.
(A) Results of the ANOVA conducted to assess if there was a significant effect of either status, dose or time on the levels of manganese or iron in treated animals
(B) Levels of iron in the sham groups compared to that in the diabetic groups at combined over the Week 10 and 15 time points
(C) Levels of manganese in the sham groups compared to that in the diabetic groups at combined over the Week 10 and 15 time points

Copper levels were found to be increased in the diabetic animals when compared to the sham animals, which is consistent with the results observed at Week six and for iron and manganese. As expected, the amount of copper excreted increased as the dose of TETA increased (independently of Status) and this mirrors the decrease in copper observed in the serum. Copper excretion was also found to significantly decrease with time in both the sham and diabetic groups (no interaction). Results are presented in Figure 5.18.

(A)

Source	Num DF	Den DF	F value	Pr>F
Status	1	60	186.79	**<.0001**
Dose	4	60	25.19	**<.0001**
Status*Dose	4	60	1.55	0.1995
Time	1	60	37.07	**<.0001**
Status*Time	1	60	0.15	0.6985
Time*Dose	4	60	1.34	0.2664
Status*Time*Dose	4	60	1.29	0.2833

(B)

(C)

(D)
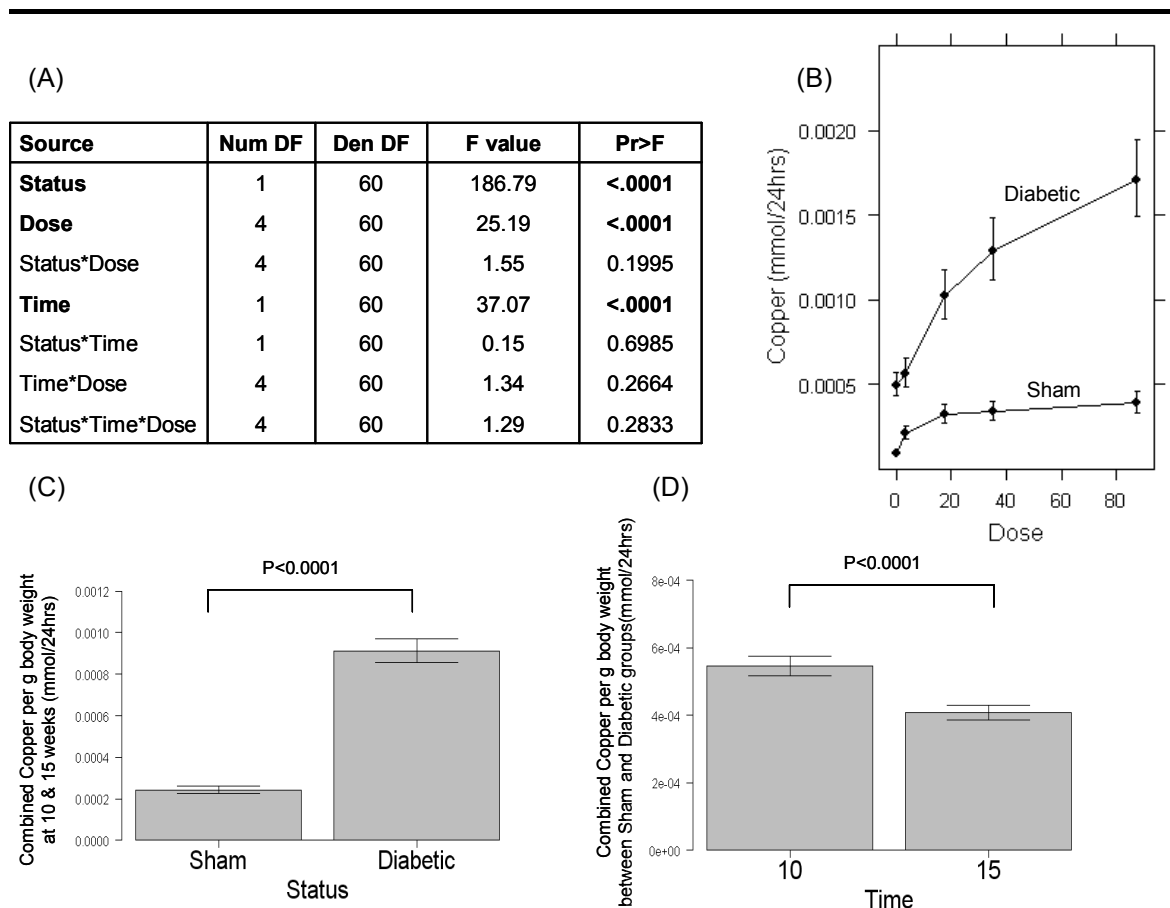
Figure 5.18 Copper excretion over time (Weeks 10 and 15)

Male Wistar rats (220-250g) were anesthetised using 5% isoflurane, 2l/min O_2, and 55mg/kg STZ dissolved in saline was immediately injected into the tail vein to induce diabetes. Control rats (sham) received the corresponding volume of saline. At 0, 6, 10 and 15 weeks post-injection, animals were placed in metabolic cages for 24hrs and urine excreted over that time was collected (Section 2.1.2). Urine metal analysis was performed using GF-AAS as outlined in Section 2.8. All copper values were corrected for 24hr volume and body weight of the animal at each time point.
(A) Results of the ANOVA conducted to assess if there was a significant effect of either status, dose or time on the levels of copper in treated animals
(B) Copper levels over presented over the range of administered doses
(C) Levels of copper in the sham groups compared to that in the diabetic groups at combined over the Week 10 and 15 time points
(D) Copper levels at the Week 10 and 15 time points combined over status

Similar to copper, zinc levels were increased in the diabetic animals compared to the sham animals (Figure 5.19) and as the dose of TETA administered increased the amount of zinc excreted also increased (independent of status). The change in zinc excretion with dose is not consistent with the serum zinc levels, which were found to have no change with TETA treatment. As with copper, zinc excretion was found to decrease with time.

(A)

Source	Num DF	Den DF	F value	Pr>F
Status	1	59	454.14	**<.0001**
Dose	4	59	6.51	**0.0002**
Status*Dose	4	59	1.14	0.3474
Time	1	60	9.98	**0.0025**
Status*Time	1	60	0	0.9773
Time*Dose	4	60	1.68	0.1657
Status*Time*Dose	4	60	1.58	0.1901

(B)

(C)

(D)
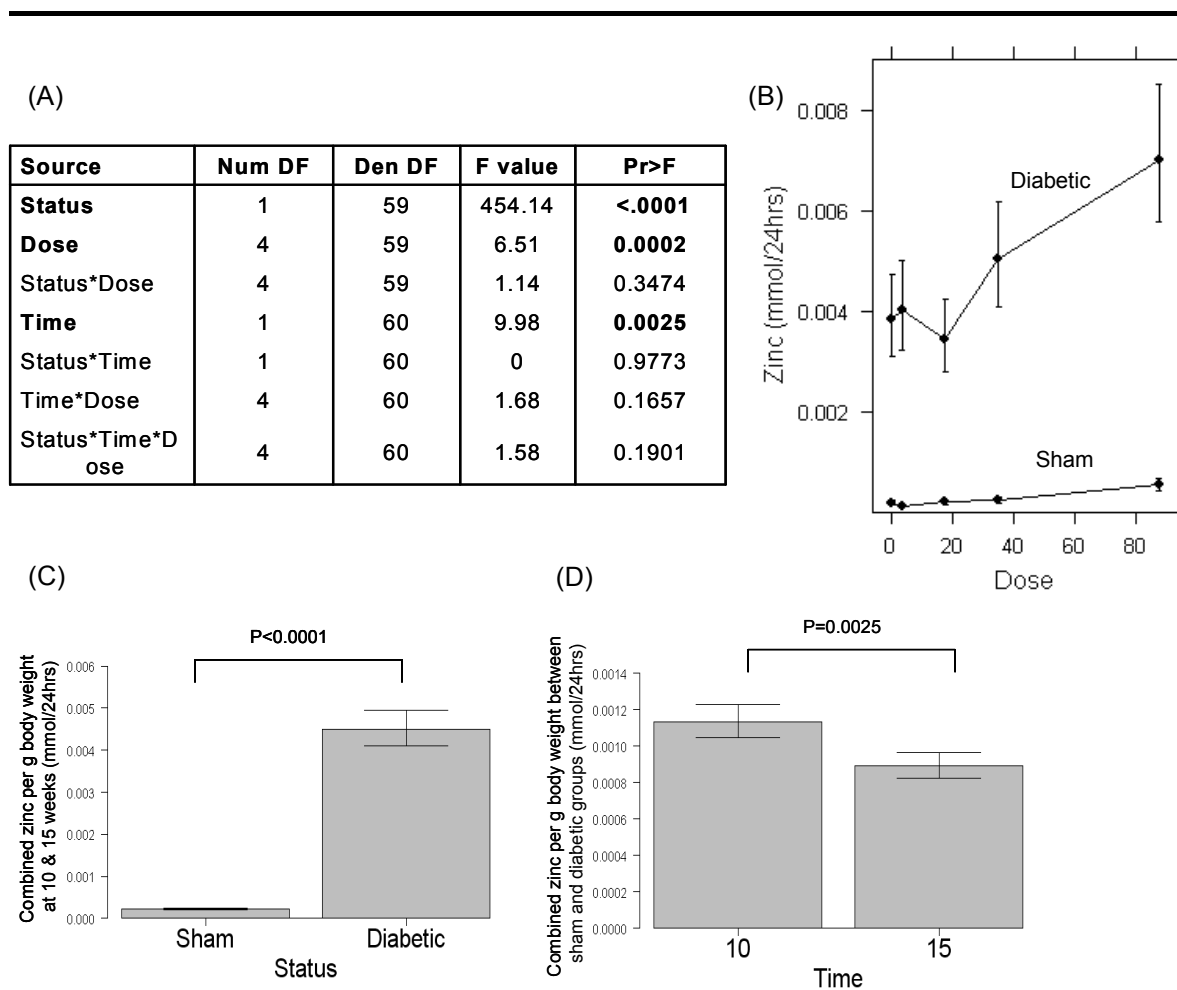
Figure 5.19 Zinc excretion over time (Weeks 10 and 15)

Male Wistar rats (220-250g) anesthetised using 5% isoflurane, 2l/min O_2, and 55mg/kg STZ dissolved in saline was immediately injected into the tail vein to induce diabetes. Control rats (sham) received the corresponding volume of saline. At 0, 6, 10 and 15 weeks post-injection animals were placed in metabolic cages for 24hrs and urine excreted over that time was collected (Section 2.1.2). Urine metal analysis was performed using GF-AAS as outlined in Section 2.8. All zinc values were corrected for 24hr volume and body weight of the animal at each time point.
(A) Results of the ANOVA conducted to assess if there was a significant effect of either status, dose or time on the levels of zinc in treated animals
(B) Zinc levels over presented over the range of administered doses
(C) Levels of zinc in the sham groups compared to that in the diabetic groups at combined over the Week 10 and 15 time points
(D) Zinc levels at the Week 10 and 15 time points combined over status

5.2.5.3. Correlation between urine levels of TETA, metabolites and trace metals

In order to understand the association between measured TETA, its metabolites and trace metals, Pearson's correlation coefficients were calculated. In order to determine if there was a significant linear association and in the case of the urine analysis if the nature of the

association was common to both time points, ANCOVA were carried out as described in Section 2.12.5.4.

5.2.5.3.1 Urine

Analysis of the association between excreted TETA, MAT and the four urine metals measured was conducted using the data from sham and diabetic animals separately. In the ANCOVA, the response was metal (Cu, Zn, Mn or Fe), the covariate was TETA/MAT and the fixed effect was time. The analysis was split into two as the amount of TETA excreted is dependent on whether animals were in the diabetic or sham group (as described by Figure 5.11). This violates the ANCOVA assumption that the x values (TETA) are independent of treatments (Status). Results for each status group are presented in Table 5.7 and 5.8.

Table 5.7 Correlation analysis in the urine of sham animals

	Is there a linear association?	Is the nature of the assoc. common to both week 10 & 15?	Correlation
TETA vs.			
Cu	Yes	Yes	0.57***
Zn	Yes	Yes	0.6***
Fe	No	n/a	n/a
Mn	No	n/a	n/a
MAT	Yes	Yes	0.89***
MAT vs.			
Cu	Yes	Yes	0.55***
Zn	No	n/a	n/a
Fe	No	n/a	n/a
Mn	No	n/a	n/a

*P<0.05, **P<0.01, ***P<.0001

There was a significant positive correlation between TETA and copper, zinc or MAT, and MAT with copper in the sham urine. As indicated by the dose responsive nature of the copper and zinc excretion, these were the only two metals that showed a strong correlation with TETA. The strongest correlation in the sham animals occurs between TETA and MAT, as would be expected.

Table 5.8 Correlation analysis in the urine of diabetic animals

	Is there a linear association?	Is the nature of the assoc. common to both week 10 & 15?	Correlation
TETA vs.			
Cu	Yes	**No**	
Week 10			0.58*
Week 15			0.83*
Zn	Yes	Yes	0.55***
Fe	No	n/a	n/a
Mn	No	n/a	n/a
MAT	Yes	Yes	0.87***
MAT vs.			
Cu	Yes	Yes	0.74***
Zn	No	n/a	n/a
Fe	No	n/a	n/a
Mn	No	n/a	n/a

*P<0.05, **P<0.01, ***P<.0001

The diabetic animals showed a stronger positive correlation with copper at Week 15 than at Week 10, which is consistent with the results presented above indicating a change in TETA and metal excretion with time. Similar to the sham animals, there is only a significant positive correlation between TETA, MAT, copper and zinc. Zinc has a positive correlation with TETA but not MAT.

5.2.5.3.2 Serum

As in the urine study, analysis of the association between TETA, MAT and the four metals measured was conducted using the data from sham and diabetic animals separately. Serum analysis was conducted at a single time point. Results for each status group are presented in Table 5.9 and 5.10.

Table 5.9 Correlation analysis in the serum of sham animals

	Is there a linear association?	Correlation
TETA vs.		
Cu	Weak	-0.45 (P=0.062)
Zn	No	n/a
Fe	No	n/a
MAT	Weak	0.51 (P=0.063)
MAT vs.		
Cu	No	n/a
Zn	No	n/a
Fe	No	n/a
Mn	No	n/a

*P<0.05, **P<0.01, ***P<.0001

Sham animals showed a weak negative correlation between TETA and copper but no other metals in the serum. There is also only a weak positive correlation between TETA and MAT.

Table 5.10 Correlation analysis in the serum of diabetic animals

	Is there a linear association?	Correlation
TETA vs.		
Cu	Yes	-0.38*
Zn	No	n/a
Fe	No	n/a
MAT	Yes	0.60**
MAT vs.		
Cu	Yes	-0.62**
Zn	No	n/a
Fe	No	n/a

*P<0.05, **P<0.01, ***P<.0001

Diabetic animals showed a significant negative correlation between TETA and serum copper, although it was not strong (38%). In this instance, MAT and copper were found to have a much stronger, significantly negative correlation (62%).

5.3 Discussion

5.3.1 Physiological characteristics

5.3.1.1 Total body and heart weight

This study demonstrates an increase in overall body weight with TETA-disuccinate treatment. The significant Status*Dose and Time*Dose interactions indicate that TETA is able to influence the weights of both sham and diabetic animals, and that this effect occurs over time. The ability of the drug to move the treated diabetic animals towards a positive weight change indicates a powerful effect on aspects of the complex metabolic disturbance in diabetes, despite no change in blood glucose.

A previous study utilising a similar experimental design (six weeks of diabetes, seven weeks of treatment) found no change in overall body weight but a decrease in the HW/BW ratio of treated diabetic animals (Cooper et al. 2004). Here, no significant change was seen in HW/BW with respect to treatment in the diabetic or sham animals (Table 5.2); however, an increase in the absolute heart weight was observed across both diabetic and sham groups. It could be hypothesised that the change in body weight observed here mirrors the change in heart weight and that this cancels out any effect. One way to confirm this hypothesis would be to conduct an analysis of heart weight/tibia length which has been proposed as an alternative to heart weight/body weight as the use of HW/BW assumes BW remains constant or that the HW changes in parallel with BW under normal conditions which may not be the case in the diabetic group (Yin et al. 1982).

5.3.1.2 Serum biochemistry

As TETA is a copper chelator it is important to understand the effect it is having on the biochemistry of the body. The majority of serum biomarkers measured were found to change only as a result of the diabetic state. However, two important biomarkers that were significantly affected by TETA treatment were serum copper and ferroxidase levels (Figure 5.6). One of the most important markers of copper in the body is levels of ceruloplasmin (ferro-O_2-oxidoreductase: EC 1.16.3.1). In rats, it is not possible to directly measure levels of ceruloplasmin since no suitable assays are available, so an indirect assay of its activity (ferroxidase activity, Section 2.6.9) was utilised instead.

Here we found that both serum copper and ferroxidase levels were raised as a result of the diabetic state, which is consistent with previous reports (serum copper; diabetic: $0.02 \pm 4\times10^{-4}$mM compared to sham: $0.014 \pm 4\times10^{-4}$mM and ferroxidase; diabetic: 349 ± 10U/l compared to sham 260 ± 11U/l, (Uriu-Adams et al. 2005)). In this study, administration of TETA decreased both copper and ferroxidase levels in both groups in a dose dependent way; however, the Status*Dose interaction indicated that TETA is acting differently on these two serum markers depending on whether the animal was in the diabetic or the sham group. The sham animals appear to be more sensitive to the administered dose of TETA with a steeply decreasing slope for both copper and ferroxidase. The slope for copper and ferroxidase levels in the diabetic groups was much shallower and indicates that TETA was unable to influence copper and ferroxidase levels as easily as in the sham animals. This is consistent with a previously published report that examined the effects of a low copper diet on STZ-induced diabetic and control rats (Uriu-Adams et al. 2005). There, STZ rats had greater plasma copper and ferroxidase levels when compared to the control animals when fed a copper-adequate diet. After five weeks on a copper–deficient diet, the ferroxidase levels of the control animals dropped to approximately 148U/l compared to that of the STZ rats on the copper-deficient diet, which only fell to approximately 200U/l (P<0.05, (Uriu-Adams et al. 2005)).

5.3.2 TETA and metabolite levels

At the Week 10 time point there were increased levels of TETA, MAT and DAT in the urine of diabetic animals compared to sham animals. There were also greater levels of TETA and MAT in the urine at the Week 15 time point and in the terminal serum sample of diabetic animals.

One hypothesis for this generally higher level may be that the absorption of TETA administered is increased in the diabetic animals due to intestinal hypertrophy observed in

STZ diabetes (Schedl and Wilson 1971; Fedorak et al. 1987). Thus the increased surface area from which TETA is able to be absorbed may lead to an overall increase in TETA.

As a result of this observation, it is probably more meaningful to look at the percentage of unmetabolised TETA in the serum and urine in order to determine whether there are differences in the ability of the different groups to metabolise TETA (Figure 5.15). Assessment of TETA in the urine as a percentage of total drug (TETA+MAT+DAT) at Week 10 demonstrated no difference in the proportion of TETA in the diabetic rats compared to the sham rats. Analysis of results obtained at Week 15 indicated an increase over time in the diabetic group. The proportion of unmetabolised TETA in diabetic urine increased from 18.9 ± 1.4% to 30.6 ± 1.4% while the proportion of unmetabolised TETA in the sham urine remained constant (13.5 ± 1.6% to 13.4 ± 1.6%) indicating a change in the ability of the diabetic animals to metabolise the drug. This result is further confirmed by the lower percentage of unmetabolised TETA in the serum at Week 16 (48.1 ± 2.7% in diabetic animals compared to 63.9 ± 6.0% in the sham animals), which points towards increased clearance from the serum.

Further evidence for a change in the diabetic animal's ability to process TETA is the decrease in DAT to below detectable limits at Week 15. MAT and DAT are thought to be processed from TETA through two independent enzyme pathways (Lu et al. 2007). The decrease in total DAT levels and concomitant increase in both absolute and percentage of unmetabolised TETA at Week 15 points towards a change in the ability of the diabetic animals to process TETA into DAT.

A recent study by Lu *et al.,* (Lu et al. 2007) in human normal and diabetic patients found no significant difference in serum TETA levels 4-6hours after dosing between normal and diabetic subjects; however, there were increased levels of both MAT and DAT present in the diabetic subjects serum. This study also found a higher percentage of unmetabolised TETA in the urine of healthy subjects (22.8%) compared to diabetic patients (7.1%, (Lu et al. 2007)). These results are not consistent with those presented here and indicate a potential species difference in the ability to absorb and metabolise TETA.

5.3.3 Levels of trace metals, copper, zinc, iron and manganese in 24hr urine

Overall an increase in metal ion excretion was observed with the onset of diabetes (Week six urine data, Figure 5.16), which is consistent with the literature (Lau and Failla 1984; Cooper et al. 2004; Cooper et al. 2005; Uriu-Adams et al. 2005). With respect to TETA treatment, a significant increase in excretion was seen in copper and zinc levels but not in iron or manganese. Consistent findings have been published previously from a human balance study (Cooper et al. 2005). *In vitro* studies have found that TETA is able to bind

stoichiometrically with zinc as well as with copper (Kodama et al. 1997). Of the physiological trace metals zinc is known to have the second highest binding stability with TETA after copper (log K (Cu) = 20.06, log K (Zn) = 11.95, log K (Fe) = 7.72 and log K (Mn) = 4.87) which may account for the effect of TETA on urinary excretion of zinc. However, Cooper *et al.,* (Cooper et al. 2005) reported that increased urinary zinc excretion in diabetic subjects following TETA treatment reflected mainly increased uptake from the gut content, whereas increased urinary copper emanated mainly from systemic stores.

An interesting result found with the current study was the significant decrease in both copper and zinc excretion in both groups between Weeks 10 and 15 of treatment (Figure 5.18 and 5.19 respectively). This may be due to an overall improvement in the condition of the diabetic animals as observed in Section 5.2.2.2 with an increase in total bodyweight. It may also reflect the change in metabolism of the drug at Week 15 described in Section 5.3.2.

5.3.4 Relationship between TETA, MAT and metal levels in the serum and urine of treated animals

Regression analysis found that in the urine of diabetic animals the association of copper and TETA changed over time (Table 5.8). This is consistent with other evidence presented in this chapter showing a shift in the metabolism of TETA and copper homeostasis over time in the treated diabetic animals (Figure 5.11). One hypothesis for this change in strength of association could be that, after two weeks of treatment, copper levels in the diabetic urine are a mixture of the excess copper found as a result of the diabetic state and copper pulled out by TETA treatment. Continued exposure to TETA over the course of the study may result in the achievement of a homeostatic state with the excess copper seen previously removed over the passage of time and the majority of copper now being excreted solely as a result of TETA treatment and, leading to a stronger correlation between TETA and copper. This may also be an explanation for the drop in total copper observed between Week 10 and 15.

There is only a very small negative association between TETA and copper in the serum of diabetic animals (38%), which reflects the reduced levels of TETA in the serum at this time point.

In the urine of both diabetic and sham animals, MAT is found to have a significant positive correlation with copper. In the serum of diabetic animals, the negative correlation between copper and MAT is stronger than the negative correlation between copper and TETA. This finding is consistent with MAT acting as a copper chelator *in vivo* as described by Lu *et al*. (Lu et al. 2007).

5.4 Conclusion

The results presented in this chapter indicate that TETA is changing the overall physiology and metal homeostasis of both sham and diabetic animals. Similar to published human studies, TETA had the most profound effect on the excretion of copper and zinc (Cooper et al. 2005). Analysis of the serum and urine levels of TETA and its metabolites MAT and DAT indicate that the diabetic state influences the ability of the animals to take up and process TETA and that this is affected by duration of exposure. This last point could be particularly important for future human studies, because if this relationship is consistent across species, then care will be required when undertaking the administration of TETA to patients with diabetes. A more comprehensive analysis of the pharmacokinetics of TETA in diabetic animals is required in order to fully understand the changes observed here. Such studies could include radioactive tracer studies similar to those conducted by Takeda *et al*. (Takeda *et al.* 1995a; Takeda *et al.* 1995b; Takeda *et al.* 1995c).

Chapter 6 Molecular changes in the left ventricle of diabetic and sham animals after eight weeks treatment with a high dose of TETA-disuccinate

6.1 Introduction

The results presented in Chapter Five described the physiological changes observed in rodents following treatment with the copper chelator TETA-disuccinate for a period of eight weeks. Our group has previously published data describing the ability of the drug to ameliorate the effects of diabetes on the heart (Cooper et al. 2004, Gong, 2006 #290; Jullig et al. 2007). These works described an improvement in cardiac mass/body mass ratio, cardiac structure, and in particular, function as a result of TETA administration (Cooper et al. 2004; Gong et al. 2006). Gene and protein expression analysis of the heart also revealed an improvement, with the expression levels of genes such as collagen III, Smad4 and TGF-β1 and proteins such as CPT II, enoyl-CoA hydratase, E2 and E3 subunits of PDH, Ndufa10, and α and β subunits of ATP synthase all returning toward normal after drug treatment (Gong et al. 2006; Jullig et al. 2007).

The focus of the data presented in this thesis was therefore aimed at further elucidating the mechanisms by which TETA treatment causes the observed changes in the LV of hearts from sham and diabetic animals. Results presented in Chapter Four and information gained through studies by colleagues in our group suggest that fuel metabolism in the mitochondria plays a fundamental role in the mechanism of action of TETA (Jullig et al. 2007). As a result of this, the work presented in this chapter was partially directed towards fuel metabolism in general, with special focus on fatty acid metabolism in the mitochondria.

TETA-induced molecular alterations of the LV were analysed at a number of different levels. Firstly, microarray technology was utilised to look at global genetic changes with subsequent confirmation by RT-qPCR. Secondly, histological methods were employed to assess three areas known to be perturbed in diabetes. They were: ECM organisation, lipid storage and mitochondrial structure. Thirdly, more specialised analysis of tissue lipid content was carried out using flame ionisation detection thin-layer chromatography (Iatroscan) and finally fuel metabolism in the mitochondria was assessed using appropriate functional enzymatic assays.

The aim of this chapter was to characterize the effect of 87.5mg/day TETA on the LV of the heart with particular focus on fuel metabolism and in so doing, attempt to elucidate the mechanisms underlying the improvement in heart function as described (Cooper et al. 2004; Gong et al. 2006). This TETA dose was chosen as a consequence of the results presented in Chapter Five and because a dose of this magnitude had not been previously studied. The animals that received 87.5 mg TETA-disuccinate/day are now referred to herein as 'treated'.

6.2 Results

6.2.1 Summary of results from Chapter Five for untreated and treated animals

Results presented in Chapter Five showed that treatment of both sham and diabetic animals with TETA-disuccinate resulted in a number of physiological changes. Tables 6.1-6.3 show a summary of these changes comparing untreated animals with those receiving 87.5 mg of TETA per day.

Table 6.1 outlines the main physiological changes and demonstrates that drug treatment caused significant (average 15%) increase in the heart weight of the diabetic animals and a non-significant trend towards increased heart weight in the sham group. The greatest effect of drug was observed in the average weight change in both the sham and diabetic animals. Treatment with TETA caused an increased average weight change in sham animals and reversed the decline in body weight observed in the untreated diabetic animals, so much so that the treated cohort actually gained weight.

Table 6.1 Physiological changes

	Heart Weight (g)	HW/BW ratio (x10^{-3})	Average weight (16 weeks)	Final weight (g)	Average Δ Weight (week 9-16)	Blood Glucose (mM)
Sham						
No Drug	1.6 ± 0.1	3.4 ± 0.1	409 ± 7	483 ± 16	28 ± 5	4.9 ± 0.1
87.5mg	1.8 ± 0.1	3.4 ± 0.2	446 ± 9***	534 ± 12*	41 ± 5**	4.9 ± 0.1
Diabetic						
No Drug	1.3 ± 0.07	4.6 ± 0.3	300 ± 3	298 ± 13	-8.1 ± 4	29.0 ± 0.4
87.5mg	1.5 ± 0.06**	4.5 ± 0.1	319 ± 4***	339 ± 15*	4.2 ± 4***	28.6 ± 0.5

*P<0.05, **P<0.01, ***P<.0001

The majority of serum biochemistry markers assessed in this study showed no change with drug treatment. One marker found to have a significant change was that of ferroxidase activity levels. These fell in the sham-treated animals to levels consistent with those of dietary Cu-restricted rats ((Uriu-Adams et al. 2005), Table 6.2). The decrease in ferroxidase levels in diabetic animals was more modest than that seen in the sham animals. The observed change is consistent with a shift in total copper levels and signifies

a shift in the copper status of these animals that was not seen in animals treated with lower doses of TETA-disuccinate (Section 5.2.3.4) and was an important validation for the choice of 87.5mg-dosed animals for further study.

Table 6.2 Serum biochemistry

	Total Cu (mM)	Ferroxidase (U/l)
Sham		
No Drug	$0.017 \pm 1 \times 10^{-3}$	310 ± 24
87.5mg	$0.009 \pm 1 \times 10^{-3}$	136 ± 23
Diabetic		
No Drug	$0.020 \pm 9 \times 10^{-4}$	345 ± 23
87.5mg	$0.018 \pm 8 \times 10^{-4}$	285 ± 20

As discussed in Chapter Five, onset of diabetes caused increased copper and zinc excretion in the absence of treatment (Figure 5.16), while treatment with TETA led to further increases in both urinary copper and zinc in both the sham and diabetic animals (Figures 5.18 and 5.19). Copper and zinc excretion levels were greatest in animals from both groups receiving 87.5mg/day (Table 6.3).

Table 6.3 Copper and Zinc excretion

	Cu/g body weight (mmol/24hrs)	Zn/g body weight (mmol/24hrs)
No Drug	$2.2 \times 10^{-4} \pm 2 \times 10^{-5}$	$8.5 \times 10^{-4} \pm 1 \times 10^{-4}$
87.5mg	$8.1 \times 10^{-4} \pm 8 \times 10^{-5}$	$1.9 \times 10^{-3} \pm 2 \times 10^{-4}$

6.2.2 Microarray analysis

Microarray analysis was conducted using RNA extracted from the LV of rat hearts collected after sixteen weeks of the study and employed Affymetrix Rat 230 2.0 GeneChips. This was done in a manner similar to that of the study outlined in Chapter Four and described in Section 2.2.2.2 and 2.3.5. Here, five arrays were used for each of the four groups (sham, sham-treated, diabetic, and diabetic-treated) to give a total of twenty arrays. The choice of five arrays per group was considered to be sufficient to provide statistically significant results based on the manufacturer's recommendations while reducing the cost of the overall experiment.

6.2.2.1 Selection criteria

The microarray procedure was carried out as described in Section 2.3.5. As only five arrays were included in each group and there were six to eight samples available, a standard *a priori* inclusion criterion was first applied uniformly across all the sample

groups in order to remove extreme outliers prior to subsequent random selection for extracting the RNA. This is of particular importance when studying the diabetic group as it has been shown to have larger animal to animal variation, consistent with the breakdown of homeostatic regulation. The first of this criterion was the average weight of each animal across the sixteen weeks and the second was copper excretion levels of each animal at the four 24hr urine collection time points. Excessive body weight gain or loss is known to be an important indicator of animal health and deranged physiology (Foltz and Ullman-Cullere 1999). Secondly, it was known from a previous study that a change in urine copper excretion is evidence for successful drug uptake (Cooper et al. 2004) and so this was used to ensure that only confirmed drug responders were included. Once the two criteria were applied it was determined statistically by outlier analysis (Grubbs test) that three animals could be legitimately excluded from various study groups. These were: animal # 6 (normal untreated) with an average body weight of 322 ± 13.2g compared to the group average of 409 ± 6.5g; animal #21 (diabetic untreated) with an average body weight of 389 ± 15.7g compared to the group average of 299 ± 3.1g and animal #54 (diabetic-treated) with a copper excretion level of 36.7×10^{-3}mg/l at Week 15 compared to the group average of 93.6 ± 9.6 $\times 10^{-3}$mg/l. Within the remaining animals in each group, five were then randomly chosen for RNA extraction and microarray analysis.

6.2.2.2 Analysis of changes in gene expression

In the sham vs. diabetic comparison, a total of 1205 significant changes were observed using the rejection point $P < 0.05$. This is slightly fewer than that seen in Chapter Four (1614 significant changes ($P < 0.05$)) and is most likely a consequence of using fewer arrays in this study (seven arrays were performed per group in Chapter Four).

Analysis of the cellular distribution of genes (similar to that described in Figure 4.3) revealed that 12.5% of the significantly differentially expressed genes were associated with the mitochondrion; this result closely matches the 13% observed in Chapter Four. Points to note from this study are that membrane-associated genes contributed 15.7% only of the total changes compared to 29% in Chapter Four, while changes in extracellular region/matrix associated genes contributed 19% of the total compared to 7% in the pilot study.

This chapter does not aim to outline changes associated with diabetes as this was covered extensively in Chapter Four. It should be noted however, that a number of changes associated with the diabetic state, as described in Chapter 4, were also present in this study indicating that it is comparable to the previous study (Tables 6.4-6.7).   A notation of >1, in Tables 6.4-6.7 for the diabetic vs. sham comparison, indicates increased

expression in the diabetic group and <1 indicates decreased expression in the diabetic compared to sham.

Table 6.4 Genes involved in carbohydrate metabolism (as defined by their GO annotation) whose expression in LV myocardium was significantly altered by diabetes

Gene Symbol	Fold Change Study 1	P-value Study 1	Fold Change Study 2	P-value Study 2	Gene Title
Slc2a1	0.5	0.000*	0.4	0.000*	solute carrier family 2 (facilitated glucose transporter), member 1
Slc2a4	0.3	0.000*	0.2	0.000*	solute carrier family 2 (facilitated glucose transporter), member 4
Pdp2	0.4	0.000*	0.4	0.000*	pyruvate dehydrogenase phosphatase isoenzyme 2
Pdk4	7.6	0.000*	4.3	0.13	pyruvate dehydrogenase kinase, isoenzyme 4

* at least $P < 5.0E-05$

One unexpected observation, for the genes involved in carbohydrate metabolism (Table 6.4), is that in the new study PDK4 is not significantly differentially expressed, despite showing a high fold-change. This may be a consequence of the lower number of microarrays used in this study causing a reduction in resolution.

Table 6.5 Genes associated with lipid metabolism (as defined by their GO annotation) whose expression was significantly altered in diabetic LV

Gene Symbol	Fold Change Study 1	P-value Study 1	Fold Change Study 2	P-value Study 2	Gene Title
Cpt1a	2.2	0.000*	1.9	0.000*	carnitine palmitoyltransferase 1, liver
Cpt2	1.4	0.0026	1.4	0.011	carnitine palmitoyltransferase 2
Cpt1b	1.2	0.036	1.3	0.007	carnitine palmitoyltransferase 1b
Mlycd	1.5	0.000*	1.4	0.000*	malonyl-CoA decarboxylase
Slc25a20	1.3	0.002	1.3	0.095	solute carrier family 25 (carnitine/acylcarnitine translocase), member 20
Hadha	1.6	0.000*	1.6	0.000*	hydroxyacyl-Coenzyme A dehydrogenase/3-ketoacyl-Coenzyme A thiolase/enoyl-Coenzyme A hydratase (trifunctional protein), alpha subunit
CD36/FAT	1.4	0.000*	1.6	0.002	CD36 antigen/similar to fatty acid translocase/CD36
Agptl4	25.1	0.000*	21.8	0.000*	angiopoietin-like protein 4
Ucp3	2.5	0.000*	2.6	0.005	uncoupling protein 3 (mitochondrial, proton carrier)

* at least $P < 5.0E-05$

Almost all changes associated with lipid metabolism (Table 6.5) were consistent with those reported in Chapter Four. The one exception was solute carrier family 25 (carnitine/acylcarnitine translocase), member 20 which, despite showing a similar fold-change to the results obtained previously, did not return a significant result.

Table 6.6 Expression changes in genes associated with activation of PKC

Gene Symbol	Fold Change Study 1	P-value Study 1	Fold Change Study 2	P-value Study 2	Gene Title
PKCδ	1.3	0.003	1.4	0.083	protein kinase C, ð type
Ednrb	1.9	0.000*	1.4	0.538	endothelin receptor type B
Ednra	1.6	0.003	1.0	0.982	endothelin receptor type A

* at least P< 5.0E-05

Of the three genes associated with activation of PKC (Table 6.6) as discussed in Chapter Four, none were found to be significant in this study, although results for PKC δ are close to significant. This is again likely to be due to the small numbers per group reducing the level of resolution achievable by the microarray system.

Table 6.7 Genes that play roles in oxidative stress (as defined by their KEGG pathway description) with expression significantly altered in diabetic LV

Gene Symbol	Fold Change Study 1	P-value Study 1	Fold Change Study 2	P-value Study 2	Gene Title
Gapdh	0.9	0.352	0.9	0.524	glyceraldehyde-3-phosphate dehydrogenase
Gapdhs	0.9	0.626	0.9	0.508	glyceraldehyde-3-phosphate dehydrogenase, spermatogenic
Tiparp_predicted	1.3	0.027	1.1	0.849	TCDD-inducible poly(ADP-ribose) polymerase (predicted)
Sod1	0.9	0.957	1.0	0.929	superoxide dismutase 1
Sod2	0.9	0.088	0.8	0.056	superoxide dismutase 2, mitochondrial
Sod3	1.0	0.998	1.0	0.980	superoxide dismutase 3, extracellular
Cat	1.4	0.001	1.5	0.000	catalase
Mt1a	1.0	0.855	0.8	0.645	metallothionein 1a

* at least P< 5.0E-05

Results presented in Table 6.7 show that the only difference between the two studies for genes involved in oxidative stress was with TCDD-inducible (poly-ADP-ribose) polymerase (predicted); the gene did not significantly change in this study.

While there where a few notable differences in gene changes observed between the two studies, which can most likely be attributed to the smaller number of arrays performed in the current study, overall the two studies produced very similar results. The two tables presented below show the top 15 gene changes from the sham (Table 6.8) and diabetic (Table 6.9) untreated vs. treated comparisons in the new study.

Table 6.8 Sham untreated vs. sham-treated, top 15 genes (based on unadjusted P-value)

Gene Symbol	Fold Change	P-value	FDR adjusted P-value	Gene Title	GO Biological Process and Molecular function annotation	
Scn3b	0.7	0.000*	1.000	sodium channel, voltage-gated, type III, beta	ion transport, sodium ion transport	voltage-gated sodium channel activity
Ssr1	0.8	0.000*	1.000	Signal sequence receptor, alpha	co-translational protein targeting to membrane	signal sequence binding, calcium ion binding
LOC683220/LOC688750	0.8	0.000*	1.000	similar to CD209 antigen	---	---
Hkr3	0.8	0.001	1.000	GLI-Kruppel family member HKR3	regulation of transcription, DNA-dependent	transcription factor activity, metal ion binding

Gene	FC	P	FDR	Title	GO BP	GO MF
Calm3	1.3	0.001	1.000	calmodulin 3	G-protein coupled receptor protein signaling pathway	calcium ion binding, protein binding
Slc39a6	0.8	0.001	1.000	solute carrier family 39 (metal ion transporter), member 6	nervous system development, metal ion transport	metal ion transporter activity
---	1.3	0.002	1.000	Transcribed locus	---	---
---	0.7	0.002	1.000	---	---	---
---	0.8	0.002	1.000	Transcribed locus	---	---
Sfn_predicted	0.8	0.002	1.000	stratifin (predicted)	regulation of cyclin-dependent protein kinase activity	protein kinase C inhibitor activity
---	1.4	0.003	1.000	---	---	---
Rpp38	0.8	0.003	1.000	ribonuclease P/MRP 38 subunit (human)	protein biosynthesis	structural constituent of ribosome
---	1.3	0.003	1.000	Transcribed locus	---	---
Zfhx1b	1.2	0.003	1.000	Zinc finger homeobox 1b	neural crest cell migration, somitogenesis	phosphatase regulator activity, SMAD binding, zinc ion binding
Scn3b	0.7	0.003	1.000	sodium channel, voltage-gated, type III, beta	ion transport	voltage-gated sodium channel activity

Fold-change: The fold-change in the sham untreated compared to sham-treated animals. >1 is increased expression in the sham untreated animals and <1 is decreased expression in the sham untreated animals compared to those treated with TETA. * at least $P < 5.0E-05$

Table 6.9 Diabetic untreated vs. diabetic-treated, top 15 genes (based on unadjusted P-value)

Gene Symbol	Fold Change	P-value	FDR adjusted P-value	Gene Title	GO Biological Process and Molecular function annotation	
---	1.5	0.000*	0.052	Similar to RIKEN cDNA2810451A06	protein folding	heat shock protein binding
Etv4_predicted	1.4	0.000*	0.127	E1A enhancer binding protein, E1AF) (predicted)	regulation of transcription, DNA-dependent	transcription factor activity
MGC125034	2.1	0.000*	0.147	similar to RNA binding motif protein 21	---	nucleotide binding, zinc ion binding
---	1.5	0.000*	0.182	---	---	---
Fbn1	0.5	0.000*	0.412	fibrillin 1	skeletal development, heart development	extracellular matrix structural constituent
Asam	0.7	0.000*	0.412	adipocyte-specific adhesion molecule	cell-cell adhesion	---
Hpd	1.9	0.000*	0.412	4-hydroxyphenylpyruvic acid dioxygenase	L-phenylalanine catabolism	4-hydroxyphenylpyruvate dioxygenase activity, iron ion binding
Slc41a3	0.6	0.000*	0.412	solute carrier family 41, member 3	cation transport	cation transporter activity
---	0.8	0.000*	0.412	---	---	---
Arntl	0.4	0.000*	0.412	aryl hydrocarbon receptor nuclear translocator-like	protein import into nucleus, translocation, regulation of transcription	DNA binding, signal transducer activity
---	2.9	0.000*	0.477	Transcribed locus	---	---
Mettl7a	1.4	0.000*	0.477	methyltransferase like 7A	---	methyltransferase activity
Il6ra	1.3	0.000*	0.547	interleukin 6 receptor	immune response, cell surface receptor linked signal transduction	interleukin-6 receptor activity, enzyme binding

| --- | 0.7 | 0.000* | 0.654 | Transcribed locus | --- | --- |
| Mig12 | 1.5 | 0.000* | 0.654 | MID1 interacting G12-like protein | negative regulation of microtubule depolymerization | protein binding |

Fold-change: The fold-change in the diabetic untreated compared to diabetic-treated animals. >1 is increased expression in the diabetic untreated animals and <1 is decreased expression in the diabetic untreated animals compared to those treated with TETA. * at least P< 5.0E-05

As can be seen in the P-value column for both tables, there were numerous changes associated with drug treatment.

Table 6.10 Gene expression changes common to both treated vs. untreated comparisons

Gene Symbol	Gene Title	Diabetic untreated vs. treated		Sham untreated vs. treated	
		Fold change	Unmodified P-Value	Fold change	Unmodified P-Value
Adam17	a disintegrin and metalloproteinase domain 17 (tumor necrosis factor, alpha, converting enzyme)	-1.20	0.01	-1.19	0.05
Fdx1	ferredoxin 1	-1.13	0.02	-1.13	0.04
Hmox1	heme oxygenase (decycling) 1	-1.35	0.00	-1.17	0.01
Wisp1	WNT1 inducible signaling pathway protein 1	1.16	0.04	1.19	0.03
Arntl	aryl hydrocarbon receptor nuclear translocator-like	-2.65	0.00	1.27	0.02
Ptpn2	protein tyrosine phosphatase, non-receptor type 2	-1.13	0.01	-1.14	0.04
Zdhhc9	zinc finger, DHHC domain containing 9	-1.12	0.05	-1.18	0.02
Postn (predicted)	periostin, osteoblast specific factor (predicted)	-2.31	0.01	1.15	0.02
Sfrs3 (predicted)	splicing factor, arginine/serine-rich 3 (SRp20) (predicted)	-1.19	0.01	-1.11	0.04
Per3	period homolog 3 (Drosophila)	1.52	0.02	-1.18	0.02
Usp2	ubiquitin specific peptidase 2	1.85	0.00	1.32	0.02
G0s2	G0/G1 switch gene 2	-1.35	0.05	1.14	0.01
Fut8	fucosyltransferase 8 (alpha (1,6) fucosyltransferase)	-1.13	0.02	1.18	0.01
Fxyd3	FXYD domain-containing ion transport regulator 3	-1.33	0.04	1.18	0.01
Lrrc10 (predicted)	leucine-rich repeat-containing 10 (predicted)	1.21	0.01	1.12	0.03
Slc25a29	solute carrier family 25 (mitochondrial carrier, palmitoylcarnitine transporter), member 29	1.22	0.05	-1.13	0.04
Smyd3	SET and MYND domain containing 3	-1.14	0.05	-1.12	0.04
Ppp2r3a	protein phosphatase 2 (formerly 2A), regulatory subunit B", alpha	1.14	0.04	1.16	0.03
Cbfb	core binding factor beta	1.21	0.04	-1.11	0.04
Abhd14a	abhydrolase domain containing 14A	1.21	0.02	-1.12	0.04
---	Transcribed locus	1.23	0.05	1.13	0.05

Fold-change: The fold-change in the untreated group (sham or diabetic) compared to treated animals (sham or diabetic). >1 is increased expression in the untreated animals and <1 is decreased expression in the untreated animals compared to those treated with TETA. * at least P< 5.0E-05

A number of significant gene expression changes (pre-FDR correction) were observed that were common to both the diabetic- and sham-treated vs. untreated comparisons. The majority of these changes appeared to be in the same direction i.e. increased in the diabetic-treated was also increased in the sham-treated. These results are presented in Table 6.10 above. This indicates that the drug may be having an effect at the gene expression level. However, an element of the statistical analysis incorporated

into microarray statistics is the adjustment for false discoveries (FDR (Benjamini and Hochberg 1995), as described in Chapter Three). The use of this adjustment resulted in there being no significant changes in gene expression after drug treatment (see FDR adjusted P-value column). This result was unexpected, particularly in light of the reported evidence for molecular effects in prior studies (Cooper et al. 2004; Gong et al. 2006; Jullig et al. 2007) and noted phenotypic and cardiac mass changes of this current work (Chapter Five). The implications of analysing microarray data using univariate statistics with a false discovery rate correction are discussed in Section 6.3 and further in Chapter Seven.

6.2.2.3 Gene Set Enrichment Analysis

As a result of the inability to detect any statistically significant changes in gene expression associated with TETA-disuccinate treatment under the stringent statistical criteria described in Section 6.2.2.2, a second method for analysing microarray datasets known as Gene Set Enrichment Analysis (GSEA) described by Subramanian *et al.,* (Subramanian et al. 2005) was applied to the data from this study. This method incorporates *a priori* pathway or gene-set information rather than analysing information from individual genes. This is thought to increase the power of the statistical analysis and so increase the chance of seeing significant changes in gene expression. Program and parameter information for GSEA are described in Section 2.12.3. Five categories of gene-sets were used in this analysis: *Apriori*, Biological Process, Cellular Compartment, KEGG and Molecular function. The construction of these categories is described in Section 2.12.3. As only two groups could be analysed at one time, planned comparisons of diabetic vs. normal, normal vs normal-treated and diabetic vs. diabetic-treated were carried out. The significance of a result is based on the enrichment score (ES). The ES reflects the degree to which a gene-set is overrepresented at the extremes (top or bottom) of a ranked gene list (generated from the microarray data). The score is calculated by 'walking down' the list, increasing a running sum statistic (Kolmogorov–Smirnov-like statistic) when a gene in the gene-set is encountered and decreasing it when a gene not in the gene-set is encountered. The magnitude of the increment depends on the correlation of the gene with the phenotype (in this case sham, diabetic or diabetic-treated). The enrichment score is the maximum deviation from zero encountered in the random walk. A positive enrichment score indicates genes found at the top of the list while a negative enrichment score indicates genes found at the bottom of the list. Table 6.11 provides a summary of the results from these planned comparisons. No changes were observed in the sham vs. sham-treated comparison.

Table 6.11 GSEA comparison summary

	Apriori	Biological Process	Cellular Compartment	KEGG	Molecular Function
Diabetic vs. Sham					
Diabetic (n=5)					
Total number of gene-sets correlated with diabetic	11/27	200/445	59/128	39/115	102/239
Gene-sets significant at FDR<25%	4	0	5	2	2
Sham (n=5)					
Total number of gene sets correlated with sham	16/27	245/445	69/128	76/115	137/239
Gene-sets significant at FDR<25%	7	0	0	0	0
Diabetic vs. Diabetic-treated					
Diabetic (n=5)					
Total number of gene-sets correlated with diabetic	22/45	245/413	68/128	70/115	152/239
Gene-sets significant at FDR<25%	0	1	2	0	0
Diabetic-treated (n=5)					
Total number of gene-sets correlated with diabetic-treated	23/45	168/413	59/128	45/115	87/239
Gene-sets significant at FDR<25%	0	0	0	0	0
Sham vs. Sham-treated					
Sham (n=5)					
Total number of gene-sets correlated with diabetic	22/45	232/413	69/128	74/115	139/239
Gene-sets significant at FDR<25%	0	0	0	0	0
Sham-treated (n=5)					
Total number of gene-sets correlated with diabetic-treated	23/45	181/413	59/128	41/115	105/239
Gene-sets significant at FDR<25%	0	0	0	0	0

Table 6.12 and 6.13 contain the data from the eleven gene-sets that were identified as significant in the *Apriori* category in the sham vs. diabetic comparison. As expected from the results obtained in Chapter Four and here above, gene-sets containing genes involved in fatty acid metabolism were significantly enriched in the diabetic group, while gene-sets containing genes involved in glucose metabolism were found to be enriched in the sham group.

Table 6.12 Gene-sets identified as significantly correlated with the diabetic group

GO ID Number	Name	Gene-set Size	ES	Normalised ES (NES)	P-value	FDR (%)
GO:0001676	long-chain FA metabolic process	19	0.76	1.5	0.000	13%
GO:0006631	FA metabolic process	87	0.50	1.5	0.004	7%
GO:0006637	acyl-CoA metabolic process	21	0.83	1.5	0.008	9%
GO:0006629	lipid metabolic process	208	0.42	1.5	0.013	8%

Abbreviations: GO ID, gene ontology identity; Gene-set size, number of genes within gene-set (based on GO ID number); ES, enrichment score; NES, normalised enrichment score.

Table 6.13 Gene-sets identified as significantly correlated with the sham group

GO ID number	Name	Gene-set Size	ES	NES	P-value	FDR (%)
GO:0016491	oxidoreductase activity	234	-0.31	-1.4	0.002	13%
GO:0005319	lipid transporter activity	38	-0.53	-1.6	0.002	13%
GO:0005975	carbohydrate metabolic process	133	-0.35	-1.4	0.019	13%
GO:0006094	gluconeogenesis	24	-0.52	-1.5	0.026	20%
GO:0015758	glucose transport	24	-0.64	-1.4	0.033	15%
GO:0005355	glucose transporter activity	15	-0.74	-1.4	0.039	15%
GO:0006869	lipid transport	35	-0.41	-1.4	0.064	17%

Abbreviations: GO ID, gene ontology identity; Gene-set size, number of genes within gene-set (based on GO ID number); ES, enrichment score; NES, normalised enrichment score

Table 6.14 outlines the remaining nine gene-sets that were significantly associated with the diabetic phenotype in the sham vs. diabetic comparison. No further gene-sets were found to be significantly correlated with the sham group.

Table 6.14 Gene-sets identified as significantly correlated with the diabetic group

GO ID Number	Name	Category	Gene-set Size	ES	NES	P-value	FDR (%)
GO:0003735	structural constituent of ribosome	Molecular Function	133	0.30	1.8	0.008	7.6%
GO:0004519	endonuclease activity	Molecular Function	27	0.48	1.7	0.015	17.5%
GO:0005840	ribosome	Cellular Compartment	80	0.39	1.9	0.000	0.5%
GO:0005843	cytosolic small ribosomal subunit	Cellular Compartment	25	0.55	1.8	0.000	0.8%
GO:0005635	nuclear envelope	Cellular Compartment	54	0.46	1.6	0.000	17.3%
GO:0001533	cornified envelope	Cellular Compartment	15	0.66	1.5	0.018	23.3%
GO:0005842	cytosolic large ribosomal subunit	Cellular Compartment	32	0.52	1.6	0.026	12.0%
KEGG: 3010	Ribosome	KEGG	66	0.544	1.840	0.008	10.0%
KEGG: 3320	PPAR signaling pathway	KEGG	93	0.446	1.627	0.012	9.9%

It is interesting to note the small number of significantly different gene-sets associated with the diabetic vs. sham comparison (Table 6.11). We would have expected that this comparison would give a high number of significantly enriched gene-sets due to the large number of significant gene changes occurring with diabetes (1205 genes, $P<0.05$). The low number of significant gene-sets identified may be either due to the small number of replicates used, giving rise to the warning message as stated in Section 2.12.3 or to the relatively stringent FDR criteria applied by the GSEA software (FDR<25%).

Comparison of the diabetic vs. diabetic-treated groups revealed three gene-sets that were significant. The first two were from the cellular component category and the third was from the biological process category. All three were found to be relatively enriched in the diabetic untreated group and are presented in Table 6.15 below.

Table 6.15 Gene-sets identified as significantly correlated with the diabetic group

GO ID Number	Name	Category	Gene-set Size	ES	NES	P-value	FDR (%)
GO:0030032	lamellipodium biogenesis	Biological process	19	0.47	1.9	0.004	6.3%
GO:0005681	spliceosome	Cellular component	50	0.45	1.8	0.000	11%
GO:0001533	cornified envelope	Cellular component	15	0.74	1.7	0.000	16%

Abbreviations: GO ID, gene ontology identity; Gene-set size, number of genes within gene-set (based on GO ID number); ES, enrichment score; NES, normalised enrichment score

Lamellipodium biogenesis is a biological process that leads to formation of the lamellipodia, a short thin band (<5% of the total cell length) at the extreme cell anterior of locomoting cells, such as fibroblasts and smooth muscle cells (Abercrombie 1980; Cramer et al. 1997; Pichon et al. 2004). Lamellipodia contain concentrated arrays of polar actin filaments that polymerize to form protrusions (for a review see (Small et al. 2002)) and participate in the first stage of cell migration (Cramer et al. 1997; Pichon et al. 2004). There is evidence for remodelling of the heart and increased collagen deposition as a result of diabetes (Cooper et al. 2004). This remodelling in the diabetic heart would require increased movement of cardiac fibroblasts and potentially lead to increased lamellipodium biogenesis.

The spliceosome is a ribonucleoprotein complex, which contains RNA and small nuclear ribonucleoproteins (snRNPs) and is assembled during the splicing of mRNA primary transcripts to excise introns. The spliceosome catalyses a two-step transesterification reaction required to remove introns and ligate exons (for reviews see (Konarska 1998; Will and Luhrmann 2001)). There has been no prior report to implicate TETA in the modulation of RNA splicing. However, there are several lines of evidence linking copper-dependent processes such as metal ion uptake and sensing to transcriptional regulation ((Pena et al. 1998; Labbe et al. 1999; Zhou, H. and Thiele 2001) and described in Section 1.4). Furthermore, there is evidence that addition of copper or zinc chelators to nuclear extracts specifically inhibit the second step in mRNA splicing (Shomron et al. 2002). Therefore, this new finding, that potentially links TETA treatment to genes relevant to spliceosome biology, deserves further scrutiny and follow up.

The cornified envelope is an insoluble protein structure formed under the plasma membrane of cornifying epithelial cells (as defined by the GO AmiGO (Ashburner et al. 2000) search engine). Of note is that this gene-set was also significantly associated with the diabetic phenotype in the diabetic vs. sham comparison (Table 6.14, Cellular compartment).

There is no prior information concerning the implications of linkages between any of these gene-sets and the pathogenesis of diabetes, treatment with a copper chelator or mitochondrial fuel metabolism, so further analysis at this level has not as yet been pursued. However, further detailed evaluation will be required before it is possible to place these findings into the broader context, and they have not been discarded at this time.

6.2.3 RTqPCR

In order to verify the performance of the microarray study, an RT-qPCR validation experiment was performed. A set of 11 *a priori* genes were used and the rationale for choosing each gene is described below:

- A number of genes were chosen for their involvement in fatty acid metabolism. These were; Angptl4 (an inhibitor of lipoprotein lipase (Yoshida et al. 2002), CPT I (a mitochondrial FA transporter (Pande 1975; Saggerson and Carpenter 1981; Saggerson 1982)), MCD (a regulator of CPT (Sakamoto et al. 2000)), and CD36 (the primary fatty acid transporter in the heart (Luiken et al. 2002)). If TETA does have effects on fuel metabolism it would be expected that changes would occur in these genes.

- Collagen III and TGF-β were chosen to determine if this dose of TETA invokes similar responses to those observed, by other group members, in a published analysis of animals treated with a lower dose (Gong et al. 2006).

- The receptor for AGE (AgeR) was chosen as an indicator of the effects of AGE accumulation on the heart. Previous studies (Qian et al. 1998; Candido et al. 2003) have indicated that AGEs accumulate on collagen after the onset of diabetes due to its slow turnover. AgeR is expressed at low levels in normal tissue and is up-regulated where ever its ligands (AGE) accumulate (Schmidt et al. 2001)). Cell culture studies have shown that the AGE-AgeR interaction alters the cellular properties that play a role in vascular homeostasis, such as causing depletion of intracellular nitric oxide concentration (Singh et al. 2001). If, as in previous studies (Cooper et al. 2004; Gong et al. 2006) collagen III is decreased following TETA treatment of diabetes, then it would be expected that AGE would also be decreased, at the level of both protein and transcript, thus leading to decreased expression of its receptor.

- Tfam was chosen as a mitochondrial marker. Although work from within this group has indicated a TETA-induced improvement in mitochondrial respiratory function (Dr. A Hickey, personal communication), it is unclear whether this is due to increased numbers of mitochondria or increased efficiency of the mitochondria already present. Tfam is known to be involved in regulating mitochondrial DNA copy number (Ekstrand et al. 2004) and so can therefore be used as a crude measurement of the number of

mitochondria present in the tissue.

- Ctr1, Cox17 and Synthesis of cytochrome oxidase deficient homolog 1 (Sco1) are all genes implicated in copper metabolism. Ctr 1 is involved in the transport of copper into the cell (Moller et al. 2000), Cox17 is a chaperone that transports copper to cytochrome c in the mitochondria (Glerum et al. 1996) and Sco1 is a copper containing protein of the inner mitochondrial membrane and is required for cytochrome c oxidase assembly (Leary et al. 2004). TETA is a copper chelator and therefore it is important to understand whether changes in copper homeostasis are occurring within the heart to provide an explanation for the observed reduction in serum ferroxidase levels resulting from TETA treatment (Table 6.2). Changes in the expression of Cox17 and Sco1 genes would also provide a link between the mitochondria and TETA induced changes in copper metabolism, given the association of each gene to both areas.

RT-qPCR was performed as described in Section 2.4. Three planned comparisons were performed on the resulting data: sham vs. diabetic (Table 6.16); diabetic-treated vs. diabetic untreated (Table 6.17) and sham-treated vs. sham (Table 6.18). These comparisons were analysed as described in Section 2.12.4.2.

Table 6.16 Sham vs. diabetic comparison

Gene	$\Delta\Delta C_t$	$\Delta\Delta C_t$ (SE)	RTqPCR Fold-change	Microarray Fold-change
Angptl4	5.0	0.6	31.1***	21.8***
Ctr1	0.01	0.3	1.0	1.0
MCD	0.6	0.2	1.5*	1.4***
Sco1	0.4	0.3	1.3	1.0
Tfam	0.5	0.3	1.4	1.3
AgeR	0.2	0.5	1.1	1.1
CD36	0.8	0.3	1.8**	1.6**
Col3a1a	0.5	0.3	1.4	1.1
CPT	0.6	0.4	1.6	1.9***
Cox17	0.2	0.4	1.1	1.1
TGF-β	-0.1	0.3	0.9	0.9

Fold-change: >1 is increased in the diabetic and <1 is decreased in the diabetic compared to sham animals. ***P<.0001, **P<0.001, *P<0.01

All of the significant changes for the sham vs. diabetic comparison using RT-qPCR were the same as those observed using microarray technology. All fold-change values from the microarray experiment corresponded reasonably well with those from the RT-qPCR experiment. One unexpected difference was the RT-qPCR result for CPT, which was highly significant on the microarray and not significant using the more sensitive technique, despite the fact that the fold-change observed using both technologies was similar.

Table 6.17 Diabetic-treated vs. diabetic comparison

Gene	$\Delta\Delta C_t$	$\Delta\Delta C_t$ (SE)	RTqPCR Fold-change	Microarray Fold-change
Angptl4	-0.5	0.8	0.7	1.8
Ctr1	0.1	0.4	1.1	1.1
MCD	0.4	0.3	1.3	1.1
Sco1	0.3	0.4	1.2	1.0
Tfam	0.1	0.4	1.1	1.1
AgeR	0.2	0.7	1.1	1.0
CD36	-0.03	0.3	1.0	1.0
Col3a1a	0.7	0.4	1.6	1.2
CPT	0.3	0.5	1.3	1.0
Cox17	-0.4	0.6	0.8	0.9
TGF-β	0.2	0.4	1.2	0.9

Fold-change: >1 is increased in the diabetic-treated and <1 is decreased in the diabetic-treated compared to untreated diabetic animals

Use of RT-qPCR technology showed no significant changes in either the diabetic or sham animals as a result of treatment with TETA (Table 6.17 and 6.18). This confirms the microarray results and provides additional specific evidence that using this technology, TETA at 87.5mg did not act at the transcriptional level with respect to the specific gene products studied.

Table 6.18 Sham-treated vs. sham comparison

Gene	$\Delta\Delta C_t$	$\Delta\Delta C_t$ (SE)	RTqPCR Fold-change	Microarray Fold-change
Angptl4	1.3	0.9	2.5	0.8
Ctr1	0.2	0.4	1.2	1.1
MCD	0.1	0.3	1.0	1.1
Sco1	0.3	0.4	1.3	1.0
Tfam	0.1	0.4	1.0	1.0
AgeR	-0.4	0.8	0.8	1.0
CD36	0.4	0.4	1.3	1.0
Col3a1a	0.2	0.5	1.1	1.1
CPT	0.8	0.6	1.7	1.0
Cox17	0.5	0.6	1.4	1.0
TGF-β	-0.3	0.4	0.8	1.0

Fold-change: >1 is increased in the sham-treated and <1 is decreased in the sham-treated compared to untreated sham animals.

6.2.4 Histology

Concurrently with the genetic studies, histological analysis was performed on the LV tissue from the four groups. Three different histological methods were used to study the effect of the drug on the gross morphology of the heart tissue and to confirm whether findings from previously published reports (Cooper et al. 2004; Gong et al. 2006) were present in this study.

6.2.4.1 Collagen III and myocyte histology

Results from the original study that first described the effects of TETA treatment on heart function (Cooper et al. 2004) showed that collagen III levels were increased as a result of diabetes and decreased with TETA treatment. Collagen III mRNA levels were also found to be reduced following drug treatment in a follow up study (Gong et al. 2006). We hypothesized that a similar change might be observed in this study.

Collagen III staining was performed as described in Section 2.5.1. Figure 6.1 (A), (B), (C) and (D) are representative images of collagen III staining in sham, sham-treated, diabetic, and diabetic-treated respectively. From these it can be seen that the myocytes in both the diabetic and diabetic-treated sections appear elongated and are more disorganised compared to controls. This indicates a perturbation in the arrangement and size of the myocytes that is likely to be due to the effects of diabetes and is consistent with earlier reports (Cooper et al. 2004).
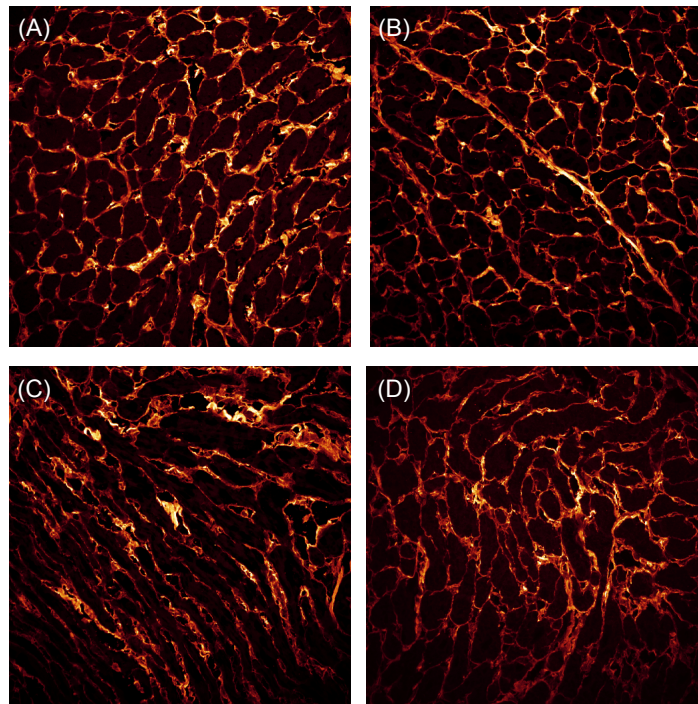
Figure 6.1 Confocal image analysis of collagen III levels in the LV

A section of tissue was cut from the base of the LV after perfusion, embedded in OCT compound and frozen in liquid N_2. Tissues were cryosectioned to 5μm using a cryo-microtome and adhered to SuperFrost slides prior to staining. Tissue sections were immunostained using the primary antibody rabbit anti-rat collagen type III and secondary antibody Alexa Fluor 488 goat anti-rabbit both diluted 1 in 100 diluted in PBS containing 1% BSA. Images were obtained using a LEICA TCS SP2 set at 40x magnification, 512*512 format and analysed using ImageJ software as described in Section 2.5.4.1. (A)- (D) are representative images obtained for each group as indicated. (A) Sham untreated group. (B) Sham-treated with 87.5mg (without rat 18). (C) Diabetic untreated group. (D) Diabetic-treated with 87.5mg TETA group

Semi-quantitative analysis (Section 2.5.4.1, Table 6.19) of these images found no significant difference between sham and diabetic animals (Status), however there was found to be a significant reduction with TETA treatment on the percentage area of Collagen III staining using two-way ANOVA (Treatment P=0.0358).

Table 6.19 Percentage area of Collagen III staining

Status		Treatment	
Sham	Diabetic	Untreated	Treated
15.0±1.2%	14.3 ± 0.8%	16.5 ± 0.9%	13.1 ± 0.8%*

Values represent percentage collagen III stain ± SEM; *P<0.05

6.2.4.2 Nile Red staining for lipid content

The increase of lipid in heart tissue in the diabetic state was first described by Orth and Morgan in a study utilising both light and electron microscopy (Orth and Morgan 1962). In order to confirm these findings in our STZ-diabetic rat model and to establish the effect, if any, of TETA on cardiac lipid levels, sections were stained with Nile red and a semi quantitative analysis similar to that used for the collagen III analysis was applied (Section 2.5.4.2)

While the original unmodified files were used for analysis, the colour of the image has been inverted to create a better contrast for presentation. As described in Section 6.2.5, phospholipids make up the greatest proportion of neutral lipids in cardiac tissue, and staining of this lipid class is the most likely explanation for the high degree of background observed (Figure 6.2, all images). In support of this, no background staining was observed in the negative control.
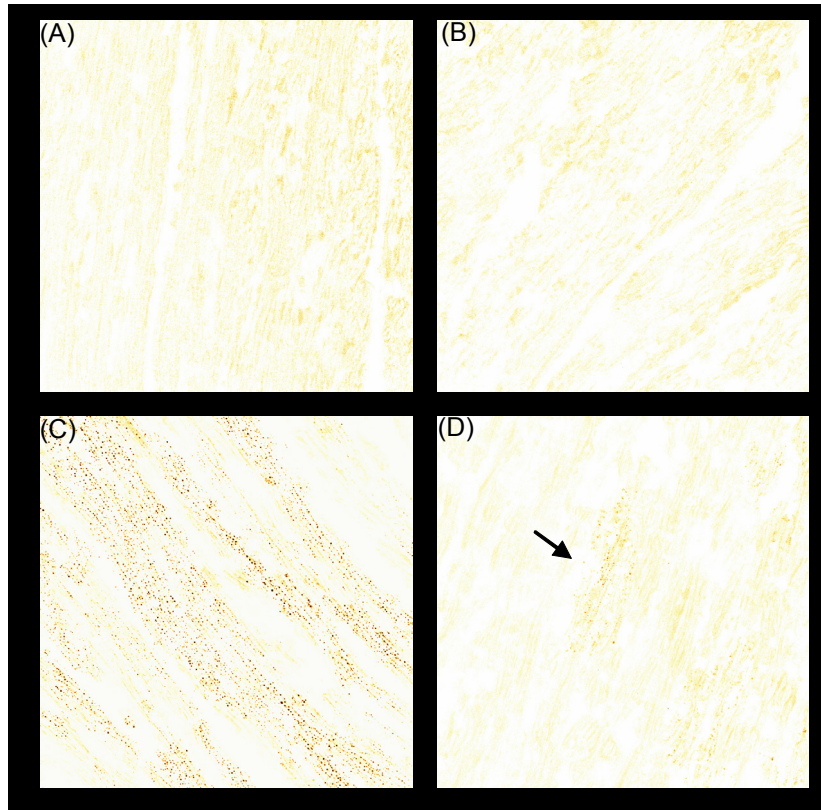
Figure 6.2 Confocal Image analysis of lipid levels in the LV

A section of tissue was cut from the base of the LV after perfusion, embedded in OCT compound and frozen in liquid N_2. Tissues were cryosectioned to 5µm using a cryo-microtome and adhered to SuperFrost slides prior to staining. Sections were stained using Nile red for lipid as described in Section 2.5.2. Images were obtained using a LEICA TCS SP2 set at 63x magnification, 1024*1024 format and analyzed using ImageJ software as described in Section 2.5.4.2. (A)-(C) are representative images obtained for each group as outlined. (A) Sham untreated. No dark spots visible. (B) Sham-treated with 87.5mg TETA. No dark spots visible. (C) Diabetic untreated. Lipid is represented by the dark spots. (D) Diabetic-treated with 87.5mg TETA group. Lipid has been highlighted using black arrow heads

In accordance with the study of Orth and Morgan (Orth and Morgan 1962), cardiac tissue from the diabetic animals in this study contained high numbers of lipid droplets when compared to the tissue from sham animals (Figure 6.2 (A) and (C)). Inspection of images taken from diabetic and diabetic-treated animals (Figure 6.2 (A) and (B)) found a decrease in the number of lipid droplets following drug treatment.

Semi-quantitative analysis (Section 2.5.4.2, two-way ANOVA) was conducted on the percentage of lipid area found in each of the four groups, similar to that used for the Collagen III percentage area. This analysis revealed that there was a significant Status*Treatment interaction (P=0.0093) for the effect of TETA on the percentage of lipid area. A significant interaction indicates that the effect of TETA is dependent on whether

the animal was in the diabetic or sham group (Status). The percentage area of lipid staining for each group is presented in Table 6.20.

Table 6.20 Percentage of Nile red (lipid) area staining

		Treatment	
		Untreated	Treated
Status	Sham	1.2 ± 0.1%	2.3 ± 0.2%
	Diabetic	4.5 ± 0.9%**	1.5 ± 0.3%*

Values represent percentage Nile red stain ± SEM
**P<.001 sham vs. diabetic; *P<0.05 diabetic untreated vs. diabetic-treated
(Bonferroni *post-hoc* test)

The percentage area of lipid staining is significantly greater in the diabetic tissue than in the sham tissue and treatment with TETA significantly decreases this staining in the diabetic-treated tissue when compared to the untreated animals. There is no significant difference between the sham-treated and untreated animals, or the sham-treated and diabetic-treated animals.

6.2.4.3 TEM scanning of muscle fibres

It is known that the onset of diabetes can evoke a perturbation in mitochondrial structure in the heart (Cooper et al. 2004; Shen et al. 2004), and improvement following TETA treatment has also been described in rat hearts (Cooper et al. 2004). Given that the focus of the thesis work centred in large part around mitochondrial responses, it was important to assess the effects of diabetes and TETA treatment on the structure of mitochondria from animals in this study.

Figure 6.3 shows TEM images captured from mitochondria in isolated interventricular septal fibres (Section 2.5.3) from animals that had received 35mg TETA per day (courtesy of Dr. A Hickey and Dr. A Turner). Images displayed are representative of the population. Inspection of the images indicated that mitochondria from diabetic tissue appeared smaller, had structural abnormalities and showed erratic placement within the tissue when compared to that from sham-treated animals (Figure 6.3(A) and (C)). Mitochondria from diabetic animals also appeared to contain small holes, which may have resulted from lipid accumulation within the tissue as described in Section 6.2.4.2. Treatment with TETA appeared to restore the shape and order of the mitochondria, such that they appear similar to those from the sham-treated animals (Figure 6.3(D)); in addition the appearance of holes within the mitochondria was diminished in TETA-treated tissue.
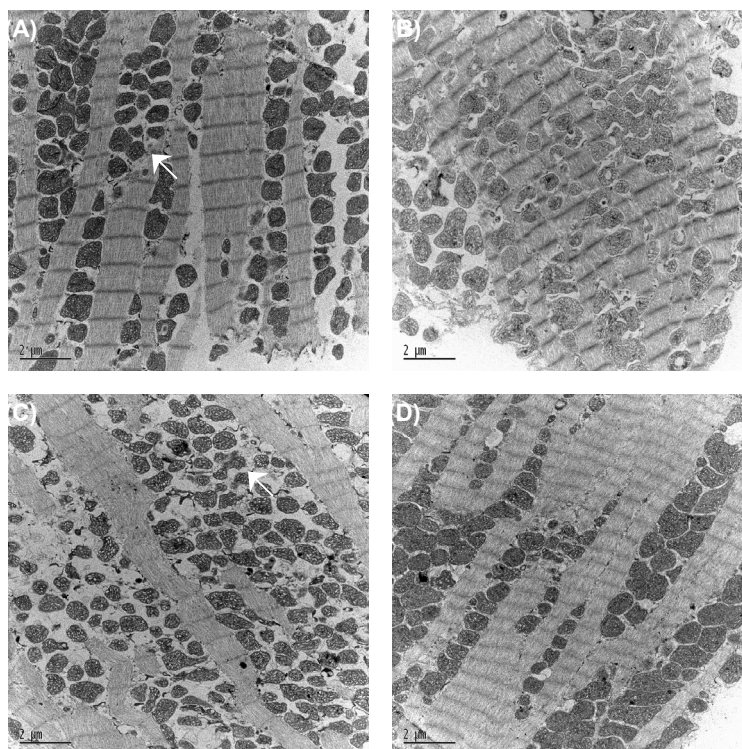
Figure 6.3 Representative TEM images of LV myocardium

Approximately 20-50 mg of endomyocardial tissue was dissected from the from the LV side (medial) of the septum and was placed into a high energy relaxing biopsy buffer (10mM EGTA-Ca$_2$EGTA buffer, free Ca^{II} concentration 0.1μM, 9.5mM MgCl$_2$, 3 mM KH$_2$PO$_4$, 20mM taurine, 5mM ATP, 15mM creatine phosphate, 49mM K$^+$ MES, 29mM imidazole-HCl, pH 7.1) and dissected into fibre bundles of 0.5 x 1mm using fine sharp forceps into fibre bundles. Several fibres were then placed into sucrose 250mM, 10mM HEPES (pH 7.1) containing 2.5% glutaraldehyde and stored at 4 ^{o}C for transmission electron microscope (TEM) ultrastructural analysis. Samples were embedded in 812 epoxy resin, sectioned to 1μm and stained with toluidine blue. Ultrathin sections were then cut to 70 nm, mounted on copper mesh grids and stained with uranyl acetate. Samples were scanned using a Philips CM12 at 120 kV. (A) Sham untreated. White arrow indicates mitochondria. (B) Sham-treated with 35mg TETA. (C) Diabetic untreated. White arrow indicates mitochondria with holes that may result from lipid accumulation. (D) Diabetic-treated with 35mg TETA group.

6.2.5 Flame-ionisation detection thin-layer chromatography (latroscan)

Results from the histological studies outlined in Section 6.2.4.2 suggested that drug treatment caused a reduction in the lipid that builds up in the LV myocardium following the onset of diabetes. There are several lipid classes present in cardiac tissue and in order to determine which class or classes where reduced by drug treatment, quantitative assessment of cardiac lipid was performed using latroscan technology. latroscan technology has been used previously to study levels of different lipid classes in an animal model of cardiac hypertrophy (Saburi et al. 2003; Takahashi et al. 2005). A comparative analysis of latroscan technology with the more commonly used phosphorous and gas

chromatographic techniques gave comparable results between the three methods and indicated that fast, accurate measurement of tissue lipid content was achievable using the Iatroscan (Kramer et al. 1985).

Analysis was conducted as outlined in Section 2.9 and confirmed the presence of four major lipid classes present in cardiac tissue: TG, FFA, cholesterol and phospholipids. This experiment contained groups with uneven numbers and so after consultation with the School of Biological Sciences statistician it was decided that a mixed model analysis would be most appropriate (Section 2.12.4.1). This analytical approach yields defined covariate factors that reduce the overall experimental variation. This is important given that the data within the diabetic group appeared to vary considerably. A summary of the results from the Iatroscan analysis are presented in Table 6.21 (further information regarding the mixed model analysis of the Iatroscan TG data can be found in Appendix 2).

Table 6.21 Lipid classes determined by Iatroscan analysis

Lipid Class	Status		Treatment	
	Sham	Diabetic	Untreated	Treated
TG	0.2 ± 0.1	1.2 ± 0.2***	1.0 ± 0.2	0.8 ± 0.2*
FFA	0.2 ± 0.1	0.09 ± 0.02	0.1 ± 0.03	0.1 ± 0.02
Cholesterol	0.7 ± 0.06	0.7 ± 0.05	0.7 ± 0.1	0.7 ± 0.04
Phospholipid	19.0 ± 0.9	19 ± 1.0	19 ± 1.0	19 ± 1.4

All values presented are µg lipid/mg wet cardiac tissue weight ± SEM. Based on the exclusion criteria defined in Appendix 2, four diabetic animals were excluded from the analysis based on body weight (Animal ID 8, 42, 145 and 168). ***$P<.0001$, *$P<0.05$

Analysis revealed that, of the four lipid classes measured, only TG levels were significantly increased in the diabetic tissue (Status) after sixteen weeks of diabetes ($P<.0001$). Increased TG levels in heart tissue as a result of diabetes has been reported previously in human patients (Alavaikko et al. 1973), the STZ-animal model (Douillet et al. 1998; Nielsen et al. 2002) and a type-2 diabetic animal model (Christoffersen et al. 2003). This indicates that one of the effects of uncontrolled diabetes on the heart is an accumulation of TG in the tissue.

Animals treated with TETA were found to have significantly lower tissue TG levels ($P=0.0179$). This indicates that treatment of animals with TETA results in reduced cardiac lipid levels and is consistent with the histological data presented in Section 6.2.4.2. Interestingly, the Status*Treatment interaction was not significant in this analysis ($P=0.3002$) signifying that the drug effect was not dependent on Status. A high degree of variability was found within the TG and FFA values from the diabetic group (as evidenced by their high SEM values). Future studies using this technology may benefit from having much larger group sizes than that used here.

6.2.6   Mitochondrial functional analysis

The results described above suggest that treatment of animals with TETA-disuccinate evoked changes in cardiac lipid metabolism.   As stated in Section 6.1, previous studies in our group indicate that there is an improvement in LV mitochondrial respiration following TETA treatment of diabetic animals (Dr. A Hickey, personnel communication) and an improvement in FAO enzyme protein levels (Jullig et al. 2007). Alterations in the lipid content of the heart provided further evidence for a change in the activity levels of enzymes involved in energy metabolism. It is widely accepted that the mitochondrion is the primary site of energy metabolism in the heart and also that lipid is often exclusively associated with mitochondria histologically (Orth and Morgan 1962); for these reasons, an analysis of specific mitochondrial enzymes within both crude homogenate and isolated mitochondria was performed. Tissue from the LV side of the interventricular septum was used in this instance as the remaining LV tissue was pre-allocated for use in RNA collection (microarray and RT-qPCR) and histology. The mitochondrial enzymes studied are outlined below with a brief indication of normal function and the data resulting from this study.

6.2.6.1 Citrate synthase

Citrate synthase (CS) is an important generator of flux in the TCA cycle (Newsholme and Start 1973), and is abundant in the mitochondrial matrix. It is routinely used as an indicator of mitochondrial content in tissue. Results from this study showed an increase in crude-homogenate CS activity in diabetic LV compared to sham LV (Figure 6.4(A), P=0.044), which suggests increases in mitochondrial number in diabetic septal homogenates. Additionally, CS activity was increased in both sham and diabetic septal following TETA treatment (Figure 6.4(A), two-way ANOVA P<.0001).

Increases in citrate synthase activity can be used as an indicator of successful mitochondrial purification from the crude homogenate. CS activity increased approximately four-fold in all groups after purification, providing evidence that the process was successful. Interestingly, the CS activity per mg of mitochondrial protein (Figure 6.4(B)) decreased in the diabetic animals relative to the sham animals (P=0.006). Following TETA treatment mitochondrial CS activity was significantly increased in the diabetic animals (P<0.001, Bonferroni *post-hoc* test). This observed increase in CS activity indicates increased amounts of CS per individual mitochondria and suggests enhanced TCA flux capacities within diabetic mitochondria following treatment with a copper chelator.
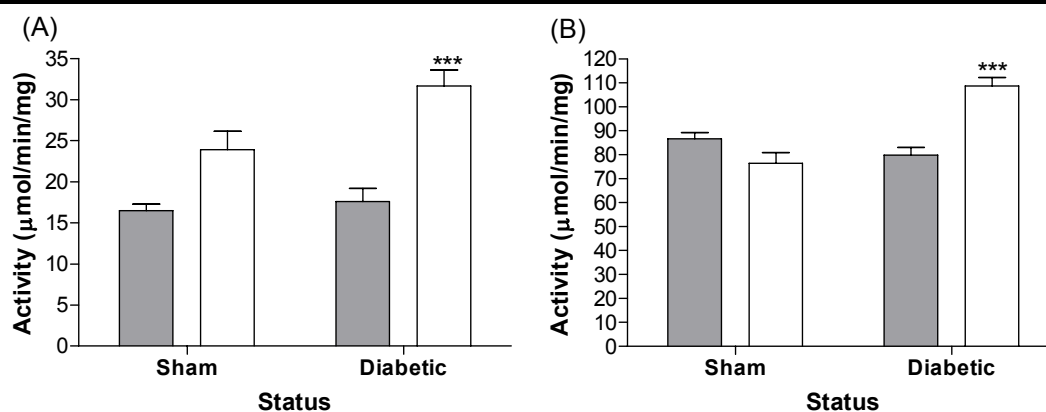
Figure 6.4 Citrate synthase

Following heart perfusion, the interventricular septum was cut into small pieces in ice-cold mitochondrial isolation buffer (MIB; 225mM D-mannitol; 75mM sucrose; 20mM HEPES; 1.0mM EGTA, 0.5mg/ml BSA (fraction V, IgG free, free fatty acid-poor); pH 7.4 at 4 ℃). The septum was homogenised (Ultra-Turrax T25) and a portion of the homogenate was collected and stored at -80℃. Mitochondria were isolated as described in Section 2.10.1. Mitochondrial pellets were stored at -80 ℃. Citrate synthase activity was determined as described in Section 2.10.2.1. Untreated group (■, sham or diabetic), Treated group (□ sham or diabetic). Values are means ± SEM (sham n=4, sham + 87.5mg n=5, diabetic n=6, diabetic + 87.5mg n=9). Statistical significance was analysed by two-way ANOVA and inter-treatment difference was assessed using Bonferroni *post-hoc* tests.

(A) Citrate synthase activity in septum homogenate fraction. Two-way ANOVA results, Dose $P<0.0001$, Status $P=0.0442$, Status*Dose $P=0.1247$. Bonferroni *post-hoc* tests ***$P<0.001$

(B) Citrate synthase activity in isolated septal mitochondria. Two-way ANOVA results, Dose $P=0.0427$, Status $P=0.0063$, Status*Dose $P<0.0001$. Bonferroni post tests ***$P<0.001$

The enzyme activity data for CPT, HOAD and IDH-NADP+ presented below represents results determined in isolated mitochondria only.

6.2.6.2 CPT

As described in Chapter Four, FA oxidation in the mitochondria is limited by the transport of FA moieties into the organelle through the specific shuttle CPT I (Pande 1975; Saggerson and Carpenter 1981; Saggerson 1982). The two isoforms of CPT I, CPT Iα and CPT Iβ are both expressed in the rat heart. Gene expression analysis (Section 6.2.2) showed that mRNA from both CPT isoforms was increased in cardiac tissue from diabetic animals. Functional data presented here indicate that CPT mRNA transcript concentration mirrored the activity of CPT (Figure 6.5). Transcript number and enzyme activity were both increased in the diabetic state and interestingly, treatment with TETA evoked further increases in CPT activity in this group (two-way ANOVA Bonferroni *post-hoc* test $P<0.001$). This increased activity may indicate an increase in FA flux into the mitochondria and potentially provides an explanation for the observed decrease in triglyceride levels in the heart (Section 6.2.4.2 and 6.2.5).
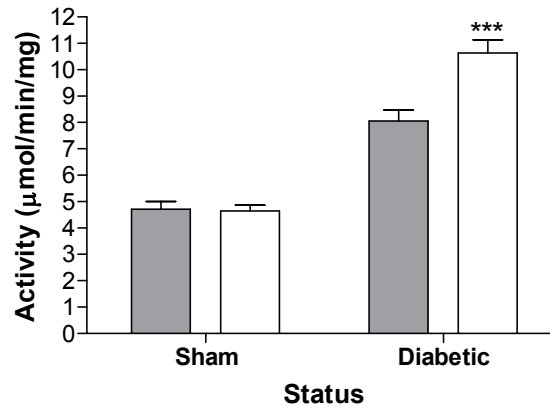
Figure 6.5 CPT activity in isolated mitochondria

Following heart perfusion, the interventricular septum was cut into small pieces in ice-cold mitochondrial isolation buffer (MIB; 225mM D-mannitol; 75mM sucrose; 20mM HEPES; 1.0mM EGTA, 0.5mg/ml BSA (fraction V, IgG free, free fatty acid-poor); pH 7.4 at 4 °C). Mitochondria were isolated as described in Section 2.10.1. Mitochondrial pellets were stored at -80°C. CPT activity was determined as described in Section 2.10.2.2. Untreated group (■, sham or diabetic), Treated group (□ sham or diabetic). Values are means ± SEM (sham n=4, sham + 87.5mg n=5, diabetic n=10, diabetic + 87.5mg n=9). Statistical significance was analysed by two-way ANOVA and inter-treatment difference was assessed using Bonferroni post-tests. Two-way ANOVA results, Dose P=0.0178, Status P<0.0001, Status*Dose P=0.0131. Bonferroni *post-hoc* tests, ***P<.0001.

6.2.6.3 HOAD

HOAD reversibly catalyzes the oxidation of a 3-hydroxyacyl CoA to 3-ketoacyl CoA in the presence of NAD (Uchida et al. 1992). It forms part of the tri-functional protein in mitochondria that oxidises fatty acids to generate the acyl-CoA that is utilised in the TCA cycle (Uchida et al. 1992). As with CPT, both HOAD mRNA transcript (Section 6.2.2) and enzyme activity levels (Figure 6.6) were elevated in the diabetic group compared to the sham group. TETA treatment led to a substantial increase in HOAD activity in the diabetic-treated group (P<0.001), mirroring the results for CPT. These data provide additional support for a role of TETA in increases in β-oxidation and hence FA clearance from diabetic LV.

Figure 6.6 HOAD activity in isolated mitochondria

Following heart perfusion, the interventricular septum was cut into small pieces in ice-cold mitochondrial isolation buffer (MIB; 225mM D-mannitol; 75mM sucrose; 20mM HEPES; 1.0mM EGTA, 0.5mg/ml BSA (fraction V, IgG free, free fatty acid-poor); pH 7.4 at 4 ºC). Mitochondria were isolated as described in Section 2.10.1. Mitochondrial pellets were stored at -80 ºC. HOAD activity was determined as described in Section 2.10.2.3. Untreated group (■, sham or diabetic), Treated group (☐ sham or diabetic). Values are means ± SEM (sham n=4, sham + 87.5mg n=5, diabetic n=10, diabetic + 87.5mg n=9). Statistical significance was analysed by two-way ANOVA and inter-treatment difference was assessed using Bonferroni *post-hoc* tests. Two-way ANOVA results, Dose P=0.0002, Status P<0.0001, Status*Dose P=0.0369. Bonferroni *post-hoc* tests, ***P<0.001.

6.2.6.4 IDH-NADP+

IDH-NADP+ catalyzes the first NADPH-yielding reaction of the TCA cycle, making it an important regulator of the cycle (Newsholme and Start 1973) and also of mitochondrial redox state. Figure 6.7 illustrates changes in IDH activity as a result of diabetes and of treatment with TETA.
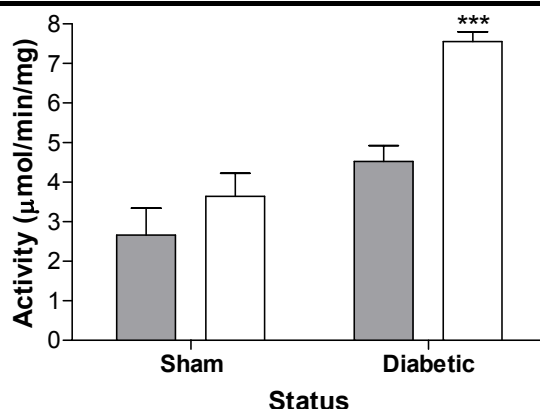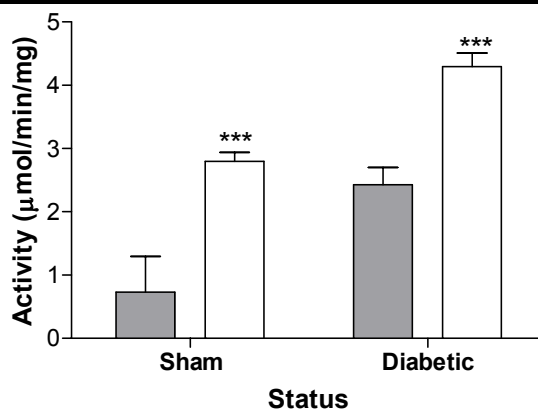
Figure 6.7 IDH activity in isolated mitochondria

Following heart perfusion, the interventricular septum was cut into small pieces in ice-cold mitochondrial isolation buffer (MIB; 225mM D-mannitol; 75mM sucrose; 20mM HEPES; 1.0mM EGTA, 0.5mg/ml BSA (fraction V, IgG free, free fatty acid-poor); pH 7.4 at 4 °C). Mitochondria were isolated as described in Section 2.10.1. Mitochondrial pellets were stored at -80 °C. IDH activity was determined as described in Section 2.10.2.4. Untreated group (■, sham or diabetic), Treated group (□ sham or diabetic). Values are means ± SEM (sham n=4, sham + 87.5mg n=5, diabetic n=10, diabetic + 87.5mg n=9). Statistical significance was analysed by two-way ANOVA and inter-treatment difference was assessed using Bonferroni *post-hoc* tests. Two-way ANOVA results, Dose $P<0.0001$, Status $P<0.0001$, Status*Dose $P=0.7476$. Bonferroni *post-hoc* tests **$P<0.01$, ***$P<0.001$

IDH-NADP+ activities were also increased in diabetic LV mitochondria; however, unlike CS, CPT and HOAD, TETA treatment significantly elevated IDH-NADP+ activity in both the diabetic and sham groups.

Taken together, the enzyme functional data indicate that diabetes alters the metabolic state of the heart. This is observed through increases in CS, CPT and HOAD activities which suggest increases in β-oxidation. Additionally, TETA treatment of diabetic animals caused further increase in activities of these enzymes in septal mitochondria, and thus provides an explanation, at least in part, for the observed drug-induced decrease in cardiac TG levels.

6.3 Discussion

In this chapter an analysis of changes occurring at the molecular level as a result of TETA treatment (87.5mg/day), in both sham and diabetic animals, for eight weeks is reported.

6.3.1 Gene expression analysis

Changes in gene expression in LV heart tissue as a result of STZ-induced diabetes in the current study were found to be consistent with the results described in Chapter Four. However, there were a few notable differences between studies, such as the finding that 1205 genes showed significant differential expression in this study compared to 1614 in

the pilot study (Chapter Four) and also that the expression of PDK4 was not significantly altered in this study. These differences can most likely be attributed to two main causes. The first is that animals in the pilot study were given a dose of 60mg/kg of STZ, while in the second study animals were given a dose of 55mg/kg. This ~10% reduction in STZ dose was applied to decrease the non-pancreatic effects of the STZ and maintain acceptable survival of the diabetic study animals. While it is possible that a lower dose of STZ could potentially result in fewer gene changes overall the principle driver for diabetes severity, blood glucose levels, were similar in both studies (26.6 ± 2.4mmol/l in this study compared to 27.7 ± 1.4 mmol/l in the pilot study), suggesting that the severity of diabetes was equivalent. A second and more likely explanation is that in the current study a total of only five microarrays were used per group, while in the results presented in Chapter Four; seven arrays were used per group. These extra arrays would have improved the power of the experiment and meant that even changes with a high degree of variation could reach significance.

In a similar manner to the experiments performed in Chapter Four, RT-qPCR was used to validate the results observed in the microarray experiment. Using this method, we were able to confirm the changes in gene expression evoked by induction of diabetes and additionally the surprising lack of change in gene expression that resulted from TETA treatment in eleven selected *a priori* genes. The lack of significant gene changes observed following treatment was unexpected due to the number of physiological effects of the drug observed in Chapter Five. However as stated by Mootha *et al.,* "When alterations in gene expression are modest, the large number of genes tested, high variability between individuals and limited sample size often makes it difficult to distinguish true difference from noise" (Mootha et al. 2003). New analysis algorithms are currently being designed that aim to overcome this problem by looking at gene changes at the pathway level or at co-regulated gene-sets rather than individual genes (Doniger et al. 2003; Draghici et al. 2003; Mootha et al. 2003). Two recent publications from the Broad Institute (Mootha et al. 2003; Subramanian et al. 2005) described an interesting new analytical technique for analysing microarray data using *a priori* defined gene-sets, such as pathways, for association with disease phenotypes (GSEA).

Diabetes mellitus is a unique systemic disease as it has such global variation in its effects on target organs (Mootha et al. 2003). There were a large number of fundamental gene changes associated with the diabetic state (in particular hyperglycaemia), creating a background level of variable gene expression changes that may decrease the ability to identify smaller alterations that have occurred with TETA treatment. In the current study the blood glucose of the animals was not reduced by treatment with TETA-disuccinate (Section 5.2.2.1, Table 6.1) and thus many of the changes associated with the diabetic state driven by high glucose and low insulin were not diminished. As a result of this issue

and taking into account the above statement by Mootha *et al.,* (Mootha et al. 2003), it was decided that GSEA analysis may allow us to identify changes associated with treatment that were not able to be identified using the univariate approach employed previously. Application of this more powerful analytical method (using "Phenotype permutation") produced fewer gene-sets than were expected for the diabetic vs. sham comparison, again almost certainly due to the underlying small sample size and variable phenotype of the STZ rats. Those gene-sets that were identified were compatible with previous results.

The use of GSEA software found three gene-sets that were significantly correlated with the diabetic group when comparing diabetic-treated against the untreated animals (Table 6.11). The first of these was the gene-set for Lamellipodium biogenesis, which was found to be significantly correlated with the diabetic group relative to the diabetic-treated group. The lamellipodia is a short thin band (<5% of the total cell length) at the extreme cell anterior of locomoting cells, such as fibroblasts and smooth muscle cells and participates in the first stage of cell migration (Abercrombie 1980; Cramer et al. 1997; Small et al. 2002; Pichon et al. 2004). Remodelling of the heart after exposure to hyperglycaemia is characterised by increased collagen deposition, increased β1-integrin levels (indicating increased myocyte movement) and damaged f-actin (Cooper et al. 2004). Remodelling of the cell configuration within the heart and increased collagen levels may lead to increased movement of cardiac fibroblasts and therefore increased lamellipodium biogenesis in the diabetic animals. Further evidence for this proposed phenomenon comes from studies indicating increased cardiac fibroblast migration when exposed to increasing collagen levels (Loftis et al. 2003). Improvement in heart structure after TETA treatment (described previously (Cooper et al. 2004)) may reduce the need for fibroblast movement and therefore reduce the level of lamellipodium biogenesis, resulting in a higher correlation of the diabetic group to this gene-set when compared to the diabetic-treated animals.

The second gene-set identified was that containing genes associated with the spliceosome. The spliceosome catalyses a two-step transesterification reaction required to remove introns and ligate exons (for reviews see (Konarska 1998; Will and Luhrmann 2001)). Shomron *et al.,* (Shomron et al. 2002) describe specific inhibition of the second step in mRNA splicing after addition of either a copper or zinc chelator to nuclear extracts of HeLa cells. Inhibition was reversed after addition of exogenous zinc to the nuclear extract in a dose dependent manner, but not addition of copper. Authors suggest that chelation of zinc removes it from the active site of a metalloprotein(s) involved in the second step of splicing thereby inhibiting this process (Shomron et al. 2002). Inhibition of splicing by a copper chelator was an unexpected finding by Shomron *et al.,* and as inhibition could not be reversed by addition of exogenous copper, authors were at a loss to explain the result (Shomron et al. 2002). They hypothesised that chelation of copper

may deplete zinc levels through binding of zinc to copper-depleted metalloproteins (Shomron et al. 2002). Data presented in Chapter Five indicated that treatment of diabetic animals with TETA-disuccinate was able to increase the levels of both urinary zinc and urinary copper in a dose-dependent manner (Figure 5.18 and 5.19 respectively). It could be hypothesised, that a reduction in zinc and copper availability in the treated-diabetic animals may result in inhibition of the second stage of splicing, changing the transcript levels of spliceosome components.

The ability of the GSEA algorithm to resolve mRNA transcript changes in the diabetic vs. diabetic-treated comparison where the original univariate analysis could not indicates the power of using this kind of method when analysing gene expression data. It also implies that there are problems in using non-pathway based univariate analysis when analysing a microarray data set as complex as this one. A more in-depth assessment of these problems are presented in Chapter Seven.

6.3.2 ECM structure in the LV

Fibrosis and subsequent alterations to the structure of the LV wall have been linked to the pathogenesis of diabetic cardiomyopathy (Fang et al. 2004). As described in Section 1.2.2, increased levels of ECM proteins are known to cause stiffening of the LV wall (Fang et al. 2004). In light of this, an analysis of collagen III staining was conducted on LV tissue from animals in this study (Figure 6.1). No increase in staining was observed in this tissue, indicating that in this model the protein levels of collagen III in the ECM did not increase as a result of diabetes. This is contrary to previously published reports which describe increases in both collagen I and III staining in diabetic animals (Candido et al. 2003; Cooper et al. 2004). A possible explanation for this discrepancy is that the technique of assessment of collagen percentage area is a semi-quantitative measure and as such is subject to a high level of user bias, making comparison between studies difficult. Another explanation may be that the model of induced diabetes described here was not as severe as that seen in the previous studies (as indicated in Section 6.3.1) resulting in less tissue fibrosis. Alternatively, as hypothesized in Chapter Four, the pathology may not arise from increases in collagen levels *per se*, but instead from increases in collagen cross-linking as a result of AGE modification. This could lead to decreased collagen breakdown and increased stiffness in the LV wall.

Visual analysis of the tissue showed that the cardiac myocytes were less well ordered in the diabetic animals and that the surrounding collagen is in a state of disarray (Figure 6.1). This result indicates that the diabetic state had some effect on the overall organisation of collagen III if not on the absolute amount of protein present. Semi-quantitative analysis revealed a significant decrease in the level of collagen III staining

from 16.5± 0.9% in the untreated animals to 13.1 ± 0.8% in the treated animals which was consistent with the results presented by Cooper *et al.,* (Cooper et al. 2004) and with the transcriptomic changes in lamellipodium biogenesis described in Section 6.2.2.3. This result indicated that TETA is affecting collagen III protein levels in the heart, although not at the level of gene expression (Table 6.17), and provides molecular evidence for an effect of TETA on the heart in this study. Alternative methods to assess changes in the ECM would be the analysis of hydroxyproline levels as a quantitative measure of collagen content or the analysis of collagen cross-linking itself. The use of these techniques may determine if it is the amount of absolute collagen or the amount of cross-linked collagen that is altered by TETA treatment.

6.3.3 Changes in fuel metabolism

In this study, induction of diabetes resulted in an increase in lipid droplets in LV wall tissue as visualised by the neutral lipid stain, Nile red (Figure 6.2). This is in concordance with studies by Orth and Morgan (Orth and Morgan 1962) that also showed an increase in the number and size of lipid droplets in the LV tissue and determined that the lipid was almost exclusively associated with the mitochondria. In the study described here, results from the histological study were confirmed by a more detailed analysis utilising flame-ionisation detection thin-layer chromatography. Use of this technique showed specifically that triglyceride levels were increased in the LV wall in the diabetic state. Taken together, these findings further strengthen the hypothesis outlined in Chapter Four and by others (Stanley et al. 1997; Rodrigues et al. 1998; Taegtmeyer et al. 2002), that increases in heart lipid contribute to the pathogenesis of diabetic cardiomyopathy.

Nile red staining indicated that treatment with TETA resulted in a significant decrease in lipid in the LV wall tissue of diabetic animals. Further analysis of the tissue by Iatroscan showed that this decrease in lipid evoked by TETA-disuccinate treatment was limited to the triglyceride pool (Table 6.21).

As discussed above the physiological changes as a result of the hyperglycaemia and hyperlipidemia induced by diabetes cover a wide spectrum of severity that can lead to increases in within-group variation ((Mootha et al. 2003), Section 6.2.2.3). Analysis of TG levels (Appendix 2) indicates that in the diabetic group, higher than average body weight tends to result in lower tissue lipid levels and this can lead to increased variation within this group. Careful study design with large group numbers and specified inclusion/exclusion criteria would reduce this variation in future studies.

He *et al.* (He et al. 2004), presented data that shows a link between the change in lipid status of skeletal muscle of type-2 diabetic patients (in this case a reduction in lipid droplet size and increased dispersion within the tissue) and increased mitochondrial

oxidative capacity. Using histochemical staining these researchers showed a negative correlation between mitochondrial number and lipid droplet size in the skeletal muscle of type 2 diabetic patients undergoing weight loss and exercise intervention (He et al. 2004). They hypothesised that decreased tissue lipid dispersion equated to an increased capacity of skeletal muscle to oxidise the available lipids. In light of this result, together with the finding that lipid droplets in the heart are almost exclusively associated with the mitochondria (Orth and Morgan 1962), and our observation of a decrease in tissue lipids as a result of TETA treatment, it could be hypothesised that a change in lipid status of the heart tissue as a result of treatment with TETA is the result of a change in mitochondrial oxidative capacity.

In order to more fully consider this hypothesis, analysis of the function of a selection of enzymes associated with the mitochondria and fuel metabolism were assessed as presented in Section 6.2.6. As described previously, the activity of hepatic CPT (Cook and Gamble 1987), HOAD (Glatz et al. 1994) and IDH-NADP+ (Cuestas and Dixit 1973) were altered as a result of diabetes indicating an increase in the uptake and metabolism of lipid.

There was a clear increase in the mRNA transcript levels of CPT and HOAD (1.9-fold and 1.65-fold respectively, from microarray data (Table 6.5)) when comparing diabetic to normal LV. These values closely match the increases in activity for both enzymes of ~1.7-fold in the mitochondria (Figure 6.5 and 6.6 respectively). Interestingly, the function of IDH-NADP+ was increased in diabetes (3.2-fold) however, results from the microarray studies performed in Chapter Four and those reported here, did not find a change in IDH-NADP+ gene expression (fold-change=0.85, P=0.21). This finding is likely to be due to the fact that complex mechanisms exist to regulate the translation of a gene into a functional enzyme and so changes in gene expression (or lack thereof) do not always correlate with changes in function levels.

In the diabetic heart, CS activity (marker of mitochondrial number) was increased in crude homogenates prepared from diabetic tissue when compared to sham, suggesting an increase in the number of mitochondria.

Taken together, these data indicate an increase in the mitochondrial content in the hearts of the diabetic animals and an increase in both the amount of gene product and functional enzyme required for lipid catabolism in the diabetic heart. This may be to facilitate an increased dependency by the heart on fatty acid metabolism following the loss of insulin mediated glucose metabolism.

Treatment of diabetic animals with TETA resulted in a further increase in the activity of CPT (1.3-fold) and HOAD (1.7-fold) and in the activity of IDH-NADP+ in both diabetic and sham animals (1.8- and 3.8-fold respectively) relative to untreated animals, despite no observed changes in gene expression changes following TETA treatment.

Increases in all three of these enzymes in the diabetic-treated group suggest an increased capacity of the diabetic mitochondria to process the excess myocardial lipid in diabetic LV.

Data presented in this study suggest that TETA may act to stabilise mitochondria thus leading to the observed increases in activity of CS, CPT, HOAD and IDH-NADP+. After purification of mitochondria from the crude homogenate, CS activity within the diabetic hearts mitochondria actually decreased slightly relative to sham tissue. This may be due either to an increase in the fragility of diabetic mitochondria (selective isolation) or that diabetic cardiac mitochondria are structurally and functionally damaged. In support of the latter, structural damage was observed in electron micrographs of diabetic cardiac mitochondria shown in this study and elsewhere (Figure 6.3, (Cooper et al. 2004; Shen et al. 2004)). The micrographs clearly illustrate structural differences between sham and diabetic mitochondria *in situ* (Figure 6.3 (A) and (C)). TETA treatment however, appears to improve mitochondrial structure ((Cooper et al. 2004) and Figure 6.3(D)) and increase levels of CS in isolated mitochondria (Figure 6.4(B)). Taken together, results from TEM and the observed increase in CS activity suggests that the additional increases in enzyme activity following TETA treatment may be a result of improved stability of protein or reduced protein turnover. The increased potential of mitochondria from treated diabetic LV to both oxidise lipids (indicated by increased activity of CPT, HOAD and reduced lipid) and increase TCA metabolism (CS, IDH-NADP+) without concomitant increases in the concentration of the various gene transcripts may also arise due to increased number of mitochondria and/or increased efficiency or stability of existing mitochondria (or the enzymes within them).

6.4 Conclusions

Analysis of the changes in gene expression, following both the induction of diabetes and treatment of the disease with TETA, using three different methods (classic microarray analysis, GSEA and RT-qPCR) confirmed the changes observed in Chapter Four. These results show an induction of diabetes evoked specific changes in gene expression and provide support for the hypothesis that TETA, at the dose used in this study, did not alter levels of expected gene transcripts in the heart. Changes in gene-sets were observed when the pathway based GSEA algorithm was applied to the microarray data and these unexpected genes have been ear-marked for further investigation. Although there was no difference observed in the mRNA transcript levels of genes associated with fuel metabolism after treatment, there were several lines of evidence that suggested TETA is altering this aspect of heart physiology: changes in histological and measured tissue TGs, improved mitochondrial appearance and increased activity of at least four enzymes known to be crucial in mitochondrial fuel metabolism. In summary, increased flux of excess

diabetic-associated lipid through the mitochondria coupled with a decrease in cardiac heart collagen (Section 6.2.4.1 and Cooper *et al.,* (Cooper et al. 2004)) may provide a possible explanation for the TETA-induced increase in heart function described by other members of our group (Cooper *et al.,* (Cooper et al. 2004) and Gong *et al.,* (Gong et al. 2006)).

Chapter 7 Final Discussion and Conclusions

7.1 Thesis findings

7.1.1 Primary aim of Thesis

The primary aims of this thesis were (i) to identify changes in expression of genes in the left ventricular wall of the heart after sixteen weeks of diabetes, (ii) to further elucidate the mechanism behind improved cardiac function occurring in the LV of the heart as a result of treatment with TETA-disuccinate by looking at the molecular level using biochemical assays and molecular techniques and at the level of gene expression using microarray technology and iv) to investigate whether the observation that TETA is metabolised differently in diabetic and normal patients (Lu et al. 2007) is concordant with the ability of STZ-diabetic and sham rats to metabolise TETA.

7.1.2 Summary of main findings

7.1.2.1 Pilot study to assess suitability of three commercially available microarray platforms for assessment of changes in gene expression

The work described in Chapter Three was important to this study for two reasons. Firstly, it allowed the comparison of four different kinds of microarray platform in order to decide which gave the best results in relation to the overall aim of this study. Secondly, this was the first time microarray technology had been used in our laboratory and it was important to establish a protocol for the use of this technology and analysis of data that would provide the best results possible.

With regard to this particular study, the results provided a valuable insight into the ability of each of the systems to perform in untrained hands. Affymetrix was the only system which provided consistently good results for an inexperienced operator. It became clear through the course of the study that one of the most critical factors to consider when choosing a microarray platform is the protocol for washing and staining of the slides provided by the manufacturer. This part of the experimental procedure impacts greatly on the quality of the results and can also be the cause of greatest user variation. Through

their automated washing and staining protocol, Affymetrix has removed the need for user intervention and therefore heavily reduced user variation. Although the other two systems assessed would eventually provide data of a similar standard to that of Affymetrix, the time and associated costs required would negate the reduced initial outlay on the other systems. The results presented in Chapter Three suggest that by reducing variation, it is possible not only to increase the robustness of the data but also to reduce the overall cost of experiments, by lowering the number of arrays required to obtain statistically significant results.

Correlation between different systems is an important factor in the sharing of data from microarray analyses between different research groups and is a topic that has been well reported on (Mecham et al. 2004; Park et al. 2004; Yauk et al. 2004; Larkin et al. 2005). Our initial analyses found that there was a very poor correlation between results from the Agilent and Affymetrix systems and that the number of common genes represented on each set of arrays was minimal when compared to the number of genes present on the microarrays from each system individually. This low number of common genes and variations in nomenclature makes comparison of the two systems difficult. Comparison studies such as that by Mecham *et al*., (Mecham et al. 2004) discussed the idea that sequence matching between two systems was necessary in order to obtain good correlation. In the current study variation within systems played a major role in determining correlation between systems. Due, at least in part, to the lack of operator experience in using microarrays, a number of mistakes occurred which increased the variation within the data. As a result, an improvement in correlation as a result of sequence matching was not obtained; however, there was a much improved correlation between Affymetrix and Agilent when the data set was reduced to genes with a significant ($P<0.05$) changes in gene expression (Figure 3.10). This indicates that only results of statistical significance (indicating low variability) should be compared in order to ensure the greatest potential for correlation between systems is met.

7.1.2.2 Assessment of differences in the transcriptome between STZ-diabetic and sham LV heart tissue at sixteen weeks

This chapter described the pilot study set up to investigate transcriptomic changes correlated with diabetic cardiomyopathy in the LV as a result of sixteen weeks of STZ-induced diabetes. These data represented a baseline from which later studies could be measured. The work performed in this chapter also allowed familiarisation with Affymetrix technology and the processes involved in data management and analysis as this technology was new to our laboratory.

Analysis of the physiological characteristics of this model (Figure 4.1, Table 4.1) indicated that the STZ-treated animals suffered from all the hallmark indicators of a mild to severe diabetes (Alberti and Zimmet 1998), including attenuated weight gain, polydipsia, hyperphagia, hyperglycaemia and hyperlipidaemia.

Genes corresponding to proteins expressed in mitochondria were found to account for a disproportionate number of those whose expression was significantly modified in DCM as identified through the GO Cellular Component classification system (Figure 4.3). This is consistent with the hypothesis that mitochondria act as key targets of the pathogenic processes that cause diabetic heart disease. Closer investigation of genes involved in fuel metabolism (specifically glycolysis and fatty acid oxidation) indicated that the majority of genes involved in glucose metabolism were down-regulated in the heart (53% of the total number of relevant genes identified) while the majority of genes involved in fatty acid metabolism were up-regulated in the heart (76% of the total number of relevant genes identified). The pattern of changes in gene expression indicated that overall, the potential of the heart to actively take up glucose (decreased GLUT1 and GLUT 4) and process it for use as a fuel source (PDH complex shifted towards inactivity through changes in regulatory enzymes PDK4 and PDP2) was decreased. Conversely, mRNAs corresponding to genes whose products mediate the ability of the heart and mitochondria to take up lipid (increased CD36 and CPT isoforms respectively) and process it into acyl-CoA (increased trifunctional β-oxidation complex enzymes) for use as an energy source, were commonly increased. The ability to observe and understand this pattern of changes in gene expression was made possible by the global nature of microarray technology.

A general hypothesis for the complications observed in diabetes has been proposed by Brownlee *et al.,* (Brownlee 2001). That work revealed perturbations in four main pathways leading to the complications associated with diabetes in cultured endothelial cells, all of which might be tied together with one underlying hyperglycaemia-induced process (Brownlee 2001). It was of interest to see if a correlation could be found between the work presented by Brownlee *et al.,* and the changes in gene expression in the diabetic rat heart observed in the current study. Overall, it appears that our study did provide some corroborating evidence for this hypothesis despite the difference in model systems used (Chapter Four uses an animal model compared to Brownlee *et al.,* who utilised an endothelial cell model (Brownlee 2001)). Of the four pathways highlighted, the current study found changes in gene expression in glutathione metabolism (Pathway One), PKC activation and subsequent activation of downstream effectors such as endothelin (increased endothelin receptor expression, Pathway Two) and a change in PAI-1, known to be altered as a result of changes in the hexosamine pathway (Pathway Four). The underlying hyperglycaemia-induced process, also known as the common

element, has been described previously (Du, X. et al. 2003). Du *et al.,* presented work indicating that it was PARP mediated inactivation of GAPDH through modification with ADP-ribose polymers that led to changes in the original four pathways. Activation of PARP was thought to be a result of increased ROS induced by hyperglycaemia (Du, X. et al. 2003). Concurrent with this work we find an increase in the gene expression of a TCDD-inducible PARP which could subsequently result in inactivation of GAPDH and lead to the aforementioned changes in genes involved in the four main pathways.

One difference between the work presented in Chapter Four and the work of Brownlee *et al.,* is that in endothelial cells, glucose uptake is not actively regulated, leading to a massive influx of glucose under hyperglycaemic conditions. The microarray data presented in Chapter Four indicates that in the heart, glucose uptake is likely to be substantively decreased. This discrepancy could be explained by the observed changes in genes associated with increased fatty acid uptake and oxidation within the mitochondria. This process would however, lead to the same endpoint as hyperglycaemia in the endothelial cell, namely accumulation of acetyl-CoA (Brownlee 2005).

In this model of diabetes we hypothesise that it is in fact increased fatty acid metabolism and dysfunctional regulation of mitochondrial β-oxidation that lead to oxidative stress damage in the heart, rather than glucose metabolism as is perhaps more widely believed. This hypothesis is strengthened by the observation that the genes for both UCP-3 and CD36 (which were found to be up-regulated in the diabetic heart), have previously been implicated in an increase in oxidative stress damage to the heart as a result of changes in lipid metabolism (Clapham et al. 2001; Brand and Esteves 2005; Farhangkhoee et al. 2005). This hypothesis is consistent with other available lines of evidence (Sakamoto et al. 2000; Lopaschuk 2002; Taegtmeyer et al. 2002; Taegtmeyer et al. 2004)

7.1.2.3 Physiological and molecular changes in the left ventricle of diabetic and sham animals after eight weeks treatment with TETA-disuccinate

This aim of this work was to evaluate the effects of continuous TETA-disuccinate administration on the physiological and molecular characteristics of male Wistar rats with or without STZ-induced diabetes over an eight week period. The physiological characteristics included blood glucose levels, total body weight, heart weight, and serum biochemistry. Within this study a variety of TETA-disuccinate doses were included with a view to understanding whether treatment elicits a dose-response and what the effects of extreme high and low doses are, as these had not been studied previously.

The molecular characteristics examined were limited to that of the LV of the heart and included changes in gene expression; structural changes in the ECM and changes in fuel metabolism in the LV of the heart.

7.1.2.3.1 Physiological changes

Previous studies conducted in this laboratory (Cooper et al. 2004; Gong et al. 2006) have pointed towards a change in the physiology of TETA-treated diabetic animals, such as changes in total body weight and heart weight/body weight; however, a comprehensive analysis of the physiological effects of TETA treatment on sham or diabetic rats over time has not been conducted.

Analysis of blood glucose levels in this study using data from Week 10 onwards (post-drug) confirmed that TETA administration had no effect on the blood glucose of the animals, consistent with prior reports (Cooper et al. 2004; Jullig et al. 2007). Blood glucose levels of the different treatment groups in both diabetic and sham animals showed no significant differences over dose or time. Any subsequent changes in the physiology of the diabetic animals with TETA treatment are therefore in spite of high blood glucose levels.

7.1.2.3.1.1 Body weight

An important factor in determining the status of animal health is weight (Foltz and Ullman-Cullere 1999). In this study, analysis of weight was split into two parts, pre- and post-TETA administration. As in Chapter Four, diabetic animals were found to have attenuated weight gain associated with mild to severe diabetes pre-TETA administration (Weeks 2-8 of the study).

It was observed during the course of this study that the weight of the diabetic animals (in particular) receiving the higher doses of TETA appeared heavier than those left untreated. Analysis of animal weights post-TETA administration (Weeks 9-16 of the study) found that that TETA treatment increased the weights of the treated animals; however, this was dependent on whether the animal was in the diabetic or sham group. The treated sham animals appeared to have increased weight compared to the untreated sham animals, but this was not dose-dependent (all doses were approximately the same). The treated diabetic animals however appeared to increase their weight in a dose-dependent way with the change in weight increasing as the dose increases (0mg~3.5mg <17.5mg<35mg<87.5mg).

7.1.2.3.1.2 Heart weight

Analysis of the heart weight and heart weight/body weight from animals in this study found that as, in Chapter Four, the diabetic hearts are significantly smaller than those of matched sham animals until corrected for body weight (Table 5.2). In the assessment of HW, it was noted that there was evidence for a significant effect of TETA administration in both groups. The data indicated that the change observed is an increase in heart weight with treatment across all groups; however this does not occur in a dose-responsive manner. Although there was an increase in the absolute heart weight across both diabetic and sham groups; no significant change was seen in HW/BW with respect to treatment in the diabetic or sham animals. It could be hypothesised that the change in body weight mirrors the change in heart weight and this removes the observed weight increase. One possible way to confirm this hypothesis would be to conduct an analysis of heart weight/tibia length. The use of the HW/BW ratio assumes BW remains constant or that the HW changes in parallel with BW under normal conditions which may not be the case in the diabetic group (Yin et al. 1982).

7.1.2.3.1.3 Serum biomarkers

A terminal serum sample was taken for each animal and used for tests of liver function (ALP, ALT, AST and Bilirubin), lipid levels (TG, HDL, FFA and cholesterol), renal function (urea, albumin, total protein and creatinine) and metal homeostasis (ferroxidase, copper, zinc and iron). Analysis indicated that in the majority of serum biomarkers tested, a significant change occurred only in the diabetic vs. sham (Status) comparison with no change observed as a result of drug treatment. Diabetic animals were found to have raised liver function enzymes and lipid markers, both hallmarks of diabetes-associated steatohepatitis. Similarly, total protein and albumin were decreased, indicating a probable overall perturbation in the synthetic function of the kidney as a result of diabetes.

In this study (Figure 5.6) it was observed however that there was a significant effect of TETA on two important markers of metal homeostasis, copper levels and ferroxidase activity. The similar outcome for both copper and ferroxidase activity indicates the interdependence of ceruloplasmin activity and serum copper levels. Overall, TETA significantly reduced the levels of copper and active ceruloplasmin in a dose-dependent manner in both the sham and diabetic animals. Control of metal homeostasis in the sham animals appeared to be more sensitive to the administered dose of TETA with a steeply decreasing slope for both copper and ferroxidase. The slope for the diabetic group's copper and ferroxidase level was much shallower and indicated that TETA is not able to influence copper and ferroxidase levels as easily as in the sham animals and provides evidence for an increase in systemic copper levels as described previously (Cooper et al. 2005).

7.1.2.3.2 Molecular changes

Results for changes occurring at the molecular level as a result of TETA treatment (87.5mg/day), in both sham and diabetic animals only were reported. Three main areas of interest were covered in this work. The first was an analysis of changes in gene expression; the second was a histological assessment of cardiac tissue lipid levels and structural changes in the ECM; and the third was an assessment of the activity of enzymes involved in mitochondrial fuel metabolism and TEM analysis of mitochondrial structure.

Changes in gene expression in LV cardiac tissue as a result of STZ-induced diabetes in the Chapter Six were found to be largely consistent with the results described in Chapter Four. Unexpectedly, no changes in gene expression were observed in either the sham or diabetic group after treatment with TETA using classical univariate microarray analysis procedures. This result was surprising given the physiological changes described in Section 7.1.2.3.1; however these results were confirmed using the more sensitive method of RT-qPCR for a subset of eleven *a priori* genes.

The explanation for why many experiments do not reach significance for changes in gene expression using microarray technology has become a topic of discussion among the microarray community (Mootha et al. 2003; Curtis et al. 2005). One hypothesis for the lack of observed changes in transcript levels is that when changes in gene expression are small, the large number of genes tested (in this case 31099), high variability between individuals due to disease status and limited sample size can make it difficult for a significant result to be obtained (Mootha et al. 2003). This is often due to the statistical method used to analyse microarray data and will be discussed more fully in Section 7.2.2.1. The use of pathway-based analytical algorithms has been investigated as a way to combat this problem. As the variation among diabetic subjects is known to be higher than that of control subjects, the pathway-based algorithm GSEA was used in an attempt to find sets of genes or pathways with significant changes in gene expression. The results from this analysis were again surprising, with fewer than expected changes observed in the sham vs. diabetic comparison and only three gene-sets that appeared plausible when comparing sham- or diabetic-treated against the untreated animals. The explanation for these limited detection changes may relate to the manner in which the software performs the analysis (permutation analysis) and the need for sufficient group sample sizes (usually >7) for it to generate a null distribution. If more experiments are to be carried out in the future using samples from this study, perhaps an increase in the number of arrays used might allow the identification of a greater number of changes in gene-sets or pathways as a result of TETA-treatment.

Semi-quantitative analysis of the cardiac ECM found no change in the level of collagen III as a result of diabetes, however revealed an overall decrease in collagen III staining following drug treatment which was consistent with the results presented by Cooper *et al.,* (Cooper et al. 2004). These results are also consistent with the GSEA pathway analysis which identified a significant difference in the gene-set for Lamellipodium biogenesis between the diabetic and diabetic-treated groups. Lamellipodia have been implicated in fibroblast movement (Abercrombie 1980; Cramer et al. 1997; Pichon et al. 2004) which may be reduced due to reduced levels of collagen present in the treated animals (Loftis et al. 2003).

Several lines of evidence were presented from this work that indicate changes in the ability of the diabetic heart to process lipid and possible changes that might have occurred as a consequence of TETA treatment. Cardiac tissue sections stained using the neutral lipid stain Nile red, revealed an increase in lipid staining of diabetic tissue when compared to sham tissue and a decrease in lipid staining when compared to diabetic animals treated with TETA-disuccinate. Confirmation of these results was obtained using Iatroscan technology (flame ionisation detection thin-layer chromatography). The Iatroscan was able to identify triglycerides as the species of lipid that was increased in the diabetic state and decreased with TETA treatment.

A hypothesis was put forward that a change in lipid status of the heart tissue as a result of treatment with TETA may result from a change in mitochondrial oxidative capacity. This hypothesis was partially tested by comparing the activity levels of a selection of mitochondrial enzymes in prepared mitochondrial fractions from the interventricular septa of animals in the sham, sham-treated, diabetic and diabetic-treated groups.

Enzyme activity levels of CPT, HOAD, and IDH were found to be altered the isolated mitochondria of diabetic animals compared to the sham animals as expected (Cuestas and Dixit 1973; Cook and Gamble 1987; Glatz et al. 1994). In accordance with this finding, the mRNA transcript levels of these enzymes were also found to be increased in the diabetic vs. sham comparison, indicating an increase in mRNA expression that potentially leads to increased enzyme activity. Conversely, CS activity of isolated mitochondria from untreated diabetic hearts was found to be decreased relative to sham mitochondria indicating fragility in the mitochondria, likely due to the effects increased ROS in diabetes.

Analysis of activity levels of CS, CPT, HOAD, and IDH unexpectedly found a further increased in the diabetic-treated animals when compared to diabetic animals. These increases in enzyme activity levels between the diabetic and diabetic-treated animals were found to occur without a concomitant increase in mRNA expression. Unlike in the diabetic-sham comparison, CS activity in isolated mitochondria was increased with

TETA treatment (diabetic-diabetic treated comparison) and TETA treatment also appeared to improve mitochondrial structure ((Cooper et al. 2004) and Figure 6.3(D)) indicating that the mitochondria are no longer as fragile after TETA treatment. The implications of this and potential links to mechanism of TETA action are discussed in Section 7.2.

7.1.2.4 Characterization of the metabolism of TETA-disuccinate by diabetic and sham rats after eight weeks of treatment and its relationship to metal ion excretion

An analysis of the levels of TETA and its metabolites, MAT and DAT, in the serum and urine of sham and diabetic animals as well as an analysis of TETA-induced changes in metal ion levels over time was conducted. Quantification of TETA, MAT and DAT was performed using an HPLC-based method developed in the School of Biological Sciences Reference Laboratory. This work aimed to establish whether the differences in metabolism observed between diabetic and matched control humans was also measurable in this animal model of diabetes.

Overall, measured levels of TETA and its metabolites were greater in the serum and urine of diabetic animals than in control animals receiving comparable daily doses. TETA levels in the drinking water were adjusted to ensure that diabetic animal's received an equivalent dose of TETA to that of the sham animals. In a recent study looking at TETA, MAT and DAT excretion in human diabetic patients, no difference was observed in the levels of TETA excreted between diabetic and normal patients treated with TETA-dihydrocholoride, while there was increased excretion of metabolites MAT and DAT. This was consistent with the hypothesis that diabetic patients metabolise TETA faster than normal patients (Lu et al. 2007). This apparent difference between the species in these studies might be explained by increased absorption of TETA in the diabetic animals due to increased gut surface area consequent from the reported hypertrophy of the digestive tract in STZ-diabetic animals (Schedl and Wilson 1971; Fedorak et al. 1987). To my knowledge the equivalent phenomenon has not been observed in human patients. There is some evidence that TETA is absorbed into the body via passive diffusion using a similar mechanism as the endogenous polyamine spermine ((Tanabe et al. 1996), for a review of polyamine absorption see (Milovic 2001)). If confirmed, this finding would provide further support for the hypothesis that the increased uptake of TETA, MAT and DAT observed in the diabetic rats is likely to be the result of increased gut surface area, as an increase in the area of the gut would provide greater area across which passive diffusion may occur. Further work in this area is required to fully understand how TETA is absorbed by the body.

It is important to note that there was no significant Status*Dose interaction observed for any of the three compounds. This indicates that although the diabetic animals excrete more TETA, MAT and DAT at the Week 10 time point, and have more TETA and MAT in their serum and at the Week 15 time point, the slope of TETA excreted over the range of administered doses was the same for both diabetic and sham animals.

A change in excretion over time was observed for both TETA and DAT with an increase in TETA excretion and a decrease in DAT excretion in the diabetic animals and a decrease in both TETA and DAT in the sham animals. These findings point towards a possible change in the enzyme systems that control the processing of these two compounds. There was no change in MAT levels over time in either diabetic or normal groups indicating relative stability in the processing of this compound.

The results presented above indicate that overall, the diabetic animals had greater amounts of the three compounds (TETA, MAT or DAT) present in their terminal serum samples and urine at both the Week 10 and 15 time points. Data from each of the groups (diabetic and sham) was normalised in order to obtain a better comparison.

Results from this analysis found that the proportion of unchanged TETA found in the urine of diabetic animals at the Week 10 time point was the same as the proportion of unchanged TETA found in the urine of sham animals at the Week 10 time point. However, as time progressed, the proportion of unchanged TETA in the diabetic animals increased, while the proportion of unchanged TETA in the sham group remained the same (Figure 5.15). This is consistent with the results presented (Figure 5.11) that show an increase in the amount of TETA excreted by the diabetic animals at Week 15 compared to Week 10.

In the serum, it was found that the proportion of unchanged TETA in the diabetic animals was significantly lower than the proportion of unchanged TETA in the sham animals. This result was expected, given that at the proportion of unchanged TETA in the diabetic animals at the Week 15 time point is greater than that of the sham animals indicating a higher level of excretion of unchanged TETA. Higher levels of excretion could be responsible for the observed lower serum levels.

7.1.2.4.1 Limitation: TETA levels in serum

Animals were administered TETA in their drinking water continuously for eight weeks of the study. As the serum sample taken was at the time of euthanasia, it is assumed that the serum data presented represents a stable equilibrium for the level TETA, MAT or DAT. A previous study by Takeda *et al.,* (Takeda et al. 1995a) found that oral administration of TETA-dihydrochloride at 25mg/kg produced a C_{max} in plasma after about one hour. This result is consistent with that reported in a recently published human study (T_{Max} for TETA was 1.9 ± 0.8hrs, (Lu et al. 2007)). It is not known whether the animals in

the present study actually reach a constant basal state or whether they have a cyclical pattern of high to low TETA levels depending on the time of day or how much water is drunk.

It will be important in future studies to identify what the minimum level required in the blood of TETA or metabolites in order to elicit a response and whether continuous dosing (such as in this study) is able to achieve this when compared to human trials that often incorporate a single dose at regular time points. This is particularly important given the evidence described here and in Section 5.2.4 for a difference in the ability of diabetic animals to absorb and metabolise TETA.

7.1.2.4.2 Metal ion excretion and relationship to TETA excretion

The onset of diabetes resulted in an increase in the excretion of all four metal ions measured (Figure 5.16), which is consistent with the literature (Lau and Failla 1984; Cooper et al. 2004; Cooper et al. 2005; Uriu-Adams et al. 2005). With respect to TETA treatment, a significant dose responsive increase in excretion was seen in copper and zinc levels but not iron or manganese. *In vitro* studies have found that TETA is able to bind stoichiometrically with zinc as well as with copper (Kodama et al. 1997). Of the physiological trace metals, zinc is known to have the second highest binding stability with TETA after copper which may account for the effect of TETA on urinary excretion of zinc.

In this study diabetic and sham animals showed a significant decrease in both urinary copper and zinc excretion between Week 10 and Week 15. This may be due to an overall improvement in the condition of the diabetic animals as observed in Section 5.2.2.2 with an increase in total body weight. It may also reflect the change in metabolism of the drug at Week 15 described in Section 5.2.4.

TETA was found to be significantly positively associated with both copper and zinc in the urine of sham and diabetic animals. Consistent with the evidence presented in Chapter Five for a shift in the metabolism of TETA and copper homeostasis over time in the treated diabetic animals, the TETA/copper relationship also appeared to strengthen over time (Pearson's correlation increasing from 0.58 to 0.83, P=0.030).

One hypothesis for this change in strength of association could be that, after two weeks of treatment, copper levels in the diabetic urine are a mixture of the excess copper found as a result of the diabetic state and copper pulled out by TETA treatment. Continued exposure to TETA over the course of the study may result in the achievement of a homeostatic state, with the excess copper seen previously removed over the passage of time and the majority of copper now being excreted solely as a result of TETA treatment and, leading to a stronger correlation between TETA and copper. One way to test this hypothesis would be to conduct more frequent metabolic cage urine collections

and measure the copper/TETA correlation over time to see if there is a linear increase in association between the two.

In the urine of both diabetic and sham animals, MAT was found to have a significant positive correlation with copper. In the serum of diabetic animals, the negative correlation between copper and MAT (Pearson's r = (-0.62), P<.0001) was stronger than the negative correlation between copper and TETA (Pearson's r = (-0.38), P<0.05). This finding is consistent with MAT acting as a copper chelator *in vivo* and provides evidence that MAT is an active rather than passive metabolite of TETA. In studies of patients with type-2 diabetes, Lu *et al.,* found that, in urine from diabetic patients, copper correlated better with [TETA+MAT] than [TETA] alone (Lu et al. 2007). Further studies of the ability of MAT to act as a chelator and whether it has the potential to act therapeutically on its own might extend our current understanding of the mechanism of action of TETA.

7.2 Potential mechanism of TETA

The evidence presented in this thesis and that of others in this laboratory point towards the potential mechanism for TETA in the treatment of diabetic cardiomyopathy as being a reduction in oxidant load on the diabetic animal resulting in improved general health and well being without a reduction in blood glucose.

As mentioned in Section 1.4 copper levels within the body (including uptake, distribution and export) are tightly regulated under normal conditions. Failure of this system to regulate copper can lead to increased ROS damage through the participation of copper in Fenton reactions leading to increased free radicals (Kadiiska et al. 1992; Frausto da Silva and Williams 2001).

As seen in this thesis, diabetic animals show a perturbation in copper balance with increased urinary copper excretion pre-TETA administration (Figure 5.16), further increased urinary copper excretion post-TETA administration and an increase in the serum activity of the copper carrying protein ceruloplasmin (Figures 5.16 and 5.6 respectively).

It has been postulated that increased serum and urinary copper emanates mainly from tissue stores (Cooper et al. 2005). Having excess copper in and around cells of the body would increase its potential to participate in Fenton reactions leading to the creation of excess free radicals and provide an explanation as to why copper is able to inflict such a high degree of cellular damage, leading to the complications associated with diabetes. This hypothesis is supported here with an increase in both serum and urinary copper levels as a result of diabetes which are further modified as a result of TETA treatment (Section 5.2.5). The removal of excess copper from tissue stores leading to an improvement in copper homeostasis with TETA treatment can only be implied from the

studies presented here (Chapter 5). An interesting set of experiments that could be carried out in this area would be to investigate tissue metal levels. There are a number of highly sensitive techniques which could be used in this instance. One such technique is known as proton-induced x-ray emission (PIXE) and has been used previously by this laboratory to quantify tissue metal levels (G. Cooper, unpublished observations). By measuring copper levels in the tissues of treated and untreated animals we would be able to better understand if TETA is indeed removing tissue copper leading to improved copper homeostasis at the cellular level.

Removal of copper by TETA may lead to a reduction in free radical production and therefore create an improvement in overall animal health. Previous studies looking at anti-oxidant therapies (see Section 1.3.1 for details) found little or no difference between patients or animals receiving anti-oxidant therapy and the control group. These therapies act at a downstream level by targeting the free radicals themselves without removing their source. TETA therapy reduces copper levels which in theory would remove the intiating factor leading to a reduction in overall free radical levels, allowing endogenous anti-oxidant mechanisms to function better, improving the general health of the animal. Evidence to support this from within this thesis comes from the observation that diabetic animals had increased total body and heart weights as a result of TETA treatment (Figure 5.4 and 5.5). The ability of TETA to shift the diabetic weight from a negative to a positive weight gain in this instance is an important indication that treated animals have improved general health. In order to pinpoint whether TETA is causing weight gain through increased peripheral fat deposition or muscle mass it may be of interest in the future to incorporate MRI scanning into the experimental protocol. This technique has been used previously to map out areas of fat deposition in rodents (Ross et al. 1991; Szayna et al. 2000) and may provide an insight into changes occurring within both diabetic and sham animals as a result of TETA treatment. Work from within this laboratory has also found that TETA is also improving kidney function (manuscript in submission, Gong *et al*.). This would again point towards a systemic rather than cardiac specific effect of TETA on the diabetic animals.

At a subcellular level we find improved mitochondrial structure and enzyme function (as seen in Chapter 6, Sections 6.2.4 and 6.2.6) which is also likely to be a consequence of a reduction in ROS. ROS are known to damage mitochondria and reduce their stability and enzyme efficiency (reviews see (Bulteau et al. 2006; Rolo and Palmeira 2006)). By alleviating the damage of the mitochondria, TETA may be improving heart function by increasing the stability of the organelle and as a consequence of this the efficiency of energy utilisation. As mentioned in Chapter 6, citrate synthase activity levels are used as a crude indicator of mitochondrial number and function. It could be hypothesised that a reduction in citrate synthase activity in the untreated diabetic

mitochondria may have occurred due an increase in the fragility of these mitochondria from increased structural and functional damage as a result of increased ROS leading to selective isolation during the mitochondrial preparation. In support of this explanation, structural damage was observed in electron micrographs of diabetic cardiac mitochondria in this study and elsewhere (Figure 6.3, (Cooper et al. 2004; Shen et al. 2004)). This increased fragility of mitochondria may result in increased turnover or lower mitochondrial efficiency leading to a requirement for the observed increases in mRNA transcript and enzyme activity levels (Section 6.2.2.2, Figure 6.4-6.7).

With treatement however we find no significant changes observed at the transcriptomic level, improved mitochondrial structure (TEM) and an increase in mitochondrial fuel metabolism enzyme activities (Chapter Six) which suggests that the additional increases in enzyme activity and improvement of mitochondrial structure following TETA treatment may be the result of improved stability of the mitochondria leading to reduced protein turnover and increased enzyme efficiency. The observed increases in mitochondrial fuel metabolism enzyme activities may provide some explanation for the reduction in TG levels in the heart tissue of treated-animals as found using Nile red staining and Iatroscan technology (Figure 6.2 and Table 6.21). The lack of observed changes in gene expression as a result of TETA treatment is likely due either to insufficient sensitivity of the technology used or the timing of the experiment (tissue taken after changes had occurred already). An extensive analysis of this finding is covered in section 7.3.2.

The potential for increased flux of excess lipid through the mitochondria through increased fuel-metabolism enzyme activities as a result of healthier mitochondria coupled with a decrease in cardiac heart collagen (Section 6.2.4.1 and as published by Cooper et al., (Cooper et al. 2004)) and an improvement in the oxidant status of the heart through copper removal may provide a possible explanation for the TETA induced increase in heart function described by other members of our group (Cooper et al. 2004; Gong et al. 2006).

Other evidence to support the hypothesis of reduced copper levels resulting in reduced ROS impact has come from work done in human Type-2 diabetic patients. Cooper *et al.,* found that EC-SOD (the major SOD isoform present in the vascular endothelium, where it acts to regulate superoxide levels) activity was elevated in Type-2 diabetic patients and was significantly correlated with serum [Cu]. TETA treatment was found to lower EC-SOD levels to control values in diabetic subjects (Cooper et al. 2005) indicating improved oxidant status of these patients. An important series of experiments to complete would be to look at EC-SOD levels in treated and untreated-diabetic animals to further strengthen this finding. Other indicators of the presence increased or reduced reactive oxygen species would also give greater understanding to the mechanism of

TETA. This could be achieved through a number of assays such as measuring the tissue level of thiobarbituric acid reactive substances (TBARS) in the tissues of treated vs. untreated animals. TBARS are an index of lipid peroxidation and oxidative stress.

Given the evidence for improved function in both the heart and the kidney and in total body weight it is important that the focus of new studies be all the organs within the animal and not just the heart. A detailed description of more studies that may add to our understanding of the mechanism of TETA are described in Section 7.4.

7.3 Limitations of the current studies

Due to the nature of this study and the experimental process used herein, a number of limitations should be taken into account when reviewing the results presented in this thesis.

7.3.1 Study design

In both animal studies presented here, harvesting of the LV tissue occurred sixteen weeks after STZ-induction of diabetes and eight weeks after treatment with TETA was begun. It is likely that there are transcriptomic changes which might occur at an earlier stage of both disease and treatment, such as those described by Knoll *et al.,* (Knoll et al. 2005) who reported changes in the diabetic LV two weeks after induction of diabetes. Limited transcriptome changes were observed with TETA treatment using microarray technology and none in selected targets using RT-qPCR technology. Assessment of whether changes are occurring at earlier time points may give an explanation as to why changes were not observed after eight weeks.

Serum analysis of both biochemical markers and TETA levels in both sham and diabetic animals was conducted using terminal serum samples collected at sixteen weeks. As with the analysis of gene expression it may be of use in future studies to collect serial serum samples in order to fully understand the progress of both the diabetic state and the metabolism of TETA.

7.3.2 Microarray technology

7.3.2.1 Statistical analysis

The change in gene expression between two samples as the result of a single influencing variable is often the main focus of microarray experiments; for example, tumour tissue compared to normal tissue (Chen, X. et al. 2002); diabetic tissue compared to non-

diabetic tissue (Glyn-Jones et al. 2007); or over/under-expression of a gene of interest (e.g. knock-out or knock-in studies) in a modified tissue compared to wild-type tissue (Castro-Chavez et al. 2003).

Classic microarray analysis of changes in gene expression utilized univariate statistical methods such as the Students *t*-test or non-parametric tests (Chen, Y. et al. 1997). However, using this form of microarray analysis creates a multiple testing problem, as the greater the number of comparisons (e.g. 30,000 comparisons using the Affymetrix system), the greater the potential for false positives. A multiple testing correction must therefore be applied to the data in order to remove the introduced error (Benjamini and Hochberg 1995; Dudoit et al. 2002; Smyth 2004). In this study, the FDR correction described by Benjamini and Hochberg (Benjamini and Hochberg 1995) was used to account for introduced error as a result of multiple testing.

Univariate analysis also has other more biologically-oriented problems. One such problem is that the analysis assumes that all genes present on the microarray are independent of each other. This assumption is false, as it is well established that there is a complex network of gene regulation leading to gene expression involving multiple genes and gene families, so independence cannot be assumed. A second problem is, the multiple testing correction required (such as FDR) may be important statistically but removes the power of an experiment biologically (for a review of multiple test correction methods see (Ge, Y. et al. 2003)) and can lead to a loss of significant changes in gene expression after correction for multiple testing, as seen in Chapter Six. Even if a list of genes with significant changes in gene expression is generated using this method, it is not always useful. For example, in our studies, the diabetic vs. sham comparison produced a list of greater than 1,000 genes in each study (Chapters Four and Six). Identification of genes that interact or form pathways is not incorporated into classical microarray analysis and so requires the researcher to manually identify commonalities between genes present on the list. This limits the analysis to only what the researcher can identify in a time consuming and error prone process. Overall, univariate microarray analysis does not adequately account for the complexities inherent in a biological system.

There is now movement towards a pathway-based approach that integrates normalised array data and annotations (Curtis et al. 2005). As described by Curtis *et al.,* (Curtis et al. 2005), there are a number of different pathway based analysis approaches now available (for review see (Curtis et al. 2005)). The ability to identify a shift in a whole pathway of genes is potentially more powerful than looking at individual genes, as it enables an accumulation effect where many genes contribute to the overall determined significance. In Chapter Six for example the GSEA method (Subramanian et al. 2005) was able to determine changes occurring at the pathway level for three different gene-sets, despite no changes detected at the individual gene level. However, even pathway based

approaches are not without problems. For example, this method requires at least some form of annotation, the minimum of which is a gene name or title. On the Affymetrix Rat 230 2.0 GeneChip, 10477 out of 31099 (33%) of the genes represented have no gene title or the title 'Transcribed Locus' with no further corresponding annotation. This considerably reduces the power associated with pathway analysis.

Another issue is that pathway-based approaches (including GSEA) also require a multiple testing correction, because as the number of pathways tested increases so does the chance of a false positive. GSEA, for example calculates an FDR adjusted P-value based on a 25% chance of a false positive (Subramanian et al. 2005). This reduces the power of this analysis, as it reduced the power of the classical univariate microarray analyses and means that more arrays are required to obtain a significant result.

A question that remains regarding microarray analysis is, by adding these extra statistical measures such as the multiple-testing correction, are we reducing our ability to fully elucidate the changes that are occurring? The majority of microarray experiments encompass a simple treatment vs. control or diseased vs. normal comparison; however, in Chapter Six a more complex untreated-diseased vs. treated-diseased comparison was conducted. Are microarrays sensitive enough to elucidate changes occurring at this more subtle level after adjustment for multiple testing? Table 7.1 presents a limited literature review of microarray studies looking at diabetic animals.

Table 7.1 Literature review of microarray studies looking at changes in gene expression in the diabetic state

Reference	Year	Species	Tissue	Groups	Array Type
(Aitman et al. 1999)	1999	Rat (SHR)	Adipose Tissue	SHR, BN and SHR.4	cDNA (Incyte) – heart specific
(Ferrante et al. 2001)	2001	Mice (ob/ob)	Liver	ob/ob vs. control	cDNA (printed in house), 2-dye
(Cardozo et al. 2001)	2001	Rat (Wistar)	Isolated pancreatic islets	Untransfected vs. AdIκB(SA)^2	Rat U34-A (Affymetrix
(Sreekumar et al. 2002)	2002	Human	Skeletal Muscle	Control, diabetic (no insulin), diabetic (insulin)	Hu680 arrays (Affymetrix)
(Yechoor et al. 2002)	2002	C57Bl6 mice (STZ)	Skeletal Muscle	diabetic, control, insulin-treated control	MG-U74A-v2 (Affymetrix)
(Mootha et al. 2003)	2003	Human	Skeletal Muscle	Normal, IR, type 2 diabetic	HG-U133A (Affymetrix)
(Dhahbi et al. 2003)	2003	Mice (STZ)	Liver	Diabetic vs. control	Mu11kSubA & B (Affymetrix)
(Wilson et al. 2003)	2003	NOD mice	Kidney	Control, early NOD, late NOD	cDNA (printed in house)
(Gauthier et al. 2004)	2004	Wistar Rats	Pancreatic Islets	control/AdCalacZ or AdRIPDN79PDX1-infected islets	Rat U34A (Affymetrix)
(Susztak et al. 2004)	2004	Mice	Kidney	Db/db, STZ C57BL/6J and respective controls	In house printed array
(Sullivan et al. 2005)	2005	Rat (STZ 35mg)	Penile Tissue	Diabetic, normal	Rat 230A (Affymetrix)
(Knoll et al. 2005)	2005	Rats (STZ, 55mg)	Renal cortex, LV wall, psoas muscle, retina	Diabetic vs. Normal, 2wks diabetes	cDNA spotted array, 2-dye

(Wolfram et al. 2006)	2006	Rat	rat H4IIE hepatoma cells	EGCG treated cells vs. solvent-treated cells.	Rat 230A
(Devi and Mehendale 2006)	2006	Rat (STZ 60mg)	Liver	Time series at 0, 6 & 12hr, 30 or 300mg thioacetamide	In house spotted cDNA array (liver specific)
(Colombo et al. 2006)	2006	Rat (ZDF)	Islets, liver, skeletal muscle, visceral fat	ZDF vs. Calorie restricted ZDF	Rat U34A
(Willsky et al. 2006)	2006	Rat (STZ)	Skeletal Muscle	control, diabetic, +VS (both)	Rat U34A
(Price et al. 2006)	2006	Rat (Wistar, STZ 55mg.kg)	Dorsal root ganglia	1,4 and 8 weeks of diabetes	Rat 230A/230B
(Lehti et al. 2006)	2006	Mice (NMRI)	Skeletal Muscle	sedentary healthy mice, trained healthy mice, sedentary diabetic mice, and trained diabetic mice	MG U74Av2
(Iwata et al. 2006)	2006	Mice (BDF-1, STZ injection)	Whole heart	Diabetic vs. Normal	Macroarray (membrane based)

This limited review found that a number of microarray studies published have looked solely at the effects of diabetes on gene expression and not at the changes in gene expression after introduction of a further treatment variable, as described in Chapter Six. However, one recent report (Table 7.1, Willsky *et al.,* bold) did present gene expression data looking at the effects of oral vanadyl-sulphate treatment on STZ-diabetic skeletal muscle (Willsky et al. 2006) in a similar study design to that described in Chapter Six. Authors were able to identify numerous changes that occurred with treatment using only five arrays per group. However, vanadyl-sulphate is an insulin-mimetic and authors were able to show a decrease in blood glucose concurrently with changes in gene expression (Willsky et al. 2006). The majority of changes in gene expression found to be associated with vanadyl-sulphate treatment were related to a drop in blood glucose levels, similar to that observed in insulin-treated diabetic animals (Willsky et al. 2006). Treatment with TETA does not alter blood glucose levels and this may lead to increased heteroscedacity among the population that can create difficulty when trying to resolve changes in gene expression. These findings indicate that there is a lack of published microarray data to date that has shown changes in gene expression of a diabetic model as a result of treatment with a therapeutic compound that has no effect on blood glucose. Such subtle changes may well be difficult to elucidate using microarray technology. The power of microarrays as a tool for identifying global gene changes under these circumstances has yet to be established.

One solution to this problem could be to look at genes considered to be of potential significance prior to the multiple testing correction but within this data there would always be the uncertainty of whether results under study are actually false positives that may lead a researcher down the wrong path. Another solution to the problem would be to increase the number of microarrays per group. While solving the statistical issues, the cost of the experiment would thus be increased. Future microarray analytical

techniques need to establish a compromise between statistical significance, cost and biological relevance in order to gain the most precise yet all encompassing results possible.

7.3.2.2 Oligonucleotide length

In Section 7.2.2.1, the sensitivity of microarray technology to detect very subtle changes and the impact statistical analysis has on determining the significance of these changes was discussed.

Another factor that may have influenced the sensitivity of the Affymetrix microarray is the length of the oligonucleotide bound to the glass support. As outlined in Chapter Three, Affymetrix technology utilises 25 nucleotide long oligonucleotides to probe gene expression levels of individual samples. Each gene is represented by eleven perfect match/mismatch pairs scattered randomly around the array and the signal intensity from each of the eleven pairs is combined to give the overall signal intensity (Affymetrix 2001). The original paper describing the development of Affymetrix technology (Lockhart et al. 1996), used the combined hybridisation signal from 300 perfect match/mismatch probe pairs per gene, and the detection limit of the array was determined to be approximately three mRNA copies per cell. If the number of probe pairs per gene was reduced to 20, then the detection limit of the array was approximately ten mRNA copies per cell (Lockhart et al. 1996). As the technology has developed however the sensitivity of the system has increased and according to an Affymetrix Technical Note, the current estimation of sensitivity is 3.5 copies per cell using 11 probe pairs per gene (Affymetrix 2001).

Agilent microarrays were also assessed in Chapter Three, but were found to have issues surrounding their washing and scanning protocol which led to an increase in the number of poor slides produced and variation within the data. It was decided not to use the Agilent system based on these results. As described in Chapter Three, Agilent microarrays contain a 60 nucleotide long oligonucleotide to probe the gene expression of two samples at once (competitive hybridisation). Each gene is represented only once per array. A study presented by Hughes *et al.,* (Hughes et al. 2001) found that using the 60-mer oligonucleotides they were able to detect mRNA at a level of <1 copy per cell. Shorter oligonucleotide probes (such as 25 nucleotides long) are thought to provide the best discrimination between related sequences (Lockhart et al. 1996). However, Hughes *et al.,* provided evidence that indicated a 60-mer oligonucleotide provided the best compromise between specificity and sensitivity (Hughes et al. 2001).

In the discussion presented above (Section 7.2.2.1) it was hypothesised that Affymetrix technology may not have been sensitive enough to detect changes occurring as a result of treatment with TETA. This may in part be due to the shorter oligonucleotides

on the Affymetrix GeneChip. Affymetrix was chosen because this system was able to provide the best results in the hands of an inexperienced user and it was believed that this would reduce the overall cost as fewer arrays would be required than if the Agilent system was used, given the apparent difficulties to obtain a consistent wash and stain protocol. However, if more Affymetrix arrays are required in order to increase the power of the experiment and the ability to detect very small changes, then the benefits gained from an easier to use system could be negated. In an ideal world, it would be of interest to conduct a similar experiment to the one described in Chapter Six using the Agilent microarrays. If the changes occurring as a result of treatment with TETA are very small then perhaps they would be able to be detected as result of the greater sensitivity of this system (Hughes et al. 2001).

7.4 Future experiments

The results presented here indicate that there are gross physiological changes in both diabetic and sham animals after treatment with TETA (as shown by changes in overall weight after treatment). They also indicated that within the heart at the molecular level, mitochondrial structure is improved and the activity of a number of enzymes involved in metabolism of lipid are up-regulated without a concomitant increase in gene expression. To further elucidate the mechanism of action of TETA on the heart and also other primary organs, several experiments are required. These experiments are beyond the scope of this thesis but have been outlined below.

7.4.1 Microarray analysis of LV heart tissue at different doses of TETA

The limited number of changes in gene expression associated with TETA treatment may be related to the dose of TETA. Previous studies by Gong *et al.,* (Gong et al. 2006) and Jüllig *et al.,* (Jullig et al. 2007) indicated that treatment with TETA was able to restore the level of mRNA expression of a number of genes involved in the ECM pathway and a number of proteins in the mitochondria towards normal. In both these studies, a dose of 35mg TETA-disuccinate per day was used to achieve the published results. In the current study a range of doses was included and heart tissue from all groups was collected (including, 3.5mg, 17.5mg and 35mg per day). In light of the findings presented in Chapter Six, future work that to be carried out is microarray analysis of the LV from all other drug groups. This would provide insight into whether changes in gene expression in the heart as a result of TETA treatment occurred only over a limited range of TETA exposure. This could explain why Gong *et al.,* (Gong et al. 2006) and Jüllig *et al.,* (Jullig et al. 2007) were able to describe changes in gene and protein expression, respectively, at a dose of 35mg

per day while, in the current studies of the 87.5mg dose, only limited changes in gene expression were observed, despite showing the greatest physiological changes.

7.4.2 Radioassays

7.4.2.1 Analysis of β-oxidation

In order to understand if the increased activity of mitochondria-associated enzymes CPT, HOAD, CS and IDH resulted in increased flux of triglyceride (as fatty acids) through β-oxidation *in vivo*, further studies using recently developed radio-tracers and positron-emission tomography (PET) imaging in a metabolic trapping protocol would allow the measurement of regional FAO rate. The general principle behind metabolic trapping is the use of substrate analogues (in this case, fatty acids) that can be taken through the first steps of an enzymatic transformation process but result in products that cannot be metabolised further due to a unique chemical structure. Under specific experimental conditions, the sum of the analogue products can be used to estimate the flux of native molecules through an irreversible transformation step (Oakes and Furler 2002). DeGrado *et al.,* (DeGrado et al. 2000; DeGrado et al. 2006) have developed 16-[^{18}F] fluoro-4-thia-palmitate (^{18}F-FTP) which has shown good retention (metabolic trapping) in the heart and is sensitive enough to be used under hypoxic conditions (DeGrado et al. 2000; DeGrado et al. 2006). Studies of the levels of FAO in hearts from diabetic-treated and untreated animals using this tracer and imaging technique concurrently with the perfused heart system already available in this lab (Cooper et al. 2004) would provide important information regarding the ability of the hearts to utilise lipid as a fuel source given the apparent decrease of TG in the heart and increase in enzymes involved in fuel metabolism.

7.4.2.2 TETA distribution

The levels of TETA found in organs, urine, faeces and serum over time after administration of a bolus of TETA into normal Wistar rats has been studied by Takeda *et al.,* (Takeda et al. 1995a; Takeda et al. 1995b) in a series of papers using ^{14}C labelled Triethylenetetramine dihydrochloride. Authors describe high levels of ^{14}C-TETA mainly in the kidney and liver with about 40% of radioactivity present in the urine after 24-48hrs (Takeda et al. 1995a). The results presented in Chapter Five and by Lu *et al.,* (Lu et al. 2007) indicate that diabetic animals and patients process TETA differently. As no work similar to that of Takeda *et al.,* has been attempted in diabetic animals to date, a similar

series of studies using radio-labelled TETA would add greatly to our understanding of the metabolism of TETA in diabetic animals.

7.4.3 Effects of insulin treatment combined with TETA treatment

When considering the therapeutic applications of TETA, one important variable not included in the studies presented here was the effect that insulin treatment might have on the action of TETA. Insulin was not administered to animals in the current study in order to allow mechanism of TETA to be investigated without the addition of complicating factors. However, both type-1 and type-2 patients use exogenously administered insulin, in an effort to control blood glucose levels. It has been shown previously that insulin treatment can improve cardiac function in the diabetic rat (Farah and Alousi 1981). It will be important to establish the impact of insulin treatment on the effects of TETA administration in a future study which incorporates diabetic insulin-treated and diabetic insulin + TETA-treated animals.

7.4.4 Effects of TETA treatment on the liver

One organ that has not yet been fully studied in relation to TETA treatment and diabetes is the liver. In Chapter Six, results indicating a reduction in tissue lipid levels and an increase in lipid metabolism in the heart as a result of TETA treatment were presented. The liver is known to be a site for metabolic control of fuel mobilisation (Krebs 1972; Hers 1976; Weickert and Pfeiffer 2006) and so it would be of interest to understand what changes in the expression of genes related to fuel metabolism were occurring as a result of sixteen weeks of diabetes and if these changes were affected by treatment with TETA. A previous microarray study looking at changes in hepatic gene expression after four weeks of STZ-induced diabetes in mice found that approximately 40% of the observed changes were linked to fuel metabolism. These changes included an increase in the rate limiting enzyme of gluconeogenesis, phosphoenolpyruvate carboxykinase (PEPK) and increases in mitochondria-related genes such as cytochrome c oxidase subunits (Dhahbi et al. 2003). Confirmation of these changes at the genetic and functional level in a rat model of diabetes over an extended time frame (sixteen weeks) and analysis of changes after TETA treatment would add to both understanding of the disease state and the mechanism of action of TETA.

The liver is also the organ responsible for processing xenobiotic compounds through the Cytochrome P-450 family of enzymes (Guengerich 1991; Lewis 2001). In a recent publication by Lu *et al.,* (Lu et al. 2007) one hypothesis for the observed differences in TETA metabolism by type-2 patients was that the diabetic patients may

have higher hepatic metabolic rates for TETA. Changes in members of the cytochrome P450 family as a result of diabetes have been described previously (Shimojo et al. 1993; Raza et al. 2000; Dhahbi et al. 2003). It could be hypothesised that this change in the ability of the liver to process xenobiotic compounds could lead to the differences seen in the metabolism of TETA as a result of diabetes. Further investigation of this is necessary to enable a full understanding of TETA metabolism in the diabetic state.

Another study of similar design to that seen in Chapter Six looking at the gene expression and enzyme function changes in the liver may aid in the elucidation of the mechanism of TETA and what changes in the Cytochrome P-450 family are occurring.

7.5 Concluding summary

With respect to the primary aims of this thesis, the results presented above have provided insight into a number of areas. The initial aim presented was to identify changes occurring in gene expression in the left ventricular wall after sixteen weeks of diabetes. The purchase of Affymetrix GeneChip® technology by the School of Biological Sciences Centre for Genomics and Proteomics enabled the identification of more than 1600 gene changes associated with diabetes in the left ventricle wall. A disproportionate number of those significant changes in expression were found to be associated with the mitochondria. Further investigation of these genes revealed changes associated with perturbed lipid metabolism and increased oxidative stress.

Results and experience gained through the pilot study provided the basis for the second aim of this thesis. The new study investigated changes in gene expression of the left ventricle from diabetic and sham animals treated with the copper (Cu^{II})-chelator TETA. Surprisingly, only a limited number of changes in gene expression were detected after eight weeks of TETA treatment using Affymetrix microarray technology, and none were able to be detected using the more sensitive method of RT-qPCR. A number of hypotheses were put forward to explain this result. These were: that the dose of TETA investigated was too high or the sensitivity of the microarray technology and the number of replicate microarrays were too low. Some evidence consistent with the latter explanation was provided using biochemical assays of enzyme function. It was observed that TETA was able to increase the activity of a number of fuel metabolism enzymes found in the mitochondria despite exerting no changes in the corresponding levels of gene expression.

The third aim of this thesis was to further elucidate the molecular mechanisms underpinning improved cardiac function occurring in the LV of the heart as a result of treatment with TETA-disuccinate. Through histology, thin-layer chromatography and functional enzyme assays, evidence was generated that TETA can probably decrease the level of triglyceride in LV heart tissue towards normal, possibly by improving the structure

and stability of the mitochondria. By protecting the mitochondria, TETA might reduce mitochondrion/protein turnover and enable the enzymes involved in fuel metabolism already present to function more effectively, without concomitant increases in gene expression. This could also explain the observed reduction in cardiac tissue lipid found to accumulate as a result of diabetes.

One of the main hypotheses for the development of DCM in diabetic patients is an increase in ROS production by the mitochondria. Increased structure and stability of the mitochondria could also potentially lead to reduced ROS production resulting in improvements in heart function previously identified (Cooper et al. 2004). Currently work in our laboratory is directed towards investigating the effects of TETA on the ability of the mitochondria to produce ROS.

The last aim of this thesis was to understand the absorption and excretion of TETA by both healthy and diabetic subjects as it is important for understanding the pharmacokinetics of the drug and establishing doses that are suitable for patients. Our study found that diabetic animals absorb and metabolise TETA differently to sham animals and that the length of TETA exposure was also an influencing factor in TETA metabolism. This will be of importance when considering the appropriate lengths of time human patients are to receive TETA as their ability to process it may change over time and potentially change the efficacy of treatment. In concordance with this, both groups appeared to reduce the production of DAT over time, while MAT remained the same, consistent with two different pathways that produce DAT and MAT, both of which may be influenced by exposure to TETA.

A number of questions and limitations were also identified by this work. These will provide a basis for the design of new studies, which will hopefully further our understanding of TETA's mechanism of action by which it can ameliorate the effects of diabetes on the heart and potentially other organs within the body.

Appendix 1: Bioanalyzer Analysis of RNA samples (Melbourne)

1.i Bioanalyzer Analysis

RNA samples were analysed on the Agilent Bioanalyzer on arrival in Melbourne and were found to be of the highest quality. The rRNA ratio for both sham and diabetic RNA is at 2.0 and from the figure (Figure 1.i) we can see that the peaks are high with no apparent background noise that would indicate degradation.
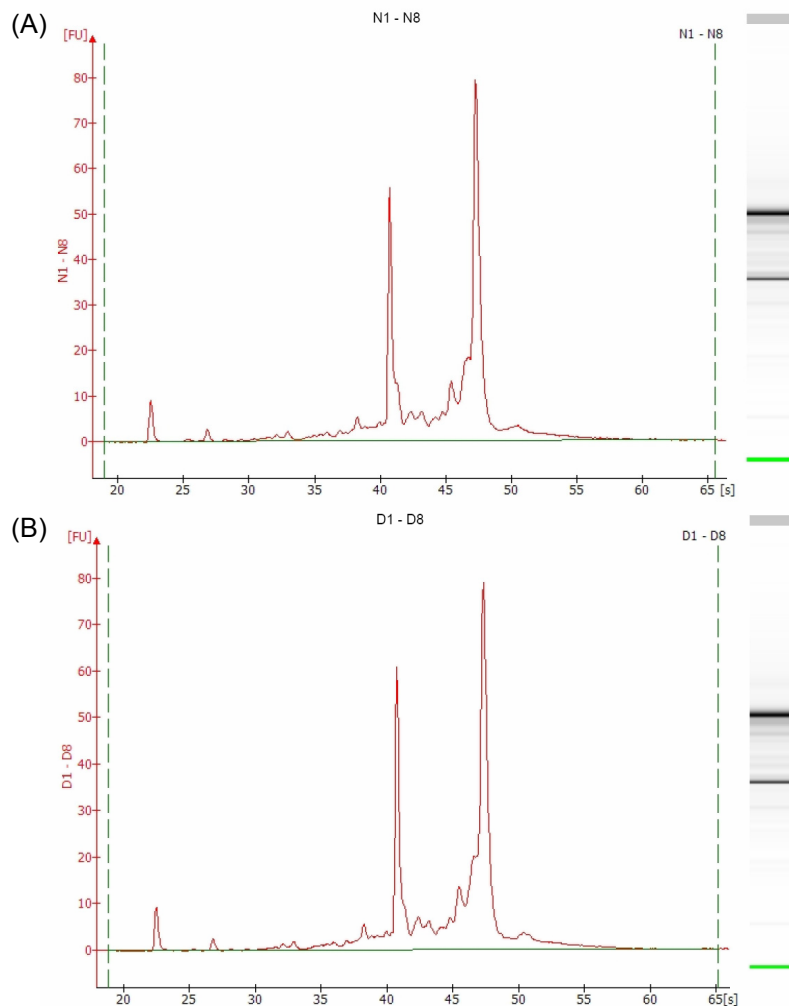
Figure 1.i Bioanalyzer results for pooled RNA samples

RNA was extracted from LV heart tissue of diabetic (n=8) or sham (n=8) male Wistar rats (Section 2.2.2.1) and then pooled. Samples were tested for degradation using the Agilent Bioanalyzer (methods Section 2.2.2.3) after being shipped to Melbourne for use in the Agilent Microarray trial.
   (A) RNA trace from Sham animals (pooled N1-N8)
   (B) RNA treace from Diabetic animals (pooled D1-D8)

Appendix 2: Statistical Analysis of Iatroscan Data

2.i Exclusion criteria

Results presented in Chapter Five (Figure 5.4) indicated that increased body weight is associated with improved animal health. It was decided that animal weight might also be significantly related to tissue lipid levels, particularly among the diabetic animals. In light of this hypothesis, a weight analysis (repeated measures ANOVA) was performed on all the diabetic animals (Figure 2.i) to identify, and allow for the exclusion of any animals that showed abnormal weight profiles over time. This analysis did not include animal #21 which had already been excluded on the basis of weight (Section 6.2.2.1).

From this analysis, four animals were identified that had significantly increased weight profiles compared to the average weight of the diabetic group. These were animals 8, 42,145,168.
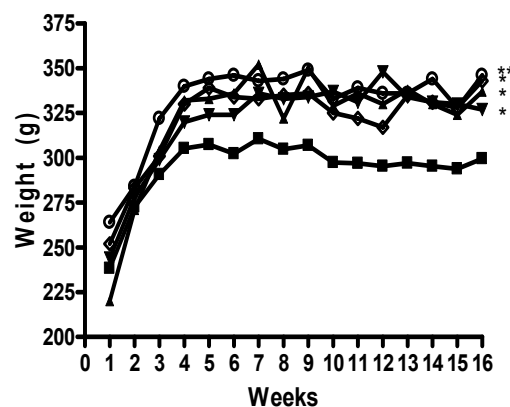
Figure 2.i Diabetic untreated group weight analysis

Male Wistar rats (220-250g) anesthetised using 5% isoflurane, 2l/min O_2, and 60mg/kg streptozotocin (STZ) dissolved in saline was immediately injected into the tail vein to induce diabetes. Animals were housed in pairs on fibrecycle bedding (12 hr light:dark cycle, 50-70 % humidity, 19-21 °C) and maintained on Teklad TB 2018 (Harlan, UK) rat chow and tap water *ad libitum*. Animals were weighed weekly for the sixteen week duration of the study. Average weight of the diabetic-untreated group over sixteen weeks (■, n=18) was plotted against weights of individual animals 8 (▲), 42 (▼), 145 (○) and 168 (◇).Repeated measures ANOVA Time P<.0001, weight P<.0001. Inter-animal differences were assessed by Tukey's *post-hoc* test * P<0.05, **P<0.01

2.ii Statistical analysis of Iatroscan TG data with and without excluded animals

Analysis was conducted on all lipid classes. Presented here are the results for the TG values only, as the other three lipid classes (FFA, cholesterol and phospholipid) were found to have no significant difference even at the level of diabetic vs. sham. Table 1.i presents the covariance parameters for the mixed model analysis of TG values when applied to the entire data set.

Table 2.i Covariance parameter estimates (all data)

Set	0.03546
Rat (Set)	0.07761
pseudoRun(Set)	0.005137
Residual	0.01117

As outlined in Table 1.ii the results from the first mixed model analysis of all the data found that there was a significant effect of status on TG levels in the heart tissue (P<0.0001); however, the effect of treatment was not significant (P=0.2263).

Table 2.ii Mixed model ANOVA table (Type III error) all data

Type III Tests of Fixed Effects				
Effect	Num DF	Den DF	F value	Pr>F
Status	**1**	**25.3**	**37.53**	**<.0001**
Treatment	1	21.6	1.55	0.2263
Status*Treatment	1	21.6	0.00	0.9722

A second mixed model analysis was then applied to the data for which the exclusion criterion was applied and data from animals 8, 42, 145 and 168 was removed. Table 1.iii outlines the new covariance estimates and Table 2.iv outlines the new ANOVA results for the TG data. It should be noted that removal of the data from these four animals in the other three lipid classes (FFA, cholesterol and phospholipid) was found to have no effect.

Table 2.iii Covariance parameter estimates (rat 8, 42, 145 and 168 data excluded)

| Set	0.04322
Rat (Set)	0.04023
pseudoRun(Set)	0.003071
Residual	0.01290

Table 2.iv Mixed model ANOVA table (Type III error), rat 8, 42, 145 and 168 data excluded)

Type III Tests of Fixed Effects				
Effect	Num DF	Den DF	F value	Pr>F
Status	**1**	**20.1**	**82.33**	**<.0001**
Treatment	**1**	**17.7**	**6.80**	**0.0179**
Status*Treatment	1	18.4	1.14	0.3002

The removal of rats 8, 42, 145 and 168 from the TG data set resulted in a significant effect of both Status (P<.0001) and Treatment (P=0.0179) and implies that body weight may have an effect of the level of TG present in the heart tissue.

2.iii Pearson's correlation analysis of lipid level and final body weight

An analysis was conducted to determine if there was an observable correlation between the final weight of an animal in our study and cardiac tissue TG level. Data correlation graph is presented in Figure 2.ii below.
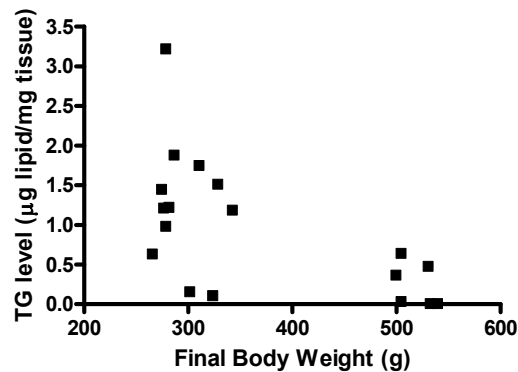
Figure 2.ii Correlation analysis between animal tissue TG level and final body weight

16 weeks after injection with either STZ (Diabetic) or saline (Sham) male Wistar rats were placed in an induction box with halothane 5%, O_2 2l/min. Once under anaesthetic animals were weighed (Final BW). Animals were thereafter maintained on halothane 2-3%, O_2 2l/min and complete anaesthesia was confirmed by testing pedal withdrawal (reflex absent). Animals were euthanized by cervical dislocation, a mid-line laprotomy was performed and hearts were excised in a laminar flow hood as described in Section 2.3.1.2. Iatroscan analysis of lipid classes present in heart tissue was conducted as described in Section 2.10. Data represents all untreated animals from the study.

Results of the Pearson's correlation analysis indicated a significant negative correlation between final body weight and heart TG levels of untreated animals (Pearson's r value of -0.6085, P=0.0074). It appears that as the weight of the animal increases the level of TG in the tissue decreases.

Reference

(2001). Beckman Coulter Synchron CX5CE/CX5 DELTA Clinical Systems Operating Instructions.

(2001). Beckman Coulter Synchron CX® Systems Chemistry Information Manual.

(2002). "MRC/BHF Heart Protection Study of antioxidant vitamin supplementation in 20,536 high-risk individuals: a randomised placebo-controlled trial." Lancet **360**(9326): 23-33.

(2006). Laboratory Handbook. Auckland, Auckland District Health Board.

Abercrombie, M. (1980). "The Croonian Lecture, 1978: The Crawling Movement of Metazoan Cells." Proceedings of the Royal Society of London. Series B, Biological Sciences **207**(1167): 129-147.

Affymetrix (2001). "GeneChip Arrays Provide Optimal Sensitivity and Specificity for Microarray Expression Analysis." Affymetrix Technical Note, Gene Expression Monitoring.

Affymetrix (2004). "Sample Tooling for Microarray Analysis: A Statistical Assesment of Risks and Biases." Affymetrix Technical Note, Gene Expression Monitoring.

Aguilar, M. V., J. M. Laborda, M. C. Martinez-Para, M. J. Gonzalez, I. Meseguer, A. Bernao and C. J. Mateos (1998). "Effect of diabetes on the tissular Zn/Cu ratio." J Trace Elem Med Biol **12**(3): 155-8.

Aitman, T. J., A. M. Glazier, C. A. Wallace, L. D. Cooper, P. J. Norsworthy, F. N. Wahid, K. M. Al-Majali, P. M. Trembling, C. J. Mann, C. C. Shoulders, D. Graf, E. St Lezin, T. W. Kurtz, V. Kren, M. Pravenec, A. Ibrahimi, N. A. Abumrad, L. W. Stanton and J. Scott (1999). "Identification of Cd36 (Fat) as an insulin-resistance gene causing defective fatty acid and glucose metabolism in hypertensive rats." Nat Genet **21**(1): 76-83.

Alavaikko, M., R. Elfving, J. Hirvonen and J. Jarvi (1973). "Triglycerides, cholesterol, and phospholipids in normal heart papillary muscle and in patients suffering from diabetes, cholelithiasis, hypertension, and coronary atheroma." J Clin Pathol **26**(4): 285-93.

Alberti, K. G. and P. Z. Zimmet (1998). "Definition, diagnosis and classification of diabetes mellitus and its complications. Part 1: diagnosis and classification of diabetes mellitus provisional report of a WHO consultation." Diabet Med **15**(7): 539-53.

Arsalane, K., C. M. Dubois, T. Muanza, R. Begin, F. Boudreau, C. Asselin and A. M. Cantin (1997). "Transforming growth factor-beta1 is a potent inhibitor of glutathione synthesis in the lung epithelial cell line A549: transcriptional effect on the GSH rate-limiting enzyme gamma-glutamylcysteine synthetase." American Journal of Respiratory Cell & Molecular Biology. **17**(5): 599-607.

Ashburner, M., C. A. Ball, J. A. Blake, D. Botstein, H. Butler, J. M. Cherry, A. P. Davis, K. Dolinski, S. S. Dwight, J. T. Eppig, M. A. Harris, D. P. Hill, L. Issel-Tarver, A. Kasarskis, S. Lewis, J. C. Matese, J. E. Richardson, M. Ringwald, G. M. Rubin and G. Sherlock (2000). "Gene ontology: tool for the unification of biology. The Gene Ontology Consortium." Nat Genet **25**(1): 25-9.

Benjamini, Y. and Y. Hochberg (1995). "Controlling False Discovery Rate - A practical and powerful approach to multiple testing." Journal of the Royal Statistical Society **Series B**(57): 289-300.

Bennett, R. A. and A. E. Pegg (1981). "Alkylation of DNA in rat tissues following administration of streptozotocin." Cancer Res **41**(7): 2786-90.

Blanchard, A. P., R. J. Kaiser and L. E. Hood (1996). "High-density oligonucleotide arrays." Biosensors and Bioelectronics **11**(6/7): 687-690.

Brand, M. D. and T. C. Esteves (2005). "Physiological functions of the mitochondrial uncoupling proteins UCP2 and UCP3." Cell Metab **2**(2): 85-93.

Brazma, A., P. Hingamp, J. Quackenbush, G. Sherlock, P. Spellman, C. Stoeckert, J. Aach, W. Ansorge, C. A. Ball, H. C. Causton, T. Gaasterland, P. Glenisson, F. C. Holstege, I. F. Kim, V. Markowitz, J. C. Matese, H. Parkinson, A. Robinson, U. Sarkans, S. Schulze-Kremer, J. Stewart, R. Taylor, J. Vilo and M. Vingron (2001). "Minimum information about a microarray experiment (MIAME)-toward standards for microarray data." Nat Genet **29**(4): 365-71.

Brownlee, M. (2001). "Biochemistry and molecular cell biology of diabetic complications." Nature. **414**(6865): 813-20.

Brownlee, M. (2005). "The pathobiology of diabetic complications: a unifying mechanism." Diabetes **54**(6): 1615-25.

Bull, P. C., G. R. Thomas, J. M. Rommens, J. R. Forbes and D. W. Cox (1993). "The Wilson disease gene is a putative copper transporting P-type ATPase similar to the Menkes gene." Nat Genet **5**(4): 327-37.

Bulteau, A. L., L. I. Szweda and B. Friguet (2006). "Mitochondrial protein oxidation and degradation in response to oxidative stress and aging." Exp Gerontol **41**(7): 653-7.

Cameron, N. E. and M. A. Cotter (1995). "Neurovascular dysfunction in diabetic rats. Potential contribution of autoxidation and free radicals examined using transition metal chelating agents." J Clin Invest **96**(2): 1159-63.

Candido, R., J. M. Forbes, M. C. Thomas, V. Thallas, R. G. Dean, W. C. Burns, C. Tikellis, R. H. Ritchie, S. M. Twigg, M. E. Cooper and L. M. Burrell (2003). "A breaker of advanced glycation end products attenuates diabetes-induced myocardial structural changes.[comment]." Circulation Research. **92**(7): 785-92.

Cardozo, A. K., H. Heimberg, Y. Heremans, R. Leeman, B. Kutlu, M. Kruhoffer, T. Orntoft and D. L. Eizirik (2001). "A comprehensive analysis of cytokine-induced and nuclear factor-kappa B-dependent genes in primary rat pancreatic beta-cells." J Biol Chem **276**(52): 48879-86.

Castro-Chavez, F., V. K. Yechoor, P. K. Saha, J. Martinez-Botas, E. C. Wooten, S. Sharma, P. O'Connell, H. Taegtmeyer and L. Chan (2003). "Coordinated upregulation of oxidative pathways and downregulation of lipid biosynthesis underlie obesity resistance in perilipin knockout mice: a microarray gene expression profile." Diabetes **52**(11): 2666-74.

Changani, K. K., A. Nicholson, A. White, J. K. Latcham, D. G. Reid and J. C. Clapham (2003). "A longitudinal magnetic resonance imaging (MRI) study of differences in abdominal fat distribution between normal mice, and lean overexpressers of mitochondrial uncoupling protein-3 (UCP-3)." Diabetes Obes Metab **5**(2): 99-105.

Chen, S., T. Evans, K. Mukherjee, M. Karmazyn and S. Chakrabarti (2000). "Diabetes-induced myocardial structural changes: role of endothelin-1 and its receptors." Journal of Molecular & Cellular Cardiology. **32**(9): 1621-9.

Chen, S., Z. A. Khan, M. Cukiernik and S. Chakrabarti (2003). "Differential activation of NF-kappa B and AP-1 in increased fibronectin synthesis in target organs of diabetic complications." American Journal of Physiology - Endocrinology & Metabolism. **284**(6): E1089-97.

Chen, X., S. T. Cheung, S. So, S. T. Fan, C. Barry, J. Higgins, K. M. Lai, J. Ji, S. Dudoit, I. O. Ng, M. Van De Rijn, D. Botstein and P. O. Brown (2002). "Gene expression patterns in human liver cancers." Mol Biol Cell **13**(6): 1929-39.

Chen, Y., E. R. Dougherty and M. L. Bittner (1997). "Ratio based decisons and the quantitative analysis of cDNA microarray images." Journal of Biomedical Optics **2**(4): 364-374.

Christoffersen, C., E. Bollano, M. L. Lindegaard, E. D. Bartels, J. P. Goetze, C. B. Andersen and L. B. Nielsen (2003). "Cardiac lipid accumulation associated with diastolic dysfunction in obese mice." Endocrinology **144**(8): 3483-90.

Chuaqui, R. F., R. F. Bonner, C. J. Best, J. W. Gillespie, M. J. Flaig, S. M. Hewitt, J. L. Phillips, D. B. Krizman, M. A. Tangrea, M. Ahram, W. M. Linehan, V. Knezevic and M. R. Emmert-Buck (2002). "Post-analysis follow-up and validation of microarray experiments." Nat Genet **32 Suppl**: 509-14.

Clapham, J. C., V. H. Coulthard and G. B. Moore (2001). "Concordant mRNA expression of UCP-3, but not UCP-2, with mitochondrial thioesterase-1 in brown adipose tissue and skeletal muscle in db/db diabetic mice." Biochem Biophys Res Commun **287**(5): 1058-62.

Colombo, M., M. Kruhoeffer, S. Gregersen, A. Agger, P. Jeppesen, T. Oerntoft and K. Hermansen (2006). "Energy restriction prevents the development of type 2 diabetes in Zucker diabetic fatty rats: coordinated patterns of gene expression for energy metabolism in insulin-sensitive tissues and pancreatic islets determined by oligonucleotide microarray analysis." Metabolism **55**(1): 43-52.

Cook, G. A., T. L. Edwards, M. S. Jansen, S. W. Bahouth, H. G. Wilcox and E. A. Park (2001). "Differential regulation of carnitine palmitoyltransferase-I gene isoforms (CPT-I alpha and CPT-I beta) in the rat heart." J Mol Cell Cardiol **33**(2): 317-29.

Cook, G. A. and M. S. Gamble (1987). "Regulation of carnitine palmitoyltransferase by insulin results in decreased activity and decreased apparent Ki values for malonyl-CoA." J Biol Chem **262**(5): 2050-5.

Cooper, C. and A. L. Lehninger (1956). "Oxidative phosphorylation by an enzyme complex from extracts of mitochondria. I. The span beta-hydroxybutyrate to oxygen." J Biol Chem **219**(1): 489-506.

Cooper, C. and A. L. Lehninger (1956). "Oxidative phosphorylation by an enzyme complex from extracts of mitochondria. III. The span cytochrome c to oxygen." J Biol Chem **219**(1): 519-29.

Reference

Cooper, C. and A. L. Lehninger (1957). "Oxidative phosphorylation by an enzyme complex from extracts of mitochondria. IV. Adenosinetriphosphatase activity." J Biol Chem **224**(1): 547-60.

Cooper, C. and A. L. Lehninger (1957). "Oxidative phosphorylation by an enzyme complex from extracts of mitochondria. V. The adenosine triphosphate-phosphate exchange reaction." J Biol Chem **224**(1): 561-78.

Cooper, G. J., Y. K. Chan, A. M. Dissanayake, F. E. Leahy, G. F. Keogh, C. M. Frampton, G. D. Gamble, D. H. Brunton, J. R. Baker and S. D. Poppitt (2005). "Demonstration of a hyperglycemia-driven pathogenic abnormality of copper homeostasis in diabetes and its reversibility by selective chelation: quantitative comparisons between the biology of copper and eight other nutritionally essential elements in normal and diabetic individuals." Diabetes **54**(5): 1468-76.

Cooper, G. J., A. R. Phillips, S. Y. Choong, B. L. Leonard, D. J. Crossman, D. H. Brunton, L. Saafi, A. M. Dissanayake, B. R. Cowan, A. A. Young, C. J. Occleshaw, Y. K. Chan, F. E. Leahy, G. F. Keogh, G. D. Gamble, G. R. Allen, A. J. Pope, P. D. Boyd, S. D. Poppitt, T. K. Borg, R. N. Doughty and J. R. Baker (2004). "Regeneration of the heart in diabetes by selective copper chelation." Diabetes **53**(9): 2501-8.

Cramer, L. P., M. Siebert and T. J. Mitchison (1997). "Identification of novel graded polarity actin filament bundles in locomoting heart fibroblasts: implications for the generation of motile force." J Cell Biol **136**(6): 1287-305.

Cuestas, R. and P. K. Dixit (1973). "Citrate metabolic enzymes in alloxan diabetes." Proc Soc Exp Biol Med **142**(3): 889-95.

Culotta, V. C., L. W. Klomp, J. Strain, R. L. Casareno, B. Krems and J. D. Gitlin (1997). "The copper chaperone for superoxide dismutase." J Biol Chem **272**(38): 23469-72.

Curtis, R. K., M. Oresic and A. Vidal-Puig (2005). "Pathways to the analysis of microarray data." Trends Biotechnol **23**(8): 429-35.

D'Elia, J. A., L. A. Weinrauch, R. W. Healy, J. A. Libertino, R. F. Bradley and O. S. Leland, Jr. (1979). "Myocardial dysfunction without coronary artery disease in diabetic renal failure." Am J Cardiol **43**(2): 193-9.

Dameron, C. T. and E. D. Harris (1987). "Regulation of aortic CuZn-superoxide dismutase with copper. Caeruloplasmin and albumin re-activate and transfer copper to the enzyme in culture." Biochem J **248**(3): 669-75.

Dancis, A., D. S. Yuan, D. Haile, C. Askwith, D. Eide, C. Moehle, J. Kaplan and R. D. Klausner (1994). "Molecular characterization of a copper transport protein in S. cerevisiae: an unexpected role for copper in iron transport." Cell **76**(2): 393-402.

de Cavanagh, E. M., F. Inserra, J. Toblli, I. Stella, C. G. Fraga and L. Ferder (2001). "Enalapril attenuates oxidative stress in diabetic rats." Hypertension **38**(5): 1130-6.

DeGrado, T. R., M. T. Kitapci, S. Wang, J. Ying and G. D. Lopaschuk (2006). "Validation of 18F-fluoro-4-thia-palmitate as a PET probe for myocardial fatty acid oxidation: effects of hypoxia and composition of exogenous fatty acids." J Nucl Med **47**(1): 173-81.

DeGrado, T. R., S. Wang, J. E. Holden, R. J. Nickles, M. Taylor and C. K. Stone (2000). "Synthesis and preliminary evaluation of (18)F-labeled 4-thia palmitate as a PET tracer of myocardial fatty acid oxidation." Nucl Med Biol **27**(3): 221-31.

Depre, C., M. E. Young, J. Ying, H. S. Ahuja, Q. Han, N. Garza, P. J. Davies and H. Taegtmeyer (2000). "Streptozotocin-induced changes in cardiac gene expression in the absence of severe contractile dysfunction." J Mol Cell Cardiol **32**(6): 985-96.

Devi, S. S. and H. M. Mehendale (2006). "Microarray analysis of thioacetamide-treated type 1 diabetic rats." Toxicol Appl Pharmacol **212**(1): 69-78.

Devlin, T. M. and A. L. Lehninger (1956). "Oxidative phosphorylation by an enzyme complex from extracts of mitochondria. II. The span beta-hydroxybutyrate to cytochrome c." J Biol Chem **219**(1): 507-18.

Dhahbi, J. M., P. L. Mote, S. X. Cao and S. R. Spindler (2003). "Hepatic gene expression profiling of streptozotocin-induced diabetes." Diabetes Technol Ther **5**(3): 411-20.

Dickinson, E. K., D. L. Adams, E. A. Schon and D. M. Glerum (2000). "A human SCO2 mutation helps define the role of Sco1p in the cytochrome oxidase assembly pathway." J Biol Chem **275**(35): 26780-5.

Doi, K., F. Sawada, G. Toda, S. Yamachika, S. Seto, Y. Urata, Y. Ihara, N. Sakata, N. Taniguchi, T. Kondo and K. Yano (2001). "Alteration of antioxidants during the progression of heart disease in streptozotocin-induced diabetic rats." Free Radic Res **34**(3): 251-61.

Doniger, S. W., N. Salomonis, K. D. Dahlquist, K. Vranizan, S. C. Lawlor and B. R. Conklin (2003). "MAPPFinder: using Gene Ontology and GenMAPP to create a global gene-expression profile from microarray data." Genome Biol **4**(1): R7.

Douillet, C., M. Bost, M. Accominotti, F. Borson-Chazot and M. Ciavatti (1998). "Effect of selenium and vitamin E supplements on tissue lipids, peroxides, and fatty acid distribution in experimental diabetes." Lipids **33**(4): 393-9.

Draghici, S., P. Khatri, R. P. Martins, G. C. Ostermeier and S. A. Krawetz (2003). "Global functional profiling of gene expression." Genomics **81**(2): 98-104.

Du, X., T. Matsumura, D. Edelstein, L. Rossetti, Z. Zsengeller, C. Szabo and M. Brownlee (2003). "Inhibition of GAPDH activity by poly(ADP-ribose) polymerase activates three major pathways of hyperglycemic damage in endothelial cells." J Clin Invest **112**(7): 1049-57.

Du, X. L., D. Edelstein, L. Rossetti, I. G. Fantus, H. Goldberg, F. Ziyadeh, J. Wu and M. Brownlee (2000). "Hyperglycemia-induced mitochondrial superoxide overproduction activates the hexosamine pathway and induces plasminogen activator inhibitor-1 expression by increasing Sp1 glycosylation." Proc Natl Acad Sci U S A **97**(22): 12222-6.

Dudoit, S., J. P. Shaffer and J. C. Boldrick (2002). "Multiple hypothesis testing in microarray experiments." U.C. Berkelely Division of Biostatistics Working Paper Series **Paper 110**: 58.

Eaton, J. W. and M. Qian (2002). "Interactions of copper with glycated proteins: possible involvement in the etiology of diabetic neuropathy." Mol Cell Biochem **234-235**(1-2): 135-42.

Eckel, R. H. (1989). "Lipoprotein lipase. A multifunctional enzyme relevant to common metabolic diseases." N Engl J Med **320**(16): 1060-8.

Ekstrand, M. I., M. Falkenberg, A. Rantanen, C. B. Park, M. Gaspari, K. Hultenby, P. Rustin, C. M. Gustafsson and N. G. Larsson (2004). "Mitochondrial transcription factor A regulates mtDNA copy number in mammals." Hum Mol Genet **13**(9): 935-44.

Elsner, M., B. Guldbakke, M. Tiedge, R. Munday and S. Lenzen (2000). "Relative importance of transport and alkylation for pancreatic beta-cell toxicity of streptozotocin." Diabetologia **43**(12): 1528-33.

Fang, Z. Y., J. B. Prins and T. H. Marwick (2004). "Diabetic cardiomyopathy: evidence, mechanisms, and therapeutic implications." Endocr Rev **25**(4): 543-67.

Farah, A. E. and A. A. Alousi (1981). "The actions of insulin on cardiac contractility." Life Sci **29**(10): 975-1000.

Farhangkhoee, H., Z. A. Khan, Y. Barbin and S. Chakrabarti (2005). "Glucose-induced up-regulation of CD36 mediates oxidative stress and microvascular endothelial cell dysfunction." Diabetologia **48**(7): 1401-10.

Fedorak, R. N., E. B. Chang, J. L. Madara and M. Field (1987). "Intestinal adaptation to diabetes. Altered Na-dependent nutrient absorption in streptozocin-treated chronically diabetic rats." J Clin Invest **79**(6): 1571-8.

Fein, F. S., L. B. Kornstein, J. E. Strobeck, J. M. Capasso and E. H. Sonnenblick (1980). "Altered myocardial mechanics in diabetic rats." Circ Res **47**(6): 922-33.

Ferrante, A. W., Jr., M. Thearle, T. Liao and R. L. Leibel (2001). "Effects of leptin deficiency and short-term repletion on hepatic gene expression in genetically obese mice." Diabetes **50**(10): 2268-78.

Firestein, G. S. and D. S. Pisetsky (2002). "DNA microarrays: boundless technology or bound by technology? Guidelines for studies using microarray technology." Arthritis Rheum **46**(4): 859-61.

Fodor, S. P., J. L. Read, M. C. Pirrung, L. Stryer, A. T. Lu and D. Solas (1991). "Light-directed, spatially addressable parallel chemical synthesis." Science **251**(4995): 767-73.

Foltz, C. J. and M. Ullman-Cullere (1999). "Guidelines for Assessing the Health and Condition of Mice." Lab Animal **28**(4): 28-32.

Frausto da Silva, J. J. and R. J. P. Williams (2001). The biological chemistry of the elements: The inorganic chemistry of life. Oxford, UK., Oxford University Press.

Galderisi, M., K. M. Anderson, P. W. Wilson and D. Levy (1991). "Echocardiographic evidence for the existence of a distinct diabetic cardiomyopathy (the Framingham Heart Study)." Am J Cardiol **68**(1): 85-9.

Gauthier, B. R., T. Brun, E. J. Sarret, H. Ishihara, O. Schaad, P. Descombes and C. B. Wollheim (2004). "Oligonucleotide microarray analysis reveals PDX1 as an essential regulator of mitochondrial metabolism in rat islets." J Biol Chem **279**(30): 31121-30.

Gautier, L., L. Cope, B. M. Bolstad and R. A. Irizarry (2004). "affy--analysis of Affymetrix GeneChip data at the probe level." Bioinformatics **20**(3): 307-15.

Ge, H., G. Yang, L. Huang, D. L. Motola, T. Pourbahrami and C. Li (2004). "Oligomerization and regulated proteolytic processing of angiopoietin-like protein 4." J Biol Chem **279**(3): 2038-45.

Ge, Y., S. Dudoit and T. P. Speed (2003). "Resampling-based multiple testing for microarray data analysis, with discussion." TEST **12**(1): 78.

Reference

Gentleman, R. C., V. J. Carey, D. M. Bates, B. Bolstad, M. Dettling, S. Dudoit, B. Ellis, L. Gautier, Y. Ge, J. Gentry, K. Hornik, T. Hothorn, W. Huber, S. Iacus, R. Irizarry, F. Leisch, C. Li, M. Maechler, A. J. Rossini, G. Sawitzki, C. Smith, G. Smyth, L. Tierney, J. Y. Yang and J. Zhang (2004). "Bioconductor: open software development for computational biology and bioinformatics." Genome Biol **5**(10): R80.

Georgatsou, E., L. A. Mavrogiannis, G. S. Fragiadakis and D. Alexandraki (1997). "The yeast Fre1p/Fre2p cupric reductases facilitate copper uptake and are regulated by the copper-modulated Mac1p activator." J Biol Chem **272**(21): 13786-92.

Gibbs, K. R. and J. M. Walshe (1986). The metabolism of trientine:animal studies. Orphan Diseases and Orphan Drugs. I. H. Scheinberg and J. M. Walshe. Manchester, Manchester University Press in Association with the Fullbright Commission.

Glatz, J. F., E. van Breda, H. A. Keizer, Y. F. de Jong, J. R. Lakey, R. V. Rajotte, A. Thompson, G. J. van der Vusse and G. D. Lopaschuk (1994). "Rat heart fatty acid-binding protein content is increased in experimental diabetes." Biochem Biophys Res Commun **199**(2): 639-46.

Glerum, D. M., A. Shtanko and A. Tzagoloff (1996). "Characterization of COX17, a yeast gene involved in copper metabolism and assembly of cytochrome oxidase." J Biol Chem **271**(24): 14504-9.

Glyn-Jones, S., S. Song, M. A. Black, A. R. Phillips, S. Y. Choong and G. J. Cooper (2007). "Transcriptomic analysis of the cardiac left ventricle in a rodent model of diabetic cardiomyopathy: molecular snapshot of a severe myocardial disease." Physiol Genomics **28**(3): 284-93.

Gong, D., J. Lu, X. Chen, S. Y. Choong, S. Zhang, Y. K. Chan, S. Glyn-Jones, G. D. Gamble, A. R. Phillips and G. J. Cooper (2006). "Molecular changes evoked by triethylenetetramine treatment in the extracellular matrix of the heart and aorta in diabetic rats." Mol Pharmacol **70**(6): 2045-51.

Goodwin, G. W., C. S. Taylor and H. Taegtmeyer (1998). "Regulation of energy metabolism of the heart during acute increase in heart work." J Biol Chem **273**(45): 29530-9.

Greenspan, P., E. P. Mayer and S. D. Fowler (1985). "Nile red: a selective fluorescent stain for intracellular lipid droplets." J Cell Biol **100**(3): 965-73.

Greenwalt, D. E., S. H. Scheck and T. Rhinehart-Jones (1995). "Heart CD36 expression is increased in murine models of diabetes and in mice fed a high fat diet." J Clin Invest **96**(3): 1382-8.

Griendling, K. K., T. Tsuda and R. W. Alexander (1989). "Endothelin stimulates diacylglycerol accumulation and activates protein kinase C in cultured vascular smooth muscle cells." J Biol Chem **264**(14): 8237-40.

Guengerich, F. P. (1991). "Reactions and significance of cytochrome P-450 enzymes." J Biol Chem **266**(16): 10019-22.

Hanna, P. M. and R. P. Mason (1992). "Direct evidence for inhibition of free radical formation from Cu(I) and hydrogen peroxide by glutathione and other potential ligands using the EPR spin-trapping technique." Arch Biochem Biophys **295**(1): 205-13.

Hayat, S. A., B. Patel, R. S. Khattar and R. A. Malik (2004). "Diabetic cardiomyopathy: mechanisms, diagnosis and treatment." Clin Sci (Lond) **107**(6): 539-57.

He, J., B. H. Goodpaster and D. E. Kelley (2004). "Effects of weight loss and physical activity on muscle lipid content and droplet size." Obes Res **12**(5): 761-9.

Hers, H. G. (1976). "The control of glycogen metabolism in the liver." Annu Rev Biochem **45**: 167-89.

Holloway, A. J., R. K. van Laar, R. W. Tothill and D. D. Bowtell (2002). "Options available--from start to finish--for obtaining data from DNA microarrays II." Nat Genet **32 Suppl**: 481-9.

Holmberg, C. G. and C. B. Laurell (1948). "Investigations in serum copper. II. Isolation of the copper containing protein, and a description of some of its properties." Acta Chemica Scandinavica **2**: 550-556.

Hsieh, H. S. and E. Frieden (1975). "Evidence for ceruloplasmin as a copper transport protein." Biochem Biophys Res Commun **67**(4): 1326-31.

Huang, B., P. Wu, K. M. Popov and R. A. Harris (2003). "Starvation and diabetes reduce the amount of pyruvate dehydrogenase phosphatase in rat heart and kidney." Diabetes **52**(6): 1371-6.

Hughes, T. R., M. Mao, A. R. Jones, J. Burchard, M. J. Marton, K. W. Shannon, S. M. Lefkowitz, M. Ziman, J. M. Schelter, M. R. Meyer, S. Kobayashi, C. Davis, H. Dai, Y. D. He, S. B. Stephaniants, G. Cavet, W. L. Walker, A. West, E. Coffey, D. D. Shoemaker, R. Stoughton, A. P. Blanchard, S. H. Friend and P. S. Linsley (2001). "Expression profiling using microarrays fabricated by an ink-jet oligonucleotide synthesizer." Nat Biotechnol **19**(4): 342-7.

Reference

Ihaka, R. and R. C. Gentleman (1996). "R: A language for data analysis and graphics." Journal of Computational and Graphical Studies **5**(3): 299-314.

Inoguchi, T., R. Battan, E. Handler, J. R. Sportsman, W. Heath and G. L. King (1992). "Preferential elevation of protein kinase C isoform beta II and diacylglycerol levels in the aorta and heart of diabetic rats: differential reversibility to glycemic control by islet cell transplantation." Proc Natl Acad Sci U S A **89**(22): 11059-63.

Irizarry, R. A., B. Hobbs, F. Collin, Y. D. Beazer-Barclay, K. J. Antonellis, U. Scherf and T. P. Speed (2003). "Exploration, normalization, and summaries of high density oligonucleotide array probe level data." Biostatistics **4**(2): 249-64.

Iwata, K., T. Nishinaka, K. Matsuno and C. Yabe-Nishimura (2006). "Increased gene expression of glutathione peroxidase-3 in diabetic mouse heart." Biol Pharm Bull **29**(5): 1042-5.

Jaksch, M., C. Paret, R. Stucka, N. Horn, J. Muller-Hocker, R. Horvath, N. Trepesch, G. Stecker, P. Freisinger, C. Thirion, J. Muller, R. Lunkwitz, G. Rodel, E. A. Shoubridge and H. Lochmuller (2001). "Cytochrome c oxidase deficiency due to mutations in SCO2, encoding a mitochondrial copper-binding protein, is rescued by copper in human myoblasts." Hum Mol Genet **10**(26): 3025-35.

Jiang, J., C. M. St Croix, N. Sussman, Q. Zhao, B. R. Pitt and V. E. Kagan (2002). "Contribution of glutathione and metallothioneins to protection against copper toxicity and redox cycling: quantitative analysis using MT+/+ and MT-/- mouse lung fibroblast cells." Chem Res Toxicol **15**(8): 1080-7.

Jullig, M., X. Chen, A. Hickey, D. Crossman, A. Xu, Y. Wang, D. Greenwood, Y. Choong, S. Schonberger, M. Middleditch, A. Phillips and G. Cooper (2007). "Reversal of diabetes-evoked changes in mitochondrial protein expression of cardiac left ventricle by treatment with a copper(II)-selective chelator." Proteomics - Clinical Applications **1**(4): 387-399.

Junod, A., A. E. Lambert, L. Orci, R. Pictet, A. E. Gonet and A. E. Renold (1967). "Studies of the diabetogenic action of streptozotocin." Proc Soc Exp Biol Med **126**(1): 201-5.

Junod, A., A. E. Lambert, W. Stauffacher and A. E. Renold (1969). "Diabetogenic action of streptozotocin: relationship of dose to metabolic response." J Clin Invest **48**(11): 2129-39.

Kadiiska, M. B., P. M. Hanna, L. Hernandez and R. P. Mason (1992). "In vivo evidence of hydroxyl radical formation after acute copper and ascorbic acid intake: electron spin resonance spin-trapping investigation." Mol Pharmacol **42**(4): 723-9.

Kang, J. H. (2003). "Modification and inactivation of human Cu,Zn-superoxide dismutase by methylglyoxal." Mol Cells **15**(2): 194-9.

Kang, J. H., K. S. Kim, S. Y. Choi, H. Y. Kwon and M. H. Won (2001). "Oxidative modification of human ceruloplasmin by peroxyl radicals." Biochim Biophys Acta **1568**(1): 30-6.

Kannel, W. B. and D. L. McGee (1979). "Diabetes and cardiovascular risk factors: the Framingham study." Circulation **59**(1): 8-13.

Karpova, T., S. Danchuk, E. Kolobova and K. M. Popov (2003). "Characterization of the isozymes of pyruvate dehydrogenase phosphatase: implications for the regulation of pyruvate dehydrogenase activity." Biochim Biophys Acta **1652**(2): 126-35.

Kaul, N., N. Siveski-Iliskovic, M. Hill, N. Khaper, C. Seneviratne and P. K. Singal (1996). "Probucol treatment reverses antioxidant and functional deficit in diabetic cardiomyopathy." Mol Cell Biochem **160-161**: 283-8.

Keegan, A., M. A. Cotter and N. E. Cameron (1999). "Effects of chelator treatment on aorta and corpus cavernosum from diabetic rats." Free Radic Biol Med **27**(5-6): 536-43.

Kersten, S. (2005). "Regulation of lipid metabolism via angiopoietin-like proteins." Biochem Soc Trans **33**(Pt 5): 1059-62.

Knight, S. A., S. Labbe, L. F. Kwon, D. J. Kosman and D. J. Thiele (1996). "A widespread transposable element masks expression of a yeast copper transport gene." Genes Dev **10**(15): 1917-29.

Knoll, K. E., J. L. Pietrusz and M. Liang (2005). "Tissue-specific transcriptome responses in rats with early streptozotocin-induced diabetes." Physiol Genomics **21**(2): 222-9.

Kodama, H., Y. Meguro, A. Tsunakawa, Y. Nakazato, T. Abe and H. Murakita (1993). "Fate of orally administered triethylenetetramine dihydrochloride: a therapeutic drug for Wilson's disease." Tohoku J Exp Med **169**(1): 59-66.

Kodama, H., Y. Murata, T. Iitsuka and T. Abe (1997). "Metabolism of administered triethylene tetramine dihydrochloride in humans." Life Sci **61**(9): 899-907.

Kolm-Litty, V., U. Sauer, A. Nerlich, R. Lehmann and E. D. Schleicher (1998). "High glucose-induced transforming growth factor beta1 production is mediated by the hexosamine pathway in porcine glomerular mesangial cells." J Clin Invest **101**(1): 160-9.

Konarska, M. M. (1998). "Recognition of the 5' splice site by the spliceosome." Acta Biochim Pol **45**(4): 869-81.

Kopp, S. J., L. M. Klevay and J. M. Feliksik (1983). "Physiological and metabolic characterization of a cardiomyopathy induced by chronic copper deficiency." Am J Physiol **245**(5 Pt 1): H855-66.

Koya, D. and G. L. King (1998). "Protein kinase C activation and the development of diabetic complications." Diabetes **47**(6): 859-66.

Kramer, J. K., E. R. Farnworth and B. K. Thompson (1985). "Quantitating heart lipids: comparison of results obtained using the Iatroscan method with those from phosphorus and gas chromatographic techniques." Lipids **20**(8): 536-41.

Krebs, H. A. (1972). "Some aspects of the regulation of fuel supply in omnivorous animals." Adv Enzyme Regul **10**: 397-420.

La Fontaine, S. L., S. D. Firth, J. Camakaris, A. Englezou, M. B. Theophilos, M. J. Petris, M. Howie, P. J. Lockhart, M. Greenough, H. Brooks, R. R. Reddel and J. F. Mercer (1998). "Correction of the copper transport defect of Menkes patient fibroblasts by expression of the Menkes and Wilson ATPases." J Biol Chem **273**(47): 31375-80.

Labbe, S., M. M. Pena, A. R. Fernandes and D. J. Thiele (1999). "A copper-sensing transcription factor regulates iron uptake genes in Schizosaccharomyces pombe." J Biol Chem **274**(51): 36252-60.

Larkin, J. E., B. C. Frank, H. Gavras, R. Sultana and J. Quackenbush (2005). "Independence and reproducibility across microarray platforms." Nat Methods **2**(5): 337-44.

Lau, A. L. and M. L. Failla (1984). "Urinary excretion of zinc, copper and iron in the streptozotocin-diabetic rat." J Nutr **114**(1): 224-33.

Leary, S. C., B. A. Kaufman, G. Pellecchia, G. H. Guercin, A. Mattman, M. Jaksch and E. A. Shoubridge (2004). "Human SCO1 and SCO2 have independent, cooperative functions in copper delivery to cytochrome c oxidase." Hum Mol Genet **13**(17): 1839-48.

Lee, G. R., S. Nacht, J. N. Lukens and G. E. Cartwright (1968). "Iron metabolism in copper-deficient swine." J Clin Invest **47**(9): 2058-69.

Lehti, T. M., M. Silvennoinen, R. Kivela, H. Kainulainen and J. Komulainen (2006). "Effects of streptozotocin-induced diabetes and physical training on gene expression of extracellular matrix proteins in mouse skeletal muscle." Am J Physiol Endocrinol Metab **290**(5): E900-7.

Lewis, D. F. (2001). Guide to Cytochromes P450. London, England, Taylor and Francis.

Lin, S. J. and V. C. Culotta (1995). "The ATX1 gene of Saccharomyces cerevisiae encodes a small metal homeostasis factor that protects cells against reactive oxygen toxicity." Proc Natl Acad Sci U S A **92**(9): 3784-8.

Lin, S. J., R. A. Pufahl, A. Dancis, T. V. O'Halloran and V. C. Culotta (1997). "A role for the Saccharomyces cerevisiae ATX1 gene in copper trafficking and iron transport." J Biol Chem **272**(14): 9215-20.

Littell, R. C., G. A. Lilliken, W. W. Stroup, R. D. Wolfinger and O. Schabenberger (2006). SAS for Mixed Models. Cary, North Carolina, SAS Institute.

Litwin, S. E., T. E. Raya, P. G. Anderson, S. Daugherty and S. Goldman (1990). "Abnormal cardiac function in the streptozotocin-diabetic rat. Changes in active and passive properties of the left ventricle." J Clin Invest **86**(2): 481-8.

Lockhart, D. J., H. Dong, M. C. Byrne, M. T. Follettie, M. V. Gallo, M. S. Chee, M. Mittmann, C. Wang, M. Kobayashi, H. Horton and E. L. Brown (1996). "Expression monitoring by hybridization to high-density oligonucleotide arrays." Nat Biotechnol **14**(13): 1675-80.

Loftis, M. J., D. Sexton and W. Carver (2003). "Effects of collagen density on cardiac fibroblast behavior and gene expression." J Cell Physiol **196**(3): 504-11.

Lopaschuk, G. D. (2002). "Metabolic abnormalities in the diabetic heart." Heart Failure Reviews. **7**(2): 149-59.

Lu, J., Y. K. Chan, G. D. Gamble, S. D. Poppitt, A. A. Othman and G. J. Cooper (2007). "Triethylenetetramine and metabolites: levels in relation to copper and zinc excretion in urine of healthy volunteers and type 2 diabetic patients." Drug Metab Dispos **35**(2): 221-7.

Luiken, J. J., Y. Arumugam, R. C. Bell, J. Calles-Escandon, N. N. Tandon, J. F. Glatz and A. Bonen (2002). "Changes in fatty acid transport and transporters are related to the severity of insulin deficiency." Am J Physiol Endocrinol Metab **283**(3): E612-21.

Mahgoub, M. A. and A. S. Abd-Elfattah (1998). "Diabetes mellitus and cardiac function." Molecular & Cellular Biochemistry. **180**(1-2): 59-64.

Mathers, C. D. and D. Loncar (2006). "Projections of global mortality and burden of disease from 2002 to 2030." PLoS Med **3**(11): e442.

Mecham, B. H., G. T. Klus, J. Strovel, M. Augustus, D. Byrne, P. Bozso, D. Z. Wetmore, T. J. Mariani, I. S. Kohane and Z. Szallasi (2004). "Sequence-matched probes produce increased cross-platform consistency and more reproducible biological results in microarray-based gene expression measurements." Nucleic Acids Res **32**(9): e74.

Reference

Medeiros, D. M., D. Bagby, G. Ovecka and R. McCormick (1991). "Myofibrillar, mitochondrial and valvular morphological alterations in cardiac hypertrophy among copper-deficient rats." J Nutr **121**(6): 815-24.

Miller, T. B., Jr. (1979). "Cardiac performance of isolated perfused hearts from alloxan diabetic rats." Am J Physiol **236**(6): H808-12.

Milovic, V. (2001). "Polyamines in the gut lumen: bioavailability and biodistribution." Eur J Gastroenterol Hepatol **13**(9): 1021-5.

Moller, L. B., C. Petersen, C. Lund and N. Horn (2000). "Characterization of the hCTR1 gene: genomic organization, functional expression, and identification of a highly homologous processed gene." Gene **257**(1): 13-22.

Mootha, V. K., C. M. Lindgren, K. F. Eriksson, A. Subramanian, S. Sihag, J. Lehar, P. Puigserver, E. Carlsson, M. Ridderstrale, E. Laurila, N. Houstis, M. J. Daly, N. Patterson, J. P. Mesirov, T. R. Golub, P. Tamayo, B. Spiegelman, E. S. Lander, J. N. Hirschhorn, D. Altshuler and L. C. Groop (2003). "PGC-1alpha-responsive genes involved in oxidative phosphorylation are coordinately downregulated in human diabetes." Nat Genet **34**(3): 267-73.

Neely, J. R., M. J. Rovetto and J. F. Oram (1972). "Myocardial utilization of carbohydrate and lipids." Prog Cardiovasc Dis **15**(3): 289-329.

Neubauer, S. (2007). "The failing heart--an engine out of fuel." N Engl J Med **356**(11): 1140-51.

Newsholme, E. A. and B. Crabtree (1986). "Maximum catalytic activity of some key enzymes in provision of physiological useful information about metabolic fluxes." Journal of Experimental Zoology **239**: 159-163.

Newsholme, E. A. and C. Start (1973). Regulation of Metabolism. London, John Wiley and Sons Ltd.

Nielsen, L. B., E. D. Bartels and E. Bollano (2002). "Overexpression of apolipoprotein B in the heart impedes cardiac triglyceride accumulation and development of cardiac dysfunction in diabetic mice." J Biol Chem **277**(30): 27014-20.

Nishikawa, T., D. Edelstein, X. L. Du, S. Yamagishi, T. Matsumura, Y. Kaneda, M. A. Yorek, D. Beebe, P. J. Oates, H. P. Hammes, I. Giardino and M. Brownlee (2000). "Normalizing mitochondrial superoxide production blocks three pathways of hyperglycaemic damage." Nature. **404**(6779): 787-90.

Nishio, Y., A. Kashiwagi, H. Taki, K. Shinozaki, Y. Maeno, H. Kojima, H. Maegawa, M. Haneda, H. Hidaka, H. Yasuda, K. Horiike and R. Kikkawa (1998). "Altered activities of transcription factors and their related gene expression in cardiac tissues of diabetic rats." Diabetes. **47**(8): 1318-25.

Oakes, N. D. and S. M. Furler (2002). "Evaluation of free fatty acid metabolism in vivo." Ann N Y Acad Sci **967**: 158-75.

Orth, D. N. and H. E. Morgan (1962). "The effect of insulin, alloxan diabetes, and anoxia on the ultrastructure of the rat heart." J Cell Biol **15**: 509-23.

Othman, A., J. Lu, T. Sunderland and G. J. Cooper (2007). "Development and validation of a rapid HPLC method for the simultaneous determination of triethylenetetramine and its two main metabolites in human serum." J Chromatogr B Analyt Technol Biomed Life Sci **860**(1): 42-8.

Pacher, P., L. Liaudet, F. G. Soriano, J. G. Mabley, E. Szabo and C. Szabo (2002). "The role of poly(ADP-ribose) polymerase activation in the development of myocardial and endothelial dysfunction in diabetes." Diabetes **51**(2): 514-21.

Pande, S. V. (1975). "A mitochondrial carnitine acylcarnitine translocase system." Proc Natl Acad Sci U S A **72**(3): 883-7.

Papadopoulou, L. C., C. M. Sue, M. M. Davidson, K. Tanji, I. Nishino, J. E. Sadlock, S. Krishna, W. Walker, J. Selby, D. M. Glerum, R. V. Coster, G. Lyon, E. Scalais, R. Lebel, P. Kaplan, S. Shanske, D. C. De Vivo, E. Bonilla, M. Hirano, S. DiMauro and E. A. Schon (1999). "Fatal infantile cardioencephalomyopathy with COX deficiency and mutations in SCO2, a COX assembly gene." Nat Genet **23**(3): 333-7.

Park, P. J., Y. A. Cao, S. Y. Lee, J. W. Kim, M. S. Chang, R. Hart and S. Choi (2004). "Current issues for DNA microarrays: platform comparison, double linear amplification, and universal RNA reference." J Biotechnol **112**(3): 225-45.

Parrish, C. C. (1999). Determination of total lipid, lipid classes, and fatty acids in aquatic samples, Springer Netherlands.

Paynter, D. I., R. J. Moir and E. J. Underwood (1979). "Changes in activity of the Cu-Zn superoxide dismutase enzyme in tissues of the rat with changes in dietary copper." J Nutr **109**(9): 1570-6.

Pena, M. M., K. A. Koch and D. J. Thiele (1998). "Dynamic regulation of copper uptake and detoxification genes in Saccharomyces cerevisiae." Mol Cell Biol **18**(5): 2514-23.

Reference

Pena, M. M., J. Lee and D. J. Thiele (1999). "A delicate balance: homeostatic control of copper uptake and distribution." J Nutr **129**(7): 1251-60.

Penpargkul, S., T. Schaible, T. Yipintsoi and J. Scheuer (1980). "The effect of diabetes on performance and metabolism of rat hearts." Circ Res **47**(6): 911-21.

Pichon, S., M. Bryckaert and E. Berrou (2004). "Control of actin dynamics by p38 MAP kinase - Hsp27 distribution in the lamellipodium of smooth muscle cells." J Cell Sci **117**(Pt 12): 2569-77.

Price, S. A., L. A. Zeef, L. Wardleworth, A. Hayes and D. R. Tomlinson (2006). "Identification of changes in gene expression in dorsal root ganglia in diabetic neuropathy: correlation with functional deficits." J Neuropathol Exp Neurol **65**(7): 722-32.

Prohaska, J. R. and L. J. Heller (1982). "Mechanical properties of the copper-deficient rat heart." J Nutr **112**(11): 2142-50.

Qian, M., M. Liu and J. W. Eaton (1998). "Transition metals bind to glycated proteins forming redox active "glycochelates": implications for the pathogenesis of certain diabetic complications." Biochem Biophys Res Commun **250**(2): 385-9.

Rae, T. D., P. J. Schmidt, R. A. Pufahl, V. C. Culotta and T. V. O'Halloran (1999). "Undetectable intracellular free copper: the requirement of a copper chaperone for superoxide dismutase.[comment]." Science. **284**(5415): 805-8.

Rakieten, N., M. L. Rakieten and M. R. Nadkarni (1963). "Studies on the diabetogenic action of streptozotocin (NSC-37917)." Cancer Chemother Rep **29**: 91-8.

Ramakrishnan, R., D. Dorris, A. Lublinsky, A. Nguyen, M. Domanus, A. Prokhorova, L. Gieser, E. Touma, R. Lockner, M. Tata, X. Zhu, M. Patterson, R. Shippy, T. J. Sendera and A. Mazumder (2002). "An assessment of Motorola CodeLink microarray performance for gene expression profiling applications." Nucleic Acids Res **30**(7): e30.

Rauscher, F. M., R. A. Sanders and J. B. Watkins, 3rd (2000). "Effects of piperine on antioxidant pathways in tissues from normal and streptozotocin-induced diabetic rats." J Biochem Mol Toxicol **14**(6): 329-34.

Rauscher, F. M., R. A. Sanders and J. B. Watkins, 3rd (2001). "Effects of coenzyme Q10 treatment on antioxidant pathways in normal and streptozotocin-induced diabetic rats." J Biochem Mol Toxicol **15**(1): 41-6.

Rauscher, F. M., R. A. Sanders and J. B. Watkins, 3rd (2001). "Effects of isoeugenol on oxidative stress pathways in normal and streptozotocin-induced diabetic rats." J Biochem Mol Toxicol **15**(3): 159-64.

Raza, H., I. Ahmed, A. John and A. K. Sharma (2000). "Modulation of xenobiotic metabolism and oxidative stress in chronic streptozotocin-induced diabetic rats fed with Momordica charantia fruit extract." J Biochem Mol Toxicol **14**(3): 131-9.

Regan, T. J., M. M. Lyons, S. S. Ahmed, G. E. Levinson, H. A. Oldewurtel, M. R. Ahmad and B. Haider (1977). "Evidence for cardiomyopathy in familial diabetes mellitus." J Clin Invest **60**(4): 884-99.

Richter, A., C. Schwager, S. Hentze, W. Ansorge, M. W. Hentze and M. Muckenthaler (2002). "Comparison of fluorescent tag DNA labeling methods used for expression analysis by DNA microarrays." Biotechniques **33**(3): 620-8, 630.

Rodrigues, B., M. C. Cam and J. H. McNeill (1998). "Metabolic disturbances in diabetic cardiomyopathy." Mol Cell Biochem **180**(1-2): 53-7.

Rodrigues, B. and J. McNeill (1999). Physiological and Pathological Consequences of Streptozotocin Diabetes on the Heart. Experimental Models of Diabetes. J. McNeill. Boca Raton, Florida, CRC Press**:** 14.

Rolo, A. P. and C. M. Palmeira (2006). "Diabetes and mitochondrial function: role of hyperglycemia and oxidative stress." Toxicol Appl Pharmacol **212**(2): 167-78.

Ross, R., L. Leger, R. Guardo, J. De Guise and B. G. Pike (1991). "Adipose tissue volume measured by magnetic resonance imaging and computerized tomography in rats." J Appl Physiol **70**(5): 2164-72.

Rubler, S., J. Dlugash, Y. Z. Yuceoglu, T. Kumral, A. W. Branwood and A. Grishman (1972). "New type of cardiomyopathy associated with diabetic glomerulosclerosis." Am J Cardiol **30**(6): 595-602.

Saburi, Y., K. Okumura, H. Matsui, K. Hayashi, H. Kamiya, R. Takahashi, K. Matsubara and M. Ito (2003). "Changes in distinct species of 1,2-diacylglycerol in cardiac hypertrophy due to energy metabolic disorder." Cardiovasc Res **57**(1): 92-100.

Saggerson, E. D. (1982). "Carnitine acyltransferase activities in rat liver and heart measured with palmitoyl-CoA and octanoyl-CoA. Latency, effects of K+, bivalent metal ions and malonyl-CoA." Biochem J **202**(2): 397-405.

Reference

Saggerson, E. D. and C. A. Carpenter (1981). "Carnitine palmitoyltransferase and carnitine octanoyltransferase activities in liver, kidney cortex, adipocyte, lactating mammary gland, skeletal muscle and heart." FEBS Lett **129**(2): 229-32.

Sajithlal, G. B., P. Chithra and G. Chandrakasan (1999). "An in vitro study on the role of metal catalyzed oxidation in glycation and crosslinking of collagen." Mol Cell Biochem **194**(1-2): 257-63.

Sakamoto, J., R. L. Barr, K. M. Kavanagh and G. D. Lopaschuk (2000). "Contribution of malonyl-CoA decarboxylase to the high fatty acid oxidation rates seen in the diabetic heart." Am J Physiol Heart Circ Physiol **278**(4): H1196-204.

Schafer, J., D. M. Turnbull and H. Reichmann (1993). "A rapid fluorometric method for the determination of carnitine palmitoyltransferase." Anal Biochem **209**(1): 53-6.

Schedl, H. P. and H. D. Wilson (1971). "Effects of diabetes on intestinal growth in the rat." J Exp Zool **176**(4): 487-95.

Schena, M., D. Shalon, R. W. Davis and P. O. Brown (1995). "Quantitative monitoring of gene expression patterns with a complementary DNA microarray." Science **270**(5235): 467-70.

Schmidt, A. M., S. D. Yan, S. F. Yan and D. M. Stern (2001). "The multiligand receptor RAGE as a progression factor amplifying immune and inflammatory responses." J Clin Invest **108**(7): 949-55.

Schnedl, W. J., S. Ferber, J. H. Johnson and C. B. Newgard (1994). "STZ transport and cytotoxicity. Specific enhancement in GLUT2-expressing cells." Diabetes **43**(11): 1326-33.

Sewell, M. A. (2005). "Utilization of lipids during early development of the sea urchin *Evechinus chloroticus*." Marine Ecology Progress Series **304**: 133-142.

Shen, X., S. Zheng, V. Thongboonkerd, M. Xu, W. M. Pierce, Jr., J. B. Klein and P. N. Epstein (2004). "Cardiac mitochondrial damage and biogenesis in a chronic model of type 1 diabetes." Am J Physiol Endocrinol Metab **287**(5): E896-905.

Shimojo, N., T. Ishizaki, S. Imaoka, Y. Funae, S. Fujii and K. Okuda (1993). "Changes in amounts of cytochrome P450 isozymes and levels of catalytic activities in hepatic and renal microsomes of rats with streptozocin-induced diabetes." Biochem Pharmacol **46**(4): 621-7.

Shipp, J. C., L. H. Opie and D. Challoner (1961). "Fatty acid and Glucose metabolism in the perfused heart." Nature **189**(4769): 2.

Shomron, N., H. Malca, I. Vig and G. Ast (2002). "Reversible inhibition of the second step of splicing suggests a possible role of zinc in the second step of splicing." Nucleic Acids Res **30**(19): 4127-37.

Singh, R., A. Barden, T. Mori and L. Beilin (2001). "Advanced glycation end-products: a review." Diabetologia **44**(2): 129-46.

Small, J. V., T. Stradal, E. Vignal and K. Rottner (2002). "The lamellipodium: where motility begins." Trends Cell Biol **12**(3): 112-20.

Smyth, G. (2004). "Linear models and empirical Bayes methods for assesing differential expression in microarray experiments." Statistical Applications in Genetics and Molecular Biology **3**(1): Article 3.

Smyth, G. (2005). Limma: Linear models for Microarray data. New York, Springer.

Sreekumar, R., P. Halvatsiotis, J. C. Schimke and K. S. Nair (2002). "Gene expression profile in skeletal muscle of type 2 diabetes and the effect of insulin treatment." Diabetes **51**(6): 1913-20.

Srinivasan, K. and P. Ramarao (2007). "Animal models in type 2 diabetes research: an overview." Indian J Med Res **125**(3): 451-72.

St-Pierre, J., J. A. Buckingham, S. J. Roebuck and M. D. Brand (2002). "Topology of superoxide production from different sites in the mitochondrial electron transport chain." J Biol Chem **277**(47): 44784-90.

Stanley, W. C., G. D. Lopaschuk and J. G. McCormack (1997). "Regulation of energy substrate metabolism in the diabetic heart." Cardiovasc Res **34**(1): 25-33.

Stekel, D. (2003). Microarray Bioinformatics, Cambridge University Press, UK.

Stevens, M. D., R. A. DiSilvestro and E. D. Harris (1984). "Specific receptor for ceruloplasmin in membrane fragments from aortic and heart tissues." Biochemistry **23**(2): 261-6.

Stohs, S. J. and D. Bagchi (1995). "Oxidative mechanisms in the toxicity of metal ions." Free Radic Biol Med **18**(2): 321-36.

Strange, R. C., M. A. Spiteri, S. Ramachandran and A. A. Fryer (2001). "Glutathione-S-transferase family of enzymes." Mutat Res **482**(1-2): 21-6.

Su, X., X. Han, D. J. Mancuso, D. R. Abendschein and R. W. Gross (2005). "Accumulation of long-chain acylcarnitine and 3-hydroxy acylcarnitine molecular species in diabetic myocardium: identification of alterations in mitochondrial fatty acid processing in diabetic myocardium by shotgun lipidomics." Biochemistry **44**(13): 5234-45.

Reference

Subramanian, A., P. Tamayo, V. K. Mootha, S. Mukherjee, B. L. Ebert, M. A. Gillette, A. Paulovich, S. L. Pomeroy, T. R. Golub, E. S. Lander and J. P. Mesirov (2005). "Gene set enrichment analysis: a knowledge-based approach for interpreting genome-wide expression profiles." Proc Natl Acad Sci U S A **102**(43): 15545-50.

Sullivan, C. J., T. H. Teal, I. P. Luttrell, K. B. Tran, M. A. Peters and H. Wessells (2005). "Microarray analysis reveals novel gene expression changes associated with erectile dysfunction in diabetic rats." Physiol Genomics **23**(2): 192-205.

Susztak, K., E. Bottinger, A. Novetsky, D. Liang, Y. Zhu, E. Ciccone, D. Wu, S. Dunn, P. McCue and K. Sharma (2004). "Molecular profiling of diabetic mouse kidney reveals novel genes linked to glomerular disease." Diabetes **53**(3): 784-94.

Szayna, M., M. E. Doyle, J. A. Betkey, H. W. Holloway, R. G. Spencer, N. H. Greig and J. M. Egan (2000). "Exendin-4 decelerates food intake, weight gain, and fat deposition in Zucker rats." Endocrinology **141**(6): 1936-41.

t Hoen, P. A., F. de Kort, G. J. van Ommen and J. T. den Dunnen (2003). "Fluorescent labelling of cRNA for microarray applications." Nucleic Acids Res **31**(5): e20.

Taegtmeyer, H. (2000). "Genetics of energetics: transcriptional responses in cardiac metabolism." Ann Biomed Eng **28**(8): 871-6.

Taegtmeyer, H., L. Golfman, S. Sharma, P. Razeghi and M. van Arsdall (2004). "Linking gene expression to function: metabolic flexibility in the normal and diseased heart." Ann N Y Acad Sci **1015**: 202-13.

Taegtmeyer, H., P. McNulty and M. E. Young (2002). "Adaptation and maladaptation of the heart in diabetes: Part I: general concepts." Circulation **105**(14): 1727-33.

Takahashi, R., K. Okumura, T. Asai, T. Hirai, H. Murakami, R. Murakami, Y. Numaguchi, H. Matsui, M. Ito and T. Murohara (2005). "Dietary fish oil attenuates cardiac hypertrophy in lipotoxic cardiomyopathy due to systemic carnitine deficiency." Cardiovasc Res **68**(2): 213-23.

Takeda, S., E. Ono, Y. Matsuzaki, Y. Wakui, Y. Mizuhara, T. Asano, S. Takeda and T. Wakamatsu (1995a). "Metabolic Fate of Triethylenetetramine dihydrochloride (Trientine hydrochloride, TJA-250) 1. Absorption, Distribution and Excretion in Rats after Single Administration of ^{14}C-TJA-250." Oyo Yakuri (Applied Pharmacology) **49**(2): 163-171.

Takeda, S., E. Ono, Y. Matsuzaki, Y. Wakui, Y. Mizuhara, T. Asano, S. Takeda and T. Wakamatsu (1995b). "Metabolic Fate of Triethylenetetramine dihydrochloride (Trientine hydrochloride, TJA-250) 2. Metabolism study in Rats Using ^{14}C-TJA-250." Oyo Yakuri (Applied Pharmacology) **49**(2): 173-178.

Takeda, S., E. Ono, Y. Matsuzaki, Y. Wakui, Y. Mizuhara, T. Asano, S. Takeda and T. Wakamatsu (1995c). "Metabolic Fate of Triethylenetetramine dihydrochloride (Trientine hydrochloride, TJA-250) 3. Bioavaliability of TJA-250 in Rats after Single Administration." Oyo Yakuri (Applied Pharmacology) **49**(2): 179-186.

Tamarat, R., J. S. Silvestre, M. Huijberts, J. Benessiano, T. G. Ebrahimian, M. Duriez, M. P. Wautier, J. L. Wautier and B. I. Levy (2003). "Blockade of advanced glycation end-product formation restores ischemia-induced angiogenesis in diabetic mice." Proc Natl Acad Sci U S A **100**(14): 8555-60.

Tanabe, R., M. Kobayashi, M. Sugawara, K. Iseki and K. Miyazaki (1996). "Uptake mechanism of trientine by rat intestinal brush-border membrane vesicles." J Pharm Pharmacol **48**(5): 517-21.

Tanzi, R. E., K. Petrukhin, I. Chernov, J. L. Pellequer, W. Wasco, B. Ross, D. M. Romano, E. Parano, L. Pavone, L. M. Brzustowicz and et al. (1993). "The Wilson disease gene is a copper transporting ATPase with homology to the Menkes disease gene." Nat Genet **5**(4): 344-50.

Thompson, A. L. and G. J. Cooney (2000). "Acyl-CoA inhibition of hexokinase in rat and human skeletal muscle is a potential mechanism of lipid-induced insulin resistance." Diabetes **49**(11): 1761-5.

Tomlinson, K. C., S. M. Gardiner, R. A. Hebden and T. Bennett (1992). "Functional consequences of streptozotocin-induced diabetes mellitus, with particular reference to the cardiovascular system." Pharmacol Rev **44**(1): 103-50.

Turko, I. V., L. Li, K. S. Aulak, D. J. Stuehr, J. Y. Chang and F. Murad (2003). "Protein tyrosine nitration in the mitochondria from diabetic mouse heart. Implications to dysfunctional mitochondria in diabetes." J Biol Chem **278**(36): 33972-7.

Turko, I. V. and F. Murad (2003). "Quantitative protein profiling in heart mitochondria from diabetic rats." J Biol Chem **278**(37): 35844-9.

Uchida, Y., K. Izai, T. Orii and T. Hashimoto (1992). "Novel fatty acid beta-oxidation enzymes in rat liver mitochondria. II. Purification and properties of enoyl-coenzyme A (CoA) hydratase/3-hydroxyacyl-CoA dehydrogenase/3-ketoacyl-CoA thiolase trifunctional protein." J Biol Chem **267**(2): 1034-41.

Reference

Urata, Y., H. Yamamoto, S. Goto, H. Tsushima, S. Akazawa, S. Yamashita, S. Nagataki and T. Kondo (1996). "Long exposure to high glucose concentration impairs the responsive expression of gamma-glutamylcysteine synthetase by interleukin-1beta and tumor necrosis factor-alpha in mouse endothelial cells." J Biol Chem **271**(25): 15146-52.

Uriu-Adams, J. Y., R. B. Rucker, J. F. Commisso and C. L. Keen (2005). "Diabetes and dietary copper alter 67Cu metabolism and oxidant defense in the rat." J Nutr Biochem **16**(5): 312-20.

Voskoboinik, I., H. Brooks, S. Smith, P. Shen and J. Camakaris (1998). "ATP-dependent copper transport by the Menkes protein in membrane vesicles isolated from cultured Chinese hamster ovary cells." FEBS Lett **435**(2-3): 178-82.

Walshe, J. M. (1969). "Management of penicillamine nephropathy in Wilson's disease: a new chelating agent." Lancet **2**(7635): 1401-2.

Walshe, J. M. (1982). "Treatment of Wilson's disease with trientine (triethylene tetramine) dihydrochloride." Lancet **1**(8273): 643-7.

Way, K. J., K. Isshiki, K. Suzuma, T. Yokota, D. Zvagelsky, F. J. Schoen, G. E. Sandusky, P. A. Pechous, C. J. Vlahos, H. Wakasaki and G. L. King (2002). "Expression of connective tissue growth factor is increased in injured myocardium associated with protein kinase C beta2 activation and diabetes." Diabetes. **51**(9): 2709-18.

Wei, M., L. Ong, M. T. Smith, F. B. Ross, K. Schmid, A. J. Hoey, D. Burstow and L. Brown (2003). "The streptozotocin-diabetic rat as a model of the chronic complications of human diabetes." Heart Lung Circ **12**(1): 44-50.

Weickert, M. O. and A. F. Pfeiffer (2006). "Signalling mechanisms linking hepatic glucose and lipid metabolism." Diabetologia **49**(8): 1732-41.

Wild, S., G. Roglic, A. Green, R. Sicree and H. King (2004). "Global prevalence of diabetes: estimates for the year 2000 and projections for 2030." Diabetes Care **27**(5): 1047-53.

Will, C. L. and R. Luhrmann (2001). "Spliceosomal UsnRNP biogenesis, structure and function." Curr Opin Cell Biol **13**(3): 290-301.

Willsky, G. R., L. H. Chi, Y. Liang, D. P. Gaile, Z. Hu and D. C. Crans (2006). "Diabetes-altered gene expression in rat skeletal muscle corrected by oral administration of vanadyl sulfate." Physiol Genomics **26**(3): 192-201.

Wilson, K. H., S. E. Eckenrode, Q. Z. Li, Q. G. Ruan, P. Yang, J. D. Shi, A. Davoodi-Semiromi, R. A. McIndoe, B. P. Croker and J. X. She (2003). "Microarray analysis of gene expression in the kidneys of new- and post-onset diabetic NOD mice." Diabetes **52**(8): 2151-9.

Wolff, S. P. and R. T. Dean (1987). "Glucose autoxidation and protein modification. The potential role of 'autoxidative glycosylation' in diabetes." Biochem J **245**(1): 243-50.

Wolff, S. P., Z. Y. Jiang and J. V. Hunt (1991). "Protein glycation and oxidative stress in diabetes mellitus and ageing." Free Radic Biol Med **10**(5): 339-52.

Wolfram, S., D. Raederstorff, M. Preller, Y. Wang, S. R. Teixeira, C. Riegger and P. Weber (2006). "Epigallocatechin gallate supplementation alleviates diabetes in rodents." J Nutr **136**(10): 2512-8.

Wu, P., J. Sato, Y. Zhao, J. Jaskiewicz, K. M. Popov and R. A. Harris (1998). "Starvation and diabetes increase the amount of pyruvate dehydrogenase kinase isoenzyme 4 in rat heart." Biochem J **329 (Pt 1)**: 197-201.

Xiang, C. C. and M. J. Brownstein (2003). Fabrication of cDNA Microarrays. Functional Genomics:Methods and Protocols. M. J. Brownstein and A. B. Kohodursky. Totowa, New Jersey, Humana Press. **224:** 1-8.

Yamamoto, H., Y. Uchigata and H. Okamoto (1981). "Streptozotocin and alloxan induce DNA strand breaks and poly(ADP-ribose) synthetase in pancreatic islets." Nature **294**(5838): 284-6.

Yao, K. W. and H. Schulz (1996). "Intermediate channeling on the trifunctional beta-oxidation complex from pig heart mitochondria." J Biol Chem **271**(30): 17816-20.

Yauk, C. L., M. L. Berndt, A. Williams and G. R. Douglas (2004). "Comprehensive comparison of six microarray technologies." Nucleic Acids Res **32**(15): e124.

Ye, G., N. S. Metreveli, J. Ren and P. N. Epstein (2003). "Metallothionein prevents diabetes-induced deficits in cardiomyocytes by inhibiting reactive oxygen species production." Diabetes. **52**(3): 777-83.

Yechoor, V. K., M. E. Patti, R. Saccone and C. R. Kahn (2002). "Coordinated patterns of gene expression for substrate and energy metabolism in skeletal muscle of diabetic mice." Proc Natl Acad Sci U S A **99**(16): 10587-92.

Yin, F. C., H. A. Spurgeon, K. Rakusan, M. L. Weisfeldt and E. G. Lakatta (1982). "Use of tibial length to quantify cardiac hypertrophy: application in the aging rat." Am J Physiol **243**(6): H941-7.

Yoshida, K., T. Shimizugawa, M. Ono and H. Furukawa (2002). "Angiopoietin-like protein 4 is a potent hyperlipidemia-inducing factor in mice and inhibitor of lipoprotein lipase." J Lipid Res **43**(11): 1770-2.

Yu, J., M. I. Othman, R. Farjo, S. Zareparsi, S. P. MacNee, S. Yoshida and A. Swaroop (2002). "Evaluation and optimization of procedures for target labeling and hybridization of cDNA microarrays." Mol Vis **8**: 130-7.

Yu, X., S. C. Burgess, H. Ge, K. K. Wong, R. H. Nassem, D. J. Garry, A. D. Sherry, C. R. Malloy, J. P. Berger and C. Li (2005). "Inhibition of cardiac lipoprotein utilization by transgenic overexpression of Angptl4 in the heart." Proc Natl Acad Sci U S A **102**(5): 1767-72.

Zargar, A. H., N. A. Shah, S. R. Masoodi, B. A. Laway, F. A. Dar, A. R. Khan, F. A. Sofi and A. I. Wani (1998). "Copper, zinc, and magnesium levels in non-insulin dependent diabetes mellitus." Postgrad Med J **74**(877): 665-8.

Zhou, B. and J. Gitschier (1997). "hCTR1: a human gene for copper uptake identified by complementation in yeast." Proc Natl Acad Sci U S A **94**(14): 7481-6.

Zhou, H. and D. J. Thiele (2001). "Identification of a novel high affinity copper transport complex in the fission yeast Schizosaccharomyces pombe." J Biol Chem **276**(23): 20529-35.